Journal

of the

AMERICAN CERAMIC SOCIETY

——— ★ ———

Ceramic Abstracts

——— ★ ———

TABLE OF CONTENTS

Journal of The American Ceramic Society (Part I)

Kinetics of Cristobalite Formation from Silicic Acid

by A. G. VERDUCH

State University of New York College of Ceramics at Alfred University, Alfred, New York

Rate experiments made on the transformation of silicic acid into cristobalite, in the temperature range 945° to 1085°C., have demonstrated the existence of a measurable nucleation period. From its variation with temperature, a value of 102.8 kcal. per mole has been calculated for the activation energy of the nucleation process. A second step of the transformation, involving the growth and perfecting of the new phase, has been shown to occur with an activation energy of 50.9 kcal. per mole. From the shape of the rate curves it has been calculated that a superstructure having fairly well-defined sequence rhythms of alternating three- and two-layer structural units might be the end product of heating silicic acid in the temperature range covered by the present experiments. It also has been demonstrated that the degree of disorder increases from the core to the surface of the transforming cristobalite crystals.

I. Introduction

IT IS well known that precipitated silica transforms into cristobalite when heated at temperatures ranging from 900° to about 1500°C., even though tridymite is generally admitted to be the stable phase in this temperature range. It is also known that this transformation is sluggish and, if the heating temperature is low enough, it yields imperfect crystals of cristobalite.

Some fifty years ago, Day and Shepherd[1] made the observation that precipitated silica does not change into a crystalline phase when heated at 900°C., even after a heating period of 1 month. A few years later, Kyropoulos[2] noticed that precipitated silica converts partly into cristobalite when heated at about 1300°C. for 2 hours. He also observed that the precipitated silica heated in this way did not yield X-ray diffraction lines as clear as those given by cristobalite made by melting water-glass with sodium phosphate. The explanation was given that the diffuse radiation due to unchanged amorphous silica was responsible for the rather diffuse X-ray diffraction lines given by the product.

Dwyer and Mellor[3] observed that precipitated silica already shows a broad diffraction band when heated at a temperature as low as 810°C. More recently, Cohn and Kolthoff[4] found that an incipient crystallization occurs after heating precipitated silica in air at 1010°C. for 5 hours. When it is heated in water vapor, signs of an incipient crystallization appear already at 865°C.

Akiyama[5] explored the transformation of precipitated silica into cristobalite by heating samples at different temperatures in the range 900° to 1500°C. for a constant period of 2 hours. His experiments showed that crystallization begins at 1100°C.

The foregoing incomplete survey shows an apparent disagreement in regard to the temperature at which the transformation begins. The fact that Akiyama does not report a noticeable transformation in a 2-hour heating period at temperatures below 1100°C., whereas Cohn and Kolthoff find an incipient crystallization at 1010°C. after a 5-hour heating period, suggests that a nucleation process involving rate-controlling factors may be present in the early stages of the transformation.

[1] A. L. Day and E. S. Shepherd, "The Lime-Silica Series of Minerals," *J. Am. Chem. Soc.*, 28 [9] 1089–1114 (1906).

[2] S. Kyropoulos, "Differentiation of Internal Structure of Different Species of Silica," *Z. anorg. u. allgem. Chem.*, 99, 197 (1917).

[3] F. P. J. Dwyer and D. P. Mellor, "X-Ray Diffraction Studies of Crystallization of Amorphous Silica," *J. Proc. Roy. Soc. N. S. Wales*, 67, 420–28 (1934); *Ceram. Abstr.*, 14 [1] 22 (1935).

[4] Günther Cohn and I. M. Kolthoff, "Thermal Aging of Silica," *Festskr. Tillägnad J. Arvid Hedvall*, 1948, pp. 97–116.

[5] Kei-iti Akiyama, "X-Ray Studies of Silica," *Waseda Applied Chem. Soc. Bull.*, 17 [1] 21–25 (1940); *Ceram. Abstr.*, 20 [8] 205 (1941).
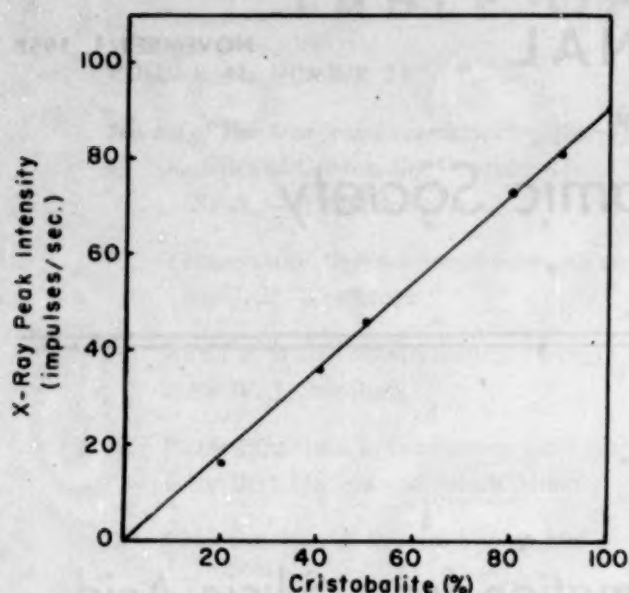
Fig. 1. X-ray calibration for mixtures of cristobalite and amorphous silica.

Fig. 2. Isothermal rate curves of transformation of amorphous silica to cristobalite.

To provide additional experimental evidence concerning the different processes involved in the crystallization of cristobalite from precipitated silica, a systematic series of rate experiments has been carried out. Attention also has been given to the nature of imperfect cristobalite and to the disorder distribution within the grains.

II. Experimental

The material used for these experiments was silicic acid from the Fisher Scientific Company, with a water content after drying at 105°C. of 3.7% and a content of impurities nonvolatile with hydrofluoric acid equal to 0.1%.

The heatings were performed in a platinum-lined porcelain boat placed in the constant-temperature zone (±1°C.) of a Kanthal-wound tubular furnace, the temperature of which was kept constant by a Celectray photoelectric controller. Constant-temperature runs were made at 945°, 985°, 1010°, 1035°, and 1085°C. In all cases the samples were heated in air. In each heating, a 5-minute period was added to allow for the time necessary for the sample to attain thermal equilibrium, when inserted into the kiln.

After each treatment, the sample was air quenched and subsequently ground in an agate mortar until no scratchiness was felt while grinding and the material appeared to be smooth under the pestle.

The quantitative determination of the transformation was done by means of X-ray diffraction analysis, by the powder method, using a General Electric XRD–3 spectrogoniometer, furnished with a 0.40-degree slit, a 0.05-degree detector, and a nickel filter. Copper radiation was used in all cases.

The calibration curve of composition vs. X-ray peak intensity (Fig. 1) was obtained by using mixtures of cristobalite and amorphous silica in different proportions. The peak selected for the calibration was the strongest one (d = 4.07 a.u.). The cristobalite was prepared by heating silicic acid at 1480°C. for 8 hours and cooling slowly with the kiln. This treatment gives a very well-built cristobalite whose interplanar spacings are the minimum attainable (see Section IV); therefore, it can be regarded as a good standard material. The amorphous silica was prepared by heating silicic acid at 800°C. for 8 hours. At this temperature, all water was driven off, and no signs of crystallization appeared under X-ray diffraction examination.

As the samples to be compared with the standard cristobalite were of widely different degrees of disorder, a direct
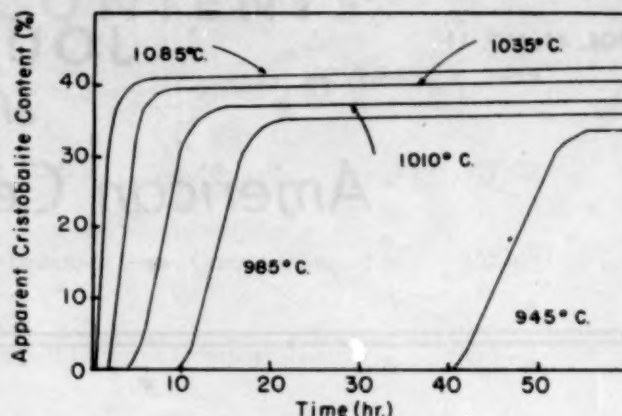
correlation between X-ray peak intensity and percentage of cristobalite formed was not to be expected. The comparison with the standard would be absolutely valid only in the hypothetical case of a transformation product (from heating silicic acid) consisting of a mixture of "perfect cristobalite" and nontransformed amorphous silica. Actually, this was not the case, but instead a partly transformed product was found in which it was not permissible to make a sharp distinction between amorphous grains and cristobalite crystals.

In spite of the inability of this method to furnish a net yield of transformation, it was accepted as the best conventional way to follow the course of the transformation. Consequently, the apparent cristobalite content of a partly transformed product was defined as the fraction of "pure cristobalite" that would give the same X-ray peak intensity as the product in question. The apparent cristobalite content values were drawn from the calibration curve mentioned.

III. Rate of Cristobalite Formation

By using the techniques described, the transformation isothermal curves shown in Fig. 2 were obtained. In view of their shape it is evident that three very distinct steps may be considered in the course of the transformation of silicic acid into cristobalite. The fact that the crystallization does not become apparent from the beginning of each heating shows that a rather slow nucleation process is the rate-controlling factor in the first stages of the transformation. This nucleation period obviously is dependent on temperature.

The second step, which is very rapid, could be described as the growth of a cristobalite-like type of structure, possibly involving short-range movements of particles such as rotation and short displacements of silica tetrahedra toward the more ordered centers formed during the nucleation period.

In the isothermal curves a sharp break is observed after the second step of the transformation has been accomplished. From there on an almost horizontal line follows, which means that a new process with a negligible rate is under course. From the practical point of view, the transformation may be considered as completed by reaching a state of apparent equilibrium. In the temperature range explored, this state seems to correspond to an apparent cristobalite content of 35 to 42%, and it is very similar for all the temperatures studied.

The experimental points obtained in the third stage of the transformation show a dispersion that is similar to the difference between two consecutive lines as drawn in Fig. 2. Even though the lines are almost parallel at higher levels for higher temperatures according to the general trend of the experimental results, it is still questionable that the separa-

Fig. 3.   Nucleation of cristobalite from silicic acid.

Fig. 4.   Crystallization of cristobalite from silicic acid (growth period).

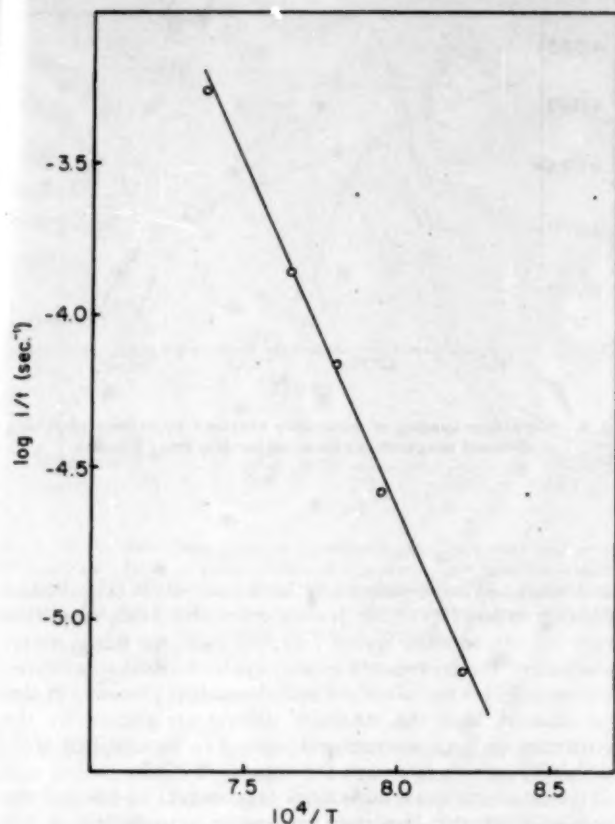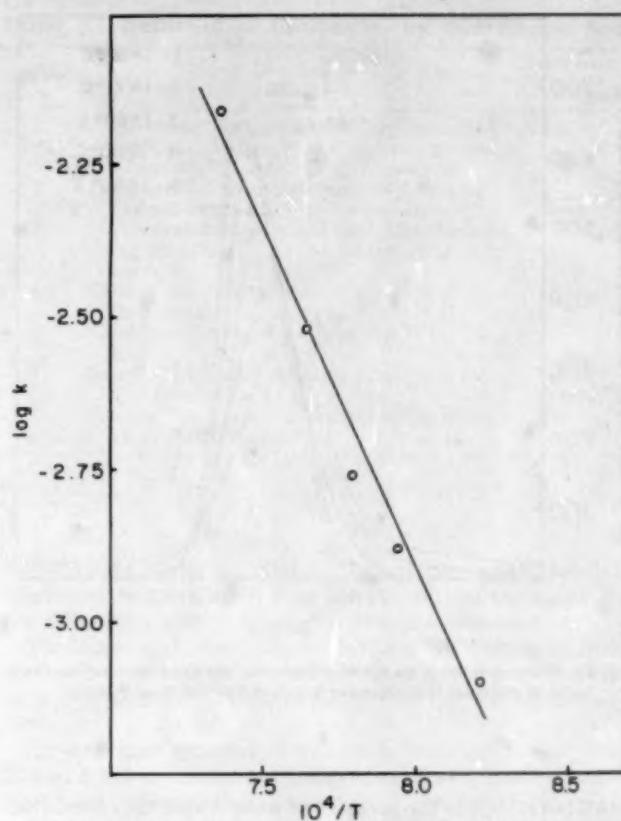tions between them have the correct values.   It would not be far from reasonable to imagine that all the isothermal curves attain one and the same level lying somewhere in between the values 35 and 42% of apparent cristobalite content.

It also has been observed that the flat parts of the isothermal curves show a tendency to increase, although the accuracy of the present experiments does not allow conclusions to be drawn concerning their slope.   The only general conclusion that can be safely drawn is that the process of building up a structure having a definite degree of order ends when the product reaches a degree of transformation corresponding to an apparent cristobalite content of about 40%.   A new process leading to another structure of a higher degree of order begins.   This second process is very slow in the temperature range studied, and it obviously will require an additional activation energy which the present experiments have not enabled the writer to calculate.

The failure of the curves to show a parabolic behavior indicates that no long-range diffusion process is involved during the transformation.

It has been demonstrated that the nucleation process occurs as a logarithm function of the reciprocal of the absolute temperature.   In Fig. 3 a plot is shown of the logarithm of the reciprocal of the nucleation period versus the reciprocal of the absolute temperature.   From the straight line obtained, a value of 102.8 kcal. per mole for the activation energy of nucleation and a pre-exponential coefficient of the Arrhenius equation of 2.09×10^{13} sec.$^{-1}$ have been calculated.

The final empirical equation derived for the nucleation of cristobalite from silicic acid is as follows:

$$\log t = \frac{22,462}{T} - 13.32$$

t = nucleation time (seconds).
T = absolute temperature.

Figure 4 shows a plot of the logarithm of the rate constant versus the reciprocal of the absolute temperature.   From this plot a value of 50.9 kcal. per mole for the activation energy of growth has been calculated.   The Arrhenius equation that holds for the growth process is

$$k = 9.55 \times 10^{5} \cdot \exp\,(-50.900/RT)$$

or in a more simplified form

$$\log k = 5.98 - \frac{11,122}{T}$$

k = per cent of apparent cristobalite formed per second.
T = absolute temperature.

In Table I a list of the nucleation and growth rate data is given.

The foregoing calculations show that the activation energy for nucleation is double that required for the growth of the crystals; therefore, any factor affecting the formation of nuclei might have a decisive influence on the over-all rate of transformation.

The observations of Cohn and Kolthoff are worth mentioning at this point.   They noticed that incipient crystallization took place when SiO_2 was heated in air at 1010°C. for

Table I.   Crystallization of Cristobalite from Silicic Acid

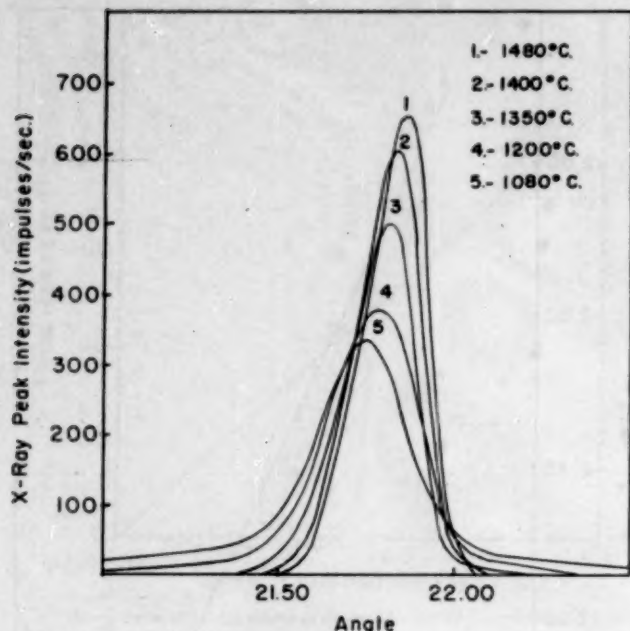| Temp.		Nucleation period		Growth period	
°C.	$10^4/T$	t (hr.)	$\log 1/t$ (sec.$^{-1}$)	k	$\log k$
945	8.21	41	−5.17	7.87×10^{-4}	−3.10
985	7.94	10.5	−4.58	1.33×10^{-3}	−2.88
1010	7.79	4	−4.16	1.74×10^{-3}	−2.76
1035	7.64	2	−3.86	3.01×10^{-3}	−2.52
1085	7.36	0.5	−3.26	7.00×10^{-3}	−2.16

Fig. 5. X-ray diffraction peaks of cristobalite obtained by heating silicic acid at different temperatures (constant heating time, 8 hours).

Fig. 6. Interplanar spacing of cristobalite obtained by heating silicic acid at different temperatures (constant heating time, 8 hours).

1 to 5 hours, but in the presence of water vapor they were able to observe signs of crystallization at temperatures as low as 865°C. They also pointed out that below 900°C. the aging of silica depended on the presence of water, which presumably acted in breaking the bonds between surface molecules, whereas at higher temperatures aging was accomplished by the motion of all the molecules without requiring the presence of water.

An additional explanation for their findings could be given on the basis of the results of this work. The presence of water molecules has a much stronger depressing action on the nucleation potential barrier than it has on the growth barrier. At low temperatures, where the nucleation period is extremely long, the effect of the presence of water should be much more noticeable than at higher temperatures where the over-all reaction rate is controlled mostly by the growth rate.

Incidentally, Cohn and Kolthoff's observation of an incipient formation of cristobalite after heating at 1010°C. for 1 to 5 hours agrees closely with the finding of a nucleation period of 4 hours at the same temperature in the present investigation.

The results reported long ago by Day and Shepherd that precipitated silica does not change into a crystalline phase when heated at 900°C., even after a heating period of 1 month, must be compared with the present observation that a nucleation period of 1 month would be required if the sample were subjected to a temperature of 870°C.

IV. Nature of Imperfect Cristobalite

The imperfect nature of cristobalite and its sensitivity to heat-treatment has been reported in many instances. In a recent paper, Flörke[6] described the idealized structure of cristobalite as being of a three-layer type, and that of the cristobalite grown at low temperatures as having anomalous sequence rhythms of alternating three- and two-layer struc-

tural units. The sequence rhythms may show periodicities of higher order, i.e. 10, 20, or even more, involving repetition every 10, 20, or more layers. In this case one has a superstructure of the cristobalite type. Such idealized superstructures usually are not observed as independent phases. It also was claimed that the structure defects are caused by the occurrence of foreign structural units, i.e., cations like Na^+, Ca^{2+}, Al^{3+}, which interrupt the regular rhythms.
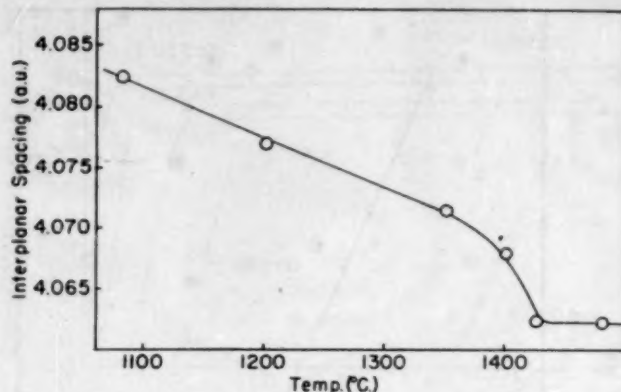
To contribute some additional information to the present knowledge of the imperfect nature of cristobalite, a few experiments were carried out.

By using the X-ray techniques already described, careful measurements of the strongest peak of cristobalite were made after heating silicic acid at various temperatures and constant time. The temperature range chosen was 1080° to 1480°C., and the constant heating time was 8 hours. The reason for this choice was that in this temperature range the nucleation period is much shorter than the selected heating time of 8 hours; therefore, all the samples were given the same length of heating for crystal growth.

In Fig. 5 it can be seen that the peaks broaden considerably at lower temperatures, and at the same time the intensities decrease and the angle for maximum intensity shifts toward lower values.

In Fig. 6 the interplanar spacing of cristobalite is plotted as a function of heating temperature. From this curve it is clear that the interplanar spacing becomes smaller as the heating temperature increases, and that at 1425°C. the curve levels off at a d value of 4.062 a.u. These results seem to show that at 1425°C. the cristobalite already possesses its maximum perfection attainable, i.e., the three-layer-type structure without any two-layer component.

Yamauchi and Kato[7] reported that cristobalite forms at a low temperature and, having imperfect crystals, changes to the high-temperature form at 170° to 180°C., whereas the transition temperature of cristobalite formed at a high temperature rises to 190° to 240°C. Walker, Holley, and Zerfoss[8] made the interesting observation that the inversion temperature of cristobalite prepared from a high-purity sil is independent of heat-treatment above 1400°C. The va ability of the inversion temperature of cristobalite when it

[6] O. W. Flörke, "Strukturanomalien bei Tridymit und Cristobalit" (Structural Anomalies in Tridymite and Cristobalite), *Ber. deut. keram. Ges.*, **32** [12] 369–81 (1955); *Ceram. Abstr.*, **1956**, July, p. 155g. This paper was reviewed by Wilhelm Eitel in *Am. Ceram. Soc. Bull.*, **36** [4] 142–48 (1957).

[7] Toshiyoshi Yamauchi and Saori Kato, "Formation Temperature of Cristobalite and Its Thermal Transition," *J. Japan Ceram. Assoc.*, **51** [606] 319–24 (1943); *Ceram. Abstr.*, **1950**, April, p. 85i.

[8] R. F. Walker, S. F. Holley, and S. Zerfoss, "The High-Low Inversion of Cristobalite," presented at the Fifty-Ninth Annual Meeting, The American Ceramic Society, Dallas, Texas, May 6, 1957 (Basic Science Division, No. 2).
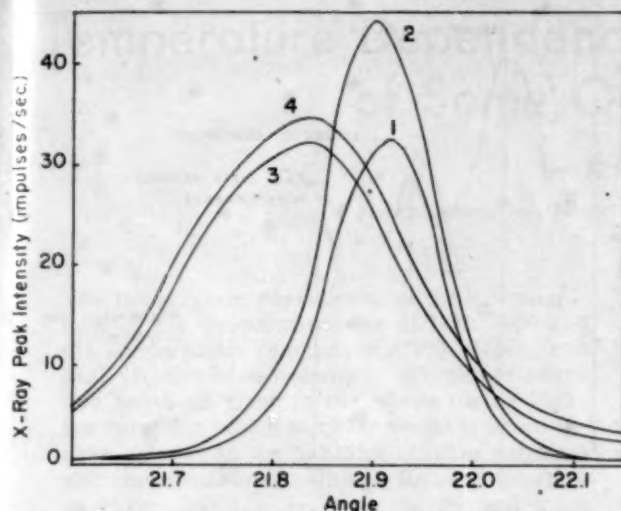
Fig. 7. X-ray diffraction peaks of cristobalite samples before and after HF treatment. (1) Mechanical mixture of cristobalite and amorphous silica, untreated; (2) mechanical mixture of cristobalite and amorphous silica, treated; (3) partly transformed silicic acid, untreated; and (4) partly transformed silicic acid, treated.

Table II. Treatment of Cristobalite by Hydrofluoric Acid

| Sample No.	Treatment	X-ray peak intensity (counts/sec.)
1	Mechanical mixture of 35% cristobalite (1400°C., 10 hr.) plus 65% amorphous silica (800°C., 8 hr.) (Fig. 7, curve 1)	33
2	Sample No. 1 after dissolving 48% of it by hydrofluoric acid (Fig. 7, curve 2)	44
3	Partly transformed silicic acid (after heating at 1010°C. for 20 hours) (Fig. 7, curve 3)	33
4	Sample No. 3 after dissolving 48% of it by hydrofluoric acid (Fig. 7, curve 4)	35
5	Cristobalite from silicic acid (1400°C., 10 hr.)	89
6	Sample No. 5 after dissolving 35% of it by hydrofluoric acid	99
7	Sample No. 5 after dissolving 48% of it by hydrofluoric acid	110

has been prepared at lower temperatures, and its constancy after heat-treatment at 1400°C. or above, may be explained by the present observation that the interplanar spacing of cristobalite varies with heat-treatment until a final state of order is attained at 1425°C.

To check the assumption of a homogeneous transformation product against a transformation product consisting of a mixture of fairly perfect cristobalite plus a fraction of remaining nontransformed amorphous silica, the following experiment was performed.

Fresh silicic acid was heated according to the following schedules: (a) single heating at 1010°C. for 89 hours, (b) heating at 1010°C. for 89 hours, with one intermediate grinding, (c) heating at 1010°C. for 89 hours, with five intermediate grindings.

After these heat-treatments, the apparent yields of transformation were evaluated by measuring the intensity of the major X-ray diffraction peak. The following results were obtained: (a) 38%, (b) 35%, and (c) 35%. Assuming an experimental error of ±2%, all these values fall under the same level, and therefore the experiment shows that the grinding does not affect the yield of the transformation.

If the transformation rate were controlled by a diffusion process, a substantial alteration of the geometry of the transforming system as imposed by a thorough grinding should be expected to have an appreciable effect on the final yield. A failure to show such an effect favors the assumption of a short-range particle movement and therefore the existence of a homogeneous transformed product.

Another structural problem which caught attention was that of the distribution of disorder within the grains. It is known that cristobalite has a poor ability to develop large crystals, in contrast to quartz, for example. On the other hand, the sluggish perfecting process of an imperfect cristobalite crystal through short-range movements might be expected to have its start either on the surface or in the core of the crystal.

To throw some light on the distribution of disorder within the cristobalite grains, the following experiments were made.

A mechanical mixture of 35% cristobalite, made by heating silicic acid at 1480°C. for 8 hours, and 65% amorphous silica, made by heating silicic acid at 800°C. for 8 hours, was suspended in distilled water in a platinum crucible. A sufficient amount of 50% HF solution was added to dissolve 48% of the solids. After drying, the product was heated at about

250°C. The apparent cristobalite content, after this HF treatment, was evaluated from the intensity of the major X-ray diffraction peak. A value of 49% was obtained.

The increase of cristobalite content, by HF treatment, from the original value of 35% to a final value of 49% shows an evident preferential attack on the amorphous fraction of the mixture.

An analogous experiment was made using silicic acid that had an apparent content of cristobalite of 34% instead of the mechanical mixture used previously. The sample was prepared by heating silicic acid at 1010°C. for 20 hours. An amount of 50% HF solution (enough to dissolve about 48% of the solids) was used, and the apparent cristobalite content after this HF treatment was found to be 38% in contrast to the original value of 34%.

Taking into account the experimental errors introduced in the determinations, a slight increase in the cristobalite content was caused by the dissolution process.

In Fig. 7 the X-ray diffraction peak of the samples before and after HF treatment are shown as obtained by the counting method. The conclusion drawn from this experiment is that the cristobalite made by heating silicic acid at 1010°C. for a long enough time to reach the apparent equilibrium is nearly a homogeneous phase.

Two additional experiments of this nature were made by dissolving 35 and 48%, respectively, of a cristobalite heated at 1400°C. for 10 hours, by means of hydrofluoric acid. The X-ray peak intensities were compared with those of the original untreated sample. It was found that the sample which had 35% of its solids removed by HF treatment had jumped from an original X-ray peak intensity of 89 impulses per second to 99 impulses per second, and the sample which had 48% of its solids removed had reached the even greater value of 110 impulses per second. These results are summarized in Table II.

The preceding results show that the disorder distribution in cristobalite fired at 1400°C. is much more heterogeneous than that existing in low-fired cristobalite. The perfection of its lattice decreases from the core to the surface of the grains. This means that the perfecting process starts from the core of the crystal rather than from the surface.

It is unlikely that the degree of crystalline disorder would be affected by the alpha–beta transition. On the other hand, the transition at 267°C. is affected by the degree of disorder. In a recent paper by Hill, Roy, et al.[9] it has been shown that the

[9] V. G. Hill, Rustum Roy, et al., "Final Report on Crystal Chemistry Studies," The Pennsylvania State University, November 1957. Contract No. DA–36–039, SC–71214.

temperature of the alpha–beta inversion in cristobalite is variable and depends on the structure of the starting material and the temperature and length of heat-treatment. It also has been shown that this variability is an index of the order achieved in the cristobalite structure.

According to these experiments, one would be inclined to regard the outer part of the cristobalite crystals as containing a high degree of disorder, as would be the case for a tridymite type of structure. This fact might probably be associated with the growth-limiting factors that in cristobalite must undoubtedly exist.

The often-observed crystallization of distinctly octahedral cristobalite in the centers of tabular tridymite crystals is explained by Flörke. He assumes "a regular intergrowth of the older high-temperature three-layer structure core (cristobalite), with the increasingly defect irregular rhythms of the intermediate cristobalite and finally with the tridymites of the peripheral parts of the complex crystallization. . ."

The present experimental results strongly support the views of Flörke in this respect and give a basis for a more detailed study on the disorder distribution in cristobalites.

One of the valuable observations of Hill and Roy refers to the constancy of the inversion temperature during either heating or cooling (as determined by differential thermal analysis) for the lower-temperature heat-treated cristobalites. The differential thermal analysis patterns of cristobalite heated at or above 1400°C. show, on the contrary, that the material contains a mixture of more than one type of cristobalite, having different inversion temperatures. These observations are in agreement with the results shown in Table II. The hydrofluoric acid experiment with partly transformed silicic acid (1010°C., 20 hours) showed a very slight increase in the apparent cristobalite content by the dissolution process. Analogous experiments with cristobalite formed by heating silicic acid at 1400°C. for 10 hours showed a higher degree of heterogeneity.

The silicic acid used in the present experiments had 0.1% of impurities nonvolatile with hydrofluoric acid. The role of such impurities must not be overlooked. It has been claimed recently[7] that the occurrence of foreign cations in the cristobalite lattice may interrupt the regular layer rhythms. As it has been proved, the degree of order of the imperfect cristobalite decreases toward the surface of the crystals. This could be explained partly by assuming that the foreign cations migrate toward the surface of the grains as the cristobalite nuclei grow. The interruption of the regular silica-layer rhythms, caused by the higher concentration of foreign ions near the surface, would account for the more disordered outer structure encountered in the present experiments.

V. Final Remarks

By looking at the isothermal curves shown in Fig. 2, one may consider that an intermediate metastable cristobalite phase, having a well-defined degree of disorder, is formed as a primary product in the heating of silicic acid. The degree of disorder exhibited by this primary product could correspond to that of a superstructure having fairly well-defined sequence rhythms of alternating three- and two-layer structural units.
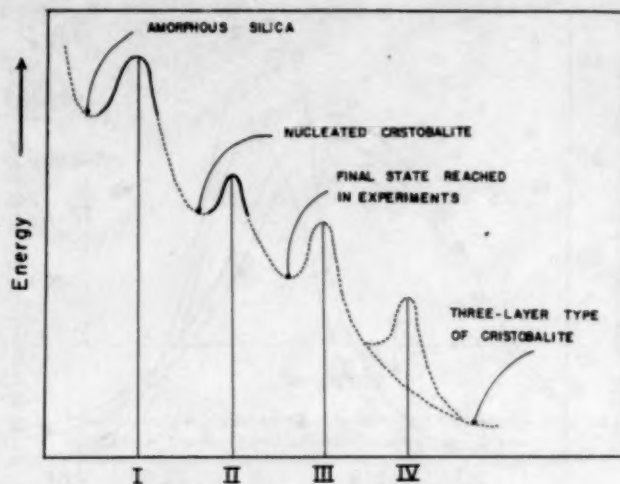
Fig. 8. Energy diagram illustrating transformation of amorphous silica into cristobalite. (I) Nucleation, $Q_I = 102.8$ kcal. per mole; (II) growth of first superstructure, $Q_{II} = 50.9$ kcal. per mole; (III) transition to second superstructure or to final three-layer type of cristobalite; and (IV) transition to third superstructure or to final three-layer type of cristobalite.

Just for the sake of discussion, an imaginary energy diagram of the transformation process has been drawn (Fig. 8). The first step of the transformation involves the overcoming of a nucleation barrier, which is rather high (102.8 kcal. per mole). After the product is nucleated, an additional activation energy of 50.9 kcal. per mole is required in order to form a first superstructure. This supposedly is the only end product of heating silicic acid throughout the whole temperature range covered by the present experiments. Another reason to support the existence of a definite metastable phase could be the fairly high degree of homogeneity within the grains, as encountered in the HF experiment with a sample heated to 1010°C. (see Fig. 7 and Table II). It seems as if the perfecting process, which starts at the original nuclei, reaches an end when it approaches the surface; then the whole crystal has the same degree of order. This degree of order persists until the supply of an additional activation energy makes it possible for the crystal to start a new perfecting process leading to the next superstructure or eventually to the final three-layer type of cristobalite.

To clarify this process, more rate experiments at higher temperatures would be desirable. They would demonstrate if the metastable phase already encountered is the only superstructure existing with a reasonable stability.

Temperature Dependence of Strength and Brittleness of Some Quartz Structures

by J. H. WESTBROOK

Research Laboratory, General Electric Company, Schenectady, New York

The temperature dependence of the microhardness of the quartz structures of both SiO_2 and the isomorphous compounds $AlPO_4$, GeO_2, and $LiAlSiO_4$ has been examined. Particular attention has been given to the effects of the high–low inversion, which has been found to be anomalous relative to the behavior of other polymorphic transformations. The high quartz structure has been found to be much harder and more brittle than low quartz, despite their very close structural similarity.

I. Introduction

THAT quartz* is a material of great commercial importance and scientific interest need hardly be mentioned. In addition to the attention that is paid to it in its own right, it also has significance as a base or prototype structure to which a whole host of other compounds may be related. It is therefore surprising that the knowledge of the mechanical properties of this material is so meager—and with respect to the temperature dependence of strength completely lacking. The writer therefore proposed an exploratory investigation of the temperature dependence of the strength and brittleness of quartz and for a tool chose the indentation hardness test that has been used successfully in previous studies on other brittle materials. The test consists essentially in measuring the size of the indentation made by an indenter of fixed geometry at a given temperature under a known load. Hardness values are calculated by dividing load by contact area of impression. The instrument used employs dead-weight loading on a balanced beam. By keeping the load and loading rate low, errors due to cracking can be avoided. Cracking incidence, however, may be used, as will be explained, as a semiquantitative measure of brittleness. In the work reported here indentations were made *in vacuo* with a 136° diamond pyramid indenter (Vickers type) at a loading rate of 1 mm. per minute and a load of 50 gm. except as noted. Further details of the technique have been reported elsewhere.[1]

The mere fact that a permanent crack-free indentation may be made in a quartz crystal at room temperature of itself poses a mechanistic problem. The deformation mechanisms that may operate in quartz have been analyzed qualitatively by Fairbairn.[2] Three twinning modes are considered to be possible: (a) on the pyramidal (11$\bar{2}$2) plane (Japanese twin),

(b) parallel to the vertical axis, with the prism plane (10$\bar{1}$0) the twinning plane (Dauphiné), or (c) parallel to the vertical axis with the twinning plane (11$\bar{2}$0) (Brazil). Of these, only the Dauphiné type has been definitely established experimentally as a result of mechanical forces,[3] although Fairbairn cites the opinions of Judd[4] and of Sander[5] regarding the possible occurrence of the Brazil and Japanese types, respectively. Zinzerling and Shubnikov,[3] however, show that twinning of the Dauphiné type results in no external deformation in the crystal; hence, this mode cannot account for the observed indentation deformation. With regard to slip, the strong, uniform three-dimensional framework of SiO_4 tetrahedra militates against *any* easy slip system. Fairbairn concludes from a study of the structure of low quartz that glide could conceivably take place in only one direction—parallel to the edge between the prism plane (10$\bar{1}$0) and the positive rhombohedral plane (10$\bar{1}$1), i.e., parallel to those rows of atoms of like charge where the minimum disturbance of tetrahedral SiO_4 bonds would occur. No preferred glide plane could be deduced. He further concludes, contrary to the implication in the earlier review of Sosman,[6] that there is no unequivocal experimental evidence for slip in quartz. In a more recent study, Wachtman and Maxwell[7] failed to observe any plastic deformation in bending up to 800°C. It therefore must be concluded that the apparent plastic flow that occurs in quartz during indentation cannot be understood in terms of known deformation mechanisms. However, the inability to identify the operative flow mechanism does not preclude use of the hardness measurements for study of all aspects of the strength behavior of quartz. There is nothing to suggest that any unique or exotic deformation mechanism should operate during indentation of quartz in contrast to those for more common types of loading. Detailed study of the deformation markings about hardness indentations in various materials (metals,[8] covalent elements,[9] $NaCl$,[10] and MgO[11]) has established that, in general, deformation modes during indentation are the normal ones. Application of various microtechniques to study of the deformed material immediately about a hard-

* The term "quartz" when used (as here) without qualification is to be understood to refer to *silica* in the quartz structure modification. Specific notation will be made when reference is to other compounds having the quartz structure.

[1] (a) J. H. Westbrook, "Microhardness Testing at High Temperatures," *Proc. Am. Soc. Testing Materials*, **57**, 873–97 (1957).

(b) J. H. Westbrook, "Temperature Dependence of Hardness of Equi-Atomic Iron Group Aluminides," *J. Electrochem. Soc.*, **103** [1] 54–63 (1956).

[2] H. W. Fairbairn, "Correlation of Quartz Deformation with Its Crystal Structure," *Am. Mineralogist*, **24** [6] 351–68 (1939); *Ceram. Abstr.*, **19** [4] 99 (1940).

[3] K. Zinzerling and A. V. Shubnikov, "Plasticity of Quartz," *Trav. inst. Lomonosoff géochem., crist., minéral.*, **3**, 67 (1933).

[4] J. W. Judd, "Lamellar Structure in Quartz," *Mineral. Mag.*, **8**, 1 (1888).

[5] Bruno Sander, Gefugekunde der Gesteine (Science of Structure of Rocks). Julius Springer, Vienna, 1930. 352 pp.; *Ceram. Abstr.*, **10** [10] 727 (1931).

[6] R. B. Sosman, Properties of Silica. American Chemical Society Monograph Series, No. 37, Chemical Catalog Co., Inc., New York, 1927. 836 pp.; *Ceram. Abstr.*, **7** [7] 505 (1928).

[7] J. B. Wachtman, Jr., and L. H. Maxwell, "Plastic Deformation of Ceramic-Oxide Single Crystals," *J. Am. Ceram. Soc.*, **37** [7] 291–99 (1954).

[8] B. W. Mott, Microindentation Hardness Testing, pp. 73 ff. Butterworths Scientific Publications, Ltd., London, 1956. 272 pp.; *Ceram. Abstr.*, **1958**, April, p. 98f.

[9] A. T. Churchman, G. A. Geach, and J. Winton, "Deformation Twinning in Materials of the *A4* (Diamond) Crystal Structure," *Proc. Roy. Soc. (London)*, **A238**, 194–203 (1956).

[10] E. Votava, S. Amelinckx, and W. Dekeyser, "Indentation Figures on Single Crystals, I," *Acta Met.*, **3** [1] 89–94 (1955) (in English).

[11] J. H. Westbrook; unpublished research.
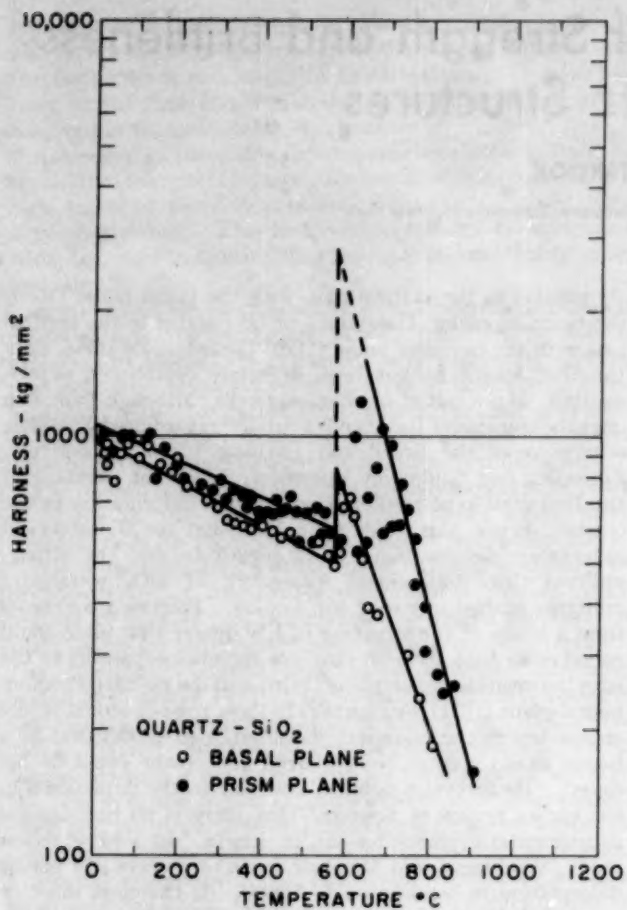
Fig. 1. Temperature dependence of hardness of quartz for two crystal orientations.

Fig. 2. Temperature dependence of quartz compared with other oxides and a typical metal (arrows here and in subsequent figures indicate half the absolute melting point).

ness indentation in quartz might lead to identification of the deformation mechanism. Subsequent studies using the indentation hardness method might then elucidate the observations to be described here of the effects of temperature, structure, and orientation on the strength of quartz. Such studies are considered to be highly important but outside the scope of the present investigation.

II. Temperature Dependence of Hardness of Quartz

The temperature dependence of the hardness of a synthetic quartz single crystal was studied for both the basal and prism plane (direction of load application perpendicular to designated plane). The results are shown in Fig. 1* and comparison made with the behavior of a typical metal and two other common oxides in Fig. 2.[11] It is apparent that the high-low quartz inversion has a marked effect on the hardness; both a hardness discontinuity and a change in slope occur at the inversion temperature. The hardness of the prism plane is observed to exceed that for the basal plane by about 15% for low quartz but by as much as 100% for high quartz. For both low quartz and high quartz the relative anisotropy is essentially independent of temperature.

These results may be compared with those in the literature. Taylor's results[12] on the Vickers hardness of surfaces perpendicular and parallel to the optic axis (1103 and 1260 kg. per sq. mm., respectively) are in fair agreement both qualitatively and quantitatively with the data reported here. Mitsche and Onitsch[13] and Winchell[14] report indentation hardness data for several orientations but not for the basal plane. In both instances, however, the highest hardness was obtained in the prism plane, i.e., parallel to the *c* axis. On the other hand,
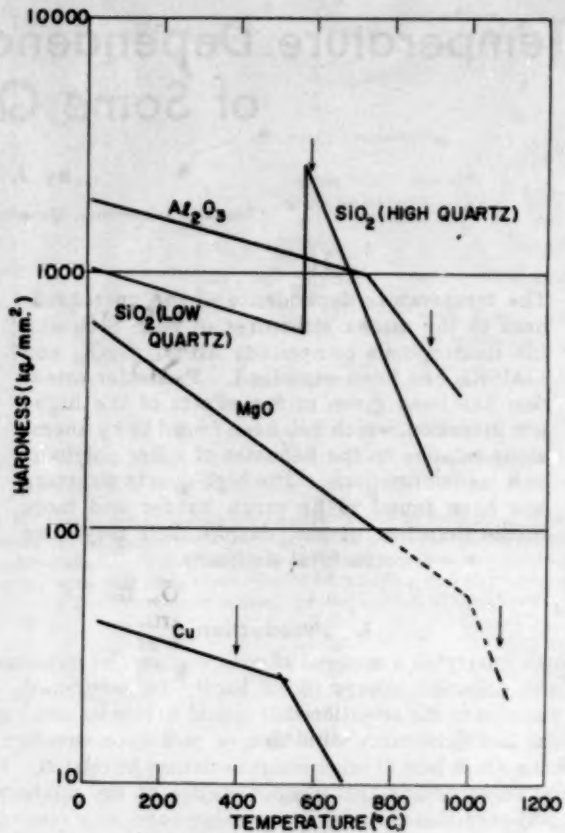
Knoop *et al.*[15] found the Knoop hardness parallel to the optic axis about 10% less than that on a plane perpendicular to the optic axis and Kuznetsov[16] found no difference in the wear resistance of the basal, prism, and positive rhombohedral planes by a mutual polishing technique. Japanese-quartz workers recognize a definite anisotropy in quartz,[17] but it is unclear whether their techniques place greater emphasis on hardness or cleavability. As has been pointed out, the 1100 kg. per sq. mm. room-temperature Vickers hardness obtained in this study for low quartz agrees well with the findings of other similar investigations (see Mott[8] for a complete tabulation), but all the Knoop data reported (again see Mott[8]) are consist-

---

* Each point shown in this and subsequent graphs represents a single hardness measurement. The effects of indenter orientation in the test plane were not considered.

[12] (a) E. W. Taylor, "Correlation of Mohs' Scale of Hardness with Vickers Hardness Numbers," *Mineral. Mag.*, 28, 718–21 (1949).
(b) E. W. Taylor, "Plastic Deformation of Optical Glass," *J. Soc. Glass Technol.*, 34 [157] 69–76T (1950); *Ceram. Abstr.*, 1951, March, p. 47e.

[13] R. Mitsche and E. M. Onitsch, "Microhardness of Minerals," *Mikroskopie*, 3, 257–309 (1948).

[14] Horace Winchell, "Knoop Microhardness Tester as a Mineralogical Tool," *Am. Mineralogist*, 30, 583–95 (1945); *Ceram. Abstr.*, 1946, March, p. 56.

[15] Frederick Knoop, C. G. Peters, and W. E. Emerson, "Sensitive Pyramidal-Diamond Tool for Indentation Measurements," *J. Research Natl. Bur. Standards*, 23 [1] 39–61 (1939); RP 1220; *Ceram. Abstr.*, 18 [11] 307 (1939).

[16] V. D. Kuznetsov, "Mutual Polishing of Different Crystals," *Doklady Akad. Nauk S.S.S.R.*, 89, 271–74 (1953); English translation issued as U. S. Atomic Energy Comm. NSF–tr–51, 1–4 (1953).

[17] S. Ichikawa, "Appendix to Etched Figures of Japanese Quartz," *Am. J. Sci.*, (4th Series), 39, 472 (1915).

LOW QUARTZ   **HIGH QUARTZ**
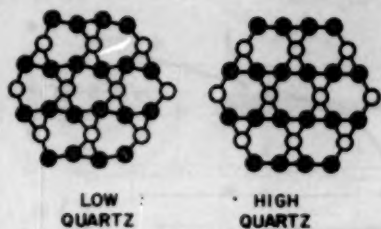
Fig. 3. Plan view of arrangement of silicon atoms in low quartz and high quartz, after Wells (A. F. Wells, Structural Inorganic Chemistry. Oxford University Press, London, 1945. 590 pp.).

Fig. 4. Schematic of temperature dependence of hardness of solids both with and without allotropic transformation.

ently lower than this figure, averaging about 800 kg. per sq. mm. in spite of the fact that Knoop numbers ordinarily are found to be somewhat higher than Vickers numbers for the same material. The relative hardness of the two orientations studied is also in accord with the anisotropy in the elastic modulus as measured by Perrier and de Mandrot.[18] Various workers have reported crushing, tensile, and bending strengths at room temperature slightly higher parallel to the c axis than perpendicular to it (see Sosman[6]). However, the low values obtained and the extreme variability in duplicate tests render these findings of questionable value. The work of Perrier and de Mandrot apparently constitutes the only mechanical-property data on high quartz in the literature. In contradiction to the present results, Perrier and co-workers found a surprising reversal from the behavior of low quartz; i.e. for high quartz $E_\perp > E_\parallel$. No explanation is apparent except that one must remember that hardness is an elastoplastic property and hence will not necessarily parallel the behavior of a purely elastic property.

The marked effects of the high-low inversion that were observed appear to be anomalous with reference to the usual behavior of materials in several respects: the magnitude of the discontinuity, the direction of the discontinuity, the change in slope at the inversion, and the sharpness of the inversion on the low-temperature side. These points are now discussed in turn.

The high-low inversion itself is rather subtle. It involves no change in bond type or coordination but only a slight distortion of the bond angle. In this instance the high-temperature form is the basic structure and the low-temperature form a distortion derivative.[19] Some indication of this is obtained from a plan view of the structure as shown in Fig. 3. It is surprising that this relatively minor change in structure evidently causes the hardness to change by a factor of about 4.

An increase in structural symmetry at a polymorphic inversion in pure metals under conditions of glide deformation results in a discontinuous softening[20] as shown schematically in Fig. 4. More recent studies by Chubb[21] and others confirm this observation. The increase in the hardness of quartz with an increase in symmetry when passed through the inversion temperature must then indicate one of the following conclusions: (a) Low-temperature deformation in quartz does not proceed by glide or (b) glide in quartz obeys different rules than in the case of pure metals, i.e., factors other than structural symmetry and melting point are determinative with
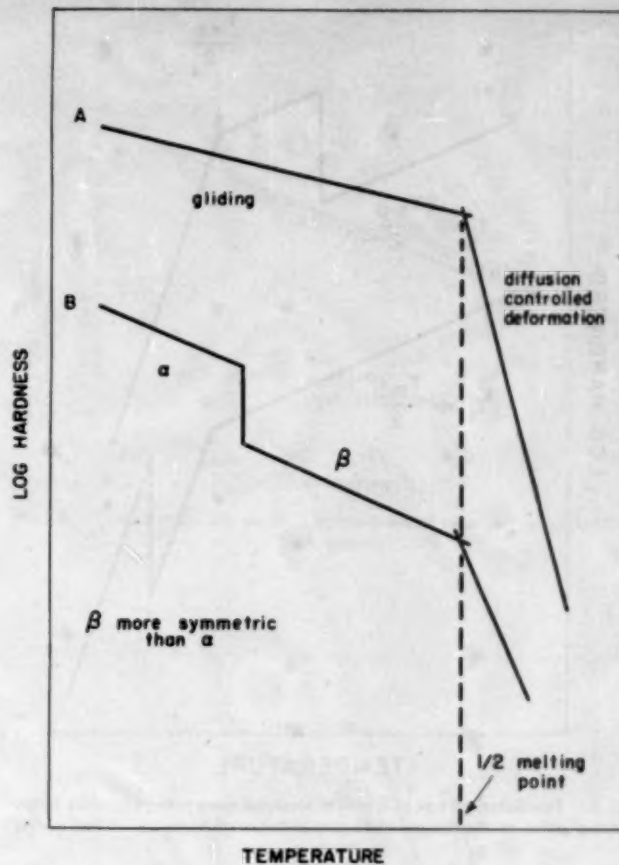
respect to strength. This question cannot be resolved on the basis of present results but is discussed further below.[*]

It has been observed further in the case of pure metals as well as in other compounds[22] that the only effect of a polymorphic transformation is discontinuous change in hardness without significant change in slope on either side of the transition. This is in accord with observations made on pure metals[20] that the temperature dependence of hardness is a function primarily of the bond strength as reflected in the melting point, and to a first approximation is independent of crystal structure. Quartz therefore presents a distinct

---

[*] It has been suggested by G. Kuczynski (private communication) that alloys which undergo an order-disorder reaction are also anomalous with respect to most materials but in agreement with the observation on quartz; i.e., that the disordered form is softer than the apparently more symmetric ordered form. It must be noted, however, that the cases are not equivalent. In the case of an alloy AB which undergoes an order-disorder transition, the lattice point symmetry is the same on both sides of the transition, and consequently no strength contribution is expected from the transition on a geometric basis. On the other hand, on disordering above O–D temperature the distribution of bond types is changed from preferential formation of A–B bonds to the case where A–A, A–B, and B–B bonds are present in approximately equal numbers. This can and does result in a decrease in hardness.

[18] A. Perrier and R. de Mandrot, "Elasticity and Symmetry of Quartz at Elevated Temperatures," *Mém. soc. vaudoise sci. nat.*, 1, 333 (1923); prelim. publ., *Compt. rend.*, 175, 622, 1006 (1922).

[19] M. J. Buerger, "Derivative Crystal Structures," *J. Chem. Phys.*, 15, 1–16 (1947).

[20] J. H. Westbrook, "Temperature Dependence of Hardness of Pure Metals," *Trans. Am. Soc. Metals*, 45, 221–48 (1953).

[21] W. Chubb, "Contribution of Crystal Structure to Hardness of Metals," *J. Metals*, 7, *Trans. Am. Inst. Mining Met. Engrs.*, 203, 189–92 (January 1955).

[22] (a) G. M. Schwab, "Some New Aspects of Strength of Alloys," *Trans. Faraday Soc.*, 45, 385–96 (1949).

(b) Friedrich Rinne and Wolfgang Riezler, "Plasticity of Rock Salt, Silver Bromide, and Silver Iodide at Different Temperatures," *Z. Physik*, 63, 752–59 (1930).

(c) V. P. Shishokin, "Relation Between Chemical Composition and Thermal Coefficient of Plastic Deformation," *Bull. acad. sci. U. R. S. S., Classe sci. math. nat., Sér. chim.*, 1937, pp. 1341–67 (in French, pp. 1367–8).

Fig. 5. Postulated effects of a shift in inversion temperature relative to the melting point on the temperature dependence of hardness of the quartz structure.
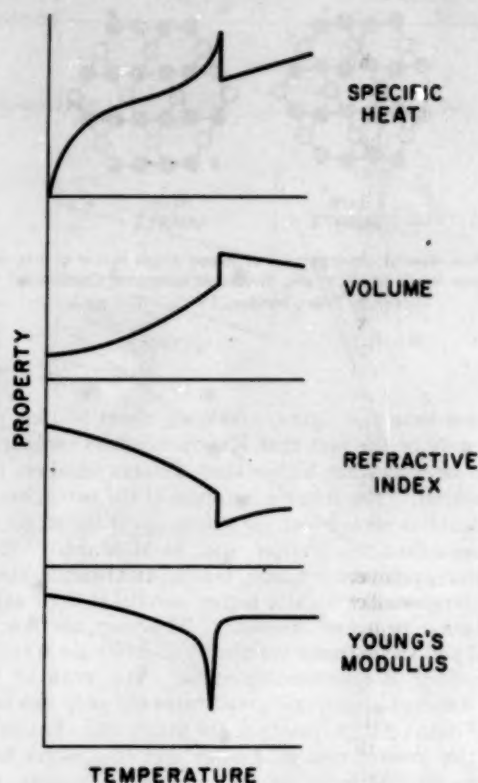
Fig. 6. Schematic of temperature dependence of various properties of quartz.

anomaly in undergoing a slope change in the log hardness-temperature curve by a factor of about 8 when passing through the high-low transition. A possible explanation for this behavior is as follows. Most substances have been shown to exhibit a semilogarithmic dependence of hardness on temperature with a rather abrupt change of slope in the general vicinity of half the absolute point (see Figs. 2 and 4). This result has been interpreted as indicating deformation predominantly by gliding at low temperature and by diffusion-controlled processes above about half the melting point. In the case of quartz, the 573°C. inversion falls near half the melting point, assuming Sosman's value of 1420°C.[6] It therefore is suggested that the observed behavior is that of low-temperature-type deformation in low quartz and high-temperature-type deformation in high quartz. Were it possible to shift the high-low inversion a substantial amount relative to the melting point, one of the two situations shown

schematically in Fig. 5 might then be expected to prevail. Specific tests of this hypothesis are discussed below.

The fourth point of interest concerns the details of the hardness-temperature curve. The temperature dependencies of various physical properties of crystalline quartz through the high-low inversion range show many common characteristics. Among others, Sosman[6] cites a discontinuous property change at the inversion, a gradual increase in the rate of change of all properties beginning 50° or more below the inversion, the absence of the latter effect above the inversion, and the small temperature dependence of all properties above the inversion relative to that between room temperature and the inversion. The curves of Fig. 6 illustrate these behaviors. Here again quartz is apparently anomalous, the hardness-temperature curve showing little, if any, deviation from a linear course below the inversion, some rounding above the inversion, and as discussed above a markedly greater slope for the high quartz form.

To summarize the problem at this point, the writer wishes to explain the anomalies just discussed, to determine if these behaviors are specific to quartz or derive more generally from the quartz structure, and to extend the knowledge of the mechanical properties of the quartz structure both by examining other properties and possible anisotropies and by studying other types of quartz structures. Consideration of the temperature dependence of hardness of a selected group of quartz-structure compounds can accomplish several of these objectives simultaneously. Data on one or more examples from each of the categories of Table I should permit conclusions as to the generality of the behavior and the effects of certain structural details as well as testing of the previously discussed hypothesis for the observed change in slope of the hardness-temperature curve through the inversion by examination of compounds having transitions at different homologous temperatures. Recent crystallographic and phase equilibrium studies indicate that many possibilities exist from

Table I. Schematic of Relations of the Quartz Isomorphs
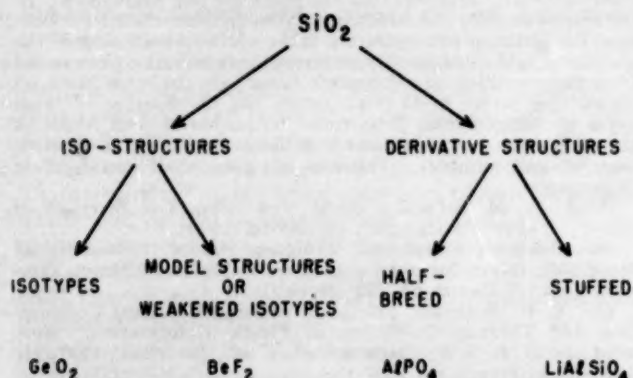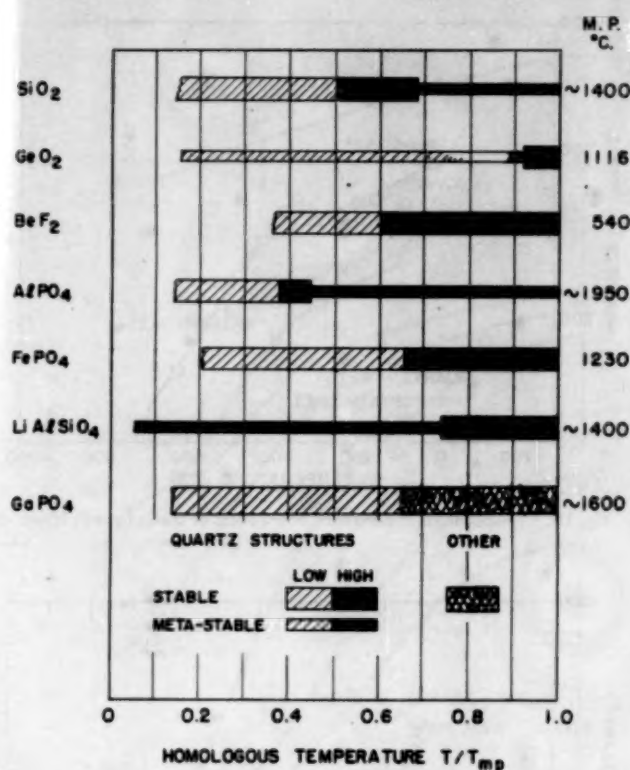
Fig. 7.   Stability range of some quartz structures with respect to the homologous temperature scale.

Fig. 8.   Temperature dependence of hardness of high eucryptite, LiAlSiO (high quartz).
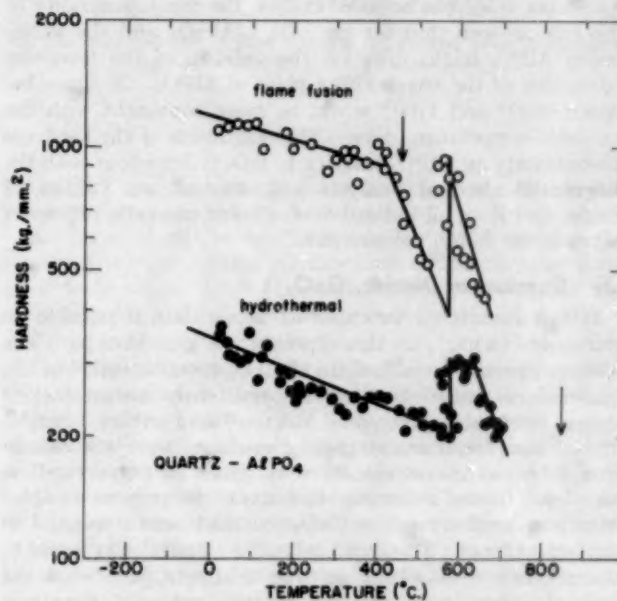
Fig. 9.   Temperature dependence of hardness of quartz form of AlPO₄ from two sources.

which to select compounds for study, a number of which are shown schematically in Fig. 7.

III.   High-Low Inversion in Other Quartz Structures

(1)   High Eucryptite, LiAlSiO₄

High eucryptite, $LiAlSiO_4$, one of the first compounds studied, has been found by Winkler[23] to be isomorphous with high quartz.   This structure has been confirmed by Roy *et al.*,[24] who also established the reconstructive inversion to the rhombohedral phenacite type of low eucryptite at 972° ± 10°C.   It has been found, however, that the high eucryptite form is readily retained on cooling and will persist metastably even with prolonged heating at low temperatures.   A similar reluctance to transform would not be expected, however, for the high-low quartz transformation, and hence one should see a discontinuity in the hardness-temperature curve for metastable high eucryptite if a high-low inversion does occur in the metastable range.   Synthetic crystals (about 1 by 2 mm.) grown from the melt were used for these experiments.*   The results shown in Fig. 8 show no discontinuity but only a change in slope slightly above half the melting point.   It is thus indicated that high eucryptite does not undergo a high-low quartz transformation at least down to liquid nitrogen.

(2)   Aluminum Orthophosphate, AlPO₄

Aluminum orthophosphate, $AlPO_4$, is unique in that it is the only known compound that exhibits all the silica iso-

morphs.   It is also of interest as an example of the half-breed derivative structure (see Table I) in contrast to $LiAlSiO_4$, which is of the "stuffed" type.   The crystal chemistry of this compound has been reviewed recently by Beck[25] and by Shafer and Roy.[26]   Samples of two different types were tested: a hydrothermally grown crystal, furnished to the writer by R. Roy but originally prepared by Stanley at the Fort Monmouth laboratories, and a crystal prepared by the Verneuil flame-fusion technique in the writer's laboratory. The identity of both crystals as low quartz structures was

[23] H. G. F. Winkler, "Synthese und Kristallstruktur des Eukryptits, LiAlSiO₄" (Synthesis and Crystal Structure of Eucryptite, LiAlSiO₄), *Acta Cryst.*, 1 [1] 27–34 (1948); *Ceram. Abstr.*, 1949, June, p. 156a.

[24] Rustum Roy, D. M. Roy, and E. F. Osborn, "Compositional and Stability Relationships Among the Lithium Aluminosilicates: Eucryptite, Spodumene, and Petalite," *J. Am. Ceram. Soc.*, 33 [5] 152–59 (1950).

* These crystals were kindly supplied by Professor Winkler of the University of Marburg.

[25] W. R. Beck, "Crystallographic Inversions of the Aluminum Orthophosphate Polymorphs and Their Relation to Those of Silica," *J. Am. Ceram. Soc.*, 32 [4] 147–51 (1949).

[26] E. C. Shafer and Rustum Roy, "Silica Structure Phases: III, New Data on the System AlPO₄," *Z. physik. Chem. (Frankfurt)*, 11, 30–40 (1957) (in English).

established by X-ray diffraction patterns.* The results of hardness runs on prism planes of both types of sample are shown in Fig. 9. Both types of crystal show distinct evidence of high-low transformation at 585° ± 10°C. However, the flame-fusion crystal is 2 to 3 times as hard as the hydrothermal crystal at all temperatures, presumably a result of low purity caused by partial decomposition. The hardness-temperature curve for the hydrothermal crystal approaches that postulated in curve (a) of Fig. 5, with the slope change occurring only slightly above the high-low inversion and some distance below half the melting point (arrow). In this case the melting point was taken as 2000°C., the lower limit estimated by Stone *et al.* from extrapolation of liquidus data in the system Al_2O_3–P_2O_5.[27] On the other hand, the flame-fusion material shows the slope change distinctly below the high-low inversion, giving a curve identical in shape to that predicted in (b) of Fig. 5. This appears to be a lowering of the melting point through partial decomposition, a view that is supported by the phase diagram presented by Stone *et al.*[27] Their eutectic temperature of 1212° was taken as approximating the melting point for the purposes of predicting the temperature at which the slope change might be expected (arrow) for the impure flame-fusion sample. The correspondence is seen to be good; in fact, the rough generality of this rule as seen thus far for SiO_2, $LiAlSiO_4$, and the flame-fusion $AlPO_4$ might question the validity of the foregoing estimation of the true melting point of $AlPO_4$. A figure between 1600° and 1700° would be more consistent with the hardness-temperature data. The magnitude of the hardness discontinuity in $AlPO_4$ relative to SiO_2 is consistent with the differential thermal analysis and dilatometric studies of Shafer and Roy, all indicative of a lower energetic difference between the $AlPO_4$ polymorphs.

(3) Germanium Dioxide, GeO₂

It was considered desirable to obtain data if possible on germania (quartz), as this represents a true isotype. The room-temperature stable form of GeO_2 is tetragonal, but the quartz form, once obtained, is persistently metastable, as shown by Laubengayer and Morton[28] and others. Single-crystal samples of macroscopic dimensions were not readily obtainable, so measurements were made on polycrystalline samples. Initial attempts were made to prepare samples from powdered crystalline GeO_2 that had been converted to the quartz form. Powdered germania (quartz) was found to sinter poorly even with long-time treatment just below the melting point; no conversion to the tetragonal form was noted. Satisfactory samples were finally made by devitrification of germania glass.† A treatment of one week at 900°C. followed by three weeks at 600° resulted in a polycrystalline material that gave a sharp X-ray diffraction pattern for the low quartz structure; no other significant lines were present.

Germania was expected to show the effects of a high-low quartz inversion, although the temperature at which this might occur was not known. Evidence for the high-low inversion in this material is as follows. All X-ray studies by Zachariasen,[29] by Shafer and Roy,[30] and in the present study indicate that samples quenched to room temperature have the low quartz form. Shafer and Roy further find a high, posi-

Fig. 10. Temperature dependence of hardness of GeO₂ (quartz form).

Fig. 11. Temperature dependence of hardness of cristobalite form of AlPO₄ inverted from quartz form.

tive thermal-expansion coefficient, generally characteristic of the low quartz structure rather than low or even slightly negative as is observed for high quartz. On the other hand, the GeO_2–SiO_2 phase diagram obtained by Shafer and Roy[30] shows complete solid solubility across the diagram at high temperatures and hence would indicate high quartz as the stable high-temperature form of GeO_2. Hot X-ray diffraction studies by these investigators bracket the inversion temperature as $700° < T_i < 1000°$.

The hardness-temperature curves obtained on germania were not as satisfying as had been hoped. Many curves were obtained both on the same sample and on duplicate samples, none of which exactly duplicated any other. The curve shown in Fig. 10 is typical.

The slope change near half the melting point was evident in all. Attempts were made at first to ascribe certain discontinuities observed in this and other curves to a high-low inversion.

* True monocrystals of quartz form $AlPO_4$ could not be consistently prepared by the Verneuil technique. In most cases partial or complete decomposition to Al_2O_3 occurred in the flame. The sample for the tests described, however, was shown by X-ray diffraction to be substantially all $AlPO_4$ (low quartz).

[27] P. E. Stone, E. P. Egan, Jr., and J. R. Lehr, "Phase Relationships in the System CaO–Al_2O_3–P_2O_5," *J. Am. Ceram. Soc.*, **39** [3] 89–98 (1956); correction, *ibid.*, [10] 361–62.

[28] A. W. Laubengayer and D. S. Morton, "Germanium: XXXIX, Polymorphism of Germanium Dioxide," *J. Am. Chem. Soc.*, **54**, 2303–20 (1932).

† The germania glass was kindly prepared for this purpose by A. G. Pincus of this laboratory.

[29] William Zachariasen, "Crystal Structure of Water-Soluble Modification of Germanium Dioxide," *Z. Krist.*, **67**, 226–34 (1928).

[30] E. C. Shafer and Rustum Roy, "Studies of the Silica Structure Phases: IV, The System GeO_2–SiO_2 and Some Remarks on the Quartz-Tridymite-Cristobalite Relations"; presented at the Fifty-Ninth Annual Meeting, The American Ceramic Society, Dallas, Texas, May 6, 1957 (Basic Science Division, No. 1).
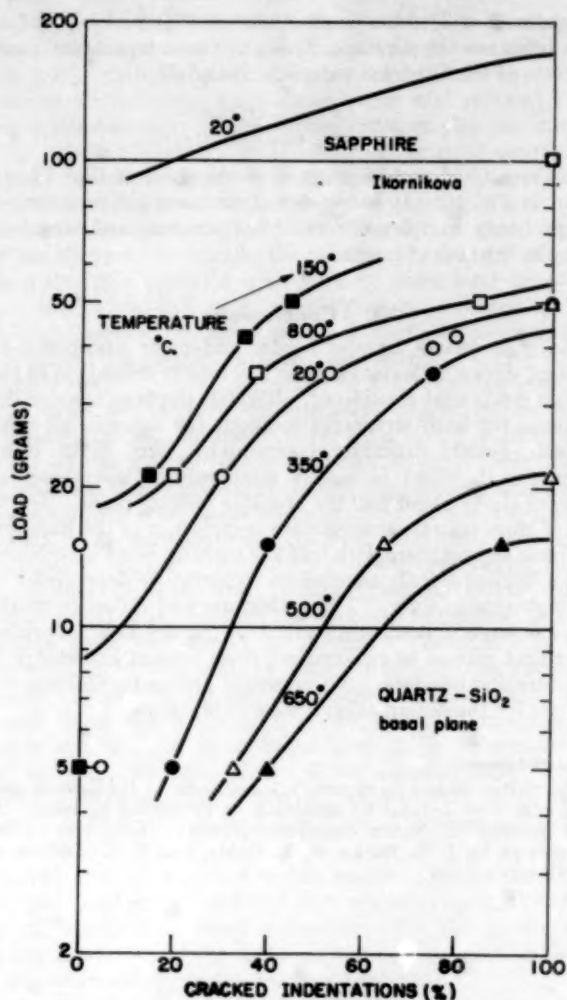
Fig. 12. Effect of load on percentage of cracked indentations in quartz at various temperatures.

Fig. 13. Reduced plot of data from Fig. 12 showing effect of temperature on ductility of a quartz single crystal.

However, the variability in the indicated inversion temperature together with microscopic and hot X-ray diffraction observations indicated that instead such effects should be attributed to crystalline anisotropy in this polycrystalline sample. Single-crystal data would still be very desirable. All diffraction patterns obtained with a high-temperature X-ray diffraction camera up to about 1000°C. showed clear patterns for low quartz; no other lines were present. This result together with that of Shafer and Roy may indicate that the high-low inversion is very close to 1000°C.

IV. Generalizations on Effects of Structure

The results described for AlPO₄ indicate that the increase in hardness obtained in going from low to high quartz is a general characteristic of this inversion and is not unique with silica quartz. It was still desired, however, to establish whether this increase is characteristic of high-low inversions in general or only of the quartz structure. A single experiment was performed, the result of which supports the former view. A crystal of the quartz form of AlPO₄ was converted to the cristobalite form by heating for less than 1 hour at 800°C. The hardness-temperature curve obtained (shown in Fig. 11) indicates very clearly the high-low inversion in cristobalite AlPO₄ at 200°C. Again the high form is harder than the low form. The change in slope with the inversion is truly anomalous and no explanation is yet apparent. The results obtained here regarding the allotropy of AlPO₄ support the findings of Shafer and Roy[26] that the quartz structure becomes unstable

below 800° and that quartz AlPO₄ inverts to cristobalite and not to tridymite as indicated by Beck.[25]

A review of all the hardness-temperature curves for the quartz structures studied permits some additional generalizations to be made. For temperatures below about half the melting point, the temperature dependence of high quartz is observed to be approximately the same as that of low quartz in the same compound. It is furthermore relatively insensitive to variations between compounds having significantly different melting points. This behavior is in contrast to that of the metallic state, where a change in average bond strength of the order indicated by the range of melting points exhibited by the quartz structures studied here would have occasioned a significant change in the temperature dependence of hardness. It also may be observed that for the quartz structure the temperature dependence of hardness is insensitive to the presence of interstitial atoms (stuffed structures behave similarly to all other quartz-structure types) and to the nature of the bonding (isotypes, model structures, and half-breed and stuffed derivatives all behave similarly). In other words, gross structure seems to be the preponderant determinative factor. Zinzerling and Shubnikov[3] claim to have observed a 15:1 reduction in "yield point" between room temperature and 573°, in contrast to the approximately 2:1 reduction in hardness measured in the present study. Although hardness data frequently can be correlated with yield points, inasmuch as Zinzerling and Shubnikov did not obtain a conventional yield point, lack of agreement in the corresponding temperature dependencies may not be significant. No correlation between the intrinsic hardness (i.e. the hardness extrapolated to absolute zero) and the melting point or bond strength could be established in this study for either the high or low quartz structures as had been done for isostructural metallic elements.

V. Brittleness of the Quartz Structure

In the course of making the hardness measurements discussed, incidental observations were made of the degree of cracking about hardness impressions. Significant variations in this respect were observed between different compounds, different polymorphs of the same compound, and different orientations of a given crystal. In general, quartz and LiAlSiO₄ were less susceptible to cracking than the other com-

pounds studied, but the high quartz form was invariably considerably more so than the low quartz form, particularly just above the inversion temperature. The basal plane also seems to be more crack-susceptible than the prism plane. As the cracking tendency increases with increasing load, Ikornikova,[31] Winchell,[32] and others have suggested using the load for a constant percentage of cracked indentations as a measure of the relative brittleness of individuals in a series of samples. As the indentations maintain similar geometry with changing load and other loading conditions are kept constant, the percentage of cracked indentations is equivalent to the probability that a particular point in the sample can sustain a certain effective strain without fracture.* An extensive series of tests of this type was made for quartz, the results of which are shown in Fig. 12. Direct comparison of relative brittleness or ductility cannot be made from this plot as the effective sample size has inadvertently changed with temperature owing to softening of the material. An approximate correction for this may be made, taking as a measure of ductility, D_T, at any temperature, T, the ratio of the load, L, for 50% cracking

---

[31] N. Yu. Ikornikova, "Brittleness of Corundum Crystals," pp. 233–36 in Fizicheskie Svoistva Sinteticheskogo Korunda (Physical Properties of Synthetic Corundum—A Symposium) (A. V. Shubnikov, M. V. Klassen-Neklyudova, and S. V. Grum-Grzhimaĭlo, Editors). *Trudy Inst. Krist. Akad. Nauk S.S.S.R.*, No. 8 (1953). 356 pp.; *Ceram. Abstr.*, 1955, February, p. 24g.

[32] H. Winchell, discussion of paper by N. W. Thibault and H. L. Nyquist, "Measured Knoop Hardness of Hard Substances and Factors Affecting Its Determination," *Trans. Am. Soc. Metals*, 38, 271–330 (1947); p. 327.

* Tabor has shown that for the 136° pyramid indenter the effective strain about an indentation is about 8%. (D. Tabor, "A Simple Theory of Static and Dynamic Hardness," *Proc. Roy. Soc. (London)*, A192, 247–74 (1948).)

as measured at T to the product of the 50% cracking load at some reference temperature, T_0 (e.g., room temperature), and the ratio of the hardness values at T and T_0.

$$D_T = \frac{L_T \ (50\% \ \text{cracked})}{L_{T_0} \ (50\% \ \text{cracked}) \ H_T/H_{T_0}}$$

The results of such treatment of the data of Fig. 12 are shown in Fig. 13. It is apparent that there are pronounced and probably complex effects of temperature and structure on the brittleness of quartz.

VI. Conclusions

The high quartz form is harder and more susceptible to cracking during indentation than low quartz regardless of the specific compound considered, although the temperature dependence for both structures is about the same in all compounds. Quartz-structure compounds, like most other materials, show an increased temperature dependence of strength above about half the absolute melting point. In the case of silica quartz, approximate coincidence of the high-low inversion temperature with half the melting point is responsible for the apparently anomalous temperature dependence of the high quartz form. The rather marked influence of the high-low inversion on mechanical properties is a surprising effect that cannot be rationalized from present knowledge of structure and bonding. No presently known mechanism can account for the deformation during indentation.

Effect of Water on Mechanical Strength of Selected Ceramic Compositions

by W. J. SMOTHERS

Ceramic Research Laboratory, The Ohio Brass Company, Barberton, Ohio

The strength of unglazed feldspathic porcelain test bars in air decreased with humidity at the time of breaking. Moderate vacuum increased strength. N_2, CO_2, O_2, and H_2 were not effective in changing porcelain strength with respect to that in ambient air. Use of a so-called compression glaze eliminated the deleterious effect of water. Several organic liquids, as coatings on unglazed test bars, were evaluated. Tests with acid and basic solutions indicated that porcelain strength decreased with an increase in the mole % of water present in the liquid coating.

I. Introduction

IN making a study of the fundamental properties of glazes and their effect on the strength of certain glaze-body combinations, several nonceramic coatings were used. After applying a coating of paraffin to a fired unglazed ceramic test bar of selected composition, it was found that the modulus of rupture increased approximately 15% over that measured in air on an uncoated bar. The writer describes the results of several experiments made in an attempt to explain this and related observations.

II. Review of Literature

Because there is very little literature on the effect of atmosphere on the strength of porcelain, selected references on glass also are cited. The basic structure of many ceramic bodies and glasses is the Si—O—Si network, and both these materials are considered to be brittle under certain conditions. Reference to the work on glass therefore is believed to be appropriate.

Milligan[1] found that the strength of small bars of window glass in which a transverse scratch was made was reduced about 20% when water was present in this scratch. Exposure to air saturated with water vapor also reduced the strength considerably. Bars wetted and then redried before testing regained slightly more than their original strength. Contrary to this action of water, the presence of dry paraffin oil in the scratch increased the strength by about 20%.

Orowan[2] discussed the so-called "fatigue" of glass; this term has been used to describe the decreased breaking strength when a load is applied for a long time. Some later investigators choose to call this effect "delayed fracture." In contrast to metals, the stress need not fluctuate periodically to develop this static fatigue phenomenon. Using the Griffith concept, Orowan suggested that the surface energy of the glass would vary considerably, depending on the surrounding media, and might differ by a factor of three or four for exposure in air compared with vacuum. He also suggested that if the diffusion of the adsorbed layer from the air into the Griffith crack were important and had an effect on the time-load characteristics, covering the glass with an impermeable varnish or with a low-thermal-expansion glaze should decrease the "fatigue" effect. Baker and Preston[3] found that this fatigue effect was eliminated when soda-lime glass was tested in vacuum. The atmosphere, however, also was found to affect relatively short-time strength (10-second duration of load). The reduction in strength from vacuum conditions to wet at atmospheric pressure was 60% for Pyrex-brand glass, 51% for soda-lime glass, and 40% for silica glass. For a ceramic body (50% clay, 39% feldspar, and 11% flint, fired to cone 9-10) the reduction in strength under comparable conditions was only 33%.

Taylor[4] pointed out that solids under tension are at a higher potential energy and therefore are more susceptible to chemical attack than when stress-free. He also predicted that the conditions of the ambient atmosphere would affect the activation energy of the fracture process.

Both water vapor and carbon dioxide were shown by Gurney and Pearson[5] to affect the delayed fracture of soda-lime glass. Levengood and Swift[6] found that the rate of lateral spread of fractures in plate glass was noticeably increased when water vapor, carbon dioxide, or ammonia was blown over the surface during scoring of the glass with a glass cutter. Stockdale *et al.*[7] pointed out that exposure to water can either decrease or increase the strength of glass, depending on the conditions. The immediate effect of water immersion was a decrease in strength of about 12% for soda-lime, lead, and borosilicate glasses. The magnitude of the effect of continued treatment was found to depend on length of exposure and composition of the glass.

Perhaps more precise measurements were made by Moorthy and Tooley[8] and by Culf.[9] Moorthy and Tooley determined

Table I. Effect of Surrounding Media on Strength or Fracture Energy of Two Glasses

Medium	Change in strength or fracture energy of glass compared with that in water (%)	
	Moorthy and Tooley	Culf
Nitrobenzene	-1 ± 5	
Air	9 ± 6	12–21
Mercury	10 ± 6	12
Acetone	18 ± 4	12
Glycerol	19 ± 5	50
n-Butyl alcohol	22 ± 5	14
Ethyl alcohol	28 ± 7	17
Ammonia (gas)		20
Silicone oil		56
Nitrogen (gas)		62
Carbon dioxide (gas)		64

the change in tensile strength of 10- to 12-mil glass fibers as a function of the surrounding medium. Culf calculated the fracture energy associated with the force necessary to cause a cone crack of a certain size in a given time in plate glass as it was affected by the surrounding medium. Selected results (Table I) show that differences in composition and in testing conditions probably play a great part in the relative position of various media in such a compilation. Moorthy and Tooley suggested that the relatively high dipole moment of nitrobenzene (3.98 × 10⁻¹⁸, and dielectric constant 36), and the strong electron-attracting character of the nitro group, might account for the apparent decrease in strength with this medium which was greater than that for water. Some of the results obtained by Culf, e.g., for ammonia and carbon dioxide, seem to contradict results of some of the previous investigators. Culf suggests that the positive effect of many of these liquids is mainly because of their action to keep moisture away from the fracture.

Comparable literature on ceramic bodies is sparse but, in addition to the early work of Baker and Preston,[3] Pearson[10] showed that the delayed fracture of commercial sintered alumina was influenced by the normal atmosphere. When the alumina was tested in vacuum, the strength at selected times of loading was considerably higher than when it was tested in air. Williams[11] suggested that both delayed fracture (static fatigue) and dynamic fatigue of sintered alumina were functions of atmospheric attack.

Sato[12] stated that the lowering of the breaking strength of solids wetted by liquids could be related to the surface tensions of the solid and the liquid; the higher the surface tension of the liquid, the greater was the decrease of breaking stress. Benedicks[13] thought he demonstrated this principle by tests on steel, glass, and sugar surrounded by various liquids.

[1] L. H. Milligan, "Strength of Glass Containing Cracks," *J. Soc. Glass Technol.*, 13 [52] 351–60T(1929); *Ceram. Abstr.*, 9 [7] 516 (1930).

[2] E. Orowan, "Fatigue of Glass Under Stress," *Nature*, 154 [3906] 341–43 (1944); *Ceram. Abstr.*, 24 [1] 7 (1945).

[3] T. C. Baker and F. W. Preston, "Effect of Water on Strength of Glass," *J. Appl. Phys.*, 17 [3] 179–88 (1946); *Ceram. Abstr.*, 1946, August, p. 137.

[4] N. W. Taylor, "Mechanism of Fracture of Glass and Similar Brittle Solids," *J. Appl. Phys.*, 18 [11] 943–55 (1947); *Ceram. Abstr.*, 1948, August, p. 191g.

[5] C. Gurney and S. Pearson, "Effect of Surrounding Atmosphere on Delayed Fracture of Glass," *Proc. Phys. Soc. (London)*, 62 [356B] 469–76 (1949); *Ceram. Abstr.*, 1949, November, p. 254f.

[6] W. C. Levengood and H. R. Swift, "Lateral Growth of Cutter Marks in Glass," *Glass Ind.*, 30 [6] 317–19, 362 (1949); *Ceram. Abstr.*, 1950, September, p. 178h.

[7] G. F. Stockdale, F. V. Tooley, and C. W. Ying, "Changes in Tensile Strength of Glass Caused by Water Immersion Treatment," *J. Am. Ceram. Soc.*, 34 [4] 116–21 (1951).

[8] V. K. Moorthy and F. V. Tooley, "Effect of Certain Organic Liquids on Strength of Glass," *J. Am. Ceram. Soc.*, 39 [6] 215–17 (1956).

[9] C. J. Culf, "Fracture of Glass Under Various Liquids and Gases," *J. Soc. Glass Technol.*, 41 [199] 157–67T (1957).

[10] S. Pearson, "Delayed Fracture of Sintered Alumina," *Proc. Phys. Soc. (London)*, 69 [444B] 1293–96 (1956); *Ceram. Abstr.*, 1957, July, p. 171d.

[11] L. S. Williams, "Stress Endurance of Sintered Alumina," *Trans. Brit. Ceram. Soc.*, 55 [5] 287–312 (1956); *Ceram. Abstr.*, 1957, January, p. 28d.

[12] M. Sato, "Wetting Effect and Surface Tension of Solids; Formula for Determining Surface Tension of Solids," *Proc. Japan Acad.*, 30, 193–98 (1954).

[13] Carl Benedicks, "Wetting Effect; Liquostriction; Method for Determining Surface Tension of Solids," *Proc. Intern. Symposium on Reactivity of Solids, Gothenburg, 1952*, pp. 477–88 (published 1954).

III. Experimental Materials, Equipment, and Methods

(1) Ceramic Bodies

A typical feldspathic porcelain composition was chosen for this series of tests: clay 50, feldspar 30, and flint 20%.

For one test, a body was prepared in which zircon was substituted for flint. To aid the uniformity and reproducibility of mixtures, all raw materials for these mixtures were stored in drums after first mixing in a Twin-shell Blender. All bodies were fired to cone 10-11 in 12 hours (total time, 24 hours) in an electrically heated laboratory kiln and, after this treatment, were completely vitrified. Measurement of sonic modulus of elasticity after each firing showed values that differed no more than ±1% from the established average value.

(2) Glaze

The glaze used in some of the tests had the following calculated composition:

$$
\begin{array}{ll}
K_2O & 0.10 \\
Na_2O & 0.06 \\
CaO & 0.60 \\
MgO & 0.24
\end{array}
\Bigg\} \quad Al_2O_3 \quad 0.54 \quad\quad SiO_2 \quad 3.81
$$

A single firing to cone 10-11 was made when glazes were used.

(3) Conditions of Testing

The modulus of rupture of test bars 4 in. long and $3/4$ in. in diameter was calculated in the usual manner from the results obtained on breaking the bars in three-point loading. With this relatively low span-to-diameter ratio, marked changes in diameter of the specimens could cause errors in the correlation of results. In each test group the maximum difference from the average diameter was never more than 0.5%. For the approximately 500 bars broken in these series of tests the difference in diameter between the largest and smallest bar was only 4%. A Dillon tester, loading at a reproducible rate of 3340 lb. per minute, was used. Each test group contained between five and ten test bars, and the coefficient of variation of the strength values for any one group was usually 1 to 3%. The liquid coatings were applied by immersion immediately before testing.

IV. Results and Discussion

(1) Effect of Aging

After the initial observation that a paraffin coating increased the modulus of rupture, tests were made on feldspathic porcelain bars that had been exposed to the atmosphere in the laboratory for 5 months or had been placed in a desiccator immediately after firing and kept there for a few days (Table II).

The effect of moisture apparently is most important at the time of mechanical stress because the decrease in strength by water immersion is approximately the same for the bars aged under these different conditions. If the effect were a result of a long-time diffusion process, the results for the bars aged 5 months would be expected to be markedly different. Kerosene was almost as effective as paraffin in increasing the strength.

(2) Effect of Atmospheric Conditions

If water were such an important factor in affecting strength, it would be expected that the amount of moisture in the air at the time of testing would influence the measured strength. At about this time, a silicone-spray (Freon-propelled) coating was found to be effective in sealing the surface so that strengths higher than that in air could be obtained. Over a period of several months, several groups of feldspathic porcelain bars were fired, kept in a desiccator,

Table II. Effect of Aging on Strength of Bars Covered with Selected Coatings

Time lapse after firing	Storage conditions	Coating treatment	Modulus of rupture (lb./sq. in.)	Coefficient of variation of strength (%)	Change in strength (%)
5 months	Air	None	11,000	1.6	Standard
" "	"	Paraffin	12,800	2.7	+16
" "	"	Water	9,800	2.5	−11
2 days	Desiccator	None	11,150	2.2	Standard
" "	"	Kerosene	12,750	4.4	+14
" "	"	Water	10,150	2.9	−9

Table III. Effect of Atmospheric Conditions on Strength of Porcelain in Air and with Silicone and Water Coatings

Relative humidity (%)	Absolute humidity (gm. H₂O/ cu. m.)	Coefficient-of variation of strength (%)			Increase in modulus of rupture over that with water (%)	
		Water	Air	Silicone spray	Air	Silicone spray
54	11.3	1.6	0.8	3.8	9	22
48	7.8	3.7	2.3	1.5	8	18
37	9.0	1.5	2.3	2.8	12	26
35	6.8	2.9	1.8		13	
34	6.2	4.0	3.7	2.2	18	31
17	2.5	4.6	2.1	1.9	15	30

Table IV. Effect of Vacuum, Gases, and Air on Strength of Porcelain

Atmosphere	Coefficient of variation of strength (%)	Increase in modulus of rupture over that in air (%)
Air*	0.8	Standard
Vacuum	2–3	3–10
Nitrogen	4.9	0
Carbon dioxide	2.5	0
Oxygen	3.3	5
Hydrogen	1.6	6

* 37% relative humidity.

and then tested on days when the humidity was within the selected range (Table III).

With the strength of water-coated bars as a base, the strength increased as the bars were tested in air of decreasing moisture content. At the indicated moisture contents, the air could be considered to be comparable to a fluid with less than 0.1 mole % water. According to observations described later in this paper, the measured strength in air (Table III) is more nearly that expected after immersion of the bars in a fluid containing approximately 50 mole % water. There therefore must be a relatively strong adsorption process in which moisture from the air is built up on the porcelain surface. The equilibrium concentration still, however, may be a function of humidity. Results with the silicone coating suggest that, although it may be an effective sealer for preventing an additional moisture supply to reach the stressed flaws, it does not remove the original adsorbed layer. Otherwise, the results with silicone would not be expected to vary with humidity.

Table V.   Effect of Surrounding Media on Strength of Glazed Porcelain

Coating treatment	Modulus of rupture (lb./sq. in.)	Coefficient of variation of strength (%)	Change in strength (%)
None*	15,500	2.7	Standard
Silicone spray	15,400	1.3	−1
Water	15,300	2.1	−1

* Air at 21% relative humidity.

Table VI.   Effect of Moisture on Strength of Zircon Body, Unglazed and Glazed

	Unglazed body		Glazed body		Change in strength (%)	
Coating treatment	Modulus of rupture (lb./sq. in.)	Coefficient of variation of strength (%)	Modulus of rupture (lb./sq. in.)	Coefficient of variation of strength (%)	Unglazed body	Glazed body
None*	12,500	5.3	10,400	1.0	Standard	Standard
Silicone spray	13,500	6.0	12,100	3.3	+8	+16
Water	11,700	2.4	9,400	2.8	−6	−10

* Air at 33% relative humidity.

(3) Effect of Vacuum or Selected Gases

Rubber tubing, ordinarily used for rubber-band stock, enclosed the test bars in this series of experiments. After evacuation (mechanical pump) of a tube containing a test bar, the tube was closed and inserted in the Dillon tester. The bar therefore was protected to some extent from the atmosphere during the test. In other tests, the tube was evacuated and a selected gas was bled into the tube so that the test bar was surrounded by the gas at approximately atmospheric pressure. The gases were dried by standing several minutes in a 1-liter flask filled with activated alumina before the small portion (a few milliliters) was bled into the rubber tube containing the test bar.

The variation in the results for the several tests in vacuum and the results in selected gases (Table IV) are believed to be a function of the amount of adsorbed water removed from the surface of the test bar by evacuation and the dryness of the various gases used. From the results, it might be suggested that nitrogen and carbon dioxide are slightly deleterious, but the experiments are not believed to be controlled sufficiently to make such a conclusion. It is believed, therefore, that water vapor, rather than any other gas contained in air, is the main factor in the reduction of strength in moist air.

(4) Effect of Glaze

The feldspathic porcelain test bars were covered with a glaze, and the strength, as a function of the surrounding medium, was determined (Table V). Because the decrease in strength of unglazed bars after immersion in water is usually 8 to 17%, and the coefficient of variation about 1 to 3%, it is believed that this glaze minimizes, or possibly eliminates, the effect of water. Interpretation of these results indicates that the origin of the fracture is no longer at the surface of the specimen, but is somewhere below the glaze surface. Microscopic observation showed that the fracture origin* was not within the body. Because of prestressing of the surface layers brought about by the use of suitable "compression" glazes, it seems likely that the fracture origin may be near the interface of glaze and body.

Table VII.   Effect of Water and Selected Organic Liquids on Strength of Porcelain

Coating liquid	Dielectric constant	Viscosity (centi-poises)	Surface tension (dynes/ cm.)	Coefficient of variation of strength (%)	Change of strength compared to that in air (%)
None*				1.4	Standard
Water	80	1	73	1.8	−8
Ethyl alcohol	26	1	22	2.4	−4
Methyl alcohol	37	1	22	3.9	−6
Ethylene glycol	41	20	48	0.9	0
Glycerol	47	950	63	1.4	+18
Nitro-benzene	36	2	44	5.8	+13
Forma-mide	110	3	58	2.9	0
Kerosene	2 (?)	1	25	2.8	+14
Hydrazine	53	1	92	2.7	−5

* Air at 54% relative humidity.

The question arose whether a "tension" glaze would also protect the bar from the effect of moisture at the time of breaking. A body in which zircon was substituted for flint was prepared and tested. The same glaze on this zircon body would be likely to cause tension rather than compression effects. Results on both unglazed and glazed test bars are shown (Table VI).

Rather than minimizing the effect of water, the tension glaze seems to magnify this effect. Note that even with the silicone treatment the strength of the glazed bar does not reach that of the unglazed bar broken in air. These results are believed to indicate that a glaze must show compression effects to protect the body against the effect of moisture. In this case, the fracture origin would be moved below the surface.

(5) Effect of Selected Organic Liquids

If the effect of water on strength were a function of the hydroxyl ion, it was thought that organic liquids containing increasing numbers of hydroxyl groups in the molecule might have an increasingly poor effect on strength. Therefore, ethyl and methyl alcohol (one hydroxyl), ethylene glycol (two hydroxyls), and glycerol (three hydroxyls) were tested (Table VII). The only significant effect was that of glycerol, which greatly increased the strength over that obtained in air. The dissociation constant of glycerol and water is practically the same, so the reason for the effect of glycerol is not likely to be ionic. The improvement in strength through the use of glycerol is even greater than that for the silicone spray. Because of the affinity of glycerol for water, it is believed that it may remove a portion of the adsorbed water layer* from the porcelain and thus increase the porcelain strength. The high viscosity of the glycerol coating may prevent rapid diffusion of water from the air to the porcelain surface within the very short time of exposure. As pointed out earlier in this paper, the silicone, which is insoluble in water, apparently does not remove an adsorbed layer of moisture.

---

* The results on glass, described by E. B. Shand, "Experimental Study of Fracture of Glass: II, Experimental Data," *J. Am. Ceram. Soc.*, 37 [12] 559–72 (1954), have been found to be applicable for determining many of the fracture characteristics of porcelain.

Because of the high viscosity of glycerol it might be thought that this property per se would be important for a liquid that influenced the fracture process. Although kerosene and water have approximately the same viscosities, the results (Table VII) show that their effect on strength is markedly different.

Moorthy and Tooley[8] showed that nitrobenzene may reduce the strength of glass, even more than when water was used. This action was said to be a function of its high dipole moment, which is reflected to some extent in its moderately high dielectric constant. Nitrobenzene increased porcelain strength. Formamide, a high-dielectric-constant liquid with a dipole moment of 3.0×10^{-18}, also increased porcelain strength.

Sato[12] and Benedicks[13] suggested that the surface tension of the liquid was an important property in determining its effect on strength of a solid. Use of a low-surface-tension liquid coating should give a high measured strength of the solid. Observation of results (Table VII) shows that a surface tension lower than that of water does not guarantee a higher strength. Hydrazine, because of its relatively high surface tension, would be expected to produce a strength lower than when water was used. The results show, however, that the opposite was obtained.

(6) Effect of Mixtures and Aqueous Solutions

As a glycerol coating was found to increase porcelain strength, and a water coating decreased strength, a series of mixtures of these two liquids was prepared for testing. The decrease in strength (Table VIII) as water was added to glycerol was shown to be essentially proportional to the mole % of water present. The viscosity of the mixtures dropped rapidly in a nonlinear fashion when water was first added to glycerol. Again, viscosity was found not to be a critical factor in differentiating liquids with respect to their effect on the strength of unglazed porcelain bars.

In an attempt to determine whether molecular water, rather than hydrogen or hydroxyl ions, is the main factor in decreasing the strength of porcelain, test bars were immersed in concentrated solutions of either HCl or NaOH just before breaking (Table IX).

The concentration of hydrogen ions in the 0.1 N NaOH is only 10^{-13}, and it is considerably less for 5 N NaOH. Of course, the concentration of hydroxyl ions is quite high. With either NaOH solution, the mechanical strength of the test bars was approximately the same as that when water was used. With the HCl solutions the hydrogen ion concentration is quite high and the hydroxyl ion concentration is low. With the 1 N HCl solution the mechanical strength was no better than that with water. With the 12 N HCl, the mechanical strength was higher than that with water. Only 82 mole % water is present in this 12 N HCl solution. From the previous relation established for glycerol-water mixtures, it was shown that a 5% increase in strength should be obtained when the mole % of water decreases from 100 to 82. For this test with 12 N HCl, a gain in strength of 5% was observed.

These results again show that water decreases the strength of unglazed porcelain and that water molecules, rather than the constituent ions, are the effective agents.

Table VIII.   Effect of Glycerol-Water Mixtures on Strength of Porcelain

Composition of coating mixture (mole %)		Modulus of rupture (lb./sq. in.)	Coefficient of variation of strength (%)
Glycerol	Water		
100	0	13,100	1.4
82	18	12,700	0.8
69	31	12,600	1.8
20	80	10,900	2.1
0	100	10,600	2.3

Table IX.   Effect of Ionic Aqueous Solutions on Strength of Porcelain

Coating treatment		Modulus of rupture (lb./sq. in.)	Coefficient of variation of strength (%)	Increase in strength (%)
Media	Mole % water			
Water	100	10,800	2.4	Standard
0.1 N NaOH	99	10,700	2.9	0
5 N NaOH	91	10,900	2.6	0
1 N HCl	91	10,800	4.5	0
12 N HCl	82	11,400	2.3	5

V. Summary and Conclusions

(1) The strength of unglazed porcelain test bars was found to decrease as the amount of moisture in the air at the time of breaking increased. This was true, even though an adsorbed layer of moisture was probably already present.

(2) No inherent physical property of the liquids in which the test bars were immersed could be correlated with their effect on modulus of rupture. Although surface tension of the surrounding medium has been suggested as a criteria of its effect on strength, this concept was shown to be invalid.

(3) Only the amount of water (mole %) present in the coating liquids was found to be significant in lowering the strength of the ceramic test pieces. Marked differences in ionic strength of hydrogen and hydroxyl ions in selected liquids were found to have little effect.

(4) A great part of the strength of a ceramic body brought about by the use of a so-called compression glaze may be due simply to the fact that the glaze keeps moisture away from the highly stressed area where the fracture begins and propagates.

Phase Equilibria in the System CaO–Iron Oxide in Air and at 1 Atm. O₂ Pressure

by BERT PHILLIPS and ARNULF MUAN

College of Mineral Industries, The Pennsylvania State University, University Park, Pennsylvania

Phase equilibrium data, obtained by the quenching technique, are presented for mixtures in the iron oxide-rich part of the system CaO–iron oxide in air and at 1 atm. O₂ pressure. Present data are combined with data available in the literature to construct phase diagrams comprising the region from liquidus temperatures to temperatures slightly below the solidus.

I. Introduction

THE steel industry consumes enormous tonnages of oxide raw materials. Combinations of oxides giving rise to low-melting mixtures are used for slags and as additives in sintering processes, whereas combinations giving rise to high-melting mixtures are used for refractories. For an understanding of steelmaking processes, reactions among these phases at elevated temperatures and the influence of atmospheric conditions on these reactions are important considerations.

Phase equilibrium data are very useful for predicting and describing such reactions. For a number of years the American Iron and Steel Institute has sponsored a research project entitled "Phase Equilibrium Studies of Steel Plant Refractories Systems" in the College of Mineral Industries. In this program of research, phase equilibria in binary, ternary, and quaternary combinations among the common oxides are studied systematically.[1] One part of this research program is an investigation of the system CaO–FeO–Fe₂O₃–SiO₂.

Working out a quaternary system is a prodigious job that must be approached in steps, proceeding from the simpler to the more complicated parts of the system. The first step in the present investigation is a study of parts of the system CaO–FeO–Fe₂O₃ in order to check and fill in gaps in previous literature reports. This system is an example of a case where changes in oxidation state are involved, and hence the atmospheric conditions must be controlled carefully. Methods for studying and describing such systems have been discussed in several recent publications from this laboratory.[2] In the present study of the system CaO–FeO–Fe₂O₃ the writers have chosen to determine the equilibria at two levels of constant O₂ pressure, namely 0.21 atm. (air) and 1 atm. Under these conditions, mixtures at liquidus temperatures have compositions that are located along the two corresponding O₂ liquidus isobaric curves through the ternary* system CaO–FeO–Fe₂O₃. The Fe₂O₃/FeO ratio at liquidus temperatures must be determined by chemical analysis. Phase equilibria for mixtures represented by points along these O₂ isobaric curves can be illustrated by projections of these compositions into a chosen join, and the resulting diagrams have the *appearance* of binary systems.

II. Previous Work

A large number of investigations of the system CaO–iron oxide have been reported in the literature. The phase relations most commonly accepted for the system in air are shown in Fig. 1. This diagram, which is reproduced in a recent compilation of phase diagrams,[3] is based on the original data of Sosman and Merwin.[4] There are, however, many data reported in the literature that are in conflict with certain features of this diagram. These data suggest revisions of the diagram with respect to the melting relations of the 2CaO·Fe₂O₃[5] phase and also indicate the probable existence of a phase of composition CaO·2Fe₂O₃. The existence of the latter phase in particular has been the subject of many controversies. Tavasci[6] twenty years ago presented evidence for the existence of this phase, but his observation has been questioned by later investigators. As recently as 1953 Malquori and Cirilli[7] claimed that CaO·Fe₂O₃ rather than CaO·2Fe₂O₃ is stable in equilibrium with Fe₂O₃ (hematite).

[1] E. F. Osborn, "Phase Equilibrium Studies of Steel Plant Refractories Systems"; pp. 145–77 of "Regional Technical Meetings," New York, 1954, American Iron and Steel Institute.
[2] (a) Arnulf Muan, "Phase Equilibria in the System FeO–Fe₂O₃–SiO₂," J. Metals, 7, September 1955; Trans. Am. Inst. Mining Met. Engrs., 203, 965–76 (1955).
(b) Arnulf Muan and E. F. Osborn, "Phase Equilibria at Liquidus Temperatures in the System MgO–FeO–Fe₂O₃–SiO₂," J. Am. Ceram. Soc., 39 [4] 121–40 (1956).
(c) Arnulf Muan and C. L. Gee, "Phase Equilibrium Studies in the System Iron Oxide–Al₂O₃ in Air and at 1 Atm. O₂ Pressure," ibid., 39 [6] 207–14 (1956).
(d) Arnulf Muan, "Phase Equilibria at Liquidus Temperatures in the System Iron Oxide–Al₂O₃–SiO₂ in Air Atmosphere," ibid., 40 [4] 121–33 (1957).
(e) Arnulf Muan, "Phase Equilibrium Relationships at Liquidus Temperatures in the System FeO–Fe₂O₃–Al₂O₃–SiO₂," ibid., 40 [12] 420–31 (1957).
(f) Arnulf Muan, "Phase Equilibria at High Temperatures in Iron Silicate Systems," Am. Ceram. Soc. Bull., 37 [2] 81–84 (1958).
(g) Arnulf Muan, "Phase Equilibria at High Temperatures in Oxide Systems Involving Changes in Oxidation States," Am. J. Sci., 256 [3] 171–207 (1958).

[3] E. M. Levin, H. F. McMurdie, and F. P. Hall, Phase Diagrams for Ceramists, Fig. 46. The American Ceramic Society, Inc., Columbus, Ohio, 1956. 286 pp.
[4] R. B. Sosman and H. E. Merwin, "Preliminary Report on the System Lime:Ferric Oxide," J. Wash. Acad. Sci., 6, 532–67 (1916).
[5] M. A. Swayze, "A Report on Studies of (1) The Ternary System CaO–C₅A₃–C₂F, (2) The Quaternary System CaO–C₅A₃–C₂F–C₂S, (3) The Quaternary System as Modified by 5% Magnesia," Am. J. Sci., 244 [1] 1–30, 65–94 (1946); Ceram. Abstr., 1946, June, p. 116.
[6] Bonaventura Tavasci, "Ricerche sul Sistema CaO–Fe₂O₃" (Research on the System CaO–Fe₂O₃), Ann. chimi. appl., 26, 291–300 (1936).
[7] G. Malquori and V. Cirilli, "The Ferrite Phase," Proc. Intern. Symposium Chemistry of Cement, 3rd Symposium, London, 1952, pp. 120–50 (1954); Ceram. Abstr., 1956, September, p. 183d.
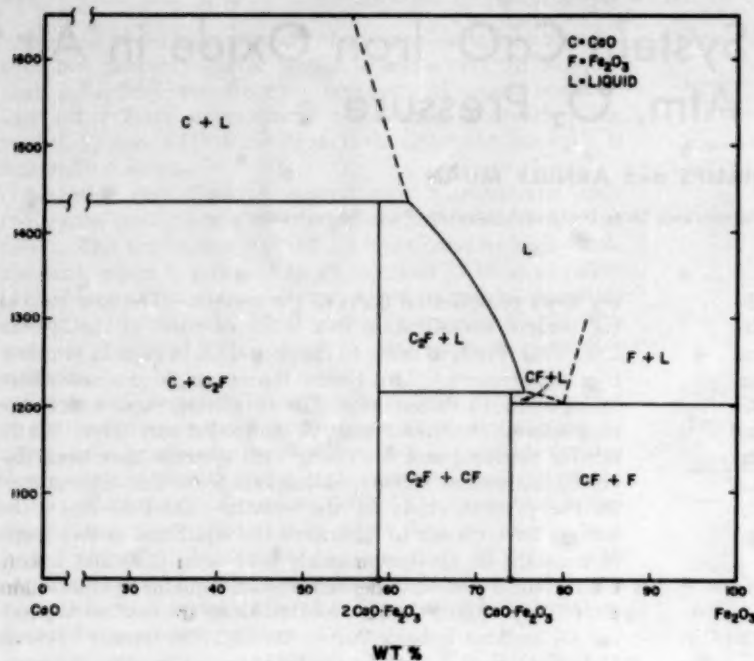
Fig. 1. Diagram illustrating phase equilibria in the system CaO–iron oxide in air, after Sosman and Merwin (footnotes 3 and 4).

Most of these controversies seem to have been resolved by the excellent work in 1956 by Edström[3] as well as by Batti.[9] Edström studied the system CaO–iron oxide at 1 atm. O_2 pressure and presented evidence for the stable existence of $CaO \cdot 2Fe_2O_3$ in the temperature interval 1120° to 1228°C., as compared with the interval 1130° to 1230°C. found by Batti. On the basis of his new data Edström constructed a revised phase diagram for the iron oxide-rich part of the system CaO–iron oxide at 1 atm. O_2. This diagram is shown in Fig. 2. Incorporated in this diagram is the change in the melting relations of $2CaO \cdot Fe_2O_3$ as suggested by Swayze.[5] Edström did not, however, determine phase equilibria at liquidus temperatures for mixtures extending in composition all the way over to the iron oxide end member, and he did not determine the effect of CaO on the temperature of decomposition of Fe_2O_3 (hematite) to Fe_3O_4 (magnetite). In the present investigation the system has been restudied in air and at 1 atm. O_2 pressure, with particular attention being paid to the stability relations of $CaO \cdot 2Fe_2O_3$, the decomposition temperature of hematite to magnetite, and the melting relations of $2CaO \cdot Fe_2O_3$.

III. Experimental Method

(1) General Procedure

Phase equilibria were determined by the quenching method. Premelted mixtures of CaO and iron oxides were held in platinum containers at constant temperature in the appropriate atmosphere until equilibrium was reached among crystalline, liquid, and gas phases. The sample was then quenched rapidly to room temperature and the phases present were determined by microscopic and X-ray examinations.

Compositions of melts at liquidus temperatures were determined by chemical analysis.

(2) Materials and Apparatus

Chemicals of highest commercial purity served as starting materials. The Fe_2O_3 was dried at 400°C. for 24 hours, and $CaCO_3$ was dried at 380°C. for 16 hours. Samples weighing 10 gm. were made up by mixing these materials in required proportions and homogenizing by mixing under alcohol for 30 minutes. Each mixture was fired in a Globar furnace at approximately 1350°C. for 16 hours. These mixtures after grinding to minus 100 mesh served as starting materials for most of the equilibration runs in the quenching furnace. To check that the equilibrium Fe_2O_3/FeO ratio of the samples was reached, a few duplicate runs for determination of liquidus temperatures were carried out, using starting materials obtained by prefiring the oxide mixture under more reducing conditions in a gas-air furnace. The results were found to be the same as for mixtures preheated in air in the Globar furnace. Each sample for determination of liquidus temperatures was held in the quenching furnace for a minimum of 12 hours and often as long as 24 hours to make sure that the equilibrium Fe_2O_3/FeO ratio, corresponding to the particular atmosphere, was reached.

Vertical-tube quenching furnaces of standard design were used. The windings consisted of platinum or a 80% platinum-20% rhodium alloy.

Temperatures were measured before and after each run with a platinum–platinum-10% rhodium thermocouple. The thermocouple was frequently calibrated at melting points defined as follows: Au, 1063°C.; $CaMgSi_2O_6$, 1391.5°C.; $CaSiO_3$, 1544°C. Temperatures in the furnaces were controlled by a second thermocouple inserted close to the heating element and connected to commercial electronic temperature-control instruments.

(3) Examination of Quenched Samples

Microscopic and X-ray methods were used to identify crystalline phases in the quenched samples. Because the samples were usually opaque, reflected-light techniques were

---

[3] J. O. Edström, "The Phase $CaO \cdot 2Fe_2O_3$ in the System CaO–Fe_2O_3 and Its Importance as Binder in Ore Pellets," *Jernkontorets Ann.*, 140 [2] 101–15 (1956) (in English); *Ceram. Abstr.*, 1956, August, p. 177c.

[9] Pietro Batti, "Stability of the Compound $CaO \cdot 2Fe_2O_3$," *Chim. e ind.* (*Milan*), 38 [10] 864–66 (1956); *Ceram. Abstr.*, 1957, February p. 48f.
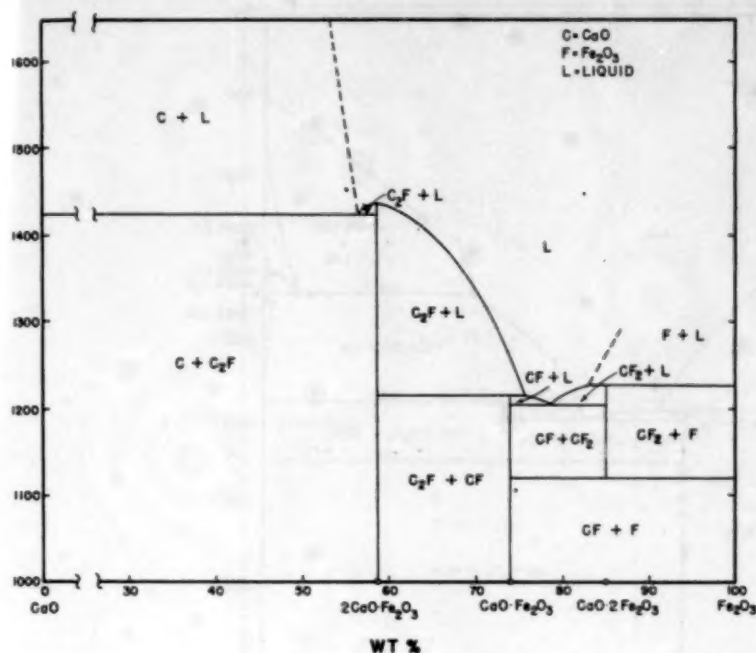
Fig. 2. Diagram showing phase equilibrium relations in the system CaO–iron oxide at 1 atm. O_2 pressure, mainly after Edström (footnote 8). Melting relations of $2CaO \cdot Fe_2O_3$ have been drawn in accordance with the data of Swayze (footnote 5).

found to be much more useful than transmitted-light examination. The melts were exceedingly fluid and gave rise to dendritic "quench crystals" even with the fastest quenching of small samples in mercury. There was usually no difficulty in distinguishing primary crystals grown in equilibrium with melts from the corresponding crystals formed during quenching. In a few cases quench crystals of $CaO \cdot Fe_2O_3$ and $CaO \cdot 2Fe_2O_3$ were difficult to distinguish from primary crystals. For further confirmation of the phase identification, high-temperature X-ray methods were used to identify the phase $CaO \cdot 2Fe_2O_3$ in the temperature interval of its stable existence. White's test[10] was used to detect trace amounts of the phase CaO.

Before analysis, the samples were crushed in a Plattner mortar to pass a 100-mesh screen. For the determination of divalent iron, approximately 0.2-gm. samples were heated to boiling in 20 ml. 1:3 H_2SO_4 in a covered platinum crucible. When steam evolved, 5 ml. HF was added and the solution was allowed to boil slowly for 5 to 10 minutes. The crucible was then plunged into a 600-ml. beaker containing 5% H_2SO_4 saturated with boric acid, and the solution was titrated with 0.05 N $KMnO_4$. For the determination of total iron, approximately 0.2-gm. samples were dissolved in 20 ml. 1:3 H_2SO_4 and 5 ml. HF in a large platinum dish by heating on a hot plate until all HF was driven off. Upon cooling of the dish the contents were diluted and reduced by running it through a Jones reductor, followed by titration with 0.05 N $KMnO_4$. Total iron was found to be, within the limits of experimental error, equal to the amount of Fe_2O_3 weighed up in the starting mixture. For this reason, analysis for total iron was abandoned, and the values for total iron given in the tables are those originally weighed up from the starting materials. Pos-

sible changes in oxidation state during quenching and the presence of mechanically intermixed platinum from the container interfere with the accuracy of analytical results.

IV. Results

The results of the quenching experiments are given in Tables I and II, for runs in air and at 1 atm. O_2, respectively. Phase equilibrium diagrams constructed from data contained in these tables as well as from literature data are shown in Figs. 3 and 4, for air and 1 atm. O_2, respectively. Each of these figures consists of two parts. The upper parts of the figures show phases present as a function of temperature. These parts of the diagrams have the *appearance* of binary systems, with CaO and Fe_2O_3 chosen as components. Because the system is not truly binary, however, the compositions of all phases cannot be read from these diagrams. In the lower parts of the figures supplementary diagrams are presented to show compositions of the liquids at liquidus temperatures (curves *A–A'* and *B–B'*). To represent phase equilibria in the upper part of the diagrams in terms of the chosen components CaO and Fe_2O_3, a method must be selected for projecting the true compositions in the ternary system CaO–FeO–Fe_2O_3 upon the join CaO-Fe_2O_3. The writers have chosen to project these compositions along straight lines pointing toward the O corner of the triangle representing the system Ca–Fe–O, of which CaO–FeO–Fe_2O_3 is a part. These reaction lines*

---

[10] Herbert Insley and V. D. Fréchette, Microscopy of Ceramics and Cements Including Glasses, Slags, and Foundry Sands. Academic Press, Inc., New York, 1955. 286 pp.; *Ceram. Abstr.*, 1956, May, p. 108c.

---

* The straight lines describing these composition changes have been referred to as iso-silica lines and iso-silica-magnesia lines, respectively, in two previous papers from this laboratory (see footnotes 2(*a*) and 2(*b*)). These lines have the same meaning as the curves referred to as dissociation paths by White and coworkers (see below). Because O_2 can either be added to or subtracted from the condensed phases, the term "reaction lines" will be used as a general term to describe these lines in this and in future papers from this laboratory.

R. G. Richards and J. White, "Phase Relationships of Iron Oxide-Containing Spinels: Part I, Relations in the System Fe–Al–O," *Trans. Brit. Ceram. Soc.*, **53** [4] 233–70 (1954).

Fig. 3. Diagram illustrating phase equilibria in the system CaO—iron oxide in air. The upper half of the figure has the appearance of a binary system, showing phases present as a function of temperature in °C. Solid dots represent temperatures along boundary curves for mixtures studied in the present investigation. ss = solid solution. The lower triangular diagram shows compositions of liquids at liquidus temperatures (heavy curve A–A'). Light straight lines are projection lines as explained in the text.

have a physical meaning. By reaction with the atmosphere during equilibration, O_2 is added to or subtracted from the condensed phases concomitant to a proportional change in the Fe_2O_3/FeO ratio of the mixture. These changes are described by the reaction lines.

The compositions of all crystalline phases except magnetite
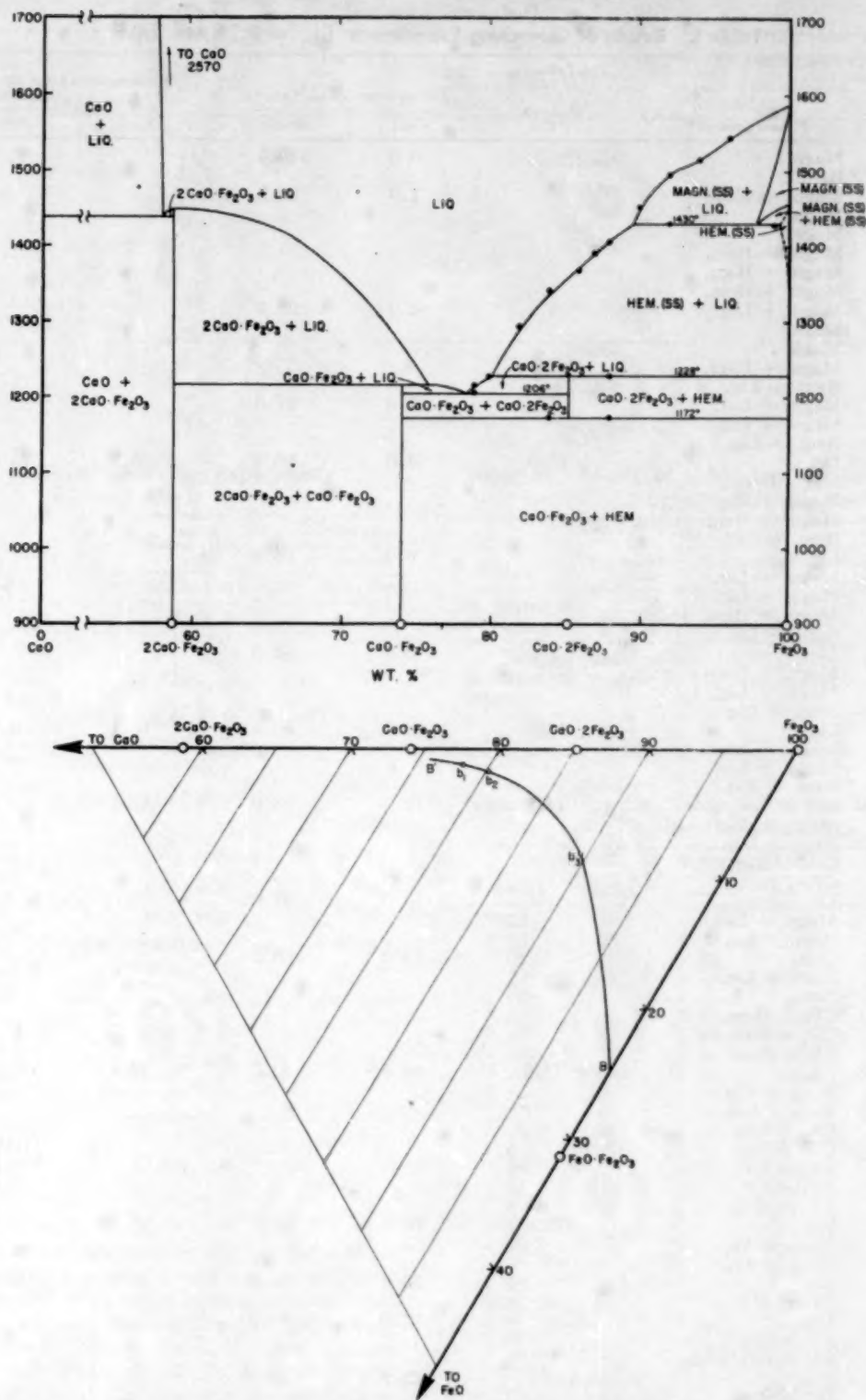
Fig. 4. Diagram showing phase equilibria in the system CaO–iron oxide at 1 atm. O₂ pressure. Line symbols have the same meanings as in Fig. 3.

are represented by points falling close to the join CaO-Fe₂O₃.* Magnetite compositions are represented by points close to the join FeO-Fe₂O₃ and slightly on the Fe₂O₃ side of the FeO·Fe₂O₃ composition. These compositions correspond to some excess

* A very small amount of Fe²⁺ can substitute for Ca²⁺ in the CaO·2Fe₂O₃, CaO·Fe₂O₃, and 2CaO·Fe₂O₃ lattices. Hence the compositions of these phases are represented by points adjacent to the join CaO-Fe₂O₃ rather than exactly along this join.

Table I. Results of Quenching Experiments ($p_0 = 0.21$ Atm. (Air))

Temp. of quenching run (°C.)	Phases present*	Temp. of run for analysis (°C.)	Initial composition (wt. %)		Composition after equilibration (wt. %) (by analysis)		
			CaO	Fe_2O_3	CaO	FeO	Fe_2O_3
1395	Magn.		0.0	100.0			
1376	Hem.						
1447	Magn. + Liq.		1.0	99.0			
1437	Magn.						
1388	Magn.						
1377	Magn. + Hem.						
1361	Magn. + Hem.						
1357	Magn. + Hem.						
1385	Magn. + Liq.		2.0	98.0			
1368	Magn.						
1362	Magn.						
1361	Magn. + Hem.						
1354	Hem. + Liq.						
1427	Magn. + Liq.		3.0	97.0			
1361	Magn. + Liq.						
1343	Hem. + Liq.						
1550	Liq.	1550	4.0	96.0	4.1	19.6	76.3
1542	Magn. + Liq.						
1366	Magn. + Liq.						
1358	Magn. + Hem. + Liq.						
1348	Hem. + Liq.						
1521	Liq.		6.0	94.0			
1503	Magn. + Liq.						
1361	Magn. + Liq.						
1358	Magn. + Hem. + Liq.						
1354	Hem. + Liq.						
1488	Liq.		8.0	92.0			
1478	Magn. + Liq.						
1417	Magn. + Liq.						
1230	Hem. + Liq.						
1449	Liq.	1452	10.0	90.0	10.1	9.9	80.0
1443	Magn. + Liq.						
1365	Magn. + Liq.						
1330	Hem. + Liq.						
1424	Liq.	1433	12.0	88.0	12.1	7.8	80.1
1419	Magn. + Liq.						
1326	Hem. + Liq.						
1155	CF_2 + Hem.						
1151	CF + Hem.						
1369	Liq.		13.0	87.0			
1360	Magn. + Liq.						
1347	Hem. + Liq.						
1342	Liq.		14.0	86.0			
1338	Hem. + Liq.						
1228	Hem. + Liq.						
1222	CF_2 + Hem.						
1191	CF_2 + Hem.						
1096	CF + Hem.						
1312	Liq.	1312	16.0	84.0	16.1	4.2	79.7
1306	Hem. + Liq.						
1230	Hem. + Liq.						
1225	CF_2 + Liq.						
1206	CF_2 + Liq.						
1202	CF_2 + CF						
1155	CF_2 + CF						
1154	CF + Hem.						
1280	Liq.	1286	18.0	82.0	18.1	2.9	79.0
1271	Hem. + Liq.						
1247	Hem. + Liq.						
1210	Liq.		20.0	80.0	20.0	1.7	78.3
1203	CF_2 + CF						
1212	Liq.		21.0	79.0			
1210	CF + Liq.						
1205	CF + CF_2 + Liq.						
1244	Liq.		25.0	75.0			
1235	C_2F + Liq.						
1222	C_2F + Liq.						
1175	CF_2 + CF						
1109	CF + Hem.						
1218	C_2F + Liq.		26.0	74.0			
1212	CF						
1298	Liq.		27.0	73.0			
1292	C_2F + Liq.						
1223	C_2F + Liq.						
1212	C_2F + CF						
1431	Liq.		35.0	65.0			
1423	C_2F + Liq.						
1448	Liq.		39.0	61.0			
1443	C_2F + Liq.						
1450	Liq.		40.0	60.0			

* Abbreviations used in this and in succeeding tables and in figures have the following meanings: Magn. = crystals of magnetite, Hem. = crystals of hematite, CF_2 = crystals of $CaO \cdot 2Fe_2O_3$, CF = crystals of $CaO \cdot Fe_2O_3$, C_2F = crystals of $2CaO \cdot Fe_2O_3$, Liq. = liquid.

Table I (Concluded)

Temp. of quenching run (°C.)	Phases present*	Temp. of run for analysis (°C.)	Initial composition (wt. %)		Composition after equilibration (wt. %) (by analysis)		
			CaO	Fe₂O₃	CaO	FeO	Fe₂O₃
1442	C₂F + Liq.						
1230	C₂F + Liq.						
1208	C₂F + CF						
1450	Liq.		41.3	58.7			
1448	C₂F						
1440	Liq.		42.0	58.0			
1436	C₂F + CaO						
1670	CaO + Liq.		43.0	57.0			
1443	CaO + Liq.						
1444	CaO + Liq.		45.0	55.0			
1437	C₂F + CaO						

Table II. Results of Quenching Experiments ($p_{O_2} = 1$ Atm.)

Temp. of quenching run (°C.)	Phases present	Temp. of run for analysis (°C.)	Initial composition (wt. %)		Composition after equilibration (wt. %) (by analysis)		
			CaO	Fe₂O₃	CaO	FeO	Fe₂O₃
1505	Magn. + Liq.		1.0	99.0			
1432	Magn. + Hem.						
1424	Hem. + Liq.						
1550	Liq.		4.0	96.0			
1542	Magn. + Liq.						
1518	Liq.		6.0	94.0			
1514	Magn. + Liq.						
1500	Liq.	1510	8.0	92.0	8.1	11.6	80.3
1494	Magn. + Liq.						
1434	Magn. + Liq.						
1427	Hem. + Liq.						
1453	Liq.		10.0	90.0			
1450	Magn. + Liq.						
1411	Liq.		12.0	88.0			
1399	Hem. + Liq.						
1230	Hem. + Liq.						
1225	CF₂ + Hem.						
1175	CF₂ + Hem.						
1170	CF + Hem.						
1394	Liq.		13.0	87.0			
1387	Hem. + Liq.						
1370	Liq.		14.0	86.0			
1365	Hem. + Liq.						
1345	Liq.	1348	16.0	84.0	16.1	3.2	80.7
1335	Hem. + Liq.						
1174	CF₂ + CF						
1170	CF + Hem.						
1297	Liq.	1313	18.0	82.0	18.0	2.3	79.7
1290	Hem. + Liq.						
1230	Liq.		20.0	80.0			
1225	CF₂ + Liq.						
1221	Liq.	1223	21.0	79.0	21.0	1.4	77.5
1212	CF₂ + Liq.						
1209	CF₂ + Liq.						
1203	CF₂ + CF						

Table III. Results of d-Spacing Measurements on CaO-Magnetite Solid Solution*

	(440) Plane		(311) Plane	
	Sample A	Sample B	Sample A	Sample B
Measured 2θ	41.39	41.32	74.15	74.06
d-Spacing	2.5310	2.5351	1.4833	1.4852

* Samples quenched from 1395°C. in air. Sample A, 0% CaO in magnetite; sample B, 1% CaO in magnetite. CoKα₁ radiation.

Table IV. Powder X-Ray Diffraction Data for Calcium Ferrites (FeKα Radiation)

2CaO·Fe₂O₃		CaO·Fe₂O₃		CaO·2Fe₂O₃	
d-Spacing	I/I_0(%)	d-Spacing	I/I_0(%)	d-Spacing	I/I_0(%)
7.22	10	4.54	10	5.26	15
3.65	25	2.60	100	5.03	15
3.03	10	2.52	55	3.00	35
2.78	30	2.24	20	2.89	25
2.68	45	2.23	25	2.76	35
2.65	100	2.11	25	2.62	50
2.61	20	1.96	15	2.60	100
2.59	15	1.83	50	2.57	25
2.35	5	1.80	15	2.55	25
2.18	10	1.74	10	2.14	15
2.07	20	1.66	15	1.98	20
1.94	30	1.54	20	1.73	20
1.90	5	1.51	45	1.72	20
1.88	15	1.46	10	1.68	15
1.84	30			1.65	20
1.74	10			1.51	15
1.66	5			1.50	15
1.62	5				
1.59	30				
1.58	5				
1.56	20				
1.54	5				
1.53	10				
1.47	5				

oxygen over the stoichoimetric ratio in Fe_3O_4,[11] and a maximum of approximately 2.5 weight % solid solution of CaO in magnetite. The results of X-ray d-spacing measurements given in Table III confirm the phase evidence for the presence of Ca^{2+} in the magnetite lattice. Table IV contains X-ray data for the phases $CaO \cdot 2Fe_2O_3$, $CaO \cdot Fe_2O_3$, and $2CaO \cdot Fe_2O_3$.

The essential features of the diagrams are as follows: Liquidus temperatures decrease sharply as CaO is added to iron oxide, from 1594° and 1583°C.[11] to a minimum of 1205° and 1206°C. in air and at 1 atm. O₂, respectively. Magnetite is the primary crystalline phase in mixtures high in iron oxide. As more CaO is added at constant O₂ pressure, with liquidus temperatures decreasing, hematite becomes the stable phase in equilibrium with liquid. The decomposition temperature of

hematite to magnetite decreases slightly as CaO is added, from 1390°²⁽ᵃ⁾ to a minimum of 1358°C. in air and from 1455°²⁽ᵃ⁾ to 1430°C. at 1 atm. O₂. A maximum amount of approximately 2.5 weight % CaO can enter into solid solution in the magnetite phase at the O₂ pressures used in this investigation. When the CaO content of the mixtures reaches 19 and 20 weight %, liquidus temperatures have decreased to 1226° and 1228°C., in air and at 1 atm. O₂, respectively, and $CaO \cdot 2Fe_2O_3$ is the primary crystalline phase. The two temperatures above are the incongruent melting temperatures of the

¹¹ L. S. Darken and R. W. Gurry, "The System Iron–Oxygen: II, Equilibrium and Thermodynamics of Liquid Oxide and Other Phases," *J. Am. Chem. Soc.*, **68** [5] 798–816 (1946); *Ceram. Abstr.*, **1947**, February, p. 50g.

Table V.   Summary of "Invariant"* Situations in the System CaO–Iron Oxide in Air and at 1 Atm. O₂ Pressure

Phases present	Composition of liquid (wt. %)			Temp. (°C.)	
	CaO	FeO	Fe₂O₃	p_{O_2} = 0.21 atm.	p_{O_2} = 1 atm.
Magn. + Liq.		27.0	73.0	1594	
" "		24.0	76.0		1583
Magn. + Hem.				1390	1455
Magn. + Hem. + Liq.	13.0	7.0	80.0	1358	
" " "	10.5	8.0	81.5		1430
Hem. + CF₂ + Liq.	19.0	2.5	78.5	1226	
" " "	20.0	2.0	78.0		1228
Hem. + CF₂ + CF				1155	1172
CF₂ + CF + Liq.	20.0	2.0	78.0	1205	
" " "	21.5	1.5	77.0		1206
CF + C₂F + Liq.	24.0	1.0	75.0	1216	
C₂F + Liq.	41.5		58.5	1449	
C₂F + CaO + Liq.	42.0		58.0	1438	

* The phase assemblages listed in reality represent univariant situations in the ternary system Ca–Fe–O. However, the existing degree of freedom has been "used up" in choosing the O₂ partial pressure of the gas phase, and hence the situations may be considered to be "invariant."

CaO·2Fe₂O₃ phase in air and at 1 atm. O₂, respectively. As more CaO is added, a "eutectic"* appears at approximately 20 and 21.5 weight % CaO and temperatures of 1205° and 1206° in air and at 1 atm. O₂, respectively, CaO·2Fe₂O₃ and CaO·Fe₂O₃ being the crystalline phases in equilibrium with the liquid. As the CaO content of the mixtures is increased still farther, liquidus temperatures start rising, with CaO·Fe₂O₃ melting incongruently to 2CaO·Fe₂O₃ and liquid at approximately 1216°C. in air.† With increasing CaO content and increasing liquidus temperatures, 2CaO·Fe₂O₃ is the primary crystalline phase. The liquidus temperature reaches a maximum of 1449°C. (in air)† at the 2CaO·Fe₂O₃ composition, and decreases to 1438°C. for a liquid which is also in equilibrium with CaO.

A notable feature of the subsolidus relations is the decomposition of the CaO·2Fe₂O₃ phase to CaO·Fe₂O₃ and Fe₂O₃ (hematite) below 1155° and 1172°C. in air and at 1 atm. O₂ pressure, respectively.

Equilibrium relations are summarized in Table V, showing temperatures at which three condensed phases (either two crystalline and one liquid phase or three crystalline phases) coexist in equilibrium with a gas. The composition of the liquid is given in cases where this is one of the phases present at equilibrium.

V.   Discussion

Phase equilibria in the system CaO–iron oxide in air (p_{O_2} = 0.21 atm.) and at 1 atm. O₂ pressure can be represented very satisfactorily in "binary-type" diagrams, as long as the mixtures are fairly high in CaO. As the iron oxide end of the system is approached, however, the deviation from binary relations becomes appreciable. To describe adequately phase equilibria in this part of the system it is necessary to consider the 0.21 and 1 atm. O₂ isobaric sections in their relation to the ternary system CaO–FeO–Fe₂O₃. A part of the latter system is represented by the triangle 2CaO·Fe₂O₃-FeO·Fe₂O₃-Fe₂O₃

in the lower halves of Figs. 3 and 4. Compositions of liquids at liquidus temperatures are represented by curves *A–A'* and *B–B'*, in air and at 1 atm. O₂, respectively. The projection of the liquidus curves into the join CaO–Fe₂O₃, plotted in the upper halves of the same figures, shows the rate of decrease in temperature along the paths *A–A'* and *B–B'* on the liquidus surface. The slope of the tangent to these curves changes continuously except at points where a boundary curve is crossed. Such points, marked a_1, a_2, a_3 in the lower half of Fig. 3 and b_1, b_2, b_3 in the lower half of Fig. 4, correspond to 'apparent invariant points in the upper "binary" projections of the same figures. On the basis of this information, phase relations in the system 2CaO·Fe₂O₃–FeO·Fe₂O₃–Fe₂O₃ may be inferred qualitatively. The probable relations are indicated by dashed lines in Fig. 5. It is emphasized that the locations of the boundary curves have not been determined, and the sketch is only intended to show the probable primary-phase areas present in the system. This diagram is at variance with the diagram of Burdese and Brisi[12] published several years ago. Their diagram lacks a primary-phase area of CaO·2Fe₂O₃ and also shows a location of the boundary curve between hematite and magnetite that is in disagreement with data for the system Fe–O by Darken and Gurry.[11]

The sharp bend of the O₂ isobaric curves at liquidus temperatures toward the CaO·Fe₂O₃ join as CaO is added to iron oxide is a noticeable feature of the lower diagrams in Figs. 3 and 4 and the sketch in Fig. 5. Two factors are responsible for this increase in the Fe₂O₃/FeO ratio of the liquids as the CaO content increases. First, as was shown by Gurry and Darken,[13] the Fe₂O₃/FeO ratio in an iron oxide liquid increases rapidly as CaO is added at constant O₂ pressure and constant temperature. This observation may be explained in different words according to the different schools of thought on liquid structure. According to one school of thought,[14] the locations of the curves reflect a strong tendency toward the formation of compounds, such as for instance CaO·2Fe₂O₃ and CaO·Fe₂O₃, in the liquid. This interpretation should not be taken to mean that the foregoing molecules exist as such in the liquid but rather that local arrangements of the ions in the melts approaching these gross compositions are energetically favored in preference to a completely statistical distribution of the ions. In the language of a different school of thought, mainly advocated by Weyl,[15] these relations would be explained in terms of the screening concept. According to this concept the important factors to consider are the relative screening demands of the two ions Fe³⁺ and Fe²⁺. The trivalent ion (Fe³⁺) has the stronger force field and hence a higher demand for screening. As the CaO content increases, the "screening power" of the liquid increases and hence Fe³⁺ becomes stabilized relative to Fe²⁺. The other factor responsible for the sharp bend of the isobaric curves toward the CaO–Fe₂O₃ join upon the addition of CaO to iron oxide is the rapid decrease in liquidus temperature resulting from this addition. Because the reaction Fe₂O₃ → 2FeO+½O₂ is strongly endothermic, the equilibrium ratio Fe₂O₃/FeO at

* These points are not true eutectics but rather points of intersection between a boundary curve and O₂ isobaric curves in the ternary system CaO–FeO–Fe₂O₃.

† No runs were made at 1 atm. O₂ with mixtures higher in CaO than 21 weight %. Because CaO stabilizes Fe₂O₃ almost to the exclusion of FeO at this and higher levels of CaO contents (compare composition curves in lower halves of diagrams in Figs. 3 and 4), the liquidus temperatures in air and at 1 atm. O₂ pressure are expected to be identical within limits of experimental error.

[12] A. Burdese and C. Brisi, "Ricerche sul Sistema CaO·Fe₂O₃–Fe₂O₄," (Research on the System CaO·Fe₂O₃–Fe₂O₄), *Ricerca sci.*, **22**, 1564–67 (1952).

[13] R. W. Gurry and L. S. Darken, "Composition of CaO-FeO-Fe₂O₃ and MnO-FeO-Fe₂O₃ Melts at Several Oxygen Pressures in Vicinity of 1600°C.," *J. Am. Chem. Soc.*, **72** [9] 3906–10 (1950); *Ceram. Abstr.*, **1951**, August, p. 145a.

[14] T. B. Winkler and John Chipman, "An Equilibrium Study of Distribution of Phosphorous Between Liquid Iron and Basic Slags," *Metals Technol.*, Tech. Pub. No. 1987, 24 pp. (April 1946); *Trans. Am. Inst. Mining Met. Engrs.*, **167**, 111–33 (1946).

[15] (a) W. A. Weyl, "Acid-Base Relationship in Glass Systems, I," *Glass Ind.*, **37** [5] 264–69, 286, 288 (1956).

(b) W. A. Weyl, "A New Acid-Base Concept Applicable to Aqueous Systems, Fused Salts, Glasses, and Solids," *ibid.*, **37** [6] 325–31, 336, 344, 346, 350 (1956).
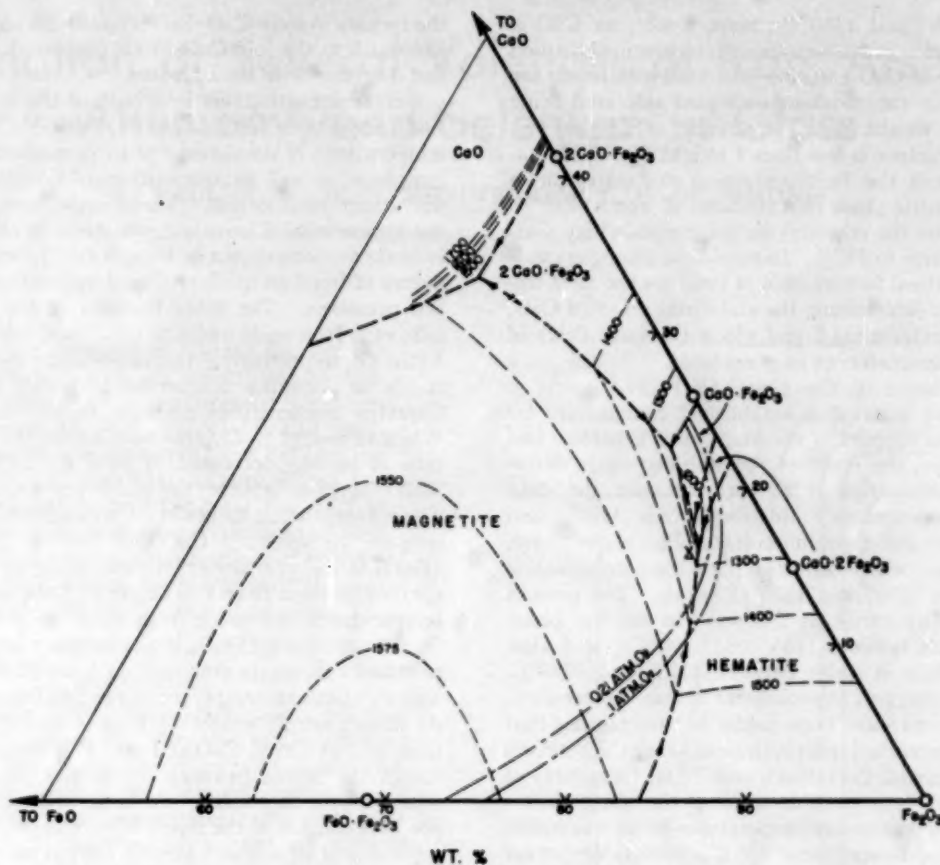
Fig. 5.   Sketch showing probable phase equilibrium relations at liquidus temperatures in the system 2CaO·Fe₂O₃–
FeO·Fe₂O₃–Fe₂O₃.   Diagram has been modified from the original version of Burdese and Brisi (footnote 12) to
incorporate a field of CaO·2Fe₂O₃ and to bring it into agreement with data of Darken and Gurry (footnote 11),
as discussed in the text.   Dashed heavy lines indicate probable approximate locations of boundary curves, light
dashed lines are approximate liquidus isotherms, and light dash-dot lines are O₂ isobars along the liquidus surface.

constant O_2 pressure and constant CaO content increases
rapidly with decreasing temperature. The decrease in
liquidus temperatures resulting as CaO is added therefore
amplifies the compositional effect of CaO, and the two factors
together account for the low FeO content of liquids in mixtures
where the CaO content exceeds 20 weight %.

The irregular shape (inflection point) of the liquidus curve
for mixtures where magnetite is the primary crystalline
phase was reconfirmed by several duplicate runs.   The effect
is particularly striking in air, but is also clearly noticeable at
1 atm. O_2 pressure.   Because no transformations in the
magnetite structure are known to take place in this tempera-
ture range, the peculiar course of the liquidus curve may be
tentatively ascribed to relatively abrupt changes in the con-
stitution of liquids in this composition range.

The exact location of the liquidus curve in the region of the
2CaO·Fe₂O₃ composition is difficult to determine because of
the extreme fluidity of the melts and the rapid formation of
relatively large quench crystals upon cooling.   Discrep-
ancies in previous versions of this part of the diagram[4,5] are
understandable on this basis.   Solidus temperatures, however,
can be determined reliably for mixtures near the 2CaO·Fe₂O₃
composition by observing the temperatures at which the
powdered samples change to a fused mass.   The writers have
established definitely that mixtures slightly higher in CaO
than the 2CaO·Fe₂O₃ composition have lower solidus tem-

peratures than a mixture of the stoichiometric 2:1 ratio.
This means that a maximum must be present on the 2CaO·-
Fe₂O₃ liquidus curve, and the incongruent melting of this
phase is ruled out.   The liquid at the "eutectic"[*] contains
only slightly more CaO than corresponding to CaO·Fe₂O₃, and
the "eutectic" temperature is only 11°C. below that of the
maximum (see data summarized in Table V).

Notice that the range of stable existence of hematite in
equilibrium with liquid decreases considerably as the O_2
pressure decreases from 1 atm. (Fig. 4) to 0.21 atm. (Fig. 3).
This also may be observed in the sketch in Fig. 5, where it will
be noticed that the O_2 isobaric curves sweep across the diagram
in a direction toward the upper left corner as the O_2 pressure
decreases.   The length of the isobar that is in the hematite
phase area thus decreases as the O_2 pressure is reduced and
hematite ceases to be stable in equilibrium with liquid at the
O_2 pressure represented by the O_2 isobar passing through point
X in Fig. 5.   This point represents liquid composition at the
invariant situation characterized by the coexistence in equilib-
rium of hematite, magnetite, CaO·2Fe₂O₃, liquid, and gas.

The temperatures of decomposition of hematite to mag-
netite, which in the pure iron oxide system are 1390° and
1455°C. in air and at 1 atm. O_2, respectively,[2(a)] decrease to

---

[*] See star footnote, page 452.

approximately 1358° and 1430°C., respectively, as CaO is added. This depression in decomposition temperature is caused by a small amount of CaO entering into solid solution in the magnetite structure, the maximum amount tolerated being approximately 2.5 weight %. The amount of CaO present in the hematite structure is less than 1 weight %. This stabilization by CaO of the Fe^{2+}-containing magnetite phase relative to the hematite phase that contains all iron as Fe^{3+} is in sharp contrast to the relations in the liquid, where CaO stabilizes Fe^{3+} relative to Fe^{2+}. In equilibria among crystalline phases, geometrical factors (size of ions) are the most important parameters determining the stabilizing effect of CaO, whereas in the homogeneous liquid phase the force fields of ions are the main parameters to be considered.

The stable existence of the phase $CaO \cdot 2Fe_2O_3$ over a limited temperature interval is established conclusively by the present data, in support of the findings of Edström[8] and of Batti.[9] However, the *extent* of the stability range determined in this investigation is at variance with the data of the other investigators. Edström gives 1120° and 1228°C. as the lower and upper limits of stability, respectively, at 1 atm. O_2 pressure, whereas Batti reports the corresponding temperatures to be 1130° and 1230°C. in air. The present data fix the stability range as follows: In air the phase $CaO \cdot 2Fe_2O_3$ is stable between 1155° and 1226°C.; at 1 atm. O_2 pressure the phase is stable between 1172° and 1228°C. The reactions are sluggish, especially at 1 atm. O_2 pressure, and great precautions have been taken in ascertaining that the equilibrium was reached from both sides, using $CaO \cdot 2Fe_2O_3$ as well as a mixture of $CaO \cdot Fe_2O_3$ and Fe_2O_3 (hematite) as starting materials. It is possible to keep the phase $CaO \cdot 2Fe_2O_3$ at 1 atm. O_2 pressure at temperatures below its equilibrium decomposition temperature for a considerable period of time (2 to 3 hours) without the formation of $CaO \cdot Fe_2O_3$ and Fe_2O_3 (hematite); given enough time (12 to 24 hours), however, the latter phases will form. In addition to the evidence obtained by quenching experiments, high-temperature X-ray examination was used in the present investigation to show that the phases $CaO \cdot Fe_2O_3$ and Fe_2O_3 (hematite) react to form $CaO \cdot 2Fe_2O_3$ in the indicated temperature interval.

The very small effect of changing O_2 partial pressure on the incongruent melting temperature of $CaO \cdot 2Fe_2O_3$ (1216°C. in air, 1218°C. at 1 atm. O_2) indicates that the FeO content of this crystalline phase must be almost the same as that of the liquid with which it is in equilibrium. Chemical analysis has confirmed this observation. The FeO content of $CaO \cdot 2Fe_2O_3$ quenched from 1192°C. in air was found to be 2.0 weight %. The increase in the lower decomposition temperature of $CaO \cdot 2Fe_2O_3$ as O_2 partial pressure increases (1155°C. in air, 1172°C. at 1 atm. O_2) shows that this phase contains more FeO than its decomposition products, $CaO \cdot Fe_2O_3$ and Fe_2O_3, combined. The FeO content of the latter phases is therefore neglected in the present investigation.

VI. Summary

Phase equilibrium relations in the system CaO–iron oxide have been investigated at two different levels of constant O_2 partial pressures. Mixtures ranging from 55 to 100 weight % iron oxide were studied in air ($p_{O_2} = 0.21$ atm.) and mixtures in the composition range 79 to 99 weight % iron oxide at 1 atm. O_2. Results of this study have been presented in terms of the ternary system $CaO-FeO-Fe_2O_3$, with supplementary projections into the join $CaO-Fe_2O_3$ presented to obtain simplified diagrams with the *appearance* of binary systems.

Univariant situations in a part of the system $CaO-FeO-Fe_2O_3$ have been summarized in Table V. The table shows temperatures of coexistence of three condensed phases and a gas phase, as well as compositions of liquids if present at the univariant equilibrium. These univariant situations have the appearance of invariant situations in the 0.21 and 1 atm. isobaric sections shown in Figs. 3 and 4, because the existing degree of freedom has been "used up" in choosing the O_2 partial pressures. The main features of the diagrams are as follows: Iron oxide melts at 1594° and 1583°C. in air and at 1 atm. O_2, respectively,[11] magnetite being the crystalline phase stable at liquidus temperatures under these conditions. Liquidus temperatures decrease rapidly as CaO is added. When 13 weight % CaO has been added, the liquidus temperature in air has decreased to 1358°C., and hematite rather than magnetite becomes the stable primary crystalline phase. The corresponding values in an atmosphere of 1 atm. O_2 pressure are 10 weight % CaO and 1430°C. The phase $CaO \cdot 2Fe_2O_3$ is the primary crystalline phase in mixtures of CaO content between 19 and 20 weight % CaO, in air, with liquidus temperatures decreasing from 1216° to 1205°C. At 1 atm. O_2 pressure $CaO \cdot 2Fe_2O_3$ is the primary crystalline phase in mixtures ranging in composition from 20 to 21.5 weight %, and with liquidus temperatures ranging from 1218° to 1206°C. As more than 20 weight % CaO is added, in air, and more than 21.5 weight % CaO at 1 atm. O_2 pressure, $CaO \cdot Fe_2O_3$ becomes the stable primary crystalline phase, with liquidus temperatures increasing. At these and higher CaO contents the FeO content of the liquid is very small, and liquidus temperatures in air and at 1 atm. O_2 are not significantly different. In the composition range 24 to 42 weight % CaO, $2CaO \cdot Fe_2O_3$ is the stable primary crystalline phase. Liquidus temperatures increase from 1216°C., go through a maximum of 1449°C. at the $2CaO \cdot Fe_2O_3$ composition, and decrease to 1438°C. for liquids in equilibrium with lime and $2CaO \cdot Fe_2O_3$. When more than 42 weight % is present, lime is the primary crystalline phase, with liquidus temperatures rising very rapidly as the CaO content of the mixtures increases.

Interesting reactions take place in the subliquidus region of the system. The hematite to magnetite decomposition temperature is lowered from 1390° to a minimum of 1358°C. in air and from 1455° to 1430°C. at 1 atm. O_2 pressure upon the addition of CaO. Approximately 2.5 weight % CaO can enter into the magnetite lattice at the temperatures and levels of O_2 pressures used in the present investigation.

The stable existence of the phase $CaO \cdot 2Fe_2O_3$ has been established conclusively. This phase is stable in the temperature interval 1155° to 1226°C. in air and in the interval 1172° to 1228°C. at 1 atm. O_2 pressure. At the upper temperature of stability under these conditions of O_2 pressures the phase decomposes incongruently to hematite and liquid, and at the lower temperature of stability it decomposes to hematite and $CaO \cdot Fe_2O_3$.

Determination of Several Valences of Iron, Arsenic and Antimony, and Selenium in Glass

by PAUL CLOSE, H. M. SHEPHERD, and C. H. DRUMMOND

General Research Division, Owens-Illinois Technical Center, Toledo, Ohio

Methods for the analysis of silicate glasses are described for ferrous iron, for tri- and pentavalent arsenic and antimony when present together, and for selenium as Se^{2-}, Se^0, Se^{4+}, and Se^{6+}. Analytical results are presented for FeO in the range 0 to 0.25%; for total As and Sb as trioxide, 0.1 to 1.25%; and for total Se, 0.05 to 0.25%. Apparatus for the determination of FeO is described, and a comparison is made of analytical data for FeO versus light transmittance at 1000 and at 1050 mμ for the same glass.

I. Introduction

THE study of color and oxidation-reduction equilibria in glass has long attracted the attention of the glass technologist. The literature on these subjects is quite large. However, applicable quantitative chemical analysis of colorants that have been reported constitutes but a small part of the whole. Published analytical procedures are somewhat rare.

The procedures presented here have been developed over a period of several years. Although the basic methods used are fundamental in analytical chemistry, the procedures and techniques developed are not of the usual kind. Particularly, the direct use of hydrofluoric acid solutions is uncommon, and yet if handled properly, can simplify what otherwise may be a cumbersome and lengthy analysis.

Reference is made to earlier analytical work in the areas covered by the writers. This work has been of interest and frequently has served as a basis for the development of the procedures used in this laboratory.

II. Determination of Ferrous Iron

(1) Introduction

The accurate determination of ferrous iron has received the close attention of silicate analysts. Of several methods proposed, that of Pratt[1] has generally been accepted for materials soluble in hydrofluoric and sulfuric acid. Several workers[2] have developed modifications directly applicable to glass.

The procedure to be described is also an adaptation of Pratt's method: Two pieces of apparatus are described that overcome the difficulty of exposing the sample to air before the complexing of HF with boric acid. Reagents are pretreated to prevent the introduction of error from this source. Ceric sulfate is chosen as the titrant because arsenic or antimony, if present, does not cause an error with this oxidant. Under the conditions obtained in the procedure, the presence of a catalyst is necessary for the ceric ion to oxidize trivalent
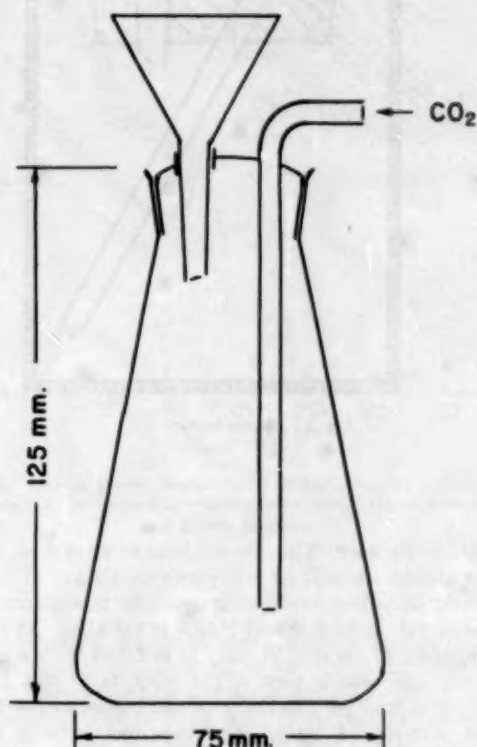
Fig. 1. Platinum flask.

arsenic or antimony. With attention to detail and careful technique, ferrous iron in the amount of 0.005% and more can be determined accurately.

(2) Apparatus

(A) *Platinum Flask:* Figure 1 shows a platinum flask with an inlet tube for the introduction of CO_2, stopper, and funnel for the addition of reagents. The flask is the same size and shape as a standard 250-ml. glass Erlenmeyer flask. This apparatus permits the boiling of the sample and attendant loss of silica, and also the rapid expulsion of sulfide from amber glasses. Although boiling is a must for many minerals to effect solution, it is not necessary for glasses. However, the volatilization of silica permits a sharper end point during the titration.

[1] W. F. Hillebrand and G. E. F. Lundell (revised by G. E. F. Lundell, H. A. Bright, and J. I. Hoffman), Applied Inorganic Analysis, 2d ed., pp. 917–19. John Wiley & Sons, Inc., New York, 1953. 1034 pp.; *Ceram. Abstr.*, 1953, July, p. 129e.

[2] (a) F. R. Harris, "Determination of Ferrous Iron in Certain Silicates," *Analyst*, 75 [894] 496–98 (1950); *Ceram. Abstr.*, 1951, January, p. 19a.

(b) R. S. Allison, "Analytical Determination of Total Iron Oxide and Ferrous Oxide Contents of Glasses," *J. Soc. Glass Technol.*, 36 [169] 124-30T (1952); *Ceram. Abstr.*, 1952, November, p. 199e.

CO₂
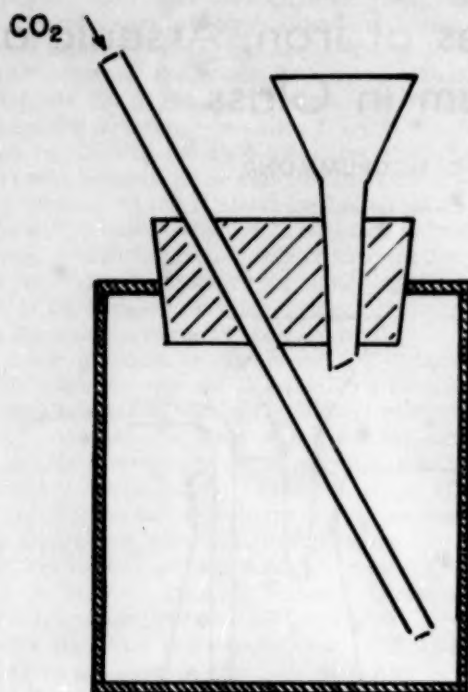
Fig. 2.　Plastic beaker.

(B) Plastic Beaker: The plastic beaker shown in Fig. 2 can serve almost as well as the platinum flask. It is preferably made of polystyrene, although any transparent material resistant to cold HF and H_2SO_4 is suitable. It should have a capacity of about 250 ml. It is fitted with a rubber stopper, through which pass a gas inlet tube and funnel. The inlet tube may be platinum or rigid plastic, the funnel plastic or wax-coated glass. The gas inlet tube is set at an angle so as to nearly touch the bottom of the beaker near the side join. Thus, when making a determination of ferrous iron in a sulfide amber glass, it is possible to sweep out the hydrogen sulfide by bubbling the CO_2 through the sample solution. The tube is retracted so as to be above the solution level for samples not containing sulfide.

(3) Reagents

(A) 0.005 N Ceric Sulfate in 0.5 to 1 N H_2SO_4: Standardize against freshly prepared 0.005 N ferrous ammonium sulfate of known quality in 0.1 N H_2SO_4; 1 ml. = 0.0003592 gm. FeO. The standardization is carried out at the same volume and concentration of H_2SO_4 as is the sample titration.

(B) Ferrous Orthophenanthroline Indicator (Ferroin): Dilute stock 0.025 mole solution 30 times. One milliliter will give a blank titer of about 0.15 ml. 0.005 N ceric sulfate.

(C) Hydrofluoric Acid: Dilute 48 to 50% reagent HF with an equal amount of water in a platinum dish. Add 0.1 N $KMnO_4$ until the solution is faintly pink. Heat until the permanganate is reduced and again add until very faintly pink. Continue heating until the permanganate is reduced. Cool for use.

(D) Sulfuric Acid: Prepare 1:1 H_2SO_4 and cool to about 50°C. Treat identically to the HF with permanganate before use.

(E) Boric Acid: Add 100 gm. H_3BO_3 to 1 liter of water and boil for 5 minutes. Cool to 60° to 70°C. for use. Cooling to a lower temperature would allow some recrystallization to occur.

(F) Water: Freshly boiled and cooled water is recommended unless stock distilled water is known to contain little dissolved oxygen.

(4) Procedure Using the Platinum Flask

Transfer to the flask a 1.000-gm. sample of amber glass, and other glasses high in iron, or a 2.000-gm. sample for flint glasses, emerald-green glasses containing chromium, or other glasses low in iron (less than 0.20%). Minus 100-mesh glass is suitable. Pass a stream of oxygen-free CO_2 (10 to 20 bubbles a second) through the apparatus for 10 minutes to flush out all air. Add 25 ml. hot water, 7 to 8 ml. 1:1 H_2SO_4, and 8 ml. 1:1 HF for each gram of glass taken. Bring quickly to a boil and boil gently for $2^1/_2$ to 3 minutes. Two or three small pieces of crumpled platinum foil will aid in smooth boiling. Gently swirling the flask while adding the reagents also will prevent caking and subsequent bumping. When boiling begins, slow the stream of CO_2 to about one-half the flushing-out rate. After boiling, remove the flask from the heat, add 60 ml. of warm 10% boric acid for 1-gm. samples and 100 ml. for 2-gm. samples, place the flask in cold water, and cool rapidly.

When the flask is cool, shut off the CO_2 and transfer the sample solution to a 250-ml. beaker. Add 8 to 10 ml. more of 1:1 H_2SO_4 and 1 ml. of the diluted indicator and titrate to the end point (orange-red to colorless). The titration is best made using a 10-ml. micro or semimicro burette. A piece of white paper is folded under and in back of the beaker to produce a good white background for judging the end point. Mechanically stirring the solution assists the operator. When the first fading of the indicator becomes apparent, additional increments of titrant (0.02 to 0.03 ml.) are added at about 20- to 30-second intervals to avoid over-titration. Subtract the indicator blank and calculate the percentage of ferrous iron.

(5) Procedure Using the Plastic Beaker

Weigh a suitable sample (as described for the platinum flask) into the beaker and flush out the apparatus with CO_2. Add 2 ml. water, 7 to 8 ml. 1:1 H_2SO_4, and 8 ml. 1:1 HF for each gram of sample taken; swirl the flask gently to prevent caking. Allow the sample to sit for 15 minutes (except sulfide ambers) and then add 5 gm. of solid boric acid for each gram of sample taken. The boric acid is washed into the beaker through the funnel. Dilute to about 125 ml. and allow to sit, with occasional swirling, for 10 minutes. Shut off the CO_2, remove the stopper, and titrate as described. Transferal to a glass beaker is unnecessary if the plastic is transparent and colorless.

When determining ferrous iron in sulfide-containing glasses, push the gas inlet tube nearly to the bottom of the beaker after the glass has dissolved, tilt or incline the beaker slightly, and allow the CO_2 to "sweep out" the hydrogen sulfide for at least 20 minutes. Then proceed as for glasses not containing sulfide.

(6) Discussion and Results

Shown in Figs. 3 and 4[3] is a series of analytical results plotted against transmittance as measured by a spectrophotometer. The solid line represents the most probable value of FeO vs. transmittance. The broken lines represent an arbitrary allowable error. These lines are drawn to include most of the data, and are also based on experience and replicate analyses. The solid line passes through 92% transmittance as the spectrophotometric data have not been corrected for reflection losses.

It is the opinion of the writers that a comparison of physical measurement and analytical data is a more severe test of analytical accuracy in this case than a simple test of the method using standard solutions carried through the pro-

[3] F. R. Bacon and C. J. Billian, "Color and Spectral Transmittance of Amber Bottle Glass," *J. Am. Ceram. Soc.*, **37** [2] 60–66 (1954).
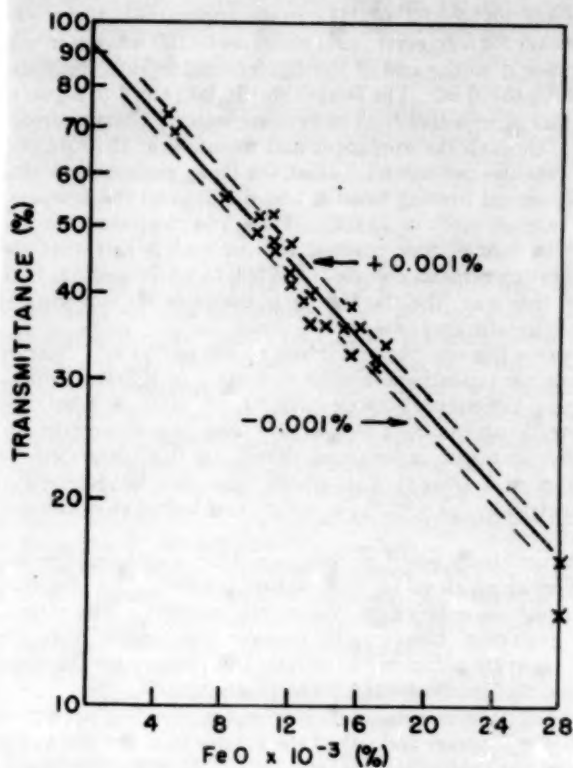
Fig. 3. Ferrous iron vs. transmittance at 1000 mμ for flint and light-green glasses 38 mm. thick (Beckman B spectrophotometer). (Data from Bacon and Billian, footnote 3.)
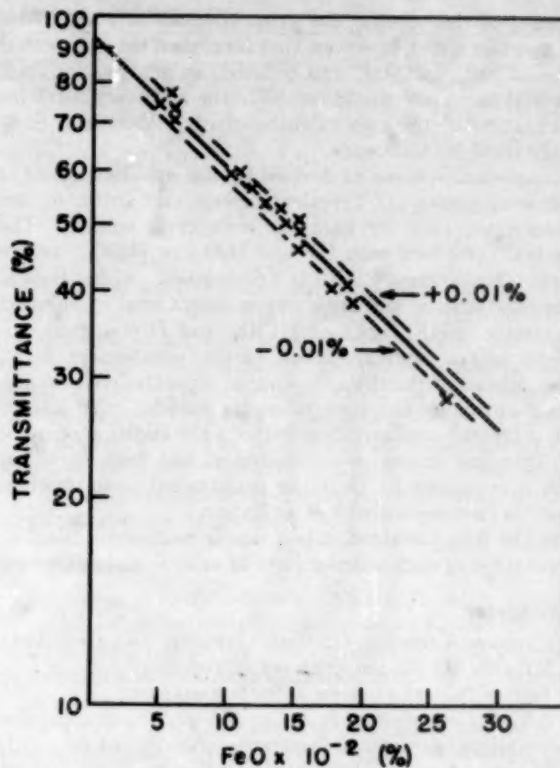
Fig. 4. Ferrous iron vs. transmittance at 1050 mμ for amber glass 2 mm. thick (Beckman DU spectrophotometer). (Data from Bacon and Billian, footnote 3.)

cedures. The actual glass sample will present influences not nearly as much under the analyst's control as relatively pure solutions. As an example, the case of amber glass is cited. Sulfide can reduce ferric iron, some of which is present in the glass. Also, any residual sulfide or sulfur compounds of lower valence than sulfate, when left in the sample solution, will be titrated by the ceric sulfate. Usually about 0.025% sulfide is present in amber glass. This quantity theoretically can reduce an equivalent of about 0.125% ferric oxide. That the effect of sulfide is nearly eliminated can be seen from the fact that the data are mostly within the ±0.01% bracket. It cannot be concluded, however, that a possible sulfide effect is entirely eliminated.

Another reason for the validity of the comparison of analytical data and spectrophotometric data is that normally only ferrous iron, of the components present in glass, has any appreciable absorbance in the 1050-mμ region. It can be expected, therefore, that the two kinds of data will have a quantitative relation.

III.   Determination of Tri- and Pentavalent Arsenic and Antimony

(1) Introduction

The effect of arsenic and antimony as oxidants and decolorizers has long been of interest to glass technologists. The quantitative measurement of the proportions of the two valency states of each has depended on the analytical chemist. For the two determinations of tri- and pentavalent arsenic in glass, analysts depended on the volatility of trivalent arsenic in HF and H_2SO_4.[4] Upon evaporation, this treatment leaves

only pentavalent arsenic in the sample, which is then separated by distillation and subsequently determined. Total arsenic is determined by the same procedure except that the trivalent arsenic is oxidized with HNO_3 before the expulsion of the HF. The difference of the two is trivalent arsenic. The presence of tri- and pentavalent antimony and arsenic together complicates the analysis when it is desired to determine the two valences of the oxides.

Heinrichs[5] estimated the ratios of Sb^{3+} and Sb^{5+} in glasses containing 0.5% arsenic as As_2O_3. Assuming 80% of the arsenic to be As^{5+}, he decomposed the sample in the presence of KI and measured the liberated iodine as representing pentavalent As and Sb; correcting for As^{5+} he obtained Sb^{5+}. Trivalent antimony was determined by solution in HF and HCl and titrating with bromate. For his purpose, results were quite satisfactory because of the high antimony-to-arsenic ratio. However, he actually had made no separate determinations. Rathsburg[6] proposed solution of the sample in HF and 15% HCl, and titrating the Sb^{3+} directly with $Ce(SO_4)_2$. After titrating the antimony, the As^{3+} is titrated with bromate. Furman,[7] who also studied the conditions for this titration, states that results are erratic unless antimony is in excess of arsenic. The acidity of the solution must be 40% in HCl; conditions are also more favorable when antimony exceeds arsenic severalfold. Because of the

[4] E. T. Allen and E. G. Zies, "Condition of Arsenic in Glass and Its Role in Glass-Making," *J. Am. Ceram. Soc.*, 1 [11] 787–90 (1918).

[5] H. Heinrichs, "Die Wertigkeit des Arsens und Antimons im Glase" (Estimation of Arsenic and Antimony in Glass), *Glastech. Ber.*, 4 [4] 130–37 (July 1926); *Ceram. Abstr.*, 6 [6] 216 (1927).

[6] Hans Rathsburg, "Salts of Cerium for Quantitative Analysis; Determination of Antimony in Presence of Arsenic," *Ber. deut. chem. Ges.*, 61B, 1663–65 (1928).

[7] N. H. Furman, "Applications of Ceric Sulfate in Volumetric Analysis: X, Determination of Antimony and Arsenic," *J. Am. Chem. Soc.*, 54 [11] 4235–38 (1932); *Ceram. Abstr.*, 12 [4] 171 (1933).

uncertainty of this scheme, the writers did not attempt to use it. It must be noted, however, that if or when the differential titration of Sb^{3+} and As^{3+} can be used, an analysis for total arsenic and antimony would complete the necessary work for the estimation of the two valences of each, As^{5+} and Sb^{5+} being obtained by difference.

The analytical scheme as devised by the writers consists of the following steps: (1) Trivalent arsenic and antimony are determined together by titration with ceric sulfate. The sample is decomposed with HF and H_2SO_4 or $HClO_4$; before titrating, the excess HF is complexed with H_3BO_3. (2) The total arsenic and antimony is determined by solution of the sample in HF, H_2SO_4 or $HClO_4$, and HNO_3, thus oxidizing all arsenic and antimony to the pentavalent form. After expulsion of fluorides, arsenic is separated by distillation, and antimony is recovered as the sulfide. (3) A third sample is treated similarly, but without the addition of nitric acid. Trivalent arsenic is volatilized as the fluoride as the solution is evaporated. Only the pentavalent form remains. The As^{5+} is then separated by distillation.

From the data obtained it is a simple matter to calculate the percentage of each valence form of arsenic and antimony.

(2) Reagents

(A) *Osmium Tetroxide Catalyst:* Prepare 0.01 mole OsO_4 in 0.1 N H_2SO_4 (0.2555 gm. OsO_4 per 100 ml.).

(B) *Ferroin Indicator:* Same as for ferrous iron.

(C) *0.02 N Ceric Sulfate in 0.5 to 1 N H_2SO_4:* Standardize against National Bureau of Standards arsenious oxide. Add a known amount of standard As^{3+} solution to about 100 ml. of 2 N H_2SO_4, add 2 drops of osmium catalyst and 1 ml. diluted ferroin, and titrate with the ceric sulfate. One milliliter 0.02 N $Ce(SO_4)_2$ = 0.0009891 gm. As_2O_3 or 0.0014576 gm. Sb_2O_3.

(D) *Other Reagents:* No special considerations are required.

(3) Procedure

(A) *As^{3+} Plus Sb^{3+}:* Weigh 1 gm. of −100-mesh sample into an 80-ml. platinum dish. Add 10 ml. H_2O and 10 ml. $HClO_4$, place the dish in a bath of cool water, and add 5 ml. HF while stirring with a platinum rod. Allow the sample to digest for about 10 minutes. Transfer the sample to a plastic dish or beaker and dilute to 100 ml. Add 6 gm. of boric acid and stir the solution for about 5 minutes; a mechanical or magnetic stirrer is most suitable. Add 1 ml. of dilute ferroin indicator (see ferrous iron). Titrate carefully dropwise with 0.02 N $Ce(SO_4)_2$ until the color of the indicator is just discharged and read the burette. This titration takes care of the indicator blank and any residual ferrous iron that still may be present. Add 2 drops 0.01 M osmium tetroxide as catalyst, and continue the titration for As^{3+} plus Sb^{3+}.

(B) *Total Arsenic and Antimony:* Weigh 1 gm. of −100-mesh sample into an 80-ml. platinum dish. Add 5 ml. water, 5 ml. 1:1 H_2SO_4 (or 8 to 10 ml. $HClO_4$), 5 ml. HNO_3, and 6 ml. HF. Perchloric acid is preferred to H_2SO_4 when the glass contains appreciable amounts of lead or barium. Evaporate to light fumes of H_2SO_4 or $HClO_4$. Wash down the sides of the dish, and if $HClO_4$ is used, add 2 to 3 ml. of saturated H_3BO_3 to assure expulsion of fluoride. Again evaporate to light fumes and cool. Fuming for any length of time is to be avoided. Add 5 ml. water and transfer to the distilling apparatus[8] with 50 to 60 ml. of concentrated HCl. Add $1/2$ gm. Hydrazine dihydrochloride dissolved in 2 ml.

hot water, and 2 to 3 ml. HBr to the apparatus. Use a 400-ml. beaker for a receiver; add about 50 to 100 ml. water to it and place it so the end of the condenser dips into the water about $1/4$ to $1/2$ in. The beaker should be placed in a pan of ice water or in a cool bath of running water. Start a stream of CO_2 through the apparatus and maintain at the rate of 5 to 10 bubbles per second. Heat the flask, preferably with a hemispherical heating mantle, and distill until the temperature reaches 108° to 111°C. Then add dropwise, via the dropping funnel, concentrated HCl at such a rate that the temperature remains constant. When 75 ml. of acid has been added this way, the distillation is complete for amounts of arsenic usually encountered in glasses.

Remove the receiver and dilute to 300 to 350 ml. Titrate the arsenic potentiometrically with 0.02 N $KBrO_3$, using a platinum-tungsten electrode pair; 1 ml. 0.02 N $KBrO_3$ = 0.0009891 gm. As_2O_3. The writers use potentiometric apparatus identical in essential details to that described by Garman and Droz.[9] The arsenic can also be determined iodometrically, or with ceric sulfate and iodine monochloride as catalyst.

The antimony could be determined by continuing the distillation at an elevated temperature, receiving the distillate and using an appropriate volumetric method. The writers have preferred, however, to transfer the sample from the flask, separate antimony as sulfide, and proceed by the usual method for handling the sulfide precipitate.

Transfer the sample solution from the distilling apparatus to a 400-ml. beaker and adjust the volume to about 200 to 250 ml. and the acidity to 1 N (8% HCl). Heat to near boiling and precipitate antimony by passing a rapid stream of H_2S through the solution as it cools. Allow the precipitate to settle for 30 minutes. Filter through a tight paper and wash with 5% HCl solution saturated with H_2S. Transfer the paper to a 300-ml. Kjeldahl flask and add 10 ml. H_2SO_4 and 5 gm. K_2SO_4. Cautiously heat to boiling and continue until all the organic matter has been destroyed. One or two boiling stones will aid in this operation. Cool the flask and add 10 to 15 ml. water and 1 ml. 6% H_2SO_3. Boil until SO_2 has been expelled. Cool, dilute to 100 ml., add 1 ml. of dilute ferroin indicator and 2 drops OsO_4 catalyst, and titrate with 0.02 N $Ce(SO_4)_2$. The titration can also be done with permanganate.

(C) *As^{5+}:* Pentavalent arsenic is determined by the same procedure as used for total arsenic except that HNO_3 is not used when decomposing the sample. Thus trivalent arsenic is not oxidized and volatilizes during the initial evaporation.

(D) *Computation:* From the several determinations made, it is a simple matter to estimate the quantities present in each valence form. From the total arsenic, as As_2O_3, the equivalent of the As_2O_5 found is subtracted. This gives the estimation of trivalent arsenic. The equivalent titer of the trivalent arsenic is subtracted from the total titer of As^{3+} plus Sb^{3+}, from which the Sb_2O_3 is calculated. The trivalent antimony is subtracted from the total antimony as Sb_2O_3, and the remainder is the equivalent amount of pentavalent antimony present.

(4) Discussion and Results

Results are shown for the analysis of six glasses in Table I. Glasses Nos. 1, 2, and 3 are simple soda-lime-silica glasses (74% SiO_2, 12% CaO, and 14% Na_2O) melted in an oxidizing atmosphere. In glass No. 1, 1.3% As_2O_3 was substituted for SiO_2; in glass No. 2, 1.0% Sb_2O_3 was substituted; and in glass No. 3, 1.3% As_2O_3 and 1.0% Sb_2O_3 was substituted. Glasses Nos. 4, 5, and 6 are commercial glasses melted in conventional glass tanks.

[8] J. A. Scherrer, "Determination of Arsenic, Antimony, and Tin in Lead-, Tin-, and Copper-Base Alloys," *J. Research Natl. Bur. Standards*, 21 [1] 95–104 (1938); RP 1116. Apparatus available commercially; sold as designated by A.S.T.M. Designation E 50–53, Apparatus No. 5; 1956 Book of A.S.T.M. Methods for Chemical Analysis of Metals, American Society for Testing Materials, Philadelphia, 1956.

[9] R. L. Garman and M. E. Droz, "An Electron Tube Direct-Current Voltmeter of New Design," *Ind. Eng. Chem., Anal. Ed.*, 11 [7] 398–99 (1939).

Table I.   Analytical Results for Arsenic and Antimony

Sample No. →	1	2	3	4		5		6	
As_2O_3 (%)	0.17		0.13	0.02	0.03	Nil	0.02	Nil	Nil
As_2O_5 (%)	1.15		1.28	0.14	0.15	0.42	0.42	0.18	0.18
Sb_2O_3 (%)		0.92	0.78	0.77	0.73	0.16	0.13	0.17	0.17
Sb_2O_5 (%)		0.12	0.19	0.09	0.12	0.02	0.04	0.01	0.01

To test the procedure for As^{3+} plus Sb^{3+}, the writers first added 3 ml. of 0.02 N standard As^{3+} solution and 5 ml. of 0.02 N standard Sb^{3+} solution to a glass containing no arsenic or antimony and then carried through the procedure. Theoretical results were obtained. Second, to test the separation of arsenic from antimony, 10 mg. of each, as trioxide in solution, were added to the distillation flask and the distillation was made as described in the procedure. Four such tests gave recoveries of 10.0, 9.9, 9.9, and 10.0 mg. As_2O_3. The volatility of As_2O_3 and the determination of antimony were not tested, as these procedures are standard practice.

From the duplicate results shown for glasses Nos. 4, 5, and 6, one can expect a precision of about 0.03% or better for each result. This is quite satisfactory, considering that only one of the four results (As_2O_5) is obtained directly.

IV.   Determination of Selenium in Its Several Valences

(1)   Introduction

The experimental work done with selenium in glass has been extensively reported in the literature. However, actual analysis and analytical methods reported are scarce. The first analytical method proposed for determining total selenium in glass was by Cousen.[10] This is a colorimetric method based on stabilizing precipitated elemental selenium with gum arabic and comparing against known standards. Using a 20-gm. sample, Cousen was able to determine 0.0005% selenium in a decolorized flint glass. Krak,[11] and Navias and Gallup[12] in their experiments, working with selenium in the order of 0.2%, and 0.5 to 25.0%, determined total selenium by precipitating as elemental selenium with SO_2, filtering, and weighing. Krak decomposed samples with HF-HNO_3, whereas Navias and Gallup used carbonate fusion and removed silica by dehydration before determining selenium. Pavlish and Silverthorn[13] developed a rapid method based on fusion with carbonate followed by distillation to separate selenium. The selenium was determined by iodometric titration. Close, Raggon, and Smith[14] devised a procedure based on a 5-gm. sample decomposed with HF, $HClO_4$, and HgO. They were able to determine selenium to 0.00025% in decolorized flint glasses.

All the foregoing procedures result only in the estimation of the total selenium in the glass. The only work known to the writers where an estimation of the valences of the selenium present was determined is that by Hirsch, Wiegand, and Dietzel.[15] The exact details of their procedures were not available to the writers, but in some respects their scheme is similar to the one used in this laboratory: Se^{4+} and Se^{6+} were determined together after reduction of Se^{6+} to Se^{4+}, Se^{4+} being determined separately without reducing Se^{6+}; Se^0 and Se^{4+} were determined together after oxidizing Se^0 with bromine. They did not encounter Se^0 and Se^{6+} in the same sample. Se^{2-} was determined by adding iodine in excess and back-titrating with thiosulfate—the same procedure as for Se^{4+}. When Se^{2-} and Se^{4+} were present together, it became necessary to add the sample to boiling 25% HCl and expel the H_2Se to determine Se^{4+}. Selenide was oxidized with bromine, and Se^{2-} and Se^{4+} were determined together.

The procedures described below allow for separation of selenium when present in its several valences or its unreac-

tivity in the final measurement when not present as Se^{4+} (selenious acid). The Norris and Fay[16] titration reaction is employed in all final measurements. The end point is detected potentiometrically, using a platinum-tungsten electrode pair. The procedures cover the determination of total Se, Se^{4+}, Se^{4+} plus Se^{6+}, Se^0, and S^{2-}; Se^{6+} = (Se^{4+} plus Se^{6+}) minus Se^{4+}. The procedures are applicable to glasses with total Se of 0.025 to 0.25%. There is no apparent reason why higher concentrations cannot be determined if stronger titrants and reagents are used.

(2)   Reagents

(A) Dilute HBr-Br Mixture: Dilute 20 ml. concentrated HBr and 20 ml. saturated bromine water to 100 ml. If the bromine fades out of the solution during initial digestion of the sample, add saturated bromine water in 1-ml. increments to maintain an excess.

(B) 0.005 N $Na_2S_2O_3$: Prepare just before use by diluting from standardized 0.1 N $Na_2S_2O_3$; 1 ml. = 0.0000987 gm. Se. This solution is the standard for the titration.

(C) 0.005 N Iodine: Prepare by diluting from 0.1 N iodine. Standardize against the 0.005 N $Na_2S_2O_3$ by titrating potentiometrically in 100 ml. of 5% acetic acid.

(D) 0.001 N $Na_2S_2O_3$ and Iodine: Prepare and standardize as for the 0.005 N solutions; 1 ml. = 0.0000198 gm. Se.

(E) Other Reagents: No special considerations.

(3)   Procedures

(A) Total Selenium: Weigh 1 gm. of −100-mesh glass into a 75-ml. platinum dish and add 5 ml. of dilute HBr-Br mixture, cool in ice water, and add 5 ml. HF. Digest for 3 to 4 minutes with occasional stirring with a platinum rod. Remove from the ice water and allow to digest at room temperature for an additional 15 minutes. Add 10 ml. water and filter through a 7-cm. medium paper. Catch the filtrate in a 125-ml. platinum dish. A plastic funnel is suitable provided it is not polyethylene; otherwise use coated glass or platinum. Wash four or five times with 1% HF solution; a polyethylene squeeze

[10] A. Cousen, "Estimation of Selenium in Glass," *J. Soc. Glass Technol.*, 7 [28] 303–307T (1923); *Ceram. Abstr.*, 3 [4] 96 (1924).

[11] J. B. Krak, "Volatility of Selenium and Its Compounds in Manufacture of Ruby Glass," *J. Am. Ceram. Soc.*, 12 [8] 530–37 (1929).

[12] Louis Navias and John Gallup, "Selenium Dioxide as a Constituent of Glasses," *J. Am. Ceram. Soc.*, 14 [5] 441–49 (1931).

[13] A. E. Pavlish and R. W. Silverthorn, "Analysis of Selenium in Glass," *J. Am. Ceram. Soc.*, 23 [4] 116–18 (1940).

[14] Paul Close, F. C. Raggon, and W. E. Smith, "Chemical Analysis of Soda-Lime-Silica Glasses for Trace Quantities of Several Colorants," *J. Am. Ceram. Soc.*, 33 [11] 345–52 (1950).

[15] W. Hirsch, H. Wiegand, and A. Dietzel, "Die quantitative Bestimmung der Oxydationsstufen des Selens in eisenoxydarmen Alkali-Kalk-Gläsern" (Quantitative Determination of Stages of Oxidation of Selenium in Alkali-Lime Glasses of Low Iron Content), *Sprechsaal*, 68 [24] 373–76 (1935); *Ceram. Abstr.*, 15 [1] 15 (1936).

[16] (a) J. F. Norris and H. Fay, *J. Am. Chem. Soc.*, 18, 703 (1896).
(b) Scott's Standard Methods of Chemical Analysis, 5th ed., Vol. 1, p. 785 (N. H. Furman, Editor). D. Van Nostrand Co., Inc., New York, 1939. 1234 pp.

bottle is suitable for this operation. Dilute to 75 to 100 ml., add 1 ml. bromine water, 5 ml. HBr, and 5 ml. formic acid and digest on the steam bath until excess bromine is reduced.

Cool and transfer to a plastic beaker or cup; polystyrene is most suitable; polyethylene cannot be used because it absorbs free halogen almost instantly. Place the sample on the titration stand and insert the electrodes. Stir the solution and add 0.005 N $Na_2S_2O_3$ to approximately a 50% excess (usually 5 to 10 ml. in excess will suffice over the amount expected). Allow the solution to sit without stirring for 5 minutes. Then titrate the excess $Na_2S_2O_3$ with 0.005 N iodine until a large permanent break occurs on the meter needle. With a full-scale sensitivity of 500 mv., the break is usually 15 to 20 scale units or about 150 to 200 mv. Difference $Na_2S_2O_3$ and I_2 = selenium.

(B) Se^{4+}: Prepare the sample as before but omit the 5-ml. HBr-Br mixture, using 5 ml. H_2O instead. Add the initial 15-minute digestion, add 10 ml. H_2O, 1 ml. acetic acid, and 10 ml. 10% barium acetate. Stir and allow to sit another 15 minutes. Filter and wash as for total Se. Add 4 ml. acetic acid, transfer to a plastic cup or beaker, dilute to 100 ml., and titrate as before. Titer equals Se^4.

(C) Se^{4+} Plus Se^{6+}: Prepare the sample as for Se^4 but omit the addition of acetic acid and barium acetate. Filter after 15 minutes as for total selenium but reserve the residue on the paper for the recovery of elemental Se. Dilute the solution to 75 to 100 ml. and add 5 ml. HBr, 2 ml. bromine water (or in excess), and 5 ml. formic acid. Digest and reduce the excess bromine and proceed as for total selenium.

(D) Se^0: Wash the residue remaining on the filter, from the sample prepared for Se^{4+} plus Se^{6+}, first with 2 ml. dilute HBr-Br mixture and then with 2 ml. 1% HF; repeat both washings. Wash the dish in which the sample was decomposed with 1 ml. dilute HBr-Br and then with a few ml. of 1% HF; pour these washings through the filter. Finally, wash the residue and paper four or five times with 2- or 3-ml. portions of 1% HF. Catch the washings in a platinum dish. Keep the volume as low as possible. Add 2 ml. HBr and 2 ml. formic acid and reduce the excess bromine on the steam bath. Transfer to a plastic beaker and titrate as before, but use 0.001 N $Na_2S_2O_3$ and I_2. The end point may be plotted, but normally the needle response is sufficient at the end point to make this unnecessary.

(E) Se^{2-}: Weigh a 3-gm. sample into a plastic bottle and evolve H_2Se as for sulfide.[14] Add 2 to 5 ml. bromine water to the absorbing alkaline solution and acidify with HCl to a 5-ml. excess; sufficient bromine must be added initially so that all selenide is oxidized on acidification. Add 5 ml. formic acid and proceed as described for total selenium. Titrate with 0.005 N $Na_2S_2O_3$.

(4) Discussion and Results

From the results shown in Table II, evaluation of the precision of each single determination is obtained by comparing the summation of results for each valence with the total selenium determined separately. The average deviation of results for this comparison is slightly less than 0.003% Se or about 0.001% for any single determination. It is not the intention of the writers to imply that this apparent precision represents the error in absolute accuracy, but rather to show that the results appear to be satisfactory for their use, an estimation of the proportion of each valence in a particular sample. The agreement, however, between the summation and the total Se determined separately does add credence to the probable accuracy of the individual results. If there was a systematic error of 0.005% Se in the individual determinations, the differences would be three to four times that shown. The accuracy of individual determinations must not be greatly different from the precision indicated.

The writers use as a standard selenium glass sample (for total Se) a glass prepared by Battelle Memorial Institute and

Table II. Analytical Results for Selenium

Sample No.	Se (%)	Se^{4+} (%)	Se^{6+} (%)	Se^{2-} (%)	Total (%)	Total Se determined separately
1	0.005	0.058	0.004		0.067	0.073
2	0.018	0.025	0.003		0.046	0.050
3	0.060	0.013	0.060	0.0038	0.137	0.136
4	0.015	0.182	0.005		0.202	0.201
5	0.029	0.181	0.022		0.232	0.235
6	0.004	0.085	0.003		0.092	0.096
7	0.029	0.206	0.043		0.278	0.277
8	0.018	0.192	0.063	0.001	0.274	0.276
9	0.025	0.169	0.033		0.237	0.240
10	0.0735	Nil	Nil	0.0005	0.074	0.077

containing 0.078% Se by their analysis. The analysis for this glass in the writers' laboratory is 0.077% Se. This is excellent agreement, as Battelle's analysis was obtained by the method of Pavlish and Silverthorn and the writers' result by the method described for total selenium. Inasmuch as there is no accepted standard such as a National Bureau of Standards glass sample, the analyst must develop his own. This is preferably accomplished by the use of two or more different procedures.

The first nine glasses shown in Table II are glasses melted in a small continuous electric furnace under neutral to oxidizing conditions. These glasses are generally characterized by the presence of Se^0, Se^{4+}, and Se^{6+}.

Glass sample No. 10 was melted under reducing conditions. This glass contains practically all its selenium as Se^0; Se^{4+} and Se^{6+} are not present and only a trace of Se^{2-} was found. It was found necessary to modify the procedure slightly for the analysis of this sample. The residue obtained in filtering the samples prepared for Se^{4+} plus Se^{6+} was sluiced from the paper back into the dish used for dissolving the glass and 6 ml. HBr-Br mixture was added. The residue was digested in the cold for 10 minutes, and then refiltered through the original paper. This treatment was found to be necessary to recover the amount of Se^0 present. This experience may indicate that some of the results for Se^0 reported for the other glasses may be slightly low. This slight change in technique should be applied whenever there is any doubt about the total recovery of Se^0.

Although the writers did not encounter any glasses with appreciable amounts of selenide (Se^{2-}), a modification may be required for such glasses. It is suggested that for such glasses, after decomposing with HF, a stream of CO_2 be bubbled through the sample solution to "wash out" the H_2Se for a period of about 15 minutes. This would be done for samples prepared for the determination of Se^{4+}, and Se^{4+} plus Se^{6+}. A possible interference of Se^{2-} probably would be eliminated in this fashion.

V. Summary

In presenting these procedures, it has been the writers' aim to show that chemical analysis for the different valence states of some of the components of glasses is feasible. The results presented are intended to show only the possibilities of the analytical procedures, and not any relations of glass compositions and melting conditions. Certainly, not all the glass technologist's problems in the study of color and oxidation-reduction equilibria in glass can be solved by the analyst. It is the writers' opinion, however, that analytical resources have never been fully employed and can complement many of the physical methods used by the glass technologist.

Note on Calculation of Effect of Temperature and Composition on Specific Heat of Glass

by JOHN MOORE and D. E. SHARP

Research Department, Libbey-Owens-Ford Glass Company, Toledo, Ohio

The specific heats of glasses reported in the literature since 1951 were studied in relation to the Sharp-Ginther equation. It was found necessary to change the factors previously furnished for K_2O and B_2O_3. The other factors were found to be satisfactory when compared with the new measurements. It was discovered that glasses containing oxides of metals with atomic weights above 50 (e.g. iron, lead, and zinc) did not accurately fit the Sharp-Ginther equation over the complete temperature range desired. Provisional factors were calculated, however, for iron and manganese oxides from 0° to 600°C.

I. Introduction

In 1951 Sharp and Ginther[1] published a paper on the specific heat of glass in which they developed an empirical equation relating composition and temperature to the mean specific heat. The equation proposed was as follows:

$$c_m = \frac{at + c_0}{0.00146t + 1}$$

where t is the temperature in degrees centigrade, c_m is the mean specific heat from 0° to t°C., c_0 is the true specific heat at 0°C., and a is a constant characteristic of the glass.

Since the publication of this paper, a large number of additional measurements on glass have appeared in the literature. It was decided that these more recent data should be brought together and investigated to determine whether they fit the foregoing equation and, if so, whether more accurate values of a and c_0 might be obtained for the components.

II. The Equation with Different Temperature Bases

The Sharp and Ginther equation was set up for mean specific heats based on 0°C. Most of the experimental data in the literature are based on 20° or 25°C., and, although the conversion to the zero base is admittedly simple, it is even more convenient to express the equation in terms of the bases of the experimental data. This does not change the form of the equation, but merely requires the replacement of c_0 by $c_m|_0^{20}$, or $c_m|_0^{25}$, as the case may be. The proof of this is given in the Appendix (see p. 463).

III. Further Investigation of Reported Data

Of the experimental data reported since the publication of Sharp and Ginther's work, the most important concern three

Table I. Factors for Calculation of Mean Specific Heat of Glass From the Composition

Oxide	Old		Revised	
	a	c_0	a	c_0
SiO_2	0.000468	0.1657		
Al_2O_3	0.000453	0.1765		
CaO	0.000410	0.1709		
MgO	0.000514	0.2142		
Na_2O	0.000829	0.2229		
SO_2	0.00083	0.189		
K_2O	0.000335	0.2019	0.000445	0.1756
B_2O_3	0.000635	0.198	0.000598	0.1935
Fe_2O_3*			0.000380	0.1449
Mn_3O_4			0.000294	0.1498

* Good only to 600°C.

sodium and potassium glasses of Schwiete and Ziegler,[2] nine glasses described in three papers by Hartmann in collaboration with Brand[3] and with Kiessling,[4] and six commercial glasses from the Battelle Memorial Institute. These data, in addition to some previously known data, are discussed in the following paragraphs.

(1) Potassium and Sodium Oxides

In 1955, Schwiete and Ziegler[2] published specific heat data on three glasses whose compositions are given by the formulas $K_2O \cdot 2.5\ SiO_2$, $Na_2O \cdot 3.3\ SiO_2$, and $Na_2O \cdot CaO \cdot 6SiO_2$. A plot of $c_m (1 + 0.00146t)$ against the temperature gave good straight lines for all three glasses.

The constants a and c_0 previously calculated for K_2O were based on just one glass: White's microcline.[5] New constants therefore were calculated, using a weighted average of his and Schwiete's glasses. The results were values for a and c_0 of 0.000445 and 0.1756, respectively, compared with the old values of 0.000335 and 0.2019 (see Table I). To check the

[1] D. E. Sharp and L. B. Ginther, "Effect of Composition and Temperature on Specific Heat of Glass," *J. Am. Ceram. Soc.*, **34** [9] 260–71 (1951).

[2] H. E. Schwiete and Günther Ziegler, "Beitrag zur spezifischen Wärme der Gläser" (Contribution on Specific Heat of Glass), *Glastech. Ber.*, **28** [4] 137–46 (1955); *Ceram. Abstr.*, **1957**, September, p. 201a.

[3] (a) H. Hartmann and Herbert Brand, "Zur Kenntnis der mittleren spezifischen Wärmen einiger technisch wichtiger Glassorten" (Determination of Average Specific Heat of Some Technically Important Glass Types), *Glastech. Ber.*, **26** [2] 29–33 (1953); *Ceram. Abstr.*, **1953**, November, p. 188f.

(b) H. Hartmann and Herbert Brand, "Zur Kenntnis der mittleren spezifischen Wärmen einiger technisch wichtiger Glassorten: II, Die spezifischen Wärmen einiger Gläser von spezieller Zusammensetzung" (Determination of Average Specific Heat of Some Technically Important Glass Types: II, Specific Heat of Glasses of Special Composition), *Glastech. Ber.*, **27** [1] 12–15 (1954); *Ceram. Abstr.*, **1955**, March, p. 46d.

[4] H. Hartmann and Karl-Heinz Kiessling, "Zur Kenntnis der mittleren spezifischen Wärmen einiger technisch wichtiger Gläser: III, Die spezifische Wärme eines Barytglases" (Determination of Average Specific Heat of Some Technically Important Glass Types: III, Specific Heat of a Barium Glass), *Glastech. Ber.*, **30** [5] 186–88 (1957).

[5] (a) W. P. White, "Specific Heats of Silicates and Platinum," *Am. J. Sci.*, [4th Series], **28**, 334 (1909).

(b) W. P. White, "Silicate Specific Heats, 2d Series," *ibid.*, [4th Series], **47**, 1 (1919).

Table II. Specific Heat of Potassium Glasses

Glass	Temp. (°C.)	c_m (observed)	c_m (old factors)	$\delta \times 10^4$	(%)	c_m (new factors)	$\delta \times 10^4$	(%)	Observer
$K_2O \cdot 2.5\ SiO_2$	25–100	0.1924	0.1964	+40	2.1	0.1924	0	0	Schwiete and Ziegler*
"	25–300	.2148	.2145	−3	0.1	.2178	+30	1.4	"
"	25–500	.2351	.2264	−87	3.5	.2336	−15	0.6	"
"	25–700	.2516	.2351	−165	6.6	.2452	−64	2.5	"
"	25–900	.2619	.2414	−205	7.8	.2540	−79	3.0	"
"	25–1100	.2659	.2463	−196	7.4	.2607	−52	2.0	"
"	25–1300	.2690	.2503	−187	7.0	.2661	−29	1.1	"
				Avg.	4.9		Avg.	1.5	
Microcline	0–100	0.1919	0.1914	−5	0.3	0.1896	−23	1.2	White†
"	0–300	.2163	.2159	−4	0.2	.2164	−1	0.0	"
"	0–500	.2321	.2322	+1	0.0	.2343	+22	0.9	"
"	0–700	.2431	.2438	+7	0.3	.2469	+31	1.3	"
"	0–900	.2515	.2524	+9	0.4	.2563	+48	1.9	"
"	0–1100	.2598	.2591	−7	0.3	.2637	+39	1.3	"
				Avg.	0.2		Avg.	1.1	

* See footnote 2.   † See footnote 5.

calculations, specific heats were calculated for the two glasses with both sets of constants and were compared with the experimental values. The average per cent deviation was 2.8% for the old constants and 1.3% for the new constants. A tabulation of the results with the new and old constants is given in Table II.

In the same way, new constants were obtained for Na_2O. The values were 0.000824 and 0.2208, a change of less than 1% from the old values of 0.000829 and 0.2229. As this would cause only 0.2% change in the specific heat of a glass with 20% Na_2O, it is recommended that the old Na_2O constants be retained. The average deviation of Schwiete's sodium glasses from the calculated c_m was 1.9%.

(2) Boron Trioxide

There were two sources giving the specific heat of pure B_2O_3 glass. Thomas and Parks[6] determined the true specific heat to around 600°C., whereas Southard[7] determined the mean specific heat for temperatures up to 1500°C. Neither of these sets of measurements, however, gave a straight line when plotted as $c_m (0.00146t + 1)$ versus t. Thomas and Parks gave a straight line to approximately 200°C., from which was computed one set of values for a and c_0. Another set was calculated from the best straight line through Southard's data, and the old constants, which had been calculated from Thomas and Parks' data by a limiting process as described by Sharp and Ginther,[1] constituted a third set. Values for the mean specific heat of Pyrex-brand glass obtained from each of these sets were compared with values in the literature.[8]

The average per cent deviation of the calculated from the experimental specific heats was 2.0% with the old constants, 1.8% with those derived from Southard's data, and 1.4% with those derived from the straight-line portion of Thomas and Parks' data. Therefore, the new constants are recommended. The values are, for B_2O_3, $a = 0.000598$ and $c_0 = 0.1935$. The results of calculations using the new and old constants are shown in Table III.

(3) Hartmann's Glasses

Hartmann, in conjunction with Brand[3] and with Kiessling,[4] reported the specific heat of nine glasses. Four of the glasses contained only components for which a and c_0 have been determined. With these glasses, the specific heat calculated from the previously determined constants was compared with experimental values. The average per cent difference was 1.3%.

Of the remaining five glasses, two contained more than 15% PbO, one contained 6% ZnO, one 9% BaO, and one 23% Mn_3O_4 with 7% Fe_2O_3. All of these, it may be noted, are oxides of metals with atomic weights well above those previously studied. None could be made to fit the Sharp and Ginther equation satisfactorily over the temperature range 0° to 300°C.

The two lead glasses did not give a straight line when $c_m(1 + 0.00146t)$ was plotted against the temperature. One had a distinct break at 600°C., whereas the other could be considered either a smooth curve or line segments with breaks near 600° and 1100°C.

The glass containing iron and manganese also showed a sharp break at 600°C. Schwiete and Ziegler[2] attempted to explain this as due to the change of the Fe^{III} ion to FeO_4 ion. They then determined constants for their heat-content equation for Fe_2O_3 and Mn_3O_4, for use only below 600°C. From these constants were calculated values of a and c_0 that gave only a 1% average deviation up to 600°C. These still cannot be trusted, however, even in this range, as the original analysis of the glass was very imprecise (the sum of the components was 96%).

The remaining two glasses, containing BaO and ZnO, gave reasonably straight lines on a graph. However, upon the calculation of a and c_0, a negative c_3 was found in each case. This result was unacceptable and it was decided that these elements, also, must await further study.

From this evidence it appears that oxides of metals with atomic weights greater than about 50 cannot be fitted easily into the Sharp and Ginther equation. Whether this is because of a transition to different forms at higher temperatures, or some other reason, cannot be said at this time.

[6] S. B. Thomas and G. S. Parks, "Studies on Glass: VI, Some Specific Heat Data on Boron Trioxide," *J. Phys. Chem.*, **35**, 2091–2102 (1931); *Ceram. Abstr.*, **12** [4] 148 (1933).

[7] J. C. Southard, "Thermal Properties of Crystalline and Glassy Boron Trioxide," *J. Am. Chem. Soc.*, **63** [11] 3147–50 (1941); *Ceram. Abstr.*, **21** [2] 51 (1942).

[8] (a) C. W. Parmelee and A. E. Badger, "Determination of Mean Specific Heats at High Temperatures of Some Commercial Glasses," *Univ. Illinois Eng. Expt. Sta. Bull.*, **32** [271] 3–22 (1934); *Ceram. Abstr.*, **14** [11] 272 (1935).

(b) J. H. Hildebrand, A. D. Duschak, A. H. Foster, and C. W. Beebe, "Specific Heats and Heats of Fusion of Triphenylmethane, Anthraquinone, and Anthracene," *J. Am. Chem. Soc.*, **39**, 2293 (1917).

(c) "Experimental Measurement of Thermal Conductivities, Specific Heats, and Densities of Metallic, Transparent, and Protective Materials," Battelle Memorial Institute, Columbus, Ohio; AF Technical Report 6145, March 1954.

(d) T. DeVries, "Specific Heat of 'Pyrex' Glass from 25° to 175°C.," *Ind. Eng. Chem.*, **22** [6] 617–18 (1930); *Ceram. Abstr.*, **9** [9] 727 (1930).

Table III. Specific Heat of Pyrex-Brand Glasses

Observer*	Temp. (°C.)	c_m (observed)	c_m (old factors)	$\delta \times 10^4$	(%)	c_m (Southard factors)†	$\delta \times 10^4$	(%)	c_m (Thomas and Parks factors)‡	$\delta \times 10^4$	(%)
Parmelee and Badger	40–800	0.271	0.270	−10	0.4	0.274	+30	1.1	0.267	−40	1.5
"	40–1000	0.287	0.279	−80	2.8	0.284	−30	1.1	0.274	−130	4.5
Hildebrand *et al.*	20–100	0.1956	0.1988	+32	1.6	0.1944	−12	0.6	0.1962	+6	0.3
"	20–135	0.2011	0.2050	+39	1.9	0.2014	+3	0.1	0.2022	+11	0.5
"	20–200	0.2157	0.2153	−4	0.2	0.2129	−28	1.3	0.2123	−35	1.6
"	20–265	0.2252	0.2242	−10	0.4	0.2224	−28	1.3	0.2209	−43	1.9
Battelle	0–(−100)	0.1445	0.1430	−15	1.0	0.1319			0.1417	−28	1.9
"	0–0	0.1695	0.1725	+30	1.8	0.1650	−45	2.7	0.1705	+10	0.6
"	0–100	0.1895	0.1945	+50	2.6	0.1896	+1	0.1	0.1920	+25	1.3
"	0–200	0.2053	0.2115	+62	3.0	0.2087	+34	1.7	0.2086	+31	1.5
"	0–300	0.2176	0.2251	+75	3.5	0.2239	+63	2.8	0.2218	+42	1.9
"	0–400	0.2270	0.2362	+92	4.1	0.2362	+92	3.9	0.2327	+57	2.5
"	0–500	0.2343	0.2454	+111	4.7	0.2465	+121	4.9	0.2416	+73	3.0

Observer*	Temp. (°C.)	c_p (observed)	c_p (old factors)	$\delta \times 10^4$	(%)	c_p (Southard factors)†	$\delta \times 10^4$	(%)	c_p (Thomas and Parks factors)‡	$\delta \times 10^4$	(%)
DeVries	26.4	0.1859	0.1851	−8	0.4	0.1791	−68	3.8	0.1828	−31	1.7
"	71.0	0.2009	0.2034	+25	1.2	0.1995	−14	0.7	0.2006	−3	0.2
"	106.4	0.2111	0.2158	+47	2.2	0.2135	+24	1.1	0.2128	+17	0.8
"	127.4	0.2178	0.2224	+46	2.1	0.2209	+31	1.5	0.2192	+13	0.6
"	155.2	0.2261	0.2304	+43	1.9	0.2298	+37	1.7	0.2270	+9	0.4
"	172.9	0.2316	0.2351	+35	1.5	0.2351	+35	1.5	0.2316	0	0.0
				Avg.	2.0		Avg.	1.8		Avg.	1.4

* See footnote 8. † See footnote 7. ‡ See footnote 6.

APPENDIX

Different Temperature Bases

If mean specific heats are required based on some temperature T other than 0°C., the following refinement of the Sharp and Ginther equation may be used:

$$c_m\Big|_T^t = \frac{at + c_m\big|_0^T}{bt + 1}$$

For simplicity in deriving the equation, let the constant $c_m\big|_0^T$ be called d. The original Sharp and Ginther equation is

$$c_m\Big|_0^t = \frac{at + c_0}{bt + 1} \tag{1}$$

and the equation for changing from the base 0 to the base T is

$$c_m\Big|_T^t = \frac{t c_m\big|_0^t - T c_m\big|_0^T}{t - T}$$

or

$$c_m\Big|_T^t = \frac{t\, c_m\big|_0^t - Td}{t - T} \tag{2}$$

From equation (1),

$$d = \frac{aT + c_0}{bT + 1}$$

giving

$$bTd - c_0 = aT - d \tag{3}$$

Substituting equation (1) in (2),

$$c_m\Big|_T^t = \frac{1}{t - T}\left(t \cdot \frac{at + c_0}{bt + 1} - Td\right)$$

and rearranging,

$$c_m\Big|_T^t = \frac{at^2 - t(bTd - c_0) - Td}{(t - T)(bt + 1)}$$

Using equation (3),

$$c_m\Big|_T^t = \frac{at^2 - t(aT - d) - Td}{(t - T)(bt + 1)}$$

$$c_m\Big|_T^t = \frac{(t - T)(at + d)}{(t - T)(bt + 1)}$$

$$c_m\Big|_T^t = \frac{at + d}{bt + 1}$$

or

$$c_m\Big|_T^t = \frac{at + c_m\big|_0^T}{0.00146t + 1}$$

Thus, if the mean specific heat from some base T other than 0 is used, the only change in the equation is the transformation of the constant c_0 from the true specific heat at 0°C. to the mean specific heat between 0° and T°C. The constants a and b retain the same values.

Optical Properties of Diatomic Glasses

by A. WINTER

Institut d'Optique Théorique et Appliquée, Paris, France

The ability of elements to form glasses, the leading part played by the elements of Group VI (O, S, Se, and Te), and the possible influence of the elements of Group VII (F, Cl, Br, and I) are discussed. New glasses suggested by previous work were melted and the refractive index (n) and coefficient of dispersion (ν) of some of them were measured. Inspection of the n, ν plots of oxide, sulfide, selenide, and telluride glasses shows that the area corresponding to them extends toward high values of refractive index (n_{max} = 5.3) and low values of dispersion coefficient (ν_{min} = 4).

I. Introduction

A NUMBER of rules concerning glass formation were discussed by the writer in previous papers[1] and may be summarized as follows: (1) The ability to form bonds that lead to a vitreous network appears to follow the periodic arrangement of the elements. (2) Elements of Group VI of the periodic table (O, S,[*] Se, and Te) form glasses containing only one kind of atom.[†] These elements are identified as "self-vitrifying" elements and the simple monatomic glasses as "primary glasses." (3) Group VI elements form a vitreous network when mixed or chemically bound to each other. (4) Elements of Group VI also form diatomic glasses, i.e., glasses containing two kinds of atoms, when combined with the elements of Group III (B, Al, Ga, In, and Tl), Group IV (C, Si, Ge, Sn, and Pb), or Group V (N, P, As, Sb, and Bi). (5) Diatomic glasses are known to exist that are composed of elements belonging to Group VII (F, Cl, Br, and I) when associated with elements of Groups II, III, IV, and V or with a transition element. (6) Elements forming primary glasses (or in some cases the elements of Group VII) are of special importance in all vitrification phenomena, as no vitreous network can be formed without them. (7) Practically all commonly known glasses consist of networks composed of elements of Group VI with elements of Group III, IV, or V. (8) Elements of Groups III, IV, and V when combined with a glassforming element form complex glasses but do not form independent vitreous networks.

Experimental evidence for these rules is summarized in Table I. This table shows all diatomic glasses known to the writer that are formed by one self-vitrifying element and a cooperative element from Groups III, IV, or V. Primary glasses

and diatomic glasses formed by two self-vitrifying elements are also given.

II. Refractive Indices and Dispersion of Glasses

Refractive indices (n) and coefficients of dispersion (ν) of some of the glasses of Table I are given in Table II.

Some of the values were taken from the literature; all others represent measurements made in the writer's laboratory. All the writer's measurements were made by the prism method; for high refractive indices a thin prism was used.

(1) Monatomic Glasses

The refractive index of pure oxygen is unknown and the value given in Table II corresponds to the refractive index of liquid oxygen at its melting point. The refractive index of a liquid in many cases approximates the refractive index of a glass of the same composition.[‡]

The refractive indices of the four primary glasses are as follows:

Oxygen glass	Unknown, possibly a value of 1.24[2] (liquid oxygen = 1.22)
Sulfur glass	1.998
Selenium glass	2.9
Tellurium glass	~5

(2) Diatomic Glasses

The refractive indices of most single-oxide glasses are known; they range from 1.46 (boric oxide glass) to 2.45 (bismuth oxide glass). Some coefficients of dispersion also are known.

The refractive indices of some of the sulfide, selenide, and telluride glasses are also known. Observed refractive index maxima and the wave length at which these maxima are observed are as follows:

$$\text{Sulfide glasses, } n_{max} = 3.9 \text{ for } \lambda = 2.8\mu$$
$$\text{Selenide glasses, } n_{max} = 4.6 \text{ for } \lambda = 5.0\mu$$
$$\text{Telluride glasses, } n_{max} = 5.3 \text{ for } \lambda = 3.6\mu$$

These measurements, although not numerous, give an over-all view of the n, ν values of the diatomic glasses of Table II. In some cases the refractive index and the contribution of different elements to its value can be estimated from the periodic classification of the elements. Thus, for a given group, the refractive index increases with the period, e.g., oxides of Group IV or the oxide, sulfide, selenide, and telluride of Pb.

[1] (a) Aniuta Winter, "Les Formateurs des Verres" (Glass Formers), Compt. rend., 240 [1] 73–75 (1955); Ceram. Abstr., 1955, July, p. 120e.
(b) A. Winter, "Glass Formation," J. Am. Ceram. Soc., 40 [2] 54–58 (1957).
[*] A clear glass is formed when plastic sulfur is cooled below −100°C.
[†] No data are available on polonium, the last element of Group VI.

[‡] The refractive index of boric oxide glass is 1.465 at 20°C. The refractive index of boric oxide liquid is 1.418 at 600°C. A borosilicate composition of approximately 12 Na_2O, 9 Al_2O_3, 9 B_2O_3, and 70 SiO_2 has a refractive index of 1.522 at 20°C. and of 1.514 at 750°C.
[2] Aniuta Winter, "Sur l'Indice de Réfraction des Verres Binaires à Base d'Oxydes" (Refractive Index of Binary Glasses on an Oxide Basis), Compt. rend., 242 [25] 2931–33 (1956); Ceram. Abstr., 1956, November, p. 237d.

Table I. Mono- and Di-Atomic Glasses of Elements from Groups III, IV, V, and VI

Periodic group	Self-vitrifying elements			
	O	S	Se	Te
Group III				
B	(a)	(a)		
Al	(b), (c)			
Ga	(c)	(c)		
In	(c)	(c)		
Tl	(c)	(c)	(c)	(d)
Group IV				
C		(e)		
Si	(f), (g)		(h)	
Ge	(i)	(j), (u)		
Sn	(c)	(c)	(c)	(c)
Pb	(c)	(c)	(c)	(c)
Group V				
N		(c)		
P	(d)	(c)	(k)	
As	(l), (d)	(m), (t)	(t)	
Sb	(l), (n)	(m)	(c)	(c)
Bi	(n)	(c)	(c)	(c)
Group VI				
O	(o)	(p)	(c)	(q), (w)
S	(p)	(c)	(r)	(c)
Se	(c)	(r)	(s)	(c)
Te	(q), (w)		(c)	(q), (v)

^a Handbook of Chemistry and Physics, 35th ed., p. 488. Chemical Rubber Publishing Co., Cleveland, 1953. 3000 pp.; *Ceram. Abstr.*, **1954**, April, p. 80h.

^b L. Hiesinger and H. König, "Optik und Struktur Kathodenzerstaübter unter besonderer Berücksichtigung der Reaktions mit dem Restgas" (Optics and Structure of Cathode Sputtered Layers with Special Reference to Reactions with Residual Gas), *Festschr. 100 Jährigen Jubiläums W. C. Heraeus G.m.b.H.*, **1951**, pp. 376–92.

^c Prepared in writer's laboratory.

^d J. W. Mellor, Comprehensive Treatise on Inorganic and Theoretical Chemistry, Vols. VIII and IX. Longmans, Green & Co., Ltd., London, 1928 and 1929.

^e P. W. Bridgman, "Recent Work in Field of High Pressures," *Am. Scientist*, **31**, 1–35 (1943).

^f See p. 588 of footnote (a).

^g A. G. Smekal, "Structure of Glass," *J. Soc. Glass Technol.*, **35** [167] 411–20T (1951); *Ceram. Abstr.*, **1952**, September, p. 159b.

^h Alarich Weiss and Armin Weiss, "Kenntniss von Silicium-diselenid Glas" (Silicon Diselenide Glass), *Z. Naturforsch.*, **8b** [2] 104–105 (1953); *Ceram. Abstr.*, **1954**, January, p. 5j.

^i L. M. Dennis and A. W. Laubengayer, "Fused Germanium Dioxide and Some Germanium Glasses," *J. Phys. Chem.*, **30** [11] 1510–26 (1926); *Ceram. Abstr.*, **6** [2] 55 (1927).

^j Kuan-Han Sun, "Glassforming Substances," *Glass Ind.*, **27** [11] 552–54, 580–81 (1946); *Ceram. Abstr.*, **1947**, November, p. 222c.

^k P. L. Robinson and W. E. Scott, "Das System Phosphor-Selen" (The System Phosphorus-Selenium), *Z. anorg. u. allgem. Chem.*, **210**, 57–66 (1933).

^l E. Kordes, "Physikalisch-Chemische Untersuchungen über dem Feinbau von Gläser: III, Binäre und pseudobinäre Gläser ohne nennenswerte Packungseffecte" (Physicochemical Researches on Fine Structure of Glasses: III, Binary and Pseudo-binary Glasses Without Appreciable Packing Effect), *Z. physik. Chem.*, **B43** [3] 173–90 (1939); *Ceram. Abstr.*, **21** [8] 167 (1942).

^m Gustav Tammann (translated by R. F. Mehl), States of Aggregation. D. Van Nostrand Co., Inc., New York, 1925. 297 pp.

^n J. T. Randall and H. P. Rooksby, "X-Ray Diffraction and Structure of Glasses," *J. Soc. Glass Technol.*, **17** [67] 287–95T (1933); *Ceram. Abstr.*, **13** [3] 56 (1934).

^o W. Wahl, "Optische Untersuchung verfestigter Gase" (Optical Investigation of Solidified Gases), *Z. physik. Chem.*, **84**, 112–22 (1913); pp. 116–17.

^p M. Gerding, "Elastische Eigenschaften des Schwefel Trioxyd" (Elastic Qualities of Sulfur Trioxide), *Naturwissenschaften*, **25**, 251 (1937).

^q G. M. Toepler, "Bestimmung der volumänderung beim Schmelzen für eine Anzahl von Elementen" (Determination of Volume Change at Fusion for a Number of Elements), *Ann. Physik. Chem. (Wiedemann Volume)*, **53**, 363 (1894).

^r H. E. Merwin and E. S. Larsen, "Mixtures of Amorphous Sulfur and Selenium as Immersion Media for Determination of High Refractive Indices with the Microscope," *Am. J. Sci.*, [4th Series], **34**, 42–47 (1912).

^s See p. 586 of footnote (a).

^t Ginette Dewulf, "Verres Transparents dans l'Infrarouge" (Infrared-Transmitting Glasses), *Rev. opt.*, **33**, 513–18 (1954); *Ceram. Abstr.*, **1956**, April, p. 73g.

^u William Pugh, "Germanium: VIII, Sulfides of Germanium," *J. Chem. Soc.*, **1930**, pp. 2369–73.

^v G. W. Morey, Properties of Glass, p. 74. American Chemical Society Monograph Series, No. 77. Reinhold Publishing Corporation, New York, 1938. 561 pp.; *Ceram. Abstr.*, **18** [2] 48 (1939).

^w J. E. Stanworth, "Tellurite Glasses," *J. Soc. Glass Technol.*, **36** [171] 217–41T (1952); *Ceram. Abstr.*, **1953**, November, p. 190b.

Table II. Refractive Index (n) and Coefficient of Dispersion (ν) for Some Mono- and Di-Atomic Glasses

Periodic group	O		S		Se		Te	
	n	ν	n	ν	n	ν	n	ν
Group III								
B	1.456	58.7						
Al	~1.56*	55*						
Ga	~1.62*	~39*						
In								
Tl	~2.3*		2.9*(1)					
Group IV								
C			1.63 liq					
Si	1.458	67.7						
Ge	1.606	41.6						
Sn	1.78*	~30*						
Pb	2.15*	~16*	3.9*(2.5)		4.6*(5)		5.3*(3.6)	
Group V								
N								
P	1.516		~2.3*	~17.1*				
As	1.799		~2.5	~6.5				
Sb	2.09		2.9(0.8)	~4	>2*			
Bi	2.45							
Group VI								
O	1.22 liq				~1.76*		~2.35	
S			1.99*	15.2*	2.2	8.27		
Se	~1.76*		2.2	8.27	2.9	~5		
Te	~2.35						~5(4)	

* Measurements made in writer's laboratory (all other values from sources indicated in Table I except for the n values of O_2 and CS_2; these are from p. 2648 and p. 498, respectively, of footnote (a)).

Note: Refractive index is stated for $\lambda = 0.589\mu$ unless otherwise indicated by superscript.
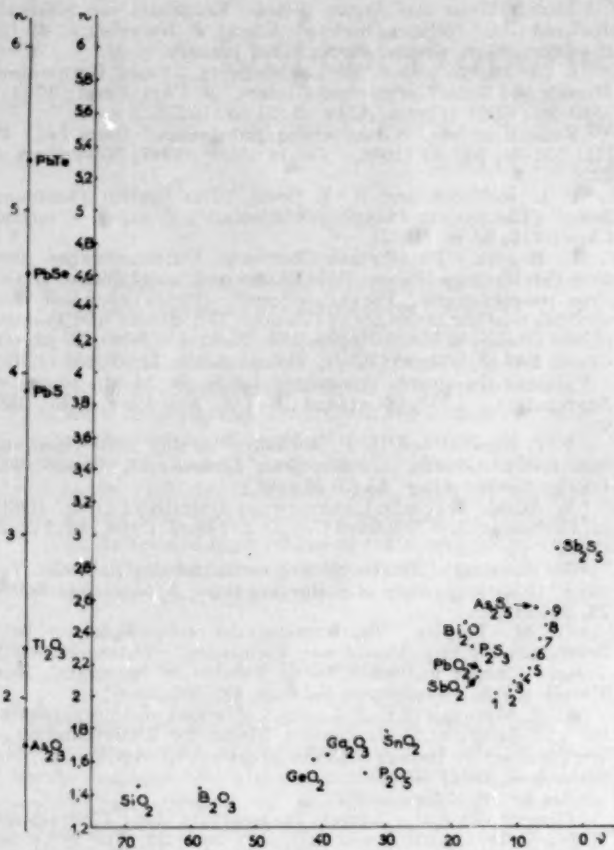
Fig. 1. Refractive indices and coefficients of dispersion of diatomic glasses. (1) 1 Se, 9 S; (2) 2 Se, 8 S; (3) 3 Se, 7 S; (4) 4 Se, 6 S; (5) 5 Se, 5 S; (6) 6 Se, 4 S; (7) 7 Se, 3 S; (8) 8 Se, 2 S; and (9) 9 Se, 1 S.

The influence of each self-vitrifying element on the values of n and ν also can be estimated graphically. Each glass may be plotted as a point in the n, ν plane as in Fig. 1.

Oxide glasses have the lowest refractive index and the highest coefficients of dispersion. Sulfide and selenide glasses appear above the oxide glasses in the direction of higher refractive indices and lower coefficients of dispersion. Only the refractive index is known for telluride glasses and the position is indicated on the refractive index axis. Several other glasses for which ν has not been determined are also marked on this axis.

The refractive index of a complex glass is always higher than that of the parent primary glass; thus, the refractive index of the parent primary glass represents the lower limit of the refractive indices of the complex glasses derived from it. Figure 1 represents only diatomic glasses; complex glasses would cover a larger area.

It is probable that complex sulfide, selenide, and telluride glasses would array themselves around the points of Fig. 1 and new n, ν values would be obtained. Thus, Table II indicates the direction in which the optical properties of glasses may be broadened.

III. Summary

Values for the refractive indices and coefficients of dispersion of monatomic and diatomic glasses composed of oxygen, sulfur, selenium, and tellurium are presented. The relation of the optical properties of such glasses to those of mixtures of these elements of Group VI with elements from other groups of the periodic table is discussed. The predominant effect of these glassforming elements on the optical properties of mixed glasses is emphasized.

Detection of Reaction Products Between Water and Soda-Lime-Silica Glass

by FRANKLIN FU-YEN WANG and F. V. TOOLEY

* Department of Ceramic Engineering, University of Illinois, Urbana, Illinois

A simulated extract approach was used to ascertain the identities of the products of reaction between a soda-lime-silica glass and water. The reaction between the glass and water was studied at 90°C. with reaction time periods up to 4 hours. The products of this reaction were found to be sodium metasilicate, calcium metasilicate, and metasilicic acid.

I. Introduction

THE reaction between glass and water* is affected by several factors: the composition of the glass, the ratio of glass surface area to volume of water, and the temperature, pressure, and time duration of the reaction. The course of the reaction is affected further by the accumulating reaction products. To study the effects of the reaction products on the reaction, the reaction products must first be identified.

II. Experimental Approach

To identify the reaction products, i.e., the constituents of the glass extracts,† a simulated extract approach was adopted. A simulated extract was prepared to approximate the exact composition of the glass extract by dissolving specified substances of definite quantities in water. When this simulated extract gave the same reaction rate on the fresh glass surfaces as that of the glass extract, it was concluded that the glass extract had the same constituents as the simulated extract and that the reaction products between glass and water were identical to the substances that were used in preparing the simulated extract.

III. Procedure

The composition, on a weight basis, of the glass used in this study was SiO_2 74, Na_2O 14, and CaO 12%. The procedures adopted for the preparation and exposure of the glass samples for the reactions were the same as The American Ceramic Society Tentative Method No. 1.[1]

* The term "water" refers to distilled water only throughout this paper.

† The term "glass extract" used in this paper refers to the liquid portion of the glass-water system. Glass extracts contain the products of reaction between glass and water.

[1] "Report of Committee on Chemical Durability of Glass," *Bull. Am. Ceram. Soc.*, 14 [5] 181–84 (1935).

A fresh glass sample was used for each reaction. Ten-gram glass samples, after digestion in 50 ml. of attacking solution at $90° \pm 0.5°C$. for a definite period of time, were filtered through a screen. The sodium, calcium, and silicon contents of these extracts were determined quantitatively.

The amount of sodium in the glass extracts was determined by the flame photometric method. The direct intensity method[2] was the only method employed. A flame photometer of the Perkin-Elmer model 52-C with an acetylene burner was used.

The volumetric determination of calcium in solutions, using Versenate as a chelating agent, was adopted. Modifications were made to the method described by Cheng and Bray.[3] Calcium was determined by using a standard magnesium solution to titrate the test solution, where excess Versenate solution was added. The dye Erichrome Black–T was used as an indicator, and the end point occurred when the color of the solution changed from blue to wine red.

The silicon content was colorimetrically determined by the molybdenum blue method.[4] Light transmittances of the solutions were measured by a Lumetron photolometer with a 650 mμ filter. Beer's law was applied.

In this study, the accuracy of the sodium determination was of the order of ± 0.02 mg. per 50 ml. of solution; of the silicon, ± 0.02 mg. per 50 ml. of solution; and of the calcium, ± 0.1 mg. per 50 ml. of solution.

IV. Results

The net amounts of sodium, calcium, and silicon‡ extracted from the glass by water, by glass extracts A and B, and by simulated extracts A_1, A_2, and A_3 are presented graphically in Figs. 1 and 2.

Examination of these data brings out the following points:

(1) The glass extracts reacted with the glass at a different rate than did water.

(2) The glass extracts, containing the same proportions of sodium, silicon, and calcium, reacted with the glass with the same reaction rate.

(3) Solutions of the same chemical composition, but of different constitutions, reacted with the glass with varied reaction rates.

(4) A solution (simulated extract A_1) was synthesized to approximate very nearly the glass extract (glass extract A) in the rate of reaction with the glass.

(5) The products of the reaction between the glass and water were found to be sodium metasilicate, calcium metasilicate, and metasilicic acid.

[2] "Instruction Manual, Flame Photometer, Model 52-C," Perkin-Elmer Corporation, Norwalk, Connecticut, 1952.

[3] K. L. Cheng and R. H. Bray, "Tests for Magnesium and Calcium in Plant Materials," *Soil Sci.*, 72 [12] 449–58 (1951).

[4] Maurice Codell, Charles Clemency, and George Norwitz, "Colorimetric Determination of Silicon in Titanium Alloys," *Anal. Chem.*, 25 [10] 1432–34 (1953).

‡ The net amounts of sodium, calcium, and silicon were obtained by subtracting the amount in the reactant solution from the total amount in the final liquid portion.
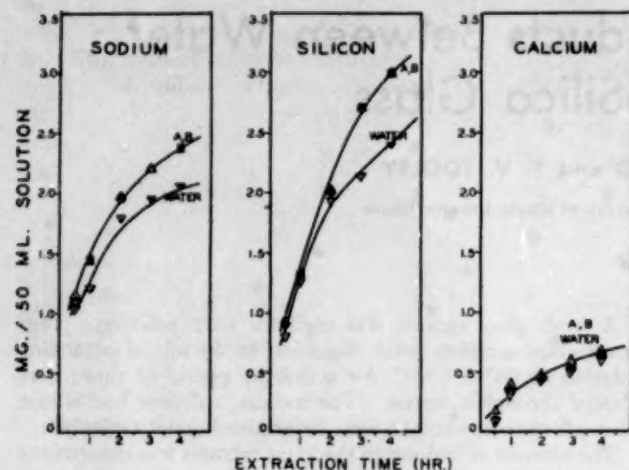
Fig. 1.   Rates of reaction between glass and water and between glass and extracts A and B.
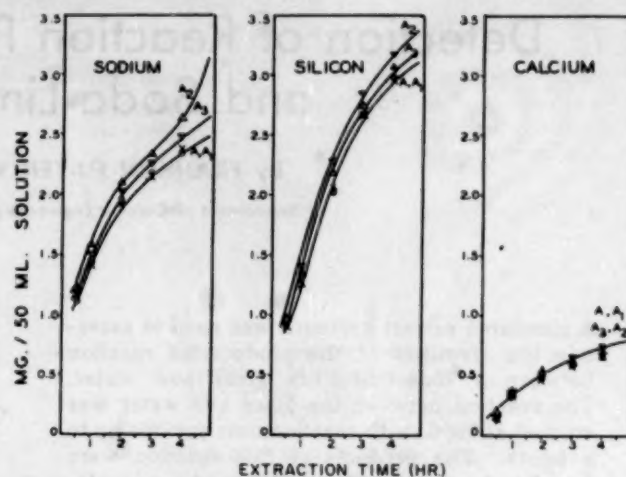

Fig. 2.   Rates of reaction between glass and glass extract A and between glass and simulated extracts A_1, A_2, and A_3.

V. Discussion

A distinction was drawn between the chemical constitution and the chemical composition of a solution.   A given solution was found by chemical analyses to contain definite amounts of sodium ions, calcium ions, and silicate ions.   These quantities represented the chemical composition of the solution.   The constituents from which these ions originated represented the constitution of the solution.   In other words, reaction products represent the chemical constitution, and ions of the reaction products represent the chemical composition of the glass extract.

The results as presented in Fig. 1 indicate that the reaction rates for the glass and water were different from the reaction rates for the glass and the glass extracts.   It shows the expected result, namely, that ions extracted from the glass affected the course of the reaction between the glass and water.

Glass extracts A and B* reacted with the glass with the same reaction rate, as shown in Fig. 1.   These two extracts had the same proportions of sodium, silicon, and calcium but different total amounts.   The fact that identical rates resulted from the reactions of glass extracts A and B on the glass suggested that in very dilute solutions the ratios of the constituents played greater roles in affecting the reaction than did the mere quantities of the constituents.

Simulated extracts A_1, A_2, and A_3 represented solutions of the same composition but of different constitution.†   Their different rates of reaction with the glass, as shown in Fig. 2, indicate that the constitution was more influential than was the composition of the reactant solution on the course of the reaction.   Figure 2 also indicates that simulated extract A_1 approximated very nearly glass extract A in its rate of reaction with the glass.

By the logic that different constitutions gave different reaction rates, such as in the case of simulated extracts A_2, and A_3 and A, it was reasoned that a solution having the same composition as a given extract and giving a similar reaction rate could be interpreted as approximating the same constitution as that of the extract.   Glass extract A therefore was considered to approximate most closely the constitution of simulated extract A_1 rather than the constitution of either A_2 or A_3.

A review of the interionic attraction theory of solutions explains how two solutions of the same composition may differ in constitution.

An electrolyte, when dissolved in water, is ionized into cations and anions.   Each ion is surrounded by an ionic sphere of another ionic species with opposite charge, and these are held together by interionic attraction forces.   These forces differ in magnitude, as ionic species and ionic concentrations vary.   When the attraction force becomes negligible, the ion becomes dissociated.   Solutions of electrolytes therefore can exhibit complete ionization but incomplete dissociation.[5]   Dilute solutions have greater degrees of dissociation, and solutions of strong electrolytes are considered to dissociate completely.

A solution that is prepared by mixing several constituents together will have an ultimate constitution when it reaches equilibrium.   This final constitution may well be different from the designated constitution of this solution, which is described by the added constituents.   It is evident that two solutions of the same composition will have the same final

---

* Glass extracts A and B were obtained from the reactions between the glass and water at 90°C. at different reaction periods. The amounts of glass and water used in each were different. Glass extracts A and B were found to have the same proportions and different amounts of sodium, silicon, and calcium.

COMPOSITION OF GLASS EXTRACT A

Sodium: 0.35 mg. per 50 ml. of solution
Silicon: 0.30 mg. per 50 ml. of solution
Calcium: 0.08 mg. per 50 ml. of solution

COMPOSITION OF GLASS EXTRACT B

Sodium: 0.60 mg. per 50 ml. of solution
Silicon: 0.52 mg. per 50 ml. of solution
Calcium: 0.14 mg. per 50 ml. of solution

† Simulated extract A_1 was prepared from sodium metasilicate, metasilicic acid, and calcium metasilicate.   Its composition was the same as that of glass extract A.

Simulated extract A_2 was prepared from sodium hydroxide, metasilicic acid, and calcium hydroxide.   Its composition was the same as that of glass extract A.

Simulated extract A_3 was prepared from sodium metasilicate, sodium hydroxide, metasilicic acid, and calcium metasilicate. Its composition was the same as that of glass extract A.

[5] I. M. Kolthoff and H. A. Laitinen, pH and Electro-Titrations, 2d ed., pp. 1–21.   John Wiley & Sons, Inc., New York, 1941.   190 pp.

constitution at equilibrium but may have different designated (initial or intermediate) constitutions.

In this study of the reaction between glass and water, it is the constitution of the glass extract at its initial stage, or its designated constitution, that draws special attention. The constituents in the glass extract at that stage are actually the products of the reaction between glass and water.

Glass extract A has the same designated constitution as simulated extract A_1, inasmuch as both solutions gave the same rate of reaction with glass.

It was concluded that the reaction products from glass and water were sodium metasilicate, calcium metasilicate, and metasilicic acid because simulated extracts made from these constituents paralleled most closely the rate curves obtained with the actual extracts.

Although hydroxyl ions were found in the sodium metasilicate solution,[6] sodium hydroxide was considered as an intermediate, rather than a major, reaction product.

$$SiO_3{}^{2-} + 2H_2O = H_2SiO_3 + 2OH^- . \qquad (1)$$

$$2Na^+ + SiO_3{}^{2-} = Na_2SiO_3 \qquad (2)$$
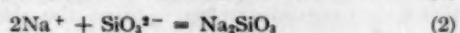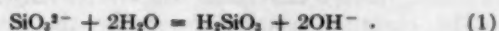
Sodium hydroxide dissociates completely in aqueous solutions. Hydroxyl ions, thus dissociated, tend to favor reaction (1) in the reverse direction, i.e., toward the left side of the reaction. Sodium ions then combine with silicate ions to form sodium metasilicate as indicated in reaction (2). The degree of hydrolysis of sodium metasilicate is not considered, however, to be unity. For a 0.1 N sodium metasilicate solution, Harman[6] found that the degree of hydrolysis was 4.8%, and for a 0.01 N solution, Bogue[7] found its degree of hydrolysis to be 27.8%; therefore, sodium hydroxide was considered as an intermediate, rather than a major, reaction product.

Similar considerations applied to the calcium metasilicate solutions.

Metasilicate salts were favored over other silicates for several reasons. Sodium metasilicate was reported to require

a smaller heat of formation than other silicates such as pyrosilicates, disilicates, and hydrates of metasilicates.[8] Glasses of metasilicate compositions dissolve readily in water.[9] Moreover, no aggregation is apparent in metasilicate solutions.[9]

Silicon could not exist in solutions as free silica or silica gel in the concentration ranges that were studied. Data by Correns[10] and by Iler[11] showed that in the pH range 8 to 11 the solubility of silica in aqueous solutions exceeded greatly the studied silicon concentrations. Metasilicic acid therefore was considered as one of the reaction products between glass and water.

It was recognized, however, that as the reaction between the glass and water proceeds, the identities of the reaction products may change. Their identities could be detected, however, by a study similar to that outlined in this paper. This type of study conceivably could be extended to glasses of varied compositions and attacking agents of all kinds.

VI. Summary

(1) A simulated extract approach was used to ascertain the identities of the reaction products between a soda-lime-silica glass and water.

(2) A solution (simulated extract A_1) was made to approximate very nearly glass extract A.

(3) The products of the reaction between the glass and water were found to be sodium metasilicate, calcium metasilicate, and metasilicic acid.

[6] (*a*) R. W. Harman, "Aqueous Solutions of Sodium Silicates: II, Transport Numbers," *J. Phys. Chem.*, **30** [3] 359–68 (1926); *Ceram. Abstr.*, **5** [6] 193 (1926).
(*b*) R. W. Harman, "Aqueous Solutions of Sodium Silicates: IV, Hydrolysis," *J. Phys. Chem.*, **30** [8] 1100–11 (1926); *Ceram. Abstr.*, **5** [10] 328 (1926).
(*c*) R. W. Harman, "Aqueous Solutions of Sodium Silicates: VII, Silicate Ions; Electrometric Titrations, Diffusion, and Colorimetric Estimation," *J. Phys. Chem.*, **31** [4] 616–25 (1927); *Ceram. Abstr.*, **6** [6] 240 (1927).
(*d*) R. W. Harman, "Aqueous Solutions of Sodium Silicates: VIII, General Summary and Theory of Constitution; Sodium Silicates as Colloidal Electrolytes," *J. Phys. Chem.*, **32** [1] 44–60 (1928); *Ceram. Abstr.*, **7** [7] 493 (1928).
[7] R. H. Bogue, "Hydrolysis of the Silicates of Sodium," *J. Am. Chem. Soc.*, **42** [12] 2575–82 (1920); abstracted in *J. Am. Ceram. Soc.*, **4** [4] 311 (1921).

[8] J. G. Vail, Soluble Silicates, Vol. I, Chemistry, pp. 72–73, 96–98, 107–108, 134, 174. American Chemical Society Monograph Series, No. 116. Reinhold Publishing Corp., New York, 1952. 357 pp.; *Ceram. Abstr.*, **1953**, January, p. 18*e*.
[9] R. V. Naumann and P. Debye, "Light-Scattering Investigations of Carefully Filtered Sodium Silicate Solutions," *J. Phys. & Colloid Chem.*, **55** [1] 1–9 (1951); *Ceram. Abstr.*, **1954**, July, p. 135*d*.
[10] C. W. Correns, "Solubility of Silica in Weakly Acid and Alkaline Solutions," *Chem. Erde*, **13**, 92–96 (1940/1941).
See also Wilhelm Eitel, Physical Chemistry of the Silicates, 3d ed., p. 365, footnote 5. University of Chicago Press, Chicago, 1954. 1592 pp.; *Ceram. Abstr.*, **1955**, January, p. 20*g*.
[11] R. K. Iler, Colloid Chemistry of Silica and Silicates, pp. 15–25. Cornell University Press, Ithaca, N. Y., 1955. 324 pp.; *Ceram. Abstr.*, **1956**, May, p. 107*g*.

Dielectric Loss and the States of Glass

by D. W. RINEHART

Glass Division Research Laboratories, Pittsburgh Plate Glass Company, Creighton, Pennsylvania

Specimens of commercial plate glass were compacted at 900°F. and cooled slowly to room temperature. Power loss was determined as the specimens were reheated and quenched from various temperatures within the range 200° to 1200°F. Irreversible increases in tan δ were found to occur at quenching temperatures below the transformation range as well as within it. The increases below the transformation range are considered to result from changes in the Na$^+$ ion distribution, established during cooling, among the interstitial holes. As shown by density measurements, the increases within the transformation range are associated with configurational changes in the basic silica network. A glass property that depends on the mobility of a constituent ion is determined by at least two states: (1) a configurational state of the silica network and (2) a distribution state of the mobile ion. The extent of compaction is clearly indicated in a family of curves of tan δ vs. quenching temperature, with compacting time as a parameter.

I. Introduction

THE behavior of inorganic glass as a dielectric depends primarily on its chemical composition. The relation of glass constituents to dielectric properties has been the subject of numerous investigations[1] designed to aid in developing glasses to fulfill specific dielectric requirements as well as to contribute to the general conception of glass constitution.

Although glass properties, in general, are fixed principally by composition, they have specific significance only with reference to that state or combination of states that characterize the glass at the time of measurement. It is known that most properties depend to some appreciable degree on the past history of the glass, particularly on its cooling history through the interval of temperatures commonly referred to as the transformation range.[2] Because of the relaxation nature of the configurational rearrangements

that occur within this temperature range, the glass fails to make complete transformations during normal cooling to the more compact states characteristic of the lower temperatures. As a result, high-temperature states may be retained in the glass and the properties observed at room temperature correspond to those of the "frozen-in" states. Inasmuch as the transformations that take place are time-dependent, the room-temperature properties become dependent on the rate of cooling through this critical temperature range.

The range of temperatures below the transformation region is sometimes referred to as the elastic range.[3] In this range properties that are transformed at higher temperatures usually are considered to show none of the thermal hysteresis that governs their behavior in the transformation range. Such a property is said to be perfectly reversible through these lower temperatures. It always will have essentially the same room-temperature value, irrespective of the rate at which the glass is cooled through this region.

Winter[2] has shown the existence of a continuum of equilibrium states within a critical range of temperatures by observing the transformation of refractive index for a borosilicate crown glass in this temperature range. Tool and Hill[4] increased the coefficient of thermal expansion (between room temperature and 200°C.) of a borosilicate composition by as much as 10% by quenching the glass from elevated temperatures. Kreidl and Weidel[5] observed an increase of more than 1% in the room-temperature density of an optical borosilicate glass as a result of annealing. These are but a few of the many studies that demonstrate the dependence of such properties as refractive index, coefficient of thermal expansion, and density on the thermal history within the transformation range of temperatures.

The electrical conductivity of glass, which involves principally the transport of alkali ions, has been observed to depend also on the thermal history of the glass. This fact was established by Foussereau[6] and by others,[7] who showed that

[1] For example:
(a) Louis Navias and R. L. Green, "Dielectric Properties of Glasses at Ultra-High Frequencies and Their Relation to Composition," *J. Am. Ceram. Soc.*, **29** [10] 267–76 (1946).
(b) H. Moore and R. C. De Silva, "Study of Electrical Properties of Alkali-Lime-Silica Glasses, Some Containing Boric Oxide or Alumina, in Relation to Glass Structure," *J. Soc. Glass Technol.*, **36** [168] 5–55T (1952); *Ceram. Abstr.*, **1952**, November, p. 201b.
(c) J. M. Stevels, "Some Experiments and Theories on the Power Factor of Glasses as a Function of Their Composition, II," *Philips Research Repts.*, **6** [1] 34–53 (1951); *Ceram. Abstr.*, **1953**, March, p. 40j.
(d) J. M. Stevels, "Dielectric Losses in Glass," *Philips Tech. Rev.*, **13** [12] 360–70 (1952).

[2] Aniuta Winter, "Transformation Region of Glass," *J. Am. Ceram. Soc.*, **26** [6] 189–200 (1943).
[3] (a) Francis Naudin, "Strains and the Transformation Region of Glass: III, Dynamic Study of Refractive Index and Birefringence as Function of Temperature," *Verres et Réfractaires*, **6** [4] 209–18 (1952); translated by K. G. Eells and N. M. Brandt in *Glass Ind.*, **35** [11] 603–608, 628 (1954); for abstract see *Ceram. Abstr.*, **1953**, May, pp. 79–80.
(b) Francis Naudin, "Strains and the Transformation Region of Glass: IV, Static Study at Constant Temperature of Refractive Index and Birefringence as a Function of the Time," *Verres et Réfractaires*, **6** [5] 282–89 (1952); translated by K. G. Eells and N. M. Brandt in *Glass Ind.*, **35** [12] 666–70, 688 (1954); for abstract see *Ceram. Abstr.*, **1953**, August, p. 138c.
[4] A. Q. Tool and E. E. Hill, "On the Constitution and Density of Glass," *J. Soc. Glass Technol.*, **9** [35] 185–207T (1925); *Ceram. Abstr.*, **5** [2] 47 (1926).
[5] N. J. Kreidl and R. A. Weidel, "Annealing of 517:645 Borosilicate Optical Glass: II, Density," *J. Am. Ceram. Soc.*, **35** [8] 198–203 (1952).
[6] G. Foussereau, "Influence de la Trempe sur la Résistance Électrique du Verre" (Influence of Tempering on Electrical Resistance of Glass), *Compt. rend.*, **96**, 785 (1883).
[7] (a) M. J. Mulligan, J. B. Ferguson, and J. W. Rebbeck, "Electrochemical Behavior of Silicate Glasses, III," *J. Phys. Chem.*, **32** [5] 779–84 (1928); *Ceram. Abstr.*, **8** [1] 21–22 (1929).
(b) J. T. Littleton and W. L. Wetmore, "Electrical Conductivity of Glass in Annealing Zone as Function of Time and Temperature," *J. Am. Ceram. Soc.*, **19** [9] 243–45 (1936).

Fig. 1. Curve showing normal rate of cooling of annealed glass specimens.

TIME (HR.)
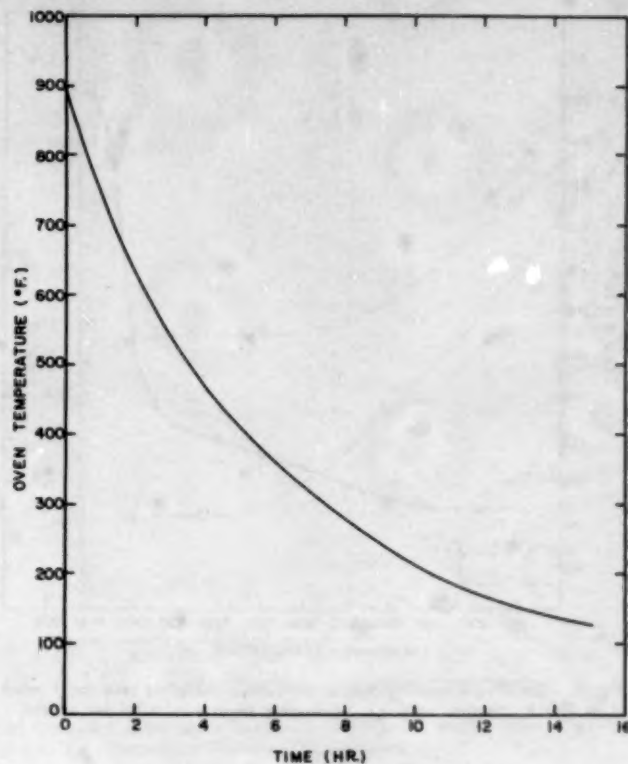
annealing is accompanied by a decrease in electrical conductivity. The conductivity of strained or quickly cooled glass has been found to be as much as several times that of annealed glass.

Inasmuch as the electrical conductivity of glass depends on the transport of certain ions within the glass, and as the room-temperature dielectric loss depends on the mobilities of similar ions, it is to be expected that the loss values also would be influenced by the thermal history of the glass. McDowell and Begeman[8] observed that the power factor of two borosilicate glasses was lowered by relieving the existing strain through annealing. Humphrys and Morgan[9] observed that the dielectric constant of several borosilicate glasses decreased continuously as the stabilizing temperature from which the specimens were quenched was lowered. In earlier work carried out in this laboratory, Imalis[10] showed that the dielectric loss of tempered plate glass is appreciably greater than that of the annealed product. Somewhat more recently, Naudin[11] observed that an increase in refractive index, as brought about by heat-treatment, was generally accompanied by a decrease in dielectric loss angle.

It is of some interest to know in more detail the effect of thermal history on the dielectric properties of glass and the significance of this relation as it concerns present-day theories of glass constitution. In this paper the writer presents the results of studies that have been carried out to show some of the effects of heat-treatment on the power loss of regular commercial plate glass.

II. Experimental Procedure

Disks of commercial plate glass approximately 2 in. in diameter were used as the dielectric specimens in this study. They were cut from ground and polished plates with a nominal thickness of $\frac{5}{64}$ in. By analytical determination the oxides in this glass were shown to be present in the following amounts: SiO_2 71.5, Na_2O 13.5, CaO 11.8, MgO 2.4, SO_3 0.5, Fe_2O_3 0.12, and Al_2O_3 0.20 weight %.

Six groups of specimens were studied, each with a different initial thermal past brought about by different degrees

of reannealing of the commercial glass. Changes in room-temperature tan δ then were observed as the specimens of each group were held for 1 hour* at various temperatures through the range 200° to 1200°F. and quenched in air. The method of quenched samples has been used extensively in studying the behavior of various properties in a range of temperatures corresponding to the transformation range. This method takes advantage of the fact that when glass is cooled quickly from temperatures in this range, it lacks sufficient time to revert appreciably to lower-temperature states, and the room-temperature measurements subsequently carried out reflect in large measure the state of the glass at the temperature from which it was quenched.

Using the substitution method of measurement, the loss determinations were made with General Radio equipment at an impressed frequency of 1000 cycles per second, a temperature of 78°F., and a relative humidity of less than 20%.

III. Results and Discussion

Before heat-treating, specimens of the first group studied were annealed by holding at 900°F. for 1 week and allowing them to cool gradually to room temperature inside an electric annealing oven, after the power input was cut. The temperature as a function of cooling time for these specimens is shown in Fig. 1. The specimens were then reheated at

[8] L. S. McDowell and Hilda Begeman, "Behavior of Glass as a Dielectric in Alternating Current Circuits: I, Relation of Power Factor and Dielectric Constant to Conductivity," *Phys. Rev.*, 31 [3] 476–81 (1928); *Ceram. Abstr.*, 7 [8] 533 (1928).
[9] J. M. Humphrys and W. R. Morgan, "Effect of Composition and Thermal History on Dielectric Constants of Soda-Borosilicate Glasses," *J. Am. Ceram. Soc.*, 24 [4] 123–30 (1941).
[10] O. Imalis; unpublished work.
[11] Francis Naudin, "Dielectric Constant and Loss Angle of Glass," *Compt. rend.*, 232 [9] 831–32 (1951); *Ceram. Abstr.*, 1951, July, p. 119j.

* To avoid excessive sample distortion above 1100°F., the holding time was limited to 10 minutes. Tests have shown that the maximum loss value is attained within this shorter heating time. Changes in the structural state apparently occur very rapidly at these temperatures.
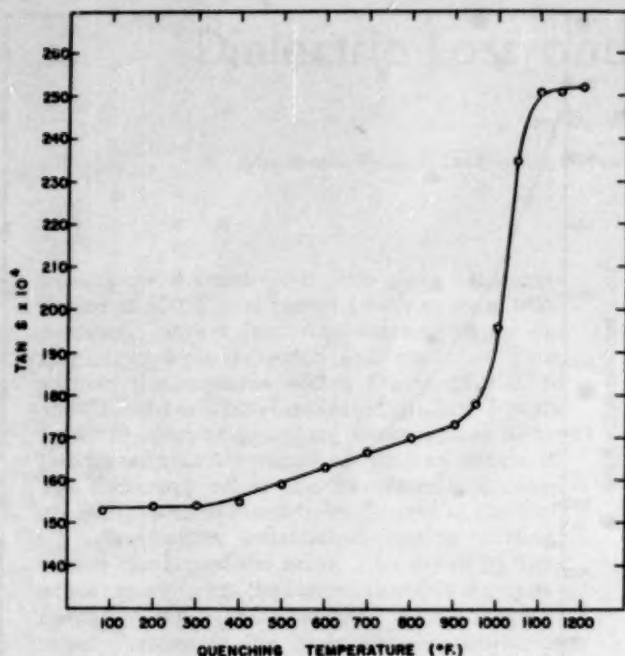
Fig. 2. Tan δ vs. quenching temperature for plate glass held for 1 week at 900°F. Normal cooling. Measuring frequency, 1 kc. per second.

Fig. 3. Tan δ vs. quenching temperature for plate glass cooled at differen rates after 1 week at 900°F. (A) Normal cooling and (B) temperature reduced 50°F. every 24 hours. Measuring frequency, 1 kc. per second.

various temperatures in the range 200° to 1200°F. and quenched. The tan δ vs. quenching temperature relation established by this set of heat-treated specimens is that shown in Fig. 2.

As shown in Fig. 2, tan δ begins to depart from its initial value when quenching temperatures of about 300° to 400°F. are reached. It continues to increase with quenching temperature at a somewhat constant rate through an interval extending to about 900°F. Here, tan δ suddenly assumes a much higher rate of increase with quenching temperature. This increased rate is maintained for nearly 200° and then falls off very abruptly.

The curve established by this series of heat-treatments demonstrates not only a marked degree of dependence of loss on thermal history but is particularly significant in these two respects:

(1) It indicates the existence of temperature-dependent states in an interval of temperatures corresponding to that in which configurational changes in the structural state are known to occur.

(2) It shows an irreversible behavior of dielectric loss at temperatures below the transformation range and the existence of a kind of temperature-dependent state for these temperatures.

Dielectric loss in glass, at the given temperature and frequency, is attributed mostly to the energy dissipated by the Na^+ ions as they migrate within the glass in response to the applied electric field. Any change brought about in the glass as a result of thermal treatment which will influence this migration would be reflected in the loss measurements. The tan δ vs. quenching temperature curve of Fig. 2 indicates that, as far as the Na^+ ion mobility is concerned, transformations of two types have taken place.

Considering the effect on tan δ of thermal history at temperatures below 900°F., it was shown that slower cooling through this region will reduce the final room-temperature loss value and will change the slope of the tan δ vs. quenching temperature curve in this range. This dependence on cooling rate is shown in Fig. 3. The top curve is that shown in Fig.
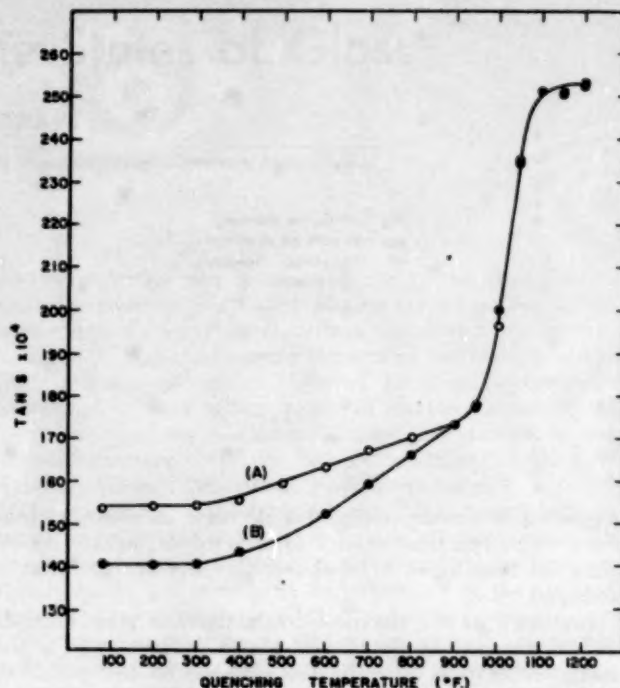
2 which represents the group of specimens that received normal cooling. The bottom curve was established by a second group of specimens that also were held at 900°F. for 1 week but were cooled below 900° by reducing the temperature in steps of 50° every 24 hours until room temperature was reached. The two curves converge to a common tan δ value at about 900° and become coincident throughout the transformation range.

The existence of temperature- and time-defined states below 900°F. is further demonstrated by the tan δ vs. quenching temperature curves of Fig. 4. Both specimen A (Fig. 4 (A)) and specimen B (Fig. 4 (B)) were held at 900° for 1 week. Specimen A had been cooled to room temperature at the normal rate, whereas specimen B had received the prolonged step cooling described earlier. Both were subjected to identical quenching treatments within this temperature range. Each was quenched following a 1-hour heating period at successively higher temperatures. Upon reaching the 900° maximum temperature, the specimens were then quenched at successively lower temperatures through this range. For the latter series of quenchings the temperature was reduced from one quenching temperature to the next lower one at the normal cooling rate. Room-temperature loss measurements followed each quenching. As shown in Fig. 4 (A), the loss data obtained as a result of the series of quenchings carried out on specimen A fall on a single curve. This coincidence shows that for the particular cooling cycle used, described as normal cooling, a continuous array of temperature-dependent states is established which limits the degree of sodium ion migration. The tan δ vs. quenching temperature relation established for specimen B by the series of quenchings is shown in Fig. 4 (B). The curve obtained during cooling lies considerably above that established during heating. The thermal history of specimen B in this temperature range apparently has been erased, for its tan δ curve during cooling is essentially the same as that of specimen A.
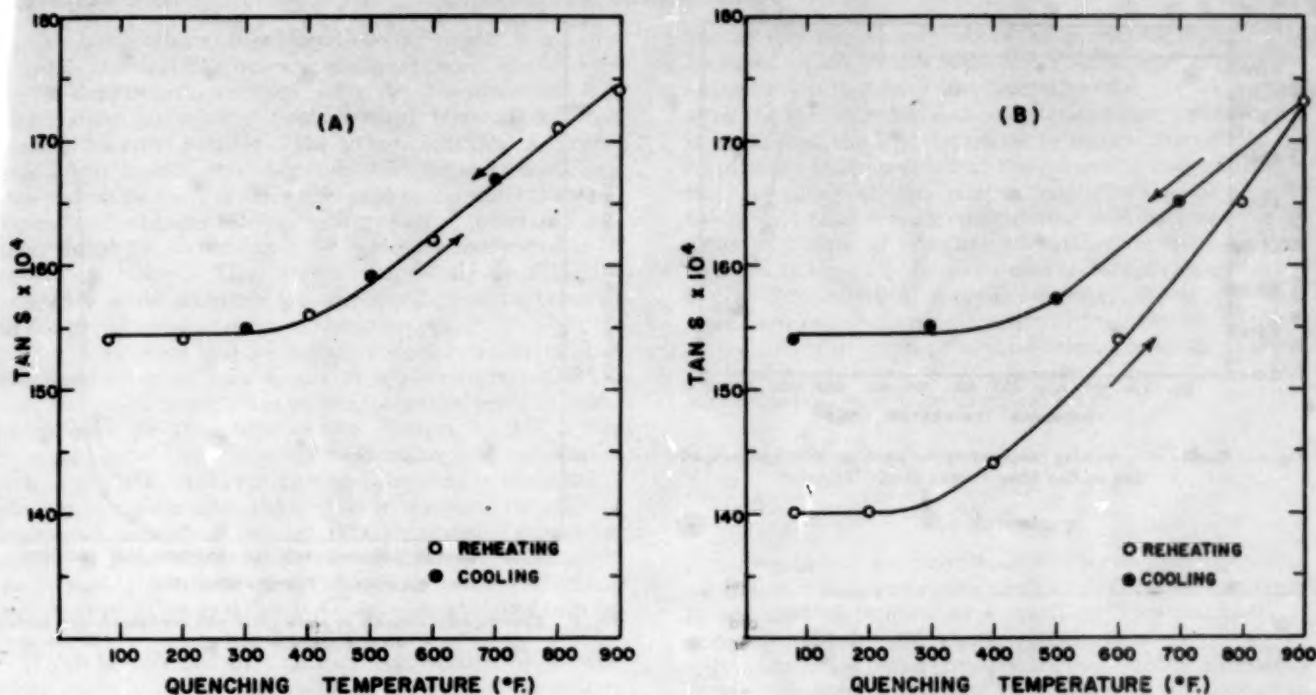
Fig. 4. Tan δ vs. quenching temperature during reheating and cooling of annealed plate glass specimens. (A) Normal cooling after 1 week at 900°F. and (B) prolonged step cooling after 1 week at 900°F. Measuring frequency, 1 kc. per second.

Table I. Values of Room-Temperature Dielectric Loss for Plate Glass Resulting from Different Degrees of Annealing and from Different Quenching Treatments

Group →	(a)	(b)	(c)	(d)	(e)	(f)
Holding time at 900°F. Cooling rate	None	1 hr. Normal	5 hr. Normal	24 hr. Normal	1 week Normal	1 week Prolonged step
Tan δ × 10⁴	216	179	171	165	153	140
After quenching (°F.)						
200	216	179	172	165	154	140
300	215	180	173	165	154	140
400	216	183	176	166	155	143
500	215	186	180	170	159	
600	216	194	186	174	163	152
700	217	197	189	179	167	159
800	216	202	194	182	170	166
900	209	207	200	187	173	173
950	209	211	204	196	178	177
1000	217	223	220	218	196	200
1050	238	237	237	238	235	233
1100	249	249	249	253	251	251
1150	253	253	254	255	251	250
1200	252	251	255	254	252	253

The effect that the degree of compaction has on the loss vs. quenching temperature relation of plate glass is shown by measurements carried out on six groups of specimens. Group (a) represents the original commercial glass without further compaction. Groups (b), (c), and (d) were compacted at 900° for periods of 1, 5, and 24 hours, respectively. Below 900° they were cooled at the normal rate. Groups (e) and (f) are those that were used in establishing the curves of Fig. 3. Descriptions of the various groups and the changes in room-temperature tan δ induced in each by the quenching treatments are summarized in Table I. The tan δ vs. quenching temperature relation is shown graphically for
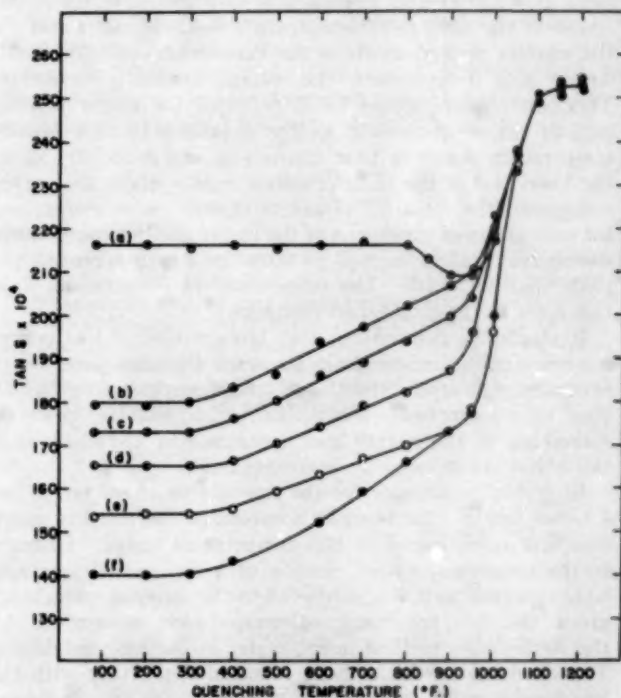
Fig. 5. Tan δ vs. quenching temperature for plate glass specimens with different degrees of annealing. (a), commercial annealing; (b), (c), (d), and (e), 1 hour, 5 hours, 24 hours, and 1 week, respectively, at 900°F. with normal cooling; (f), 1 week at 900°F. with prolonged step cooling. Measuring frequency, 1 kc. per second.

each group in the curves of Fig. 5. The extent of compaction is evidenced in this family of curves by a lowering of the tan δ value which corresponds to that temperature at which configurational changes in structure first begin to
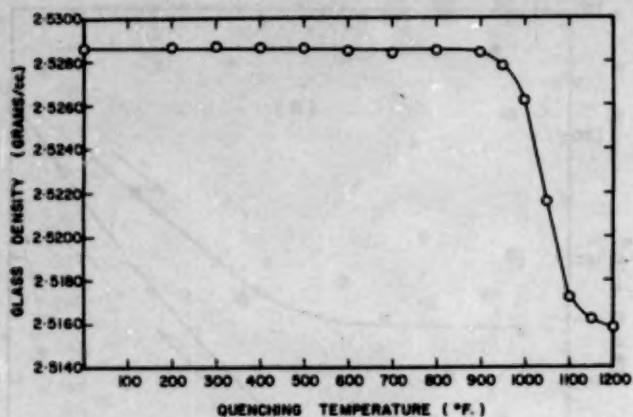
Fig. 6. Density vs. quenching temperature for plate glass with prolonged step cooling after 1 week at 900°F.
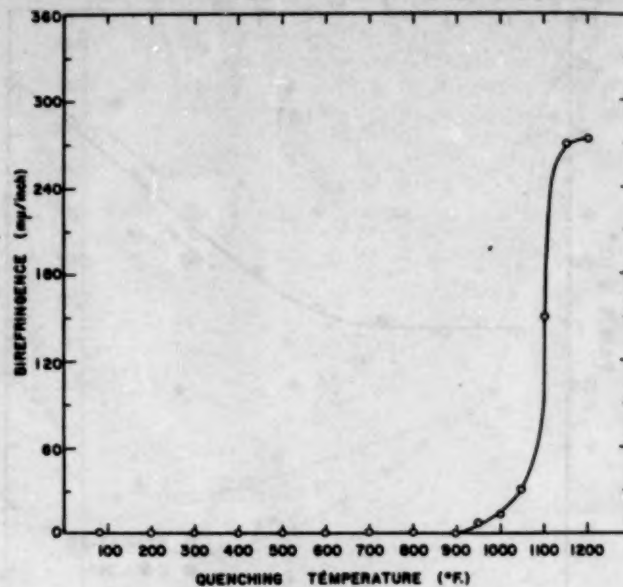
Fig. 7. Birefringence induced in plate glass with prolonged step cooling after 1 week at 900°F.

appear. Curve (*a*) shows that the initial commercial glass has considerable thermal history below 900° as well as above it. At holding temperatures above 800° the indicated decrease in tan δ is probably caused mainly by a gradual reversion of higher-temperature states frozen in during manufacture. For the groups of specimens that received the same cooling, greater compaction is responsible for a decrease in the final room-temperature value of tan δ and for the relative displacements of the various curves below 900°. Above this temperature the curves gradually converge. This convergence would be more rapid for longer heating periods before quenching, as the approach to new higher-temperature states is time consuming and especially so at the lower end of the transformation region where the curves are spread the most. The points at 900° were determined for each group of specimens at the end of the holding periods, during reannealing, as well as after the 1-hour reheating periods that followed. The coincidence of these values fixes this point in the established relations.

It should be pointed out that the established loss curves are not equilibrium curves in the sense that the glasses were necessarily at equilibrium at all temperatures from which they were quenched. They clearly demonstrate, however, something of the nature and magnitude of the changes in tan δ that are induced by heat-treatment.

In trying to account for the irreversible character of tan δ below 900°F., the reversible nature of thermal expansion was first investigated in this temperature range. Changes in the room-temperature density of a step-cooled specimen were observed as it was subjected to the series of quenchings given the loss specimens. Densities were determined by the Archimedes method, using water as the buoyant liquid. The specimen used had been reannealed together with the loss specimens of group (*f*). The results of this study, as shown in Fig. 6, indicate that within the limits of experimental error, which is approximately $\pm 2 \times 10^{-4}$ gm. per cc., no significant dimensional changes have been retained in the glass at quenching temperatures below about 900°F. Thus, no evidence has been found to support any dependence of tan δ variations on changes in structural configuration below the critical temperature. Other tests have shown that permanent strains are not introduced in similarly reannealed specimens by quenching until the quenching temperatures have reached the second interval defined by the loss experiments. The results of such tests are shown in Fig. 7.

It is apparent that some room-temperature properties of well-annealed glass are unchanged by heat-treatment within the lower temperature interval whereas others are not. Properties that differ in this respect would not be expected to show good correlation if a part of this interval were included in the thermal treatments employed in varying the magnitude of these properties. In showing the inadequacy of the fictive temperature concept to specify the structural state of a glass, Ritland[12] has shown that a plot of electrical resistivity vs. refractive index for "rate" and "soak" samples of a borosilicate crown glass is not a continuous curve. Rather, two curves corresponding to the two types of thermal treatments employed seem to be indicated by the data, with the points for the rate specimens falling at a higher resistivity level than those for the soak specimens. It is undoubtedly true that direct-current electrical conductivity depends on thermal history within the range of temperatures below the transformation region, just as the present work has shown tan δ to be. The effective mobility of the current-carrying ions in the rate samples apparently has been lowered more, as these specimens were cooled slowly through temperatures extending below that from which the soak specimens were rapidly cooled.

IV. Interpretation

Most of the power loss occurring in a soda-lime-silica glass, in the audio range of frequencies and at room temperature, can be attributed to the motion of certain sodium ions, which have sufficient thermal energy to move across the potential barriers separating certain interstitial positions that they may occupy. Any change in the size distribution of these interstitial holes would affect the sodium ion mobility and consequently the dielectric loss. This apparently is what happens in the transformation range during the quenching treatments. Because of the relaxation nature of glass

12 H. N. Ritland, "Limitations of Fictive Temperature Concept," *J. Am. Ceram. Soc.*, **39** [12] 403–406 (1956).

in this temperature range, rapid cooling results in an irreversible increase in room-temperature volume as indicated by the density measurements of Fig. 6. The interstitial-hole distribution accordingly tends toward larger holes with smaller potential barriers. The sodium ions, which become less tightly bound, move between positions more freely and dissipate more energy. It would thus be expected that configurational changes leading to increased or decreased volume would be accompanied by correspondingly higher or lower loss values. This is shown to be the case by the similarity of the dielectric loss and specific volume behavior in the transformation range of temperatures.

If it is assumed that no configurational rearrangement of the basic silica network occurs at temperatures below the transformation range, some other explanation must be found to account for the observed loss changes in this region. It would seem that the room-temperature loss can change only if the heat-treatment to which the glass is subjected in this range redistributes the sodium ions among the existing interstices in such a manner that the number remaining mobile at room temperature will be different. This would mean that a greater number of sodium ions must remain mobile at room temperature to produce the observed increase in loss that results from more rapid cooling below 900°F.

It can be assumed that for each temperature below 900° there exists a unique equilibrium distribution of the sodium ions among the interstitial holes of the glass. Such a distribution may be considered to be analogous to the equilibrium configurational states of the transformation range of temperatures. For any given hole size there is a minimum amount of thermal energy that an ion must have to enable it to move out of the influence of this hole. If the thermal energy of an ion suddenly drops below the minimum amount for escape, it becomes trapped in the hole. The smallest holes, which have the greatest trapping tendencies, would have their maximum populations of sodium ions when the distribution approached that which would exist at equilibrium. Thus, a larger number of ions would tend to be continuously immobilized with a slower rate of cooling below 900°, as indicated by the curves in Fig. 3. At the conclusion of the cooling cycle, there are still many untrapped sodium ions located in the larger holes that remain mobile and continue to contribute to dielectric loss.

When the annealed specimens are now reheated to some temperature T within the temperature range under consideration, those ions that were previously trapped during cooling through temperatures below T are released and redistributed in some manner which approaches the characteristic distribution for that temperature. The dielectric loss at this temperature would, of course, be considerably increased in accordance with the greater number of more energetic ions that have now become mobile. If the temperature is suddenly reduced to room temperature, as is the case in quenching, the Na^+ ions tend to become trapped in the distribution that prevailed at the quenching temperature T. But quenching at this temperature allows fewer ions to be trapped than was the case during slow cooling from T. Thus, as a result of reheating and quenching annealed glass it seems likely that the room-temperature dielectric loss is increased by virtue of a smaller number of Na^+ ions that have been immobilized as a result of this treatment. Such a mechanism is proposed as an explanation of that part of the characteristic tan δ vs. quenching temperature curve which lies below the transformation range.

V. Summary

Studies have been carried out which establish experimental evidence that irreversible changes in dielectric loss occur in annealed plate glass as a result of heat-treatments at temperatures below the transformation range.

It is concluded that a property of glass which is determined by the migration of ions through the network will depend on at least two states that characterize the glass:

(1) A configurational state that specifies the structural arrangement of the silica network and determines the size and distribution of the interstitial holes in which the ions are located.

(2) A distribution state that defines the way in which the mobile ions are distributed among the holes.

The first, which depends on thermal history within the transformation range of temperatures, affects both specific volume and ionic mobility. The second, which depends on thermal history through temperatures below the transformation region, appears to affect only ionic mobility.

High-Temperature-Resistant Ceramic Adhesives

by HENRY G. LEFORT and DWIGHT G. BENNETT

Department of Ceramic Engineering, University of Illinois, Urbana, Illinois

Ceramic adhesives were developed for bonding metal in the operational range 500° to 1000°F. When glassy-bond adhesives were suitably prepared and properly applied to types 302 and 17-7 PH stainless-steel specimens, shear strengths of the order of 2000 lb. per sq. in. were obtained at a test temperature of 800°F. and shear strengths of more than 800 lb. per sq. in. were obtained at 1000°F. Factors affecting adhesive strength included thermal-expansion fit between ceramic adhesive and metal, metal or metallic oxide additions to the adhesive glass, and the use of metal screens of selected wire and mesh dimensions as carriers in the adhesive joint. The ceramic adhesive could be applied to a precipitation hardenable type of stainless steel during part of the precipitation hardening treatment, which included heating the metal for various times at temperatures up to 1750°F.

I. Introduction

BONDING metal to metal with ceramic-type adhesives is under study as a result of demands for adhesive materials that will function at elevated temperatures. Specific interest in ceramic adhesives is for use in metal joining and honeycomb sandwich construction in aircraft and missiles that develop high skin temperatures while operating at high speeds in the earth's atmosphere.

The advantages of organic adhesive bonding in airframes, instead of welding, soldering, brazing, or riveting, have been brought out by Epstein.[1] Organic adhesives, however, lose their strength as temperature increases and currently are not usable as structural adhesives much above 400°F. As it was desirable to extend the use of adhesives into the hot zone of operation, it was natural to turn to ceramic-type adhesives because of their relative stability at elevated temperatures.

The property of a high-temperature adhesive that is most desired is high strength for extended periods of time at elevated temperatures. The adhesive must also have good thermal-shock properties and be resistant to moisture. For economic reasons and tolerance factors of the fabricated parts, the maturing temperature of the adhesive should be as low as possible.

In this investigation the method used for evaluating ceramic adhesives was to determine their shear strength from room temperature to 1000°F. The lap-joint specimens used conformed to military specifications for heat-resistant organic adhesives.[2]

Preliminary work indicated that air setting or maturing materials such as oxychlorides, sodium silicate cements, and ceramic oxide-organic mixtures lost their strength with tem-
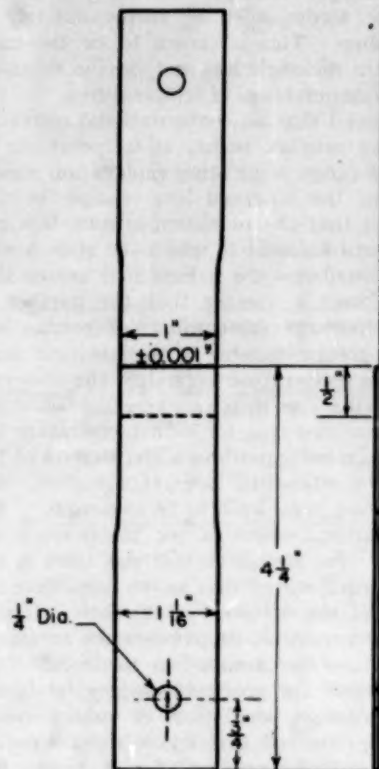
Fig. 1. Shear specimen with lap joint.

perature increase or had poor moisture resistance. Porcelain enamels showed promise in bonding ingot iron shear specimens. Modified ceramic coatings bonded stainless-steel shear specimens successfully when the thermal expansion of the coating properly approached that of the metal. Such adhesives decreased in effectiveness when their thermal expansion fell considerably below that of the metal.

In this paper, ceramic adhesives of the glassy-bond type that showed promise, either alone or with metal or metal oxide additions in the frit or in the slip, are discussed.

II. Experimental Procedures

(1) Preparation and Bonding of Specimens

(A) Metal Preparation: Several hundred shear strength specimens of ingot iron and types 302 and 17–7 PH stainless steel were cut from sheet stock. One end of each specimen was machined to the tolerances indicated in Fig. 1, so that acceptable overlap joints might be formed. The ingot iron varied from 0.030 to 0.071 in. in thickness (22 to 15 U. S. Standard gauge); types 302 and 17–7 PH stainless steel varied from 0.047 to 0.060 in. (18 to 16 gauge). The overlap areas of all specimens were lightly sandblasted to remove scale

[1] George Epstein, Adhesive Bonding of Metals. Reinhold Publishing Corp., New York, 1954. 218 pp.

[2] "Adhesives, Heat Resistant, Airframe Structural, Metal to Metal," Parts 4.3.4.1 and 4.3.4.2. Military Specifications MIL–A–8431 (USAF), 2 March, 1955.

Table I. Mill Batch and Fineness of Milling of Porcelain Enamels Used as Ceramic Adhesives

| | | Mill composition | | | | |
Adhesive	Frit	X-brand clay	Borax	MgCO₃	Water	Fine-ness*
High-expansion enamel	100	7	0.5		45	5.4
Intermediate-expansion enamel	100	7	0.5		45	2.1
Low-expansion enamel	100	7	0.5	0.25	36	1.5

* Grams residue on a 200-mesh screen from a 50-ml. sample.

and dirt; there was little or no warpage of the overlap area.

(*B*) *Development of Ceramic Adhesive and Preparation:* It appeared early in the investigation that the thermal expansion of the ceramic adhesive and metal played an important part in the quality of bond that could be developed. To check further on this, three porcelain enamels, having mean linear thermal expansions of approximately 10, 11, and 12 × 10⁻⁶ cm. per cm. per °C., respectively, up to 400°C., were used as adhesives for ingot iron. The expansion for the ingot iron was approximately 14.5 × 10⁻⁶ cm. per cm. per °C. up to 400°C. The enamels were prepared in the conventional manner from commercially available ground-coat frits. Table I gives the mill batch and fineness of milling of these enamel adhesives.

Table II. Frit and Ceramic Adhesive Compositions Used for Bonding Stainless Steels

(*A*) Frit Composition (parts by weight)

	UI 117	UI 1036	UI 1037	UI 1038	UI 1040	UI 1041	UI 1042	UI 1043	UI 1045
Potash feldspar	34.8	32.2	32.2	32.2	32.2	32.6	32.6	32.6	32.6
Borax	9.2	8.5	8.5	8.5	8.5	8.6	8.6	8.6	8.6
Soda ash	16.5	14.1	14.1	14.1	14.1	11.0	11.0	11.0	11.0
Soda niter	4.2	6.3	6.3	6.3	6.3	11.6	11.6	11.6	11.6
Flint		0.3	0.3	0.3	0.3	0.2	0.2	0.2	0.2
Barium carbonate	0.7	1.7	1.7	1.7	1.7	1.8	1.8	1.8	1.8
Whiting	8.0	7.4	7.4	7.4	7.4	7.3	7.3	7.3	7.3
Zinc oxide	9.2	8.5	8.5	8.5	8.5	8.6	8.6	8.6	8.6
Sodium silico-fluoride	4.2	3.9	3.9	3.9	3.9	3.9	3.9	3.9	3.9
BaO·P₂O₅	6.9	6.5	6.5	6.5	6.5	6.5	6.5	6.5	6.5
88% vanadium pentoxide	2.5	2.7	2.7	2.7	2.7	2.6	2.6	2.6	2.6
Aloxite	3.8	3.8	3.8	3.8	3.8	3.7	3.7	3.7	3.7
Fe₂O₃		4.1			3.1	1.6			1.3
NiO			4.1		0.7		1.6		0.2
Cr₂O₃				4.1	0.3			1.6	0.1

(*B*) Ceramic Adhesive Slip Compositions (parts by weight)

Adhesive No.	Frit	Colloidal silica	Water	Powdered aluminum	Powdered copper	Carbonyl iron	Carbonyl nickel	Powdered silicon
UI 117–50	100	2	50					
UI 1036–1	100	2	35					
UI 1037–1	100	2	35					
UI 1038–1	100	2	35					
UI 1040–1	100	2	35					
UI 1041–1	100	2	35					
UI 1042–1	100	2	35					
UI 1043–1	100	2	35					
UI 1045–1	100	2	35					
UI 117–52	65.8	1.3	32.9	5				
UI 117–53	65.8	1.3	32.9		5			
UI 117–54	65.8	1.3	32.9			5		
UI 117–55	65.8	1.3	32.9				5	
UI 117–56	65.8	1.3	32.9					5

Fig. 2. Rack for alignment and support of specimens during development of adhesive bond. Bonding pressure, up to a maximum of 50 lb. per sq. in., is applied normal to the specimens as indicated by the arrow.

In further consideration of the significance of the adhesive fit, modifications of a ceramic coating having a thermal expansion considerably above that of most ceramic coatings ordinarily designed for application to stainless steel or other high-alloy metals were used in this study to bond stainless-steel shear specimens. The basic ceramic adhesive, UI 117–50, from which all other adhesives discussed in this paper were derived, consisted of a high-expansion frit (mean linear thermal expansion, 14.1 × 10⁻⁶ cm. per cm. per °C. up to 400°C.), designated UI 117, suspended in water with 2% colloidal silica. Such a small amount of silica used instead of 5 or 6% clay resulted in a reduced maturing temperature for the adhesive and did not appreciably change the thermal expansion of the adhesive from that of the frit. The compositions of this frit and adhesive are given in Table II.

King, Tripp, and Duckworth[3] found that porcelain enamels that contained oxides of the metals on which the enamel would be applied exhibited better adherence than the same enamel with no such addition. As it appeared that such findings might be directly applicable to ceramic-adhesive bonding, a series of adhesives was made that consisted of frits based on UI 117 with additions of the oxides of the metals contained in stainless steel smelted into the frit. It was hoped that these additions would improve the adherence of the resulting adhesives and in so doing increase the over-all shear strength of the adhesive bond. Frit and adhesive compositions for this series are given in Table II.

An additional series of compositions was made by stirring fine metal powders into wet-milled ceramic adhesive UI 117–50. It was thought that such additions might improve the shear strength and thermal-shock resistance of the adhesive. These compositions also are given in Table II.

(*C*) *Ceramic Adhesive Bonding:* At least six shear specimens were dipped in each of the respective adhesives so that about 1 in. of the machined end of each specimen was coated. They were then placed in a horizontal position and allowed to dry. The dried specimens were placed on a firing rack in such a manner that an overlap of ¹/₂ in. resulted as indicated in Figs. 1 and 2. A stack of six specimens was assembled with

³ B. W. King, H. P. Tripp, and W. H. Duckworth, "Nature of Adherence of Porcelain Enamels to Metals"; presented at the Fifty-Eighth Annual Meeting, The American Ceramic Society, New York, N. Y., April 25, 1956 (Enamel Division, No. 23).
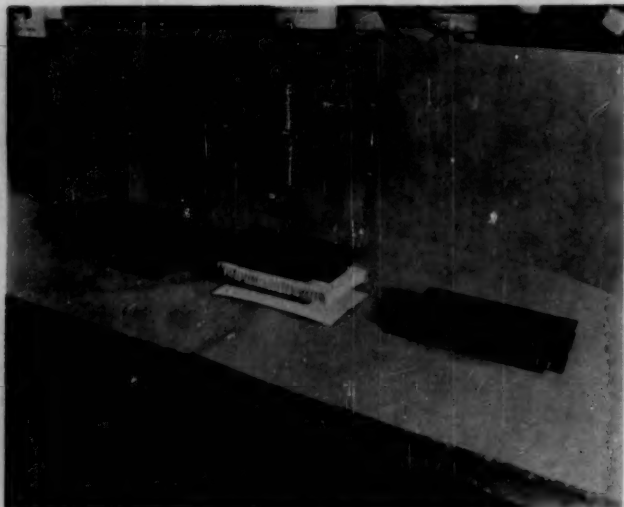
Fig. 3. Honeycomb panel assembly of type 17–7 PH stainless steel. Left, expanded view of heat-scaled components; center, expanded view of adhesive-coated components; and right, finished panel after bonding of ceramic adhesive and heat-hardening treatment for the steel.

Fig. 4. Shear specimen and split-tube heating furnace.

spacers being used to hold them in position. A bonding pressure of 50 lb. per sq. in. was applied to the stack in a direction perpendicular to the individual planes of the specimens as indicated in Fig. 2. As there was a tendency for the molten adhesive to be squeezed out during bonding, a thin foil of stainless steel was used between the specimens to keep them from sticking.

Shear specimens were fired for 20 minutes in place on the firing rack under the bonding pressure. The high-expansion porcelain enamel used as an adhesive was fired at 1500°F., the intermediate-expansion enamel at 1550°F., and the low-expansion enamel at 1600°F. to bond ingot iron. Ceramic adhesive UI 117–50 and all modifications of it were fired at 1750°F. on types 302 and 17–7 PH stainless steel. The firing at 1750°F. was especially applicable for type 17–7 PH stainless steel specimens as that temperature is part of one of the heat-hardening treatments which may be selected to precipitation harden that alloy.

The bonded specimens were allowed to cool in place under the bonding pressure until they were within a few hundred degrees of room temperature. The bonding pressure was then removed; the type 302 stainless-steel specimens then were ready for testing and the type 17–7 PH stainless-steel specimens were ready for further heat hardening.

All shear specimens of type 17–7 PH stainless steel were precipitation hardened to condition RH 950 from received condition A according to the schedule given in Table III. Note particularly that in the RH 950 hardening treatment one of the steps in heating permits the application of the ceramic adhesive completely within the time-temperature limits of the specification.

Stainless-steel screen was used as a carrier in the adhesive bonded joint during the later portion of the investigation.

Table III. Metal Precipitation Hardening Treatment of Type 17–7 PH Stainless Steel from Condition A to Obtain Condition RH 950

(1) Heat at 1750°F. ± 15°F. for 20 minutes
(2) Cool to 60°F. within 1 hour after removal from furnace
(3) Cool at −100°F. for 8 hours
(4) Harden at 950°F. ± 10°F. for 1 hour; air cool
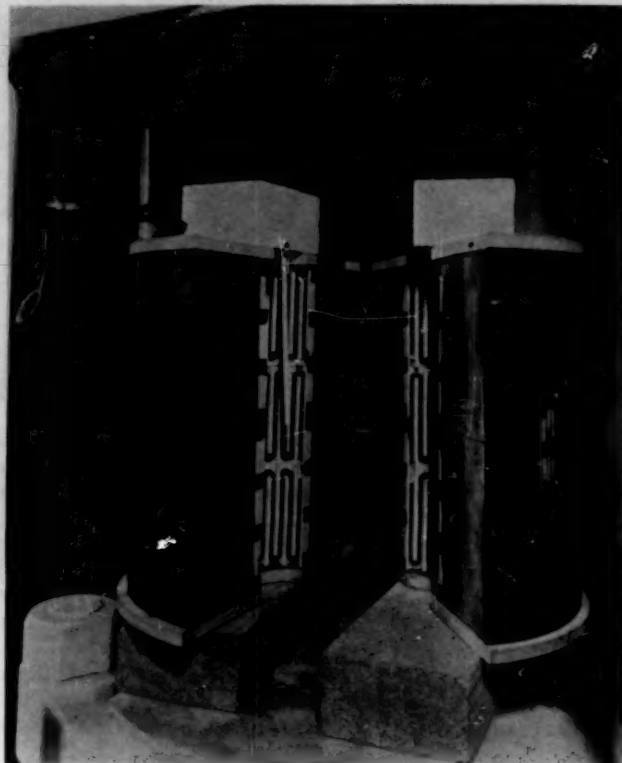
During the preliminary stages in which porcelain enamel-type adhesives were used to bond ingot iron, or ceramic adhesive UI 117–50 was used to bond type 302 stainless steel, screen carriers were not used.

During the course of the investigation, stainless-steel space screen of $1/_{32}$ in. space with 0.004-in. diameter wire, designated 28-mesh space screen, was tried on type 302 stainless steel bonded with ceramic adhesive UI 117–50. It was noted that an increase in shear strength occurred. This particular space screen was used regularly during the rest of the investigation. One series of tests, however, was conducted to see how the screen size and wire diameter of regular-mesh stainless-steel screen would affect shear strength when used as a carrier.

A few pieces of type 17–7 PH stainless-steel honeycomb sandwich panels were prepared to see if ceramic adhesive UI 117–50 would adhere over larger areas than on shear specimens and to obtain an idea of the strength of the bond. Figure 3 shows the various stages of honeycomb panel assembly.

The honeycomb cores were approximately 3 by 6 in. and had nominal cell sizes of $3/_{16}$ and $9/_{32}$ in., a ribbon thickness of 0.0015 in., a core thickness of $1/_{2}$ in., vents of 0.025 in., and continuous welds. The skins were approximately 3 by 6 in. and were 0.047 in. thick. The skins and cores were heat-scaled for 20 minutes at 1700°F. to remove grease and dirt. The skins were sandblasted on one side only (the side that would be bonded to the core).

The cores were coated with ceramic adhesive UI 117–50 by dipping and then were dried for 20 minutes at 200°F. The skins were dipped in the adhesive, wiped clean on the unsandblasted surface, and dried for 20 minutes at 200°F. The cores were placed between the skins on a stainless-steel firing rack, a bonding pressure of 2.25 lb. per sq. in. was applied, and the honeycomb panels were fired for 20 minutes at 1750°F. They were then given the remaining hardening treatments required to reach condition RH 950 as indicated in Table III.

(2) Testing of Bonded Specimens

Shear strength tests of specimens bonded with ceramic adhesives were conducted over the range room temperature to 1000°F. A Tinius Olsen Super L-type hydraulic testing machine was used with a split-tube furnace for making these tests.

The shear specimen was mounted in the stainless-steel grips as shown in Fig. 4, and the furnace was closed around it. The furnace was next brought to the desired temperature and held at that temperature for 10 minutes so that it might approach equilibrium. The specimen was then loaded at a scale reading of 1200 lb. per minute until failure occurred. As the overlap area of the adhesive bond was only $1/2$ sq. in., the scale reading was doubled to obtain the shear strength in pounds per square inch. In room-temperature tests the split-tube furnace was merely allowed to remain open and unheated.

It should be mentioned that the shear strengths reported probably deviate slightly from true values as a small bending moment was introduced because of the overlap of the specimen. It also was somewhat difficult to keep the specimens in exact alignment during adhesive bonding, which may have introduced additional bending moments. The reported values of the shear strengths of the ceramic adhesives may therefore sometimes be below the true values.

No tests were conducted on the honeycomb panels bonded with ceramic adhesive; they appeared to be well bonded, however, and there was no evidence of defects in the ceramic adhesive in the bonding areas.

III. Results of Shear Strength Testing

(1) Porcelain Enamel on Ingot Iron

When the three different porcelain enamels of different thermal expansions were used as ceramic adhesives to bond ingot iron, the enamel with the highest expansion yielded the highest shear strengths at any one of the three temperatures of test (see Fig. 5). In general, higher values resulted at room temperature than at elevated temperatures for all the porcelain enamels. This trend, however, became less pronounced as the expansion of enamel increased. It appears that when the expansion of the porcelain enamel is relatively high, i.e., when it is, up to some limiting value, approaching that of the metal, the shear strength of the enamel when used as an adhesive is high.

The thermal expansions of the ingot iron and porcelain enamel adhesives are shown in Table IV.

In studying and reporting on thermal expansion vs. adhesive strength, it is important to identify the area under investigation. When a ceramic adhesive with an expansion factor well below that of the metal was adjusted so that its factor increased and approached that of the metal, shear strength was found to increase. If, however, the factor for the adhesive continued to grow larger and approach closer and closer to that for the metal, shear strength might be expected to diminish. This thought is based on the consideration of porcelain enamels that can be made to exhibit either strongly

Fig. 5. Shear strength of (A) low-, (B) intermediate-, and (C) high-expansion porcelain enamels used as adhesives for 16-gauge ingot iron.
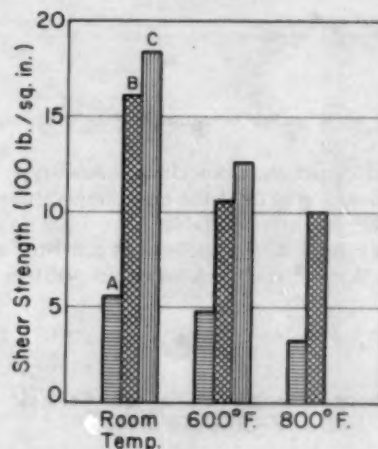
Fig. 6. Shear strength of intermediate-expansion porcelain enamel used as adhesive for (A) 22-gauge, (B) 16-gauge, and (C) 15-gauge ingot iron.

chipping or strongly crazing stresses by appropriate adjustment in their coefficient of thermal expansion.

When the intermediate-expansion enamel was used as an adhesive for different-gauge ingot iron specimens, it was found that in general the thicker the shear specimens, the higher was the resulting shear strength (see Fig. 6). This held true at any one temperature, even though shear strength decreased with temperature for specimens of all thicknesses. Shear strengths of 1840 lb. per sq. in. at room temperature and 1250 lb. per sq. in. at 600°F. on 0.071-in. stock were the highest values obtained using porcelain enamel as an adhesive on ingot iron.

(2) Ceramic Adhesive UI 117–50 on Types 302 and 17–7 PH Stainless Steel

Ceramic adhesive UI 117–50 when applied early in the investigation to type 302 stainless steel with no space-screen carrier yielded moderately successful shear strengths. Shear strength values increased to 960 lb. per sq. in. with an increase in temperature to 800°F. At 1000°F. shear strengths

Table IV. Approximate Linear Thermal Expansion of Ingot Iron and Porcelain Enamel Adhesives

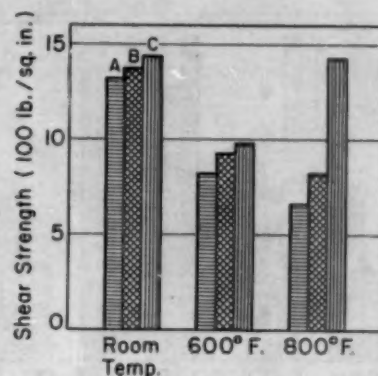| Material	Linear thermal expansion $\times 10^{-6}$ (cm./cm./°C.) up to 400°C.
Ingot iron	14.5
High-expansion porcelain enamel adhesive	12
Intermediate-expansion porcelain enamel adhesive	11
Low-expansion porcelain enamel adhesive	10
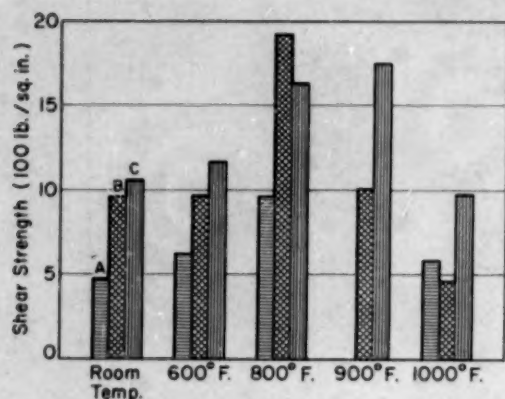
Fig. 7. Shear strength of ceramic adhesive UI 117–50 used to bond (A) type 302 stainless steel with no carrier, (B) type 302 stainless steel with 28-mesh stainless-steel space screen as a carrier, and (C) type 17–7 PH stainless steel hardened to condition RH 950 from condition A with 28-mesh stainless-steel space screen as a carrier.

Fig. 8. Enlarged view of surface of broken specimens with 28-mesh stainless-steel space screen as a carrier. Shear strength of ceramic adhesive UI 117–50 and several modifications at 800°F.: (A) no addition, 2150 lb. per sq. in.; (B) 5% Cu, 2110 lb. per sq. in.; and (C) 5% carbonyl iron, 3160 lb. per sq. in.

had decreased to a value comparable to that obtained at 600°F.

It was noted earlier that porcelain enamel-type adhesives decreased in shear strength as the test temperature increased to 800°F. This might reasonably have been expected, as the porcelain enamels used as adhesives consisted essentially of a glassy frit that softened at a lower temperature (1500° to

1600°F.) than the glass in ceramic adhesive UI 117–50 that was used to bond stainless steel (1750°F.). The results noted do not preclude the possibility that even the porcelain enamel-type adhesive would exhibit some increase in strength between room temperature and 600°F. Such an increase, actually noted for adhesive UI 117–50, is known* to be in keeping with the behavior of some glasses when heated.

When a 28-mesh stainless-steel space screen with 0.004-in.-diameter wire was used as a carrier in type 302 stainless-steel specimens bonded with ceramic adhesive UI 117–50, a marked increase in shear strength resulted for test temperatures up through 800°F. (see Fig. 7). Values were nearly 1000 lb. per sq. in. at room temperature; they increased to more than 1900 lb. per sq. in. at 800°F. and were more than 1000 lb. per sq. in. at 900°F. At 1000°F. values were 440 lb. per sq. in. These results indicate that a space screen improves the shear strength of stainless-steel specimens bonded with a ceramic adhesive up through 800°F. In fact, values were almost doubled at every temperature of test through 800°F. At temperatures above 800° to 900°F. the adhesives appeared to soften, as indicated by lower shear strength. This tended to obscure any effective evaluation of the benefit of a screen carrier above such temperatures.

The data presented in Fig. 7 were obtained on multiple specimens as shown in Table V. The average of two specimens per test temperature was used in compiling the data shown in all bar graphs other than Fig. 7. Although the average of two specimens can contribute but little to a statistical presentation, it can serve to represent the general trend that may be expected from ceramic-type adhesives.

It can be seen in the enlarged views of Fig. 8 how much the wire screen becomes an integral part of the joint. Tested to joint failure, the screen wires are observed to have been pulled, distorted, and torn. It is possible that perforated foil of some selected metals would act in the same way. In view of such results, it was decided to continue to use this type of screen as a carrier in most of the future tests on ceramic adhesives of this nature.

As shown in Table V, a few specimens of type 302 stainless steel bonded with adhesive UI 117–50 and tested at 800°F. approached 3000 lb. per sq. in. and one approached 4000 lb. per sq. in. The average of all specimens tested at that temperature was more than 1900 lb. per sq. in., as shown in both Table V and Fig. 7. These results suggest that, as a few specimens can give such good values, it should be possible to increase the shear strength by controlling variables in the

Table V. Shear Strength Data for Ceramic Adhesive UI 117–50 Used in Fig. 7

Metal used	28-mesh space screen used	Shear strength at				
		Room temp.	600°F.	800°F.	900°F.	1000°F.
302	No	100	70	600		340
"	"	400	80	740		550
"	"	410	740	840		620
"	"	640	810	1180		640
"	"	660	840	1520		800
"	"	240	840	1860		
"	"	500	780	1000		
"	"	880	200	1050		
"	"	400	840	460		
"	"			940	360	
	Avg.	470	614	961		590
302	Yes	880	860	2300	770	400
"	"	1200	920	2400	1020	420
"	"	520	790	1780	1250	500
"	"	980	1140	1860		
"	"	1400	1190	1880		
"	"	1400	1220	2460		
"	"	1520	1280	2800		
"	"	1800	1320	3680		
"	"	400	720	1020		
"	"	360	620	820		
"	"	500	700	910		
"	"	500	860	1100		
	Avg.	950	970	1920	1010	440
17–7 PH*	Yes	1000	1400	1400	1830	1160
"	"	860	1300	4000	1210	800
"	"	860	960	1070	2220	
"	"	970	1070	1070		
"	"	1030	1050	1000		
"	"	1090	1070	1000		
"	"	1390	1270	2150		
"	"	1250	1210	1270		
	Avg.	1060	1170	1620	1750	980

* RH 950 hardening.

* Private communication from K. C. Lyon, Ball Brothers Company, Incorporated, Dunkirk, Indiana.
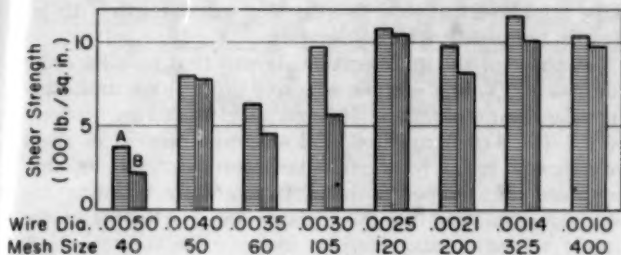
Fig. 9.   Effect of various sizes of stainless-steel screen on shear strength of ceramic adhesive UI 117–50 used to bond type 302 stainless steel. (A) 800°F. and (B) room temperature.

Fig. 10.   Shear strength of modifications of ceramic adhesive UI 117–50 used to bond type 302 stainless steel. The adhesive frit UI 117 was modified by (A) 2% Fe_2O_3, (B) 2% NiO, (C) 2% Cr_2O_3, and (D) 1.6% Fe_2O_3, 0.3% NiO, and 0.1% Cr_2O_3.

Fig. 11.   Shear strength of modifications of ceramic adhesive UI 117–50 used to bond type 302 stainless steel. The adhesive frit UI 117 was modified by (A) 5% Fe_2O_3, (B) 5% NiO, (C) 5% Cr_2O_3, and (D) 4% Fe_2O_3, 0.75% NiO, and 0.25% Cr_2O_3.

specimen preparation and bonding procedures.   Note, however, that the identification and control of variables in a research study of this type are in themselves major problems.

When ceramic adhesive UI 117–50, with 28-mesh stainless-steel space screen as a carrier, was used to bond 18-gauge type 17–7 PH stainless steel during part of the heat-hardening treatment required to bring it to condition RH 950, shear strengths generally increased at all temperatures except at 800°F. when compared with the 16-gauge type 302 stainless steel specimens.   This was especially true at 900° and at 1000°F., where shear strengths of 1750 and 980 lb. per sq. in., respectively, were obtained.   The increase in shear strength that resulted when using type 17–7 PH stainless steel instead of type 302 could have been due to (1) the differences in metal composition, which influence thermal expansion, (2) a difference in the hardness or dimensional stability of the metal, (3) a difference in the state of the glassy adhesive due to the added hardening treatments, and (4) a difference in metal thickness.   Undoubtedly all these factors were involved to some extent.

(3)   Effect of Various Sizes of Screens as Carriers

The effect of varying the sizes of regular-mesh stainless-steel screen used as a carrier in type 302 stainless-steel specimens bonded with ceramic adhesive UI 117–50 was in general to increase the shear strength as the screen became finer in mesh and the wire became smaller, as shown in Fig. 9.   The 28-mesh space screen, which is of a different mesh construction than regular-mesh screen, is not included in Fig. 9 because it was felt that it did not fit in with the comparison of the different sizes of regular-mesh screens.   Screen meshes of 120 to 400, when used as carriers, influenced the shear strength to about the same degree.   With screen coarser than 150 mesh there tended to be a reduction in shear strength as both the openings and wire diameter became larger.

When the mesh size was between 120 and 400 and the wire diameters between 0.0025 and 0.001 in., shear strengths at room temperature were comparable to those obtained using 28-mesh space screen as a carrier.   When, however, the test temperature was increased to 800°F., the use of 28-mesh space screen with its 0.031-in. opening and 0.004-in.-diameter wire served to produced shear strengths of more than 1900 lb. per sq. in., whereas when 120- to 400-mesh regular screen was used, the shear strength varied between 980 and 1160 lb. per sq. in.   Such results again indicated that 28-mesh space screen should be continued to be used when studying other variables in future tests.

(4)   Effect on Shear Strength of 2 and 5% Additions of Stainless-Steel Metal Oxides to Adhesive Frit UI 117

Shear strengths of adhesives made from frits that contained 2 and 5% additions of Fe_2O_3, NiO, and Cr_2O_3, individually or collectively, to frit UI 117 were obtained.   Since these adhesives, with 28-mesh stainless-steel space screen as a carrier, were applied to type 302 stainless-steel specimens exactly as
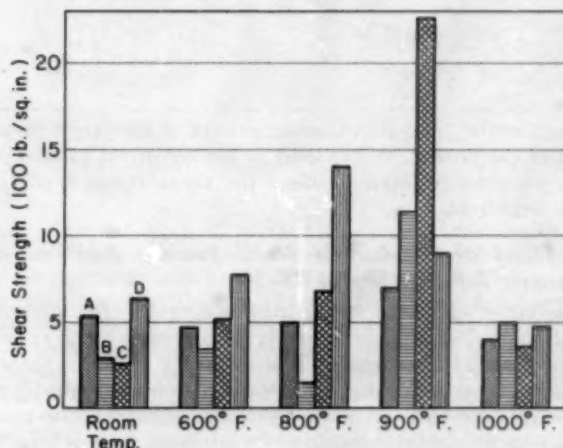
adhesive UI 117–50 was previously applied, all the resulting shear strength values can be directly compared.   The values for adhesive UI 117–50 are shown in Fig. 7; those for the adhesives with the metal oxide additions are shown in Figs. 10 and 11.

The general effect of adding stainless-steel metal oxides to the frit was to increase shear strength at 900° and at 1000°F. to some extent and to decrease shear strength at room temperature, 600°, and 800°F. to about the same extent.   No one modification of UI 117–50 was particularly outstanding over the entire temperature range studied.

An addition of 2% Cr_2O_3 to frit UI 117 produced a frit that showed the best general shear-strength values over the temperature range studied.   An addition of 5% Cr_2O_3 produced an adhesive that gave a high value of 2270 lb. per sq. in. at 900°F. but showed somewhat low values at the other test temperatures.   It appeared, therefore, that a 2% addition was more effective in increasing shear strength than a 5% addition.   Although time did not permit doing the work, some reversals in values indicated that a statistical analysis of an adequate number of specimens would be necessary to establish exact relations between 2 and 5% metal additions.

Since ceramic adhesive UI 117–50 yielded shear strengths of approximately 1000 lb. per sq. in. at all temperatures up
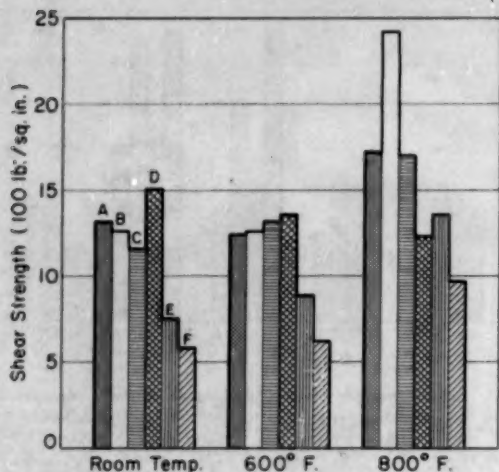
Fig. 12. Shear strength of ceramic adhesive UI 117–50 with 5 weight % of powdered metals added to the slips (adhesive used to bond type 17–7 PH stainless steel). (A) No addition, (B) carbonyl iron, (C) copper, (D) silicon, (E) carbonyl nickel, and (F) aluminum.

through 900°F., and thus approached one of the target properties of the project, it was used in further investigations of other variables believed to affect the shear strength of ceramic adhesives.

(5) Effect of Fine-Particle Metal Powder Additions to Ceramic Adhesive Slip UI 117–50

The effect on shear strength of adding 5% fine-particle metal powders of aluminum, copper, silicon, carbonyl iron, and carbonyl nickel to ceramic adhesive slip UI 117–50 is shown in Fig. 12 for temperatures up to 800°F. A control sample of UI 117–50 slip with no metal powder addition was also used as an adhesive in this phase and its resulting shear strengths are included in Fig. 12.

The additions of metal powders to the adhesive slip selectively affected the shear strength of the resulting adhesive. Some additions acted to decrease shear strength, e.g., aluminum dust and carbonyl nickel. Carbonyl iron did not affect the shear strength at room temperature and at 600°F., but did increase it at 800°F. by several hundred pounds per square inch. Copper powder had almost no effect on shear strength. Silicon powder increased shear strength at room temperature, did not affect it at 600°F., and reduced it at 800°F. Silicon powder was the only metal powder addition that acted to decrease shear strength as the test temperature increased; with all other metal additions the normal tendency for ad-

hesive UI 117–50 to show increased shear strength with increase in temperature was observed.

This phase of the investigation showed that metal powder additions of 5% to a ceramic adhesive slip will not uniformly affect the shear strength. If the metal additions are properly selected (e.g., carbonyl iron and silicon), increase in shear strength will result for certain temperatures. These additions, and also copper, although not greatly affecting the shear strength, may act to decrease the brittleness of the ceramic adhesive, and thereby improve its thermal-shock properties.

(6) Bonding of Honeycomb Sandwich Panels

Honeycomb sandwich panels were successfully bonded with ceramic adhesive UI 117–50 during part of the metal heat-treatment required to harden type 17–7 PH stainless steel to condition RH 950. Although no adhesion tests were made, the ceramic-bonded honeycomb showed no indication of adhesive defects that might cause weakening of the bond.

It was encouraging to note that relatively large areas of honeycomb sandwich panels could be bonded and that the ceramic-adhesive bond could withstand rather severe heat-treatments ranging from 1750° to −100° to 950°F. without rupture.

IV. Summary

Ceramic-type adhesives, prepared and applied to metal in a manner similar to the application of porcelain enamels or ceramic coatings, except for the inclusion of a cure pressure step, yielded shear strengths in excess of 1000 lb. per sq. in. on type 17–7 PH stainless steel and nearly 1000 lb. per sq. in. on type 302 stainless steel over the range room temperature to 900°F. when a 28-mesh stainless-steel space screen was used as a carrier.

Factors that acted to increase the shear strength of ceramic adhesives included (1) the thermal expansion of the ceramic adhesive, which must be such as to put the adhesive in an effective state of stress, (2) the use of a carrier, preferably of the space screen type, and (3) the addition of certain fine metal powders to the ceramic adhesive slip, such as carbonyl iron (particularly when tested at 800°F.) and silicon powder (particularly when tested at room temperature). Oxides of the metals contained in stainless steel, when added to the ceramic adhesive frit, acted to improve shear strength at 900° and at 1000°F. but to reduce it below those temperatures.

A ceramic adhesive can be conveniently employed to bond type 17–7 PH stainless steel, as one of the steps of heat-treating to obtain hardened condition RH 950 permits the application of the ceramic adhesive completely within the time-temperature limits of that specification.

Honeycomb panels were bonded with ceramic-type adhesives and no visible defects were noticeable.

CERAMIC ABSTRACTS

Compiled by the American Ceramic Society

I—Abrasives

PATENTS

Abrasive material with porous grains. WALTER WAGNER (Deutsche Gold- und Silber-Scheideanstalt vorm. Roessler). **Ger. 939,377,** June 21, 1956; *Chem. Abstr.,* **52** [17] 15009c (1958). —Finely dispersed Al_2O_3 is made porous by decomposition of H_2O_2 at 60° to 70° and is divided into single grains. Distribution, shape, and size of the pores achieve a higher degree of uniformity with H_2O_2, Mn compounds being added as catalysts, than with NH_4HCO_3 or other CO_2-forming substances. Addition of surface-active substances promotes the even distribution of the bubbles. The porous cake is dried and solidified by burning. Complete sintering is not permitted. It is crushed in the usual way, avoiding destruction of the porous grain structure. The different grain sizes are separated from each other, heated to 1800° to 1900°, mixed with an artificial resin, rubber, finely dispersed Al_2O_3, or a $MgCl_2$-MgO-silicate or clay-feldspar mixture, and molded; small amounts of a binder are added. If the droplets are sprayed before gas is formed, their size regulates the grain size. To prevent mutual adhesion, the droplets are dusted with finely dispersed Al_2O_3, C powder, or flour. If the grains are made by crushing, their pores must be blocked before addition of the cementing substances by filling them with swelling masses, e.g., solutions of gelatin or glue, which disappear during burning. Example: 560 gm. of Al_2O_3 was stirred with 250 cc. of water, 14 cc. of H_2O_2 solution, and a decomposition catalyst, and a surface-active substance was added. The mixture was placed in a mold, heated to 50° to 60°, and dried when gas formation was complete. The resulting cake was heated to 1900°, the final pore volume being 80%. An edge runner transformed the cake into grains 1 to 2 mm. in diameter. Mixed with a 4% methylcellulose solution and then with 15% of a cement (88 parts clay and 12 parts Pb-B frit), the mass was pressed into a grinding wheel die at 250 kg./cm.², dried, and heated to 980° to 1000°.

Electric furnace product. LEON J. FROST (National Lead Co.). **U. S. 2,849,305,** Aug. 26, 1958.—2. A fused abrasive material consists essentially of fine crystals of titanium carbide dispersed in a matrix consisting essentially of crystalline α-alumina, the carbide being present in an amount of about 10 to 50% by weight. D.J.B.

II—Art, Design, and Archeology

Antique ceramic pieces of importance. IRENE R. MAUCERI. *Ceramica* (Milan), **13** [6] 42–43 (1958).—M. describes vases and urns of the 5th and 6th centuries with decorations in Hellenic style. 3 photos. M.HA.

[Chün glazes.] IVAN ENGLUND. *Pottery Quart.,* **5** [18] 76–77 (1958).—A glaze based on a Seger formula, made of dolomite, feldspar, bone ash, slag, soda frit, clay, and flint and fired at 1280°C. in a reducing atmosphere, had an excellent Chün color. Analyses of the dolomite, slag, and clay used are given. Cf. *Ceram. Abstr.,* 1958, Jan., p. 2g. A.B.S.

Contemporary Korean kiln. HAROLD P. STERN. *Far East. Ceram. Bull.,* **10** [1–2] 1–4 (1958).—Two contemporary kilns in the vicinity of Seoul devoted to the reproduction of ancient celadon ware were visited. One, which has since failed, is described in detail. Out of 1000 vases fired in a reducing atmosphere in a wood-fired kiln, perhaps 100 are satisfactory while the others must be destroyed. 4 photos. M.F.

Contemporary studio potter. BERNARD LEACH. *Pottery Quart.,* **5** [18] 43–58 (1958).—Modern trained studio potters have an essential contribution to make in clarifying and fighting for the basic principles of that work which is at the same time recreation and labor, in which the use and beauty of the product are inseparable. A.B.S.

Cut crystal glass in the Midlands [England]. P. A. G. OSLER. *Edgar Allen News,* **37** [427] 15–19 (1958).—Historical. 7 photos. M.HA.

Good design is not enough. JULES R. GULDEN. *Am. Ceram. Soc. Bull.,* **37** [9] 416 (1958).—Market testing of dinnerware patterns is discussed.

Guide to glasses: V, Hock [wine]. ANON. *Pottery and Glass,* **36** [7] 194–98 (1958).—The graceful tulip-shaped bowl is preferred. 38 photos. For part IV see *Ceram. Abstr.,* 1958, Oct., p. 258j. C.M.C.

Koryo ceramics—problems and sources of information. GREGORY HENDERSON. *Far East. Ceram. Bull.,* **10** [1–2] 5–28 (1958). —The sources on Koryo pottery which survive deal mainly with celadon and are (a) the "Kao-li-t'u-ching" by Hsü Ching, the best and most explicit source on Koryo pottery known; (b) the "Koryo-sa" (History of Koryo), which was written between 1395 and 1451 and contains a few passing references to celadon; (c) inscriptions on stone stelae; (d) poems; (e) inscriptions on the ware; (f) archeological evidence; and (g) kiln sites. On the

basis of these sources, the major problems in the study of Koryo ceramics, which are, for the most part, unresolved, are listed as follows: (*a*) origin of Koryo celadon; (*b*) influence of Chinese pottery; (*c*) other foreign influences; (*d*) Koryo influence on Japan; (*e*) organization and direction of kilns; and (*f*) development of native Korean techniques. 6 photos, 20 references.
                                  M.F.

Majolicas of Marseille. GIUSEPPE MORAZZONI. *Ceramica* (Milan), **13** [6] 26–27 (1958).—Decorative majolica ware of the 18th century is described. 7 photos.   M.HA.

Masterpieces of yesteryear: 12, Wedgwood Museum. ANON. *Pottery Gas.*, **83** [974] 967–70 (1958). 9 photos. For part 11 see *Ceram. Abstr.*, 1958, Sept., p. 220a.   C.M.C.

Oldest document known on the production of majolica in Sicily. NINO RAGONA. *Faenza*, **44** [1] 5–7 (1958).—A Latin document of about 1309 gives certain rules for the workers in faience. Ceramic fragments found in Caltagirone and Gela are shown. 4 photos, 9 references.   M.HA.

Rare majolica vase from a pharmacist's shop in Naples. FERDINANDO SACCHI. *Ceramica* (Milan), **13** [6] 32–33 (1958).—A vase made in 1665 by Brandi is described. 2 photos. M.HA.

Romano-British kiln—building and firing a replica. F. J. WATSON. *Pottery Quart.*, **5** [18] 72–75 (1958).—Three replicas of ancient Romano-British kilns in Norfolk, England, were built with modifications suggested by experience. The kilns are circular and of the updraft type, with a central hollow pedestal serving as the kiln floor and as a flue. Wood was used for the firing, and a temperature of 850° to 1000°C. was reached. The products compared well with ancient Romano-British pots of similar shapes. Magnetization tests showed that the iron in the clay had developed magnetic properties during cooling. After the kilns had been emptied, the magnetization of the foundations was high enough to indicate that similar magnetic tests may be used to locate other ancient kiln sites. 15 photos. A.B.S.

Sang de boeuf **glaze: its Chinese historical references and local reduction experiments in electric firing kilns.** JOHN M.

MATHEWS. *Emporia* (*Kansas*) *State Research Studies*, **6** [1] (1957); reprinted in *Far East. Ceram. Bull.*, **10** [1–2] 35–61 (1958).—Experiments to reproduce this glaze were unsuccessful. 55 references.   M.F.

Thrown glazes. DAVID P. HATCH. *Pottery Quart.*, **5** [18] 67–71 (1958).—Thrown glazes are applied to pots on a wheel during the last stages of throwing, the glaze slip serving as a lubricant instead of water. The slip may be applied with a brush or poured over the pot with its distribution controlled by the potter's fingers; the shaping is then completed. A special procedure is described for handles and spouts. Feldspar glazes (with or without volcanic ash) are recommended. The use of a plastic ingredient ensures adequate adhesion of the glaze. Similarity in the physical and chemical properties of the body and glaze is important. 5 figures.   A.B.S.

Tropical fish in bone china. ANON. *Pottery Gas.*, **83** [974] 963–66 (1958).—The design and the production of a new tropical fish series for collectors are described. The large models are limited to a production of 500, and then the molds will be destroyed. 9 photos.   C.M.C.

Wood-burning kiln. IVAN McMEEKIN. *Pottery Quart.*, **5** [18] 59–66, 71 (1958).—M. summarizes the advantages of wood firing for a studio pottery, particularly where wood is plentiful and not too expensive; he stresses its reliability in firing stoneware and porcelain under suitable conditions, especially for colors produced with a reducing atmosphere near the end of the firing. The construction and operation of a kiln built in Mittagong, N.S.W., Australia, are described, and an insert shows the plan of the kiln. The method of firing differs considerably from that used with coal. A temperature of 1200°C. is reached in most parts of the kiln, and 1260°C. in the hottest parts. About 11 tons of timber is used in each firing. 3 figures.   A.B.S.

Additional abstract

Sect. IV: (*book*) Enamel Art on Metals.

III—Cements, Limes, and Plasters

ACL system. KARL HAUSER. *Rock Prods.*, **61** [7] 82–85, 136 (1958).—This system consists essentially of a traveling grate and a rotary kiln in series. The raw materials must make good pellets, and maximum performance is required of pelletizing equipment, grates, feeders, and other equipment not normally employed in cement manufacture. High operating efficiency, low initial investment, good fuel economy, and low dust losses are claimed. Once established, the process is less sensitive to changes in material fineness, composition, and temperature than conventional methods. The pan-type pelletizer is preferred for pellet uniformity and ease of control. Diagrams for a pilot plant unit are shown. 3 figures.   D.J.B.

Change in the chemical composition of clinker grains as a function of their size. W. WIELAND. *Zement-Kalk-Gips*, **11** [6] 253–58 (1958).—A study was made to determine whether the chemical composition of clinker grains is changed on grinding or whether it remains constant over the whole range of grain size. By the usual analysis the effective quantity of free lime can be determined only by using the finest grains, as the ethylene glycol penetrates the surface only to a depth of 1.5 to 3 μ. The quantity of K_2O and SO_3 in the grain fractions is mainly proportional to the specific surface. The decrease in specific weight with increasing fineness is a function of loss on ignition. Calcium disilicate and calcium trisilicate have different grindabilities. 6 figures, 3 references.   M.HA.

Composition of the ferrite phase in Portland cement. H. G. MIDGLEY. *Mag. of Concrete Research*, **10** [28] 13–16 (1958).—The composition of the ferrite phase in commercial Portland cements was investigated by powder X-ray diffraction techniques. The results of an examination of 31 samples show that the most frequently occurring composition lies between $4CaO \cdot Al_2O_3 \cdot Fe_2O_3$ and $6CaO \cdot Al_2O_3 \cdot 2Fe_2O_3$. 2 figures, 7 references.
                               V.R.E.

Determination of free CaO and free Ca(OH)₂ in Portland cements and Portland cement clinkers. MARIA WALLRAF. *Zement-Kalk-Gips*, **11** [5] 216–18 (1958).—The content of CaO in free lime ($Ca(OH)_2$ + CaO) important in the behavior of a cement is obtained as the difference between the free lime determined by means of organic solvents and the proportion of $Ca(OH)_2$. The latter value can be derived from the amount of

water formed in the range 350° to 600°C. according to the reaction $Ca(OH)_2 \rightarrow CaO + H_2O$. The amount of water is determined by absorption with Mg perchlorate. 1 figure, 9 references.   M.HA.

Electron microscope study of the hydration of Portland cement and its constituent minerals: I, Hydration of tricalcium aluminate. KUNIHIRO TAKEMOTO. *Semento Gijutsu Nenpo*, **6**, 158–65 (1952).—Hydration products of C_3A with or without $Ca(OH)_2$, $CaSO_4 \cdot 2H_2O$, or $Ca(OH)_2$ + $CaSO_4 \cdot 2H_2O$ were studied with the electron microscope and by X-ray analysis. When C_3A was hydrated at 20°C. with small amounts of water, hexagonal crystals showing the X-ray pattern of $C_3A \cdot 8H_2O$ formed, but at temperatures above 20°C. hexagonal crystals showing the X-ray pattern of $C_2A \cdot 8H_2O$ formed. The higher the temperature and the larger the amount of water used, the earlier does the formation of trapezohedral crystals of cubic $C_3A \cdot 6H_2O$ through $C_3A \cdot 8H_2O$ or $C_2A \cdot 8H_2O$ occur; the presence of $Ca(OH)_2$ retards the formation of $C_3A \cdot 6H_2O$. In the presence of large amounts of gypsum, needlelike crystals of $C_3A \cdot 3CaSO_4 \cdot 31H_2O$ are formed, but in the presence of smaller amounts of gypsum the crystals formed change to hexagonal crystals (perhaps $C_3A \cdot CaSO_4 \cdot 12H_2O$). 25 figures, 16 references. **II, Hydration of pentacalcium trialuminate, monocalcium aluminate, and tetracalcium aluminoferrite.** *Ibid.*, **7**, 19–27 (1953).—When C_5A_3 is hydrated at 20°C., the unstable gels formed initially change to crystalline aluminum hydroxide, and simultaneously hexagonal crystals of $C_2A \cdot 8H_2O$ are formed. The formation of $C_3A \cdot 6H_2O$ through $C_2A \cdot 8H_2O$ is observed only when C_5A_3 is hydrated with larger amounts of water at higher temperatures. Hydration products of CA are essentially identical with those of C_5A_3, but the hydration of CA proceeds more slowly than that of C_5A_3. In the presence of $Ca(OH)_2$, no formation of gel is observed, and $C_2A \cdot 8H_2O$ is formed immediately. Results are the same when alumina cement is hydrated in the presence of $Ca(OH)_2$. The quick setting of alumina cement brought about by adding Portland cement or $Ca(OH)_2$ seems to be intimately related to this phenomenon. Hydration products of C_4AF are similar to those of C_3A except for the formation of unknown calcium ferrite hydrates at later ages. 31 figures, 9 references. **III, Hydration of tricalcium silicate and β and γ dicalcium silicate.** *Ibid.*, **8**, 76–83

(1954).—Hydration products of the calcium silicates with or without CaO, $CaSO_4 \cdot 2H_2O$, or C_3A are reported. Spindle-shaped crystals (length $<1\mu$, width $<0.3\mu$) composed of needlelike crystals are observed in the hydration products of C_3S, and the higher the reaction temperature, the shorter is the time required for the formation. The electron diffraction pattern is different from that of $CaCO_3$ (cf. discussion by Grudemo in the report of Bernal, *Ceram. Abstr.*, 1956, Sept., p. 184b). It seems to be a calcium silicate hydrate. No formation of the crystals was observed in the hydration products of C_2S. 44 figures, 12 references. Cf. following abstract.   Y.S.

Electron microscope and X-ray investigation of the hydration of tricalcium aluminate. KOZABURO WATANABE AND TADASHI IWAI. *Semento Gijutsu Nenpo*, 8, 101–106 (1954).—C_3A is hydrated to trapezohedral crystals showing the X-ray pattern of $C_3A \cdot 6H_2O$ through hexagonal plates. Electron diffraction data on the hexagonal plates agree with the X-ray data of $C_3A \cdot 8H_2O$ reported by Thorvaldson in 1929. The sharp N pattern of hexagonal plates disappears and changes to halo during irradiation with the electron beam, showing the disintegration of the crystal structure due to dehydration. Electron microscope observation with the one-step collodion replica showed that hexagonal plates have a layer structure. No electron diffraction pattern of trapezohedral crystals was obtained. $C_3A \cdot 6H_2O$ changes to C_5A_3 with liberation of CaO and H_2O when heated at 700°C. for 10 hr., but in spite of showing the X-ray pattern of C_5A_3, no liberation of free lime was observed when it was heated at 300°C. for 10 hr. In the presence of gypsum, the hydration product of C_3A is the high sulfate form of calcium sulfoaluminate, and this form changes to the low sulfate form of hexagonal plates. 22 figures, 11 references. Cf. preceding abstract.   Y.S.

Factors in design of cement plant milling rooms. C. A. ROWLAND. *Pit and Quarry*, 51 [1] 163–65, 168–70 (1958).—A single room used for raw and finish grinding simplifies maintenance, labor, and electrical requirements. If possible, the mills should be duplicates; even in wet process, where compartment mills are used for raw grinding and ball mills for finish grinding, the same power supply setup will save on motors, gears, pinions, and couplings. The room should be planned for expansion to grow from the middle out. Proper arrangement of the control center is also covered. 4 figures.   D.J.B.

Fields of application of gypsum products. EDUARD EIPELTAUER. *Berg- u. hüttenmänn. Monatsh. montan. Hochschule Leoben*, 103 [4] 65–71; [5] 85–93 (1958).—The use of gypsum instead of clay in building materials is discussed at length. Insulating brick containing gypsum have a compressive strength of about 140 kg./cm.² compared with only 20 to 40 for clay insulating brick, and they need not be fired, have almost twice the mechanical strength for the same porosity, are more homogeneous, and are cheaper to make. Anhydrite is used in concretes instead of Portland cement; it gives better compressive and flexural strengths than the usual cements and high resistance to chemical attack. Curves for temperature gradients in walls and linings, composition of brick, etc., influence of composition on setting time, and compressive and tensile strength as function of setting time are given, and methods of preparation and application are described. Heavy concretes of this type are particularly suitable for radiation protection (atomic reactors). BeO_2 cannot be added to Portland cement as it reduces strength and delays setting time, but when added to anhydrite binder (as BeO_2 solution or in slags) it increases the strength and neutron absorption of the concrete. 16 references.   M.HA.

Grinding quantities of cement mill: I. SUEO SUZUKI. *Semento Gijutsu Nenpo*, 6, 95–104 (1952).—Based on the particle size distribution formula of Rosin and Rammler (1933), the grinding of clinker in an open circuit mill was studied. In the scope of normal grinding, the relation between the amount of particles (R) larger than a constant diameter and grinding quantity (Q in tons/hr.) can be expressed as follows: $R = 100e^{-k_1 Q^{-m}}$, where k_1 and m are constants. 12 figures, 10 references. **II.** *Ibid.*, 8, 39–44 (1954).—The formula reported in part I can be rewritten by inserting the amount of grinding media (M, in tons) as follows: $R = 100e^{-(aM+b) \cdot x^n \cdot Q^{-m}}$, where a, b, and n are constants and the value of n is nearly equal to 1. 2 figures, 8 references. **III.** *Ibid.*, 9, 189–94 (1955).—In the equation reported in part II, the effects of Q on n and m were studied, and also the effects of abnormal grinding on these values. Intersecting charts representing the relations between the specific surface (Blaine), Q, and M for normal and abnormal grinding are shown. 7 figures, 4 references. **IV.** *Ibid.*, 10, 143–50 (1956).—The effects of M

on the particle size distribution and specific surface of cements and on the power consumption and Q were studied. In the particle size distribution formula of Rosin and Rammler, n increased and k decreased with increase in M, i.e., cement of uniform size particles was obtained with increase in M. 9 figures, 6 references.   Y.S.

Hydraulic properties of glasses: I, Glasses of the system CaO–SiO_2–Al_2O_3 with and without MgO. F. KEIL AND F. W. LOCHER. *Zement-Kalk-Gips*, 11 [6] 245–53 (1958).—Thirty-two glasses of the ternary system CaO–SiO_2–Al_2O_3, with 36 to 52.5% CaO and 10 to 55% Al_2O_3, and fifteen glasses with an addition of 5% MgO were tested for their hydraulic hardening properties with clinker, anhydrite, and $Ca(OH)_2$ activation. The results are given in lines of equal strength in the diagram of the system. With clinker activation, two regions of high compressive strength are found at about 18% SiO_2 and at 30% SiO_2. Sulfate and $Ca(OH)_2$ activation give only one region of high strength. For all three types of activation the strength optimum lies within a narrow range of the ternary system, the center being at about 50 CaO, 31 SiO_2, and 19% Al_2O_3. MgO addition increases the strength in certain ranges for clinker and sulfate activation, but it has no effect with $CaO(OH)_2$ activation. The hydraulic properties of the glasses depend on their solubility and their solution rate in the activator solutions and on the type of the hydrate phases formed. The determining factor for the dissolving properties of the glasses is apparently the manner in which the Al ion is incorporated in the glass lattice, i.e., as a network former or a network modifier. The action of the clinker and lime activators is ascribed to their capacity to increase the lime concentration of the solution so that dicalcium silicate hydrate can be formed, which effects a rapid disintegration of the glasses. 15 figures, 20 references.   M.HA.

Influence of the constituent minerals and of the forming process on the firing behavior of cement nodules. G. HILL AND H. E. SCHWIETE. *Zement-Kalk-Gips*, 11 [5] 181–96 (1958).—The influence of the method of preparation of nodules on the firing process in rotary or shaft kilns was investigated. Shrinkage cracks are formed with raw mixes which have no bursting tendency, while bursting of the nodules is due to considerable consolidation of their surfaces in the nodulizing process. The porosity of nodules with bursting tendencies is less than that of nodules that can be fired normally. Plasticity and abrasion resistance are lower in difficultly firing mixes. These phenomena are ascribed to the clay minerals possessing swelling properties (in this case montmorillonite and illite), which prevent the destruction of the nodules. Efforts to eliminate the difficulties by changing the method of preparation are discussed. 22 figures, 26 references.   M.HA.

Lime around the world: 2, Research is imperative in Australia. VICTOR J. AZBE. *Rock Prods.*, 61 [7] 94–102, 128, 136 (1958).—Properties of limes from various parts of the world are compared with those of Australian limes. Manufacturing practices in Australia seem to be rather primitive. A proposed research program is outlined. 5 figures.   D.J.B.

Lime-slag cement for use in masonry: I. SHOICHIRO NAGAI, SADAO UEDA, AND YOSHIMICHI IROKAWA. *Sekko to Sekkai*, 1958, No. 35, pp. 5–10.—Cement samples were prepared by mixing (by weight) slag 60 to 80, slaked lime 10 to 30, and various admixtures 0 to 25%. Setting time and mortar strength values of samples kneaded with 0 to 15% solutions of NaOH or Na_2CO_3 are shown. A superior product was obtained with a cement consisting of (by weight) slag 80, slaked lime 10, and admixture 10% kneaded with 5 to 10% solutions of NaOH. 4 figures, 3 references.   Y.S.

Long-time tests of various types of cements for use in road pavement. TOKUJI YAMANE AND SHIGEJIRO MURI. *Semento Gijutsu Nenpo*, 10, 260–66 (1956).—Based on test results of various types of Portland cements up to the age of three years, a standard for manufacturing a Portland cement having superior properties for use in road pavement was determined. The compositions and fineness are C_3S 55.5, C_2S 22.9, C_3A 3.6, and C_4AF 12.8%; specific surface (Blaine) 2800 to 3000 cm.²/gm. The cement was burned in a rotary kiln. Comparative tests of mortar and concrete made with the cement, various types of Portland cements, and a Portland pozzolan cement showed that the cement has a lower ratio of drying shrinkage to bending strength. 3 figures.   Y.S.

Manufacture and properties of magnesia-rich Portland cements. P. P. BUDNIKOV AND KH. S. VOROB'EV. *Silikattech.*, 9 [4] 158–60 (1958).—Supplementing incomplete data on the properties of clinkers and cement with different MgO contents, tests are reported on the effect of certain additions on the hydration of

the Mg in the cements. The addition of Ca aluminate ferrite to clinkers with 10 to 25% MgO fired at 1475° did not prevent the destruction of more than 10% MgO in the clinker. Additions of 1 to 2% $MgCl_2$ or $CaCl_2$ delay the change in volume of cements containing up to 15% MgO, but gypsum and Mg sulfate have hardly any effect. In batches with 9.5 to 18.5% Mg the firing time at all temperatures from 1250° to 1550° was reduced; with increasing temperature, however, the contents of periclase and of free Mg in the clinker increase and are almost doubled at 1350° to 1550°. Gypsum is an undesirable addition in Mg-rich Portland cement, while 1 to 2% $CaCl_2$, $MgCl_2$, and $MgSO_4$ exert a favorable effect. 6 figures, 11 references.   M.HA.

New research on the pozzolanic cements. A. CERESETO AND A. RIO. *Chim. & ind.* (Paris), 69 [6] 1043–53 (1953).—The presence of pozzolans brings about a complete change in the normal hydration process of Portland cement by appreciably modifying the structure of the hydrated and hardened pastes and thus the hardening curve. Mechanical and chemical resistance, shrinkage, and heat of hydration are in general improved, as shown by many curves and tables. 4 figures, 6 references.
M.HA.

Nuclear gauge sees through slurry pipe to control density. HARRY F. UTLEY. *Pit and Quarry*, 51 [1] 162 (1958).—A continuous record of density is obtained by using the radiation from cesium 137. Only slight corrections are required owing to the decay of the source. The water in the slurry is controlled to 35 ± 0.5%, and it is feasible down to 0.25%.   D.J.B.

Portland cement for use in road construction: I. KIMBE CHUJO, SHINJI SEKINO, AND MINORU KONDO. *Semento Gijutsu Nenpo*, 5, 149–56 (1951).—Physical properties of Portland cement for use in road construction and factors affecting drying shrinkage, such as chemical compositions and fineness, are discussed. The relation between drying shrinkage (mm./10 m.) of neat cement paste at 28 days and the composition can be expressed as follows: $S^{28} = 0.25 \times C_3S + 0.16 \times C_2S + 1.03 \times C_3A + 0.28 \times C_4AF$. Based on the results, desirable chemical compositions and fineness seem to be as follows: C_3S 59%, C_2S 22, C_3A 3, and C_4AF 12; specific surface (Blaine), 2600 to 3000 cm.^{2}/gm. 5 figures. **II.** *Ibid.*, 6, 211–16 (1952).—Cement having the composition reported in part I was burned in a test kiln and ground to a Blaine specific surface of 2000 to 4000 cm.^{2}/gm. Physical properties of the prepared cement were compared with those of ordinary, rapid-hardening, and moderate heat cements. The most desirable specific surface is 2000 to 3000 cm.^{2}/gm. 5 figures, 7 references.   Y.S.

Portland pozzolan cements containing fly ash prepared by blending with cement and by intergrinding with clinker. GORO KASAI, SHIGEO SASAKI, AND HISASHI TANAKA. *Semento Gijutsu Nenpo*, 10, 227–32 (1956).—Comparative tests were made on cements prepared by both methods. No marked differences due to the preparation method were observed in the physical properties of the resulting cements. Chemical resistivity to sulfate solutions of the cement prepared by intergrinding is a little greater than that of the cement prepared by blending. Microscopic observation showed that during grinding with clinker, fine spherical particles of fly ash remain unchanged, but larger irregular particles are ground selectively. 6 figures, 16 references.   Y.S.

Pozzolanic reaction of fly ash. GUNJI SHIKAMI. *Semento Gijutsu Nenpo*, 10, 221–27 (1956).—X-ray analysis of an original fly ash and of the same samples reheated at 1000° to 1300°C. for 2 hr. showed that the residual SiO_2 beyond the amounts required for the formation of glassy phase is present as quartz and the Al_2O_3 is present mainly as a component of the glassy phase. The formation of $3CaO \cdot Al_2O_3 \cdot 3CaSO_4 \cdot 31H_2O$ and calcium silicate hydrates was observed when fly ashes were treated with solutions containing different amounts of CaO and $CaSO_4$ for 2 months. The reaction amounts of Al_2O_3 decreased with decreasing concentration of CaO in the solutions. 24 figures, 7 references.   Y.S.

Problems in lime burning. J. WUHRER. *Chem.-Ing.-Tech.*, 30, 19–30 (1958); abstracted in *J. Appl. Chem.* (London), 8 [7] ii-44 (1958).—Laboratory experiments made to investigate the effects on lime burning of temperature, time, lump and crystallite size, inert gases, and water vapor are described. The results are applied to coke-heated limekilns. Studies of combustion and temperature distribution are described. Requirements for satisfactory operation are close control of lump size of limestone, large coke of correct quality well mixed with limestone, a tall kiln, even movement across the cross section, and even and correct air distribution. 11 references.   V.R.E.

Rate of heat liberation of cements at early ages. HITOAKI

MORI AND SHIGEO AKAIWA. *Semento Gijutsu Nenpo*, 8, 60–67 (1954).—The effects of adding various amounts of gypsum dihydrate, gypsum hemihydrate, $CaCl_2$, NaOH, Na_2CO_3, and Na_2SO_4 on the rate of heat liberation (determined with a conduction calorimeter of the Lerch type), heat of hydration, and mortar strength of cements containing different amounts of $3CaO \cdot Al_2O_3$ and alkalis are reported. 26 figures, 12 references.   Y.S.

Reaction mechanism of cement raw mixes during burning: I, Reaction mechanism by differential thermal analysis. MEGUMI UEDA. *Semento Gijutsu Nenpo*, 6, 116–23 (1952).—The mechanism of the reaction of cement raw mixes was studied, mainly by differential thermal analysis and X-ray analyses and by microscopic observation. After the decomposition of $CaCO_3$, four thermal peaks were observed at about 1200°, 1280°, 1380°, and 1420°C. X-ray analysis showed that the formation of belite is approximately complete after the exothermic peak at about 1200°C. The exothermic peak at about 1280°C. is due to the formation of the liquid phase and alite. The endothermic peak at about 1420°C. seems to be due to the transformation of $2CaO \cdot SiO_2$ from the β form to the higher temperature form. 8 figures, 13 references. **II, Formation mechanism of celite.** *Ibid.*, 7, 11–19 (1953).—Raw mixes in the system $3CaO \cdot Al_2O_3$–$5CaO \cdot 3Al_2O_3$–$2CaO \cdot Fe_2O_3$ (Al_2O_3/Fe_2O_3 ratio by weight 1.2 to 1.8%) were prepared from c.p. reagents. No thermal change was observed during the formation of calcium ferrite and calcium aluminoferrite. The thermal peak at about 1380°C. is due perhaps to the melting of celite. 9 figures, 9 references. **III, Formation mechanism of alite.** *Ibid.*, 8, 16–23 (1954).—The effects of adding MgO, K_2O, Na_2O, or their combinations to cement raw mixes in the system CaO–Al_2O_3–Fe_2O_3–SiO_2 on the temperature of the beginning of the formation of alite are reported. 5 figures, 9 references.   Y.S.

Reactivity of blast-furnace slags as a raw material of supersulfated cement: I. SOJI TSUMURA. *Semento Gijutsu Nenpo*, 7, 90–94 (1953).—A method for evaluating the reactivity of blast-furnace slags is proposed on the basis of the fact that ettringite is formed during the hydration of supersulfated cements. To the mixture of slag powder 100 parts and Portland cement 5 parts by weight, 100 cc. of solution containing 100 mg./100 cc. of SO_3 is added, and the mixture is stirred for a constant period at 20° ± 1°C. After filtration, the residue is washed with dilute $Ca(OH)_2$ solution. The amount of combined SO_3 calculated from the residual SO_3 in the filtrate is regarded as a measure for evaluating the reactivity of slags. An intimate relation was observed between the reactivity of slags determined by this method and the dynamic modulus of elasticity of the resulting supersulfated cements. 9 figures. **II.** *Ibid.*, 8, 136–39 (1954).—The relation of the chemical composition of synthetic slags in the systems CaO–Al_2O_3–SiO_2–MgO and CaO–Al_2O_3–SiO_2–MgO–CaS, the reactivity of the slags determined by the method reported in part I, and the dynamic modulus of elasticity of the resulting supersulfated cements were studied. The effects of adding 1% by weight of Fe_2O_3 or MnO on the reactivity of slags in the system CaO–Al_2O_3–SiO_2–MgO–CaS were also investigated. No influence was observed when Fe_2O_3 was added, but the dynamic modulus of elasticity of the resulting cements decreased about 10% when MnO was added. 9 figures, 3 references. **III.** *Ibid.*, pp. 140–43.—The effects of the methods of grinding the slags, such as dry grinding in a ball mill or air-swept mill, wet grinding (water or acetone), and grinding with jet mill (superheated steam), on the dynamic modulus of elasticity of the resulting supersulfated cements were studied. Dry grinding in a ball mill and wet grinding with acetone are desirable. 3 figures, 4 references.   Y.S.

Reactivity of blast-furnace slags in slag cements. TOSHIYOSHI YAMAUCHI AND RENICHI KONDO. *Semento Gijutsu Nenpo*, 6, 180–86 (1952).—The chemical compositions of slags suitable for Portland blast-furnace slag cement, gypsum slag cement, etc., were determined by a mortar strength test. The results obtained are shown in the triangular diagram of the system CaO–Al_2O_3–SiO_2. 6 figures, 11 references.   Y.S.

Regenerated material from used gypsum molds. B. N. OL'-SHEVSKIĬ. *Steklo i Keram.*, 15 [6] 43–45 (1958).—The Krasnyĭ porcelain factory obtained good results in an attempt to regenerate plaster from used molds. The laminar composition of the plaster in old molds was studied, and it was established that more than 90% of the plaster is completely suitable for processing, only the layer immediately adjacent to the casting slip being contaminated and unsuitable for regeneration. Analysis of this layer showed clay-quartz-spar inclusions. Such penetration (together with salts from the slip) filled the pores to a certain

depth, depending on the time the mold had been in use, and considerably reduced the absorbing capacity. Tables show comparative data for used and new molds (different shapes and sizes). Tests were made in which certain amounts of new plaster were added to the regenerated material, and molds were then cast from these mixtures. Repeated regeneration showed that 20% new plaster is needed after the first regeneration, 30 after the second, 40 after the third, and 50 after the fourth. The factory uses 4-fold regenerated plaster for making objects for which fineness of detail is unimportant. 1 figure.   K.S.

Relation between the change of gypsum and clinker during grinding and the false set of cement: I. YOSHIKAZU MURAKAMI. *Semento Gijutsu Nenpo*, **7,** 94–101 (1953).—A thermobalance for determining the content of various forms of gypsum in commercial cements was constructed. Gypsum is present mainly as hemihydrate when the temperature of cement at the outlet of the mill is >110° to 120°C., and the content of soluble anhydrite increases with rising temperature. Soluble anhydrite changes easily to hemihydrate when cement is exposed to air at room temperature, so that soluble anhydrite is not present in commercial cements. The relation between the content of gypsum hemihydrate and that of alkali carbonate is intimately connected with the appearance of false set. In the presence of large amounts of alkali carbonate, false set occurs when gypsum hemihydrate is not present. 3 figures, 23 references. **II.** TOYOFUJIMARU YOSHII AND YOSHIKAZU MURAKAMI. *Ibid.*, **8,** 95–101 (1954).—False set due to gypsum hemihydrate was studied on mixtures of gypsum hemihydrate and siliceous sand or limestone powder. False set occurred when 0.50 and 0.75% by weight of gypsum hemihydrate were added and the mixtures were kneaded for 3 min. The shorter the kneading time, the stronger is the false set. These results showed that the set of gypsum hemihydrate occurs during kneading. The effects of adding 0.01 to 0.3% by weight of sodium salts on the false set of siliceous sand powder containing gypsum hemihydrate corresponding to 1.8% by weight of SO_2 were tested. When the mixture is kneaded for 3 min., the false set is strengthened by adding Na_2CO_3, $NaHCO_3$, and sodium citrate, which retard the setting of gypsum hemihydrate, and it is weakened by adding $NaOH$ and Na_2SO_4, which accelerate the setting. These results showed that the false set of cements aerated in dry air seems to be due to the formation of alkali carbonate, which retards the setting of gypsum hemihydrate. 3 figures.   Y.S.

Relation between the specific surface ratio of cement raw mixes and the strength—application of the Jander formula for clinker burning. KOZABURO WATANABE AND MOTOHIKO KAJII. *Semento Gijutsu Nenpo*, **6,** 10–18 (1952).—The most desirable and economical ratio between the specific surface of clay and that of limestone is 1.2. The applicability of the Jander formula for clinker burning at 1450° to 1550°C. is discussed. The contents of free lime calculated by the modified formula of Jander agreed with those actually determined. 4 figures. Cf. *Ceram. Abstr.*, 1958, Sept., p. 223g.   Y.S.

Segregation and mixing of cement raw mixes in the dry process. SHIGEO SASAKI. *Semento Gijutsu Nenpo*, **7,** 102–105 (1953).—The variation of the hydraulic modulus of the raw mix due to segregation in the tank before the grinding mill and the equalization of the hydraulic modulus of finished raw mixes during transportation are analyzed mathematically. 4 figures, 2 references.   Y.S.

Studies on the surface hardening of sulfated slag cement by an orthogonal array experiment. TOSHIYOSHI YAMAUCHI, RENICHI KONDO, AND NAOBUMI MORITA. *Yogyo Kyokai Shi*, 66 [749] 103–10 (1958).—To examine the surface hardening of sulfated slag cement, an orthogonal array experiment including 16 different factors and 15 interactions was carried out. The main cause of failure in surface hardening is the presence of CO_2 in the air, which lowers the pH value of the liquid phase and disturbs the hydration of the surface of specimens. For the surface hardening of sulfated slag cement, the following conditions are desirable: (1) slag having higher basicity and finer particle size, (2) coarse sand for mortar preparation and a rich mix with low water-cement ratio, and (3) storage in a highly humid atmosphere after curing in lime solution. 11 figures, 3 references.   K.Y.

Sulfate susceptibility of Portland cements: I. SHIGEO TAKATA, RANZO NAGANO, AND KINICHI KITAGAWA. *Semento Gijutsu Nenpo*, **6,** 73–79 (1952).—Sulfate reaction values of commercial cements in Japan determined at 20°C. by the method of Taylor and Bogue (1950) were 42 to 99. The results obtained were compared with the expansion and dynamic modulus of elasticity

of mortars immersed in solutions of Na_2SO_4, $MgSO_4$, and Na_2SO_4 + $MgSO_4$ for 3 months. 8 figures, 3 references. **II.** SHIGEO TAKATA, RANZO NAGANO, AND SHIGEYOSHI HOSOTANI. *Ibid.*, **7,** 45–50 (1953).—Test results for 3 months to 1 year are shown. The results obtained on the relation between sulfate reaction values and sulfate resistivity agreed with those of Taylor and Bogue. The sulfate reaction value of Portland cement is decreased or increased slightly by adding pozzolan consisting mainly of amorphous silica or by adding siliceous sand and blast-furnace slag. 3 figures.   Y.S.

Surkhi as a pozzolan. N. R. SRINIVASAN. *Road Research Papers* (Delhi), **1956,** No. 1, 74 pp.; abstracted in *J. Appl. Chem.* (London), **8** [7] i-13 (1958).—The mineralogy and physicochemical properties of some Indian soils and their surkhis (I) (fired clays) were studied to elucidate the function of I as a pozzolan (II) and to facilitate selection of soils for making I under controlled conditions. Brick loams do not yield very reactive I, but clays do, especially if high in 300-mesh fraction. Clay minerals strongly influence reactivity and firing temperature. Montmorillonitic clays should be fired at 600° to 800° C., kaolinitic clays at ≯ 800°, and illitic clays at ~1000° for maximum reactivity. Oxides of Fe and Al (of fine particle size) lower these optimum temperatures and improve subsequent II action. Firing beyond the optimum temperature increases particle size but lowers II reactivity. Red clays yield better I than do black-cotton clays, while laterites, bauxites, and ochers with free Fe oxides can produce reactive II when fired. A lime-reactivity/compressive-strength test for grading I according to reactivity is described. 19 figures, 74 references.   V.R.E.

Thermodynamic investigation of the solid reactions in silicate systems. O. P. MCHEDLOV-PETROSYAN AND V. I. BABUSHKIN. *Silikattech.*, **9** [5] 209–12 (1958).—The little known reactions occurring in silicate solids were investigated thermodynamically by determining the decrease in free energy (the isobaric thermodynamic potential) during the process and its dependence on the temperature. The principles of the measurement are described and applied to 10 reactions in the system CaO–Al_2O_3, 12 reactions in the system Ca–SiO_2, 10 in the system Al_2O_3–SiO_2, and 4 reactions in dolomite. The calculated heats of formation and free energies of formation from the elements are given. In the reactions of CaO with SiO_2, C_2S is formed as the principal reaction product in solid phase; without the influence of liquid or gaseous phases C_3S cannot be obtained except by special treatment. In the system CaO–Al_2O_3, $C_{12}A_7$ is formed at temperatures up to 1000°C. as the most probable primary compound, and from this CA and C_3A are formed. At 1100°, $C_{12}A_7$ becomes very unstable, and the possibilities for the formation of C_3A increase. In the decomposition of dolomite, the first stage is the disintegration into carbonates followed by MgO_2, CO_2, and $CaCO_3$. At about 900°C. the disintegration product is a mixture of the oxides. 2 figures, 40 references.   M.HA.

X-ray study for evaluating the activity of pozzolans. GORO YAMAGUCHI AND AKIHISA KATO. *Semento Gijutsu Nenpo*, **10,** 214–21 (1956).—A method is described for determining the uncombined $Ca(OH)_2$ in the reaction products of pozzolan-lime mixtures with a Geiger-counter X-ray diffractometer. The contents determined are smaller than those determined by the CH_3-$COONH_4$ and the 2,4,6-tribromophenol methods. This is due to the fact that the combined $Ca(OH)_2$ dissolves gradually in the extraction liquids. X-ray analysis of pozzolan-lime mixtures heated at 550°C. showed that the uncombined $Ca(OH)_2$ reacts with the SiO_2 present, and no decomposition of the $Ca(OH)_2$ to CaO occurs. Accordingly, the principle on which the calorimetric method of Bessey and its modification (*Ceram. Abstr.*, 1958, July, p. 165b) for determining the $Ca(OH)_2$ in hydrated cements are based is doubtful. 4 figures, 13 references.

    Y.S.

PATENTS

Bactericidal dental cements. MAXWELL B. COLTON (Edgar Schaefer). U. S. 2,846,322, Aug. 5, 1958.—A bactericidal dental filling cement consists essentially of an intimate admixture of a zinc cement set with phosphoric acid and a multiple antibiotic consisting of aureomycin, bacitracin, Chloromycetin, and streptomycin, the quantity of antibiotic being about 10 to 40 mg. to each 5 gm. cement.   D.J.B.

Dehydrating apparatus. CHARLES E. COMPTON. U. S. 2,848,-209, Aug. 19, 1958.—15. A dehydrating apparatus comprises a closed drum within which gypsum, etc., to be dehydrated is adapted to be disposed, a tube within the drum, an annular accor-

dionlike structure disposed about the tube and forming alternate internal pockets for heating medium and external pockets for the gypsum, etc., the internal pockets being in communication with the interior of the tube, means for introducing heating medium into the tube, and means connected with the annular accordionlike structure at the outer ends of the internal pockets receiving and conveying away the heating medium.   D.J.B.

Dehydrating gypsum, etc. CHARLES E. COMPTON. U. S. 2,848,210, Aug. 19, 1958.—A method of treating gypsum in a batch process comprises at least partially dividing a mass of gypsum in a closed chamber into smaller masses confined at their sides by generally upright heating surfaces, causing the gypsum to shift relatively to the surfaces while maintaining at least the partially divided smaller masses confined at their sides by the upright heating surfaces by turning the chamber about a generally horizontal axis, preheating the gypsum by conducting heat thereto through the upright heating surfaces while the chamber is turning about the horizontal axis so that the free moisture driven off from the gypsum builds up steam pressure in the chamber, and subsequently calcining the gypsum by driving off the water of crystallization by conducting heat thereto through the upright heating surfaces also while the chamber is turning about the horizontal axis and during the calcining venting the chamber to atmosphere to gradually reduce the pressure of the steam in the chamber.   D.J.B.

Dehydrating gypsum, etc. RICHARD R. RUEHLE (Charles E. Compton). U. S. 2,848,211, Aug. 19, 1958.—1. A method of dehydrating gypsum comprises introducing into a dehydrating chamber a mass of pieces of gypsum, substantially sealing the gypsum in the dehydrating chamber, applying heat to the gypsum by conduction through the wall of the dehydrating chamber while the gypsum remains sealed in the dehydrating chamber, resulting in driving off moisture from the pieces of gypsum and forming steam in the dehydrating chamber, and, while continuing to apply heat to the gypsum by conduction through the wall of the dehydrating chamber, alternately venting and sealing the dehydrating chamber for periods of at least several minutes during which the pressure in the dehydrating chamber builds up and thereby causing the pressure in the chamber to alternately rise and fall until the gypsum is substantially dehydrated to calcium sulfate hemihydrate.   D.J.B.

Method and apparatus for mixing. MORRIS M. BEAN (Morris Bean & Co.). U. S. 2,846,726, Aug. 12, 1958.—1. The process of preparing a settable and moldable slurry including a water-setting constituent, such as gypsum plaster, consists in mixing the dry constituents of the slurry with water, chilling the slurry to a temperature sufficiently below atmospheric to strongly retard the setting of the slurry, rubbing and squeezing the wetter solid particles of the slurry during the mixing until occluded gases have been substantially completely expelled while retaining the temperature of the slurry substantially below atmospheric, and then ejecting the slurry under pressure into a form with heating of the slurry as it is discharged.   D.J.B.

Oil well cement composition. JOHN A. WOOD AND EDWARD P. CHAPMAN, JR. (Vernon F. Taylor, Jr.). U. S. 2,846,327, Aug. 5, 1958.—1. A cement slurry of slow-setting characteristics and moderate set strength with low set shrinkage consists of anhydrous calcium sulfate 33 to 67% by volume of solid constituents, Portland cement 67 to 33% by volume of solid constituents, Wyoming bentonite about 2 to 4% by weight of cement, and water in amount of about 45 to 75% of solid constituents to impart slurry characteristics.   D.J.B.

Slow setting cement compositions. WALTER J. HALDAS (Lone Star Cement Corp.). U. S. 2,848,340, Aug. 19, 1958.—1. A slow setting cement composition suitable for the cementation of oil wells at depths in excess of 8000 ft. consists essentially of Portland cement and about 0.1 to 2.0% by weight, based on the dry cement, of a lower alkyl acid phosphate.   D.J.B.

Additional abstracts

Sect. X: Electrostatic precipitators. **Sect. XII:** Factors of dust suppression in small- to medium-size rotary kiln systems. Kiln ring removal.

IV—Enamels and Refractory Coatings for Metals

Description and measurement of white surfaces—report of ISCC Subcommittee on White Surfaces. RICHARD S. HUNTER. *J. Opt. Soc. Am.*, 48 [9] 597–605 (1958).—Present practices in the evaluation of white and near-white colors are reviewed. Whiteness as an attribute of surfaces and methods used to evaluate it are discussed. 9 figures, 4 tables, 20 references.   J.J.D.

Effect of heat-treatment on properties of enamel-steel composites. J. H. HEALY AND L. K. BREEZE. *J. Am. Ceram. Soc.*, 41 [10] 381–86 (1958).—Tangential deflection was measured on glass-steel strips that were heat-treated below, as well as in, the transition zone of the glass. The change in tangential deflection after heat-treatment was similar to the change in flexure breaking stress, thermal-shock resistance, resistance to fish scaling, and spalling of glass in an acid environment after heat-treatment. 10 figures, 18 references. **Discussion.** J. C. RICHMOND. *Ibid.*, pp. 386–87. 4 references. J. H. LAUCHNER. *Ibid.*, pp. 387–88. 1 figure, 4 references. B. J. SWEO. *Ibid.*, pp. 388–89. 1 figure, 4 references.

Electrophoretic deposition of ceramic insulating materials. ROLF BAHN. *Silikattech.*, 9 [7] 299–303 (1958).—Similar to the electrolytic deposition of metals, ceramic powders are deposited by electrophoresis on an electrically conductive support. The formed layers are densely packed and can be made to adhere firmly for further processing by the addition of a binder. The principle is to make a fairly concentrated suspension of finely ground glass powder in alcohol, into which two electrodes of a conducting material are immersed. By connecting a direct current of 100 or more volts, a deposit is formed at the anode of a thickness proportional to voltage, time, and concentration of the suspension. An apparatus was developed in which alumina-methanol suspensions of 400 to 1200 gm. of Al_2O_3 per liter are used to which some collodion is added as binder. Alumina suspensions, which are deposited by the addition of an electrolyte on the cathode, are called cataphoresis pastes, and suspensions in which the natural state of charge of the alumina particles remains intact are anaphoresis pastes. The amount (A) deposited in unit time is $A = (Icw)/\kappa$, where I is current, c is concentration of the suspension, w is migrating velocity of the particles, and κ is conductivity of the suspension. Directions for preparing the suspensions are given. 7 figures, 5 references.   M.HA.

Frit for vitreous enameling. ANON. *Engineer*, 206 [5348] 139–40 (1958).—Production and control methods used at a large frit plant in the U. K. are described. 1 figure.   V.R.E.

How to treat pickle liquors in a small plant. EDWARD W. LANG. *Metal Progr.*, 73 [5] 93–96 (1958).—Methods of disposal practical for small plants employing batch pickling are discussed. The tests were based on a 1200-gal. tank. It was found most practical to draw off 400-gal. portions, crystallize ferrous sulfate for disposal, and return the regenerated liquor to the pickling tank. Flow sheets, cost studies, and analytical control procedure are included. 3 figures.   D.J.B.

Porcelain enamels and ceramic coatings. ROBERT J. FABIAN. *Materials in Design Eng.*, 48 [1] 103–18 (1958).—F. gives a guide to the types of coatings available and their service properties, principal uses, and design factors. A glossary of basic enamel terms and diagrams showing recommended metal fabrication procedures for best results with enamel are included. Under ceramic coatings are included high-temperature enamels and refractory oxides. Some references to cermet coatings are given. Properties of the refractory oxide coatings are tabulated. This article comprises Manual No. 150 of *Materials in Design Eng.* and can be obtained as a separate reprint. 19 photos, 3 references.   D.J.B.

BOOK

Enamel Art on Metals. EDWARD WINTER. Watson-Guptill Publications, Inc., New York 18, 1958. 160 pp., illus. $9.75.— Winter has long been an enthusiast for porcelain enamel on metal as a medium for the artist who is hoping for permanence of design and color. He early acknowledges the necessity for good design and, to a certain extent, useful design. The many illustrations will give the art enameler some conception of the diversity of subject and the flexibility of usage. After design comes metalworking. Preparation of the metal base is deemed sufficiently important to occupy more than half of the book. Application of enamel to the base reflects the knowledge of the artist, who has per-

formed all of the operations himself. The chapters on raw materials and preparation of enamels are well advanced for those who will probably refer to this book. The glossary will be helpful to those who wish to properly express themselves, and the bibliography will provide additional references in related fields. One of the weaknesses of the book is the lack of illustrations from other artists and designers. Except for ancient pieces, few examples come from beyond the Winter family. This book is not only a text of the manufacture of enameled art pieces, but a beautiful assortment of designs by the author.   CHARLES S. PEARCE

PATENTS

Flame spraying process. HAROLD L. RECHTER AND MARVIN EISENBERG (Armour Research Foundation of Illinois Institute of Technology). U. S. 2,848,349, Aug. 19, 1958.—1. The method of coating an object with an adherent coating comprises directing a high temperature flame at the object and injecting into the flame a particulated mixture comprising lithium aluminate and zirconia.   D.J.B.

Refractory vitreous ceramic coating materials. DWIGHT G. BENNETT AND WILLIAM J. PLANKENHORN (United States of America, as represented by the Secretary of the Air Force). U. S. 2,846,325, Aug. 5, 1958.—An alkali- and alumina-free frit is intended particularly for use with stainless steels and nickel alloys known as Inconel and is effective for use at 2000° F. for extended periods. The frit components fall in the following ranges (by weight): SiO_2 34 to 40, B_2O_3 5 to 10, BaO 22 to 28, BiO_2 8 to 12 CeO_2 4 to 6.5, ZnO 4 to 6, CaO 4 to 6, and TiO_2 3 to 10%. A preferred raw batch formula (by weight) is quartz 31.2, boric acid 12.0, barium carbonate 26.3, bismuth trioxide 6.2, bismuth nitrate 4.2, cerium oxide 4.2, zinc oxide 4.2, calcium carbonate 7.5, and titania 4.2%. This mixture produces a frit with the following oxide composition (by weight): SiO_2 37, B_2O_3 8, BaO 25, BiO_2 10, CeO_2 5, ZnO 5, CaO 5, and TiO_2 5%. Chromic oxide contributes greatly to high temperature stability and may be a frit or a mill batch constituent. If no chromium is added in the mill batch, 10 to 25 parts by weight of titania per 100 parts of frit increases the resistance to acids or alkalis and improves other properties. Melting of the frit (at about 2550°F.) is followed by water quenching and grinding to 30- to 40-mesh size. In one mill batch (parts by weight) 100 frit was used with 25 chromic oxide, 6 enamelers clay, and 40 water. It was adjusted to give a dipping weight of 20 to 25 gm. on a sandblasted steel plate (both sides covered) and a fired coating 2 to 2.5 mils thick. The plate was fired at 1800°F. for 6 min. The preferred metals are AISI Nos. 302, 310, 321, and 347.   D.J.B.

Additional abstracts

Sect. VIII: Determination of the optical characteristics of enamels and glazes. **Sect. IX:** (*patent*) Method of making thorium oxide cathodes. **Sect. XII:** (*patent*) Induction heating apparatus for fusing vitreous enamel.

V—Glass

Acid polishing of lead glass. M. M. SKORNYAKOV. *Steklo i Keram.*, 14 [4] 19–22 (1957).—The polishing agent was 2 vol. of HF (sp. gr. 1.13) and 3 vol. of H_2SO_4 (sp. gr. 1.84). The glass had the following composition: 57 SiO_2, 25 PbO, 3 BaO, 11 K_2O, 4 Na_2O, and 0.5% As_2O_3. S. concluded that polishing with freshly prepared solutions of these acids should be done at 35° with a 2-sec. immersion. Increase in temperature and immersion time leads to the formation of holes on the surface of the ware. Polishing acids may be recovered at any stage of polishing. They should be controlled during recovery by density measurements. Drying of the ware after washing does not lower its quality. The use of the recovery technique considerably reduces the acid consumption. 1 reference. Cf. *Ceram. Abstr.*, 1958, June, p. 143*j*.   K.S.

Aluminum determination in glass. O. LOODIN. *Glastek. Tidskr.*, 13 [2] 43–45, 53 (1958).—For Al_2O_3 exceeding 1% in glass, L. recommends treatment with H_2SO_4, HNO_3, and HF, followed by heating for 30 min. at 300° to 350°C. to expel the last traces of F. The residue is dissolved in hot diluted H_2SO_4. After dilution to about 150 ml., 2 ml. of concentrated HCl is added. For the R_2O_3 precipitation, a mixed indicator is used of the composition 0.1 gm. of bromcresol green and 0.05 gm. of methyl red dissolved in 120 ml. of 96% alcohol + 8 ml. of water. The color changes from red over blue to green. Ammonium hydroxide is added until the green color appears. An Al_2O_3 content below 1% is determined colorimetrically with ferron, which combines with Al to form a complex having an absorption peak at 365 mμ. A coincidence with a peak belonging to the iron complex is corrected for by means of the iron peak at 600 mμ. Analyses carried out on National Bureau of Standards glasses agree with the recommended values. 1 figure, 3 references.   S.A.L.

Anomalous regions of glasses in the system Na_2O–SiO_2–B_2O_3. O. S. MOLCHANOVA. *Steklo i Keram.*, 14 [5] 5–7 (1957).—Certain glasses (within the limits of 3 to 12 mole % R_2O and 60 to 80% SiO_2 with proportional amounts of B_2O_3) undergo anomalous changes in density and refraction in the zone from the initial firing range to the softening point. Here, diffusion increases and opalescence appears; the latter disappears at high temperatures and changes the chemical resistance of the glass to water, acids, and alkalis. Graphs show the variation in chemical stability of glasses containing 20, 40, 60, and 70% SiO_2, the Na_2O varying constantly in each case. Data are also given on the change in density in relation to temperature of several normal and anomalous sodium borosilicate glasses containing 20 to 25% SiO_2. Experiments were carried out to define the limits of the anomalous regions. Earlier work by M. produced an explanation of the phenomena: glasses containing a small percentage of SiO_2 have the borate structure. The properties and structure of glasses in the composition of which SiO_2 predominates over B_2O_3 are determined by the first of these, i.e., it is a silicate glass and occupies an intermediate position. Its structure is not strong and depends on the small changes in composition and on its thermal history. An important role is probably played by the variation in coordination of the boron atoms. The existence of two lines (on the Na_2O–SiO_2–B_2O_3 diagram) of maximum chemical resistance to acids and water, especially the line passing through the 2 to 3% Na_2O region, needs further elucidation. 3 figures, 5 references. K.S.

Biologically processed wood for glassworking molds. M. HÜBSCHER, W. LUTHARDT, AND H. TISCHER. *Silikattech.*, 9 [7] 312–13 (1958).—Myco-treated wood has proved to be very advantageous for working glass. The molds are made up of wood sections which are inoculated on their front surfaces with fungi to make them more porous. This porosity holds the water in longer and prevents burning of the molds by the too early disappearance of the steam layer between glass and mold. The life of such molds is 15 times as long as that of other wooden molds and equivalent to that of carbon molds. 2 references. M.HA.

Color and light scattering of platinum in some lead glasses. R. J. RYDER AND G. E. RINDONE. *J. Am. Ceram. Soc.*, 41 [10] 415–22 (1958).—The coloration and light scattering of sodium lead silicate, borate, and phosphate glasses containing platinum, introduced as $PtCl_4$, were studied. In the normal atmosphere of a furnace heated by silicon carbide elements, the platinum is retained in the colloidal state in the sodium lead silicates and borates, producing gray glasses. In the phosphate glasses yellow to orange ionic colors as well as grays are produced. Lead oxide increases the stability of platinum ions in the phosphate glasses. Under strong oxidizing conditions, ionic platinum can also be obtained in the borate and silicate glasses. Tyndall scattering can be detected in what appear to be clear, colorless glasses. This light scattering has been observed in some glasses containing as little as 1 p.p.m. of platinum. 10 figures, 5 references.

Common salt—a good accelerator for glassmelting. V. P. SMIRNOV. *Steklo i Keram.*, 15 [7] 40–41 (1958).—NaCl can be used as an accelerator, but fluorides work more quickly. Chlorides are effective with glasses colored with sulfides. A formula for a glass fused with the aid of NaCl is given. The salt increased the output of the tank by 28%, and the quality was improved (gas inclusions reduced and working properties bettered). The salt was first sieved (36 apertures/cm.^{2}) and mixed with the sodium sulfate and coal, 15 to 20 kg. of salt being used per ton of glass. Amounts in excess of this and water contents of > 5% slowed down the rate of melting and the fining. 1 figure. K.S.

Complexometric determination of calcium and magnesium in window glass. M. HOLMBERG. *Glastek. Tidskr.*, 13 [2] 39–42 (1958) (in Norwegian).—The determination of Ca and Mg in window glass by means of EDTA is described. 1 figure, 1 reference.   S.A.L.

**Density change of glass due to heating: III, Analysis of den-

sity change by a reaction model. Toru Kishii. *Yogyo Kyokai Shi*, 66 [749] 117–24 (1958).—A theory is proposed to explain the density change of glass. Glass is postulated to be composed of small cubes which are in the energy levels $L_1 L_2, \ldots L_i$. The probability of the transition of a cube from L_i to L_j is calculated. The relation between the probability of transition of a cube and the anomalous density change observed experimentally is discussed. 12 figures, 19 references. For part II see *Ceram. Abstr.*, 1958, Aug., p. 197*e*.   K.Y.

Density studies on the function of rare-earth ions in glass matrices. R. C. Vickery and R. Sedlacek. *J. Am. Ceram. Soc.*, 41 [10] 422–26 (1958).—The effect on density of the inclusion of low concentrations of rare-earth ions in lead silicate, soda-lime, and phosphate glass matrices was studied. Significant changes in these density values are particularly noticeable in phosphate glasses and least noticeable in lead glasses. It is considered that the variable function of the Pb^{2+} ion obscures the general effect of rare earths in lead silicate glasses; in soda-lime and phosphate glasses, however, evidence indicates that the lanthanons (La through Lu) function only as network modifiers, and that scandium and yttrium in concentrations of >0.2 and 1.0 atomic % function strongly as network formers. This is shown to be in accord with concepts associating glass function with cation electronegativity. 2 figures, 7 references.

Determination of the elastic constants of some glasses and glass solders with optical supersonic methods. Adelbert Thiele. *Glastech. Ber.*, 28 [10] 384–91 (1955).—The wave lengths of transverse and longitudinal supersonic vibrations generated in glass cubes by a piezoelectric quartz plate at measured frequencies were determined by photographing the cubes in polarized light. From the velocities of the elastic waves and the densities of the glasses, the elastic constants were calculated. For 6 optical glasses the results were parallel to those of previous workers, but generally lower. The differences are explained by changes in composition of the glasses. Measurements on the glass solders met with difficulty because it was not possible to make cubes free from inhomogeneities and schlieren and because of the small stress optical constants of the high lead compositions. For 5 glass solder compositions (% PbO, % SiO_2, and % B_2O_3) densities and elastic constants (shear modulus, Poisson's ratio, and Young's modulus) were as follows: 70%, 20%, 10%, 5.075 gm./cm.³, 2159 kg./mm.², C. 0.2856, 5553 kg./mm.²; 70%, 5%, 25%, 4.936 gm./cm.³, 3122 kg./mm.², 0.2055, 7524 kg./mm.²; 80%, 5%, 15%, 5.931 gm./cm.³, 3405 kg./mm.², 0.1413, 7762 kg./mm.²; 80%, 10%, 10%, 6.00 gm./cm.³, 3434 kg./mm.², 0.1626, 7988 kg./mm.²; 85%, 5%, 10%, 6.45 gm./cm.³, 2954 kg./mm.², 0.3093, 7733 kg./mm.². 10 figures, 16 references.   C.H.G.

Development, construction, and operation of a direct-fired glassmelting furnace called the "Unit Melter." A. K. Lyle. *Glastek. Tidskr.*, 13 [2] 33–37, 42 (1958).—L. describes the development of the Unit Melter since its introduction in 1951 and summarizes its operation data, advantages, and limitations. Some unique features are discussed. The construction cost is approximately half that of an ordinary furnace. The repair and maintenance costs are estimated to be < 15% of the initial cost per annum. 3 figures.   S.A.L.

Electrosparking method for sharpening [glass] cutters. S. N. Evsyutin. *Steklo i Keram.*, 14 [6] 20 (1957).—A circuit diagram and a brief description of the method are given. 2 figures.   K.S.

Entry of water into silica glass. A. J. Moulson and J. P. Roberts. *Nature*, 182 [4629] 200–201 (1958).—Some specimens of silica glass absorb infrared radiation of about 2.7μ wave length. Garino-Canina (1954) observed that the occurrence or absence of the band in his specimens depended on whether or not water vapor was present when the glass was made (by fusing quartz crystal). Following Harrison (1947), he attributed the absorption to hydroxyl groups bound to some of the silicon ions of the glass. The present authors demonstrated the ability of the absorbing centers to diffuse into the glass at temperatures low compared with the softening point. Values of diffusion coefficient and solubility were obtained. The dependence of the equilibrium concentration of absorbing centers on the pressure of water vapor at constant temperature is being studied.   V.R.E.

Gases in glass. V. T. Slavyanskii. *Steklo i Keram.*, 14 [2] 11–17 (1957).—Details of a method for extracting and analyzing the gases contained in solid glasses are given. The equipment for extraction consists of a degassing flask containing a funnel-shaped platinum heating spiral, two traps, a Tepler pump, and an absolute manometer developed by Pirson. A special feature of the apparatus is the complete isolation of the reaction space of the system from the lubricant, rubber, and other materials. Extraction operations are as follows: a piece of glass (0.1 to 0.2 gm.) is placed in the entry tube of the degassing flask and sealed in. A vacuum is created throughout the system, and in about 1 hr. the surface of the specimen is degassed by heating up to 400°, i.e., heating the Pt spiral to 1200°. Usually at the end of degassing there is a pressure of 10^{-4} to 10^{-5} mm. The system is then shut off from the pump with a Hg seal, and liquid air enters the trap. To establish the specimen in the Pt spiral, the degassing flask is filled with Hg (this process is shown in a detailed diagram). The heating is increased, and further degassing of the specimen begins at 900°. Water vapor and CO_2 immediately condense in the cold liquid air at the top of the trap. Gas is best extracted at high temperatures. Extraction of gas takes 20 to 30 min. The flask is then filled again with Hg (it was emptied in one of the intermediate processes), the temperature is brought to room temperature, and all of the gas is pumped to the analytical apparatus. Full details of construction and operation of the apparatus and its principles are given. 3 figures, 11 references.   K.S.

Glass lubricant in metallurgy. L. K. Kovalev and V. A. Ryabov. *Steklo i Keram.*, 15 [7] 8–12 (1958).—The application, composition, and properties of glass lubricants used in hot pressing and extruding metal articles are discussed. The coefficient of friction during the hot pressing of steel with a lubrication of graphite mixed with petrolatum is 0.026 to 0.03, with graphite and glass 0.026 to 0.035, and with glass 0.027 to 0.033. The thickness of the glass layer on the pressed article is about 20 to 100μ. The main properties influencing lubrication are thermal conductivity, viscosity, degree of wetting of the metal by the glass, the critical nature of the glass film, and the corrosion of the metal by the glass. Ni and Cr alloys immersed for 15 min. in glass at 1300° were completely wetted and covered by the glass, but the same treatment given to Mo-W alloys produced no wetting and the alloy was completely free of glass. Ti alloys develop a wettability at 1050° to 1100°, particularly for glasses containing BeO, B_2O_3, and Li_2O. The greater the difference between the coefficients of expansion of glasses and metals, the easier is the separation after forming and cooling. Volume coefficients of expansion for glasses suitable for lubricants lie in the range 17.5×10^{-7} to 300×10^{-7} and rise with increasing temperature. The most important factor is the length of time over which the glass keeps its working viscosity. Glass formulas suitable for lubricants are tabulated. Russian work suggests the following composition: 56 SiO_2, 21 Na_2O, 0.5 Al_2O_3, 15 CaO, 3 K_2O, 2 BaO, 2.2 CaF_2, and 0.3% Fe_2O_3. Best results in application are obtained by immersing the metal in the glass; this prevents oxidation and does not harm the metal. The stages of this process are described, and a diagram shows a mechanical assembly for immersing rods in a glass bath ready for pressing. The method was first used by an Italian firm, Mazzagera. A second method is also described. Glass powder, wool, textile, or fibers may replace the molten glass, but the application is different. An emulsion (glass with 3 to 5% kaolin) is sometimes used. Few data on the reactions between the glass and the metals are available, but the importance of the new lubricants warrants further research. 3 figures.   K.S.

Glasses for nuclear applications. E. Umblia. *Glastek. Tidskr.*, 13 [3] 67–70 (1958).—Glasses containing 0.5 to 2% CeO_2 are discolored only slightly or not at all by γ radiation. They are therefore used in optical instruments for nuclear applications. Calculation of the mass absorption coefficients of different oxides indicate that the following oxides have maximum absorption of γ rays below 1 mev.: PbO, Bi_2O_3, Ta_2O_5, WO_3, BaO, CaO, and CdO. The low-melting glass Bi_2O_3 60, PbO 30, and B_2O_3 + SiO_2 10% absorbs even hard γ rays efficiently. It has, however, low hardness and chemical durability. The main properties of Corning's three cerium-stabilized glasses, 8365, 8362, and 8363, are given. Thermal neutrons are most efficiently absorbed by Cd, B, Li, and rare earth metals such as Sm, Gd, and Eu. Cd, however, causes a strong induced radioactivity. Pb and Fe have a strong retarding effect on fast neutrons. Glasses in the system PbO–CdO–B_2O_3, therefore, should protect efficiently against mixed neutron radiation. The use of photosensitive glasses for dosimetric purposes is discussed. 3 figures, 8 references.   S.A.L.

Increasing the efficiency of glassmelting tanks. D. B. Ginzburg, M. A. Matveev, S. I. Zherebin, and I . V. Lebedeva. *Steklo i Keram.*, 14 [4] 5–9 (1957).—The following data are given and discussed to show how the output of glass tanks can be increased from the very low value of 15 to 25%: temperature cycle

of tank, composition of gases in different parts of the tank, distribution of dry and wet gases and consumption of air, heat balance, and relation between heat work of gas generator and addition of air to the outside and into the regenerator system. Sealing of the regenerator system is important in saving fuel and improving working conditions. Special magnesium and silicate compounds are used as sealers in the U.S.S.R. 4 figures, 4 references. K.S.

Inductive regulation of a glassmelting furnace. HORST MARTIN. *Silikattech.*, 9 [6] 250–56 (1958).—As fluctuations in furnace atmosphere affect the quality of glass, a system was developed which inductively and automatically controls the O_2 content as the most characteristic component of the waste gases; it also controls the melting temperature and furnace room pressure, giving a more uniform output and better glass quality. The installation is described in full. 13 figures, 2 references. M.HA.

Influence of temperature on the optical constants of glass in the region of strong absorption. NORBERT NEUROTH. *Glastech. Ber.*, 28 [11] 411–22 (1955).—The reflection of infrared radiation in the 7 to 12µ region by window glass, household glass, and silica glass was measured for 70° and 20° angles of incidence at temperatures up to 1300°C. The radiation was polarized by a pile of six thin sheets of selenium, and measurements were made with the direction of polarization both parallel and perpendicular to the plane of incidence of the radiation on the glass. From these measurements of reflectivity, the optical constants, refractive index η and absorption index κ, were obtained by the graphical procedure of Tousey and Simon. At room temperature the silica glass showed a strong sharp maximum in absorption index at about 8.85µ with indication of a weaker neighbor band at 8.26µ. With increasing temperature this principal absorption band increased in width and decreased in height while the position of its maximum shifted to longer wave lengths. The neighbor band at 8.26µ disappeared, and a new neighbor band appeared at 9.90µ. The optical properties of the window glass were similar to those of the household glass. At 18°C. both showed a variation of absorption index with wave length resembling that of silica glass at 1270°C. or above. With rising temperatures the maxima of these curves were also decreased in height and displaced toward longer wave lengths, although the changes were less pronounced than in the case of the silica glass. Devitrification in the range 600° to 1100° caused large and erratic changes in the optical properties of the soft glasses. The marked widening of the absorption band of silica glass by increasing temperature may be explained by the silica network being more and more broken up with consequent damping of the Si-O vibrations. Both the half width of the absorption band and the variation of refractive index from minimum to maximum indicate that the damping approximately doubles for a temperature rise from 18° to 1270°C. In the window and household glasses the addition of metal oxides disrupts the silica network to about the same extent as heating the silica glass to 1270°C. From the fact that the alteration in optical constants above and below the devitrification range is continuous and reversible for the soft glasses, it is concluded that the same molecular structure is present in the glass whether it is solid or liquid. 17 figures, 12 references. C.H.G.

Internal pressure testing. LOTHAR H. LEHNERT. *Glastech. Ber.*, 28 [10] 380–83 (1955).—The bursting pressures for several types of bottles decreased from approximately 25 to 15 atm. as the out-of-roundness increased from 0 to 5 mm. Bursting pressures were found to increase as the rate of application of pressure increased. Diamond scratches made parallel to the axis of 0.5-liter brown beer bottles on the outside surface decreased the bursting pressure from 28 to 18 atm. with a scratching force of 2 kg. The decrease in bursting pressure was proportional to the load on the diamond over this range. Artificial aging by passing alternately through a heating tunnel at 40° and a water spray at 15° for 360 hr. decreased the bursting pressure of 0.33-liter brown beer bottles by about 12%. Tempering by cooling from 520° at 1000°C./hr. increased the bursting pressure of new 0.33-liter brown beer bottles from 36 to 46 atm. Increasing the temperature at which the test was made decreased the bursting pressure of 0.33-liter brown water bottles from 33 atm. at 0°C. to 23 atm. at 75°C. More investigations are needed to determine how far these results may be generalized. 9 figures, 6 references. Cf. *Ceram. Abstr.*, 1957, Oct., p. 234d. C.H.G.

Means of studying glass batches in a glass tank. V. A. DUBROVSKIĬ. *Steklo i Keram.*, 14 [6] 1–6 (1957).—The radioactive isotope Sr-89 was used to trace glass flow in a 330-ton tank (22.1 m. long, the melter 5.9 m. wide, and the cooler 7.1 m. wide), with

a daily output of 32 to 33 ton. The mixture was loaded in 5 parts by automatic means. The isotope, in quantities of 50 millicuries, was added as the carbonate precipitated from $Sr(NO_3)_2$ with Na_2CO_3. Samples were drawn from different parts of the tank, ground, and sieved. The activity of the powders was measured on the standard radiometric apparatus of B. Velichina and directly compared with that of untreated batches. Results are shown in diagrams and are discussed. D. recommends this method of marking atoms without an intermediate agent for studying the gradual blending of glass components in the tank during continuous feeding of the batch. 3 figures, 1 reference. K.S.

Modernization of the glass annealing furnace LN-18Kh1000. V. L. INDENBOM AND L. F. YURKOV. *Steklo i Keram.*, 14 [5] 22–24 (1957). 2 figures, 2 references. K.S.

New method for the production of thin and thinnest plate glass. JOHANNES RÖDER. *Silikattech.*, 9 [7] 297–99 (1958).—In a manner similar to the Fourcault process, thin glass plates (0.1 to 0.2 mm.) are drawn from a band of about 2 mm., which is suspended on a cable in a furnace until it has a low viscosity and flows off by its own weight. This foil is pulled between two rolls and equalized to a tolerance of ±0.01 mm. A successful installation is described. 5 figures. M.HA.

Optimum conditions for drying extruded films of "butafol." A. P. ALEKSANDROV. *Steklo i Keram.*, 15 [7] 41–42 (1958).—"Butafol" is a polyvinyl butyral plasticized with dibutyl sebacinate in the form of films or coatings. It is used as an adhesive intermediate layer in safety glass. The technique, which includes washing and drying at 45° to 50° in 4 to 5 hr., leads to undesirable shrinkage of the sheets. This fault can be eliminated by a special drying schedule. K.S.

Optimum temperature cycle for the melting zone of glass tanks. K. K. VILNIS, V. V. POLLYAK, AND M. G. STEPANENKO. *Steklo i Keram.*, 15 [4] 1–5 (1958).—The output of glass tanks is directly related to the length of the melting zone and the temperature of the superstructure. An increase in the dimensions of the melting area covered by the batch results in a lowering of the temperature of the glassmelt under the charge and may, under certain conditions, decrease the uniformity and clarity of the glass. The dimensions of the zone of actual melting at the existing level of temperature should not exceed 35 to 40% of the "mirror" area of the melting tank of the kiln (up to the baffle). To improve the use of the melting area and increase its specific productivity, there should be maintained near the charging chamber (for the existing type of refractory), a temperature <1420° for tanks melting technical plate glass and 1400° for window glass (containing increased Na_2SO_4). The high level of temperature at the top of the structure near the charging chamber has practically no influence on the temperature of the glass under the charge and consequently on the force of the convection streams. With increased temperature in the region of the first two burners, the length of the melting zone is not increased but reduced. A formula is given for the relation between the output of the melting zone and the temperature above it. 3 figures, 3 references. K.S.

Progressive method of air cooling glass tanks. K. I. BORISOV AND A. A. SVETLOV. *Steklo i Keram.*, 14 [2] 22–25 (1957).—The authors describe a system for protective cooling of the upper courses of a glass tank to prevent destruction in service. One meter of cooled kiln perimeter requires 0.3 to 0.4 m.³/sec. of air at a nozzle speed of 30 to 40 m./sec. 3 figures. K.S.

Rapid determination of manganous oxide in glass. V. M. YASINENKO. *Steklo i Keram.*, 14 [4] 22–23 (1957).—The new method does not use hydrofluoric acid. The determination is carried out on the filtrate obtained after separation of the SiO_2 in analysis of the glass by the double evaporation method. A brief account of the analytical method is given. K.S.

Rationalization of fuel economy at the Gor'ki glass factory. D. B. GINZBURG AND S. I. ZHEREBIN. *Steklo i Keram.*, 15 [7] 3–8 (1958).—An increase in the heating capacity of peat producer gas is obtained by adding propane-butane mixtures and artificially drying the peat. Such enrichment of the gas and the use of pitch for combustion in the kiln makes it possible to eliminate scrubbing and drainage of the phenolic liquids. The use of the heat from the waste exhaust gas in the drying of the peat is mentioned. Tests made at this plant are discussed, and data are given on the fuels and burners used. 11 figures, 4 references. K.S.

Refractive index of arsenic trisulfide. WILLIAM S. RODNEY, IRVING H. MALITSON, AND THOMES A. KING. *J. Opt. Soc. Am.*, 48 [9] 633–36 (1958).—The refractive index of a sample of arsenic

sulfide glass was determined at three temperatures near 19°, 25°, and 31°C. for a series of wave lengths in the range 0.57 to 11.8μ, and a five-term Sellmeier type dispersion equation was fitted to the average data reduced to 25°C. The computed dispersions and thermal coefficients of refractive index are given. 4 figures, 3 tables, 7 references.   J.J.D.

Semiautomatic machine for silver plating Christmas tree decorations. YA. S. ZAPOLYANSKIĬ. *Steklo i Keram.*, **14** [6] 21–22 (1957). 2 figures.   K.S.

Shape of the liquidus surface as a criterion of stable glass formation. EDGAR H. HAMILTON AND GIVEN W. CLEEK. *J. Research Natl. Bur. Standards*, **60** [6] 593–96 (1958).—The slope of the liquidus curve or surface at a point in a phase diagram representing a specific chemical composition was found to be a reliable indication of the glassforming tendency of that composition. The observed effect is interpreted in terms of the structure of the glass. 4 figures, 15 references.   M.J.K.

Silicone films on glass surfaces: II. HANS WESSEL. *Silikattech.*, **9** [5] 201–208 (1958).—Results are given in diagrams of experiments made on the behavior of silicone-treated glass surfaces under different conditions. The silicone is used as a protection from the action of different substances, particularly in the pharmaceutical industry. 18 figures, 11 references. For part I see *Ceram. Abstr.*, 1955, June, p. 104g.   M.HA.

Spectrophotometric study of colored glasses: I, Spectrophotometric study of glasses colored by iron and manganese. MASAYOSHI IHARA AND TOKUJI YAMAMOTO. *Yogyo Kyokai Shi*, **66** [750] 144–52 (1958).—The base glass was a soda-lime-silica type, and the coloring agents added were rouge, copper slag, manganese dioxide, and manganese ore. The transmission of the glass specimen between 350 and 1000 mμ was measured spectrophotometrically, and the results are expressed according to the C.I.E. color specification. With increase of total iron the color of the glass changes from blue to green. If the partial pressure of oxygen is kept constant during the melting, the equation $[FeO]^2/[Fe_2O_3] = k/[O_2]^{1/2} = \alpha$ (constant) holds. The ratio $[FeO]/[Fe_2O_3]$ decreases with increase in total iron; this means that the yellowish green tint of Fe_2O_3 becomes stronger than the blue tint of FeO. FeO makes the glass nine times as dark as does Fe_2O_3. The luminous transmission, Y, was found to be in linear relation with the content of FeO. By using this relation 0.5 to 2.5% Fe_2O_3 can be determined without chemical analysis. The color of glass with additions of both iron and manganese changes with the ratio of manganese to iron. From the types of transmittance curves, three reactions are assumed to be present: $MnO_2 + 3Fe_2O_3 \rightleftharpoons 2Fe_2O_3 + 2FeO + MnO + O_2$ for high iron ratio, $2MnO_2 + 2Fe_2O_3 \rightleftharpoons 2Fe_2O_3 + 2MnO + O_2$ for medium ratio, and $3MnO_2 + Fe_2O_3 \rightleftharpoons Fe_2O_3 + Mn_2O_3 + MnO + O_2$ for low ratio. 13 figures, 15 references.   K.Y.

Theoretical bases of the process of glassmaking. I. D. TYKACHINSKIĬ. *Khim. Nauka i Prom.*, **3** [1] 65–71 (1958).—The processes involved in the melting of glass have been identified by such observational procedures as sample analysis, gas analysis, dynamic and static weight analyses, electrical conductivity methods, petrographic and X-ray analyses, and the use of radioactive isotopes. The various stages in glass formation are identified and listed as a function of the temperatures reached at various times during the process for two glasses. T. identifies the important factors in the rate at which the various processes occur and gives empirical equations for the magnitudes of the effects under simple circumstances. The time required for dissolving sand grains is proportional to the cube of the molar concentration of the sand and inversely proportional to the square of the molar proportion of soda lye, the constant of proportionality depending on the size of the sand particles. This relation is reasonable since it can be related to the mass of sand as compared to its surface where dissolution occurs. Specifically, the velocity per unit surface is found to be proportional to the difference in concentration of SiO_2 at any time after complete dissolution of the sand, and it is inversely proportional to the viscosity of the melt and the thickness of the diffusion layer (presumably dependent on temperature and mixing rate). The effect of temperature is found to be expressed by $\tau = a \cdot b^{-bT}$, where τ is duration of the process, T is temperature, and a and b are constants for the glass. The time of melting is also found to increase with the surface of the component materials, i.e., as the degree of dispersion is increased. The increase is somewhat more than linear. The addition of accelerators, in the form of fluorides, B_2O_3, or both, decreases the time substantially. When all possible means of accelerating the processes of glassmelting are used, the effectiveness

of each factor is more or less limited. T. concludes that the capacity of glass furnaces in the Soviet Union might be increased by at least 50% if fine dispersions of raw materials were used with temperatures of 1500° and additions of appropriate amounts of accelerators. 7 figures, 15 references.   D.T.W.

Thermochemistry of nitrate glasses. C. KRÖGER AND W. JANETZKO. *Z. anorg. u. allgem. Chem.*, **287** [1–2] 28–32 (1956).—Several glasses in the system KNO_3–$Ca(NO_3)_2$ were investigated by calorimetric methods, and their heats of formation and heats of devitrification were determined. The compound $4KNO_3 \cdot Ca(NO_3)_2$ shows an incongruent melting point at 174°C. Its heat of formation was calculated from the values obtained for the binary nitrate glasses. From the relation between the maximum of the heats of devitrification and the maximum of the glassiness, it was concluded that the maximum of stability of the compound $4KNO_3 \cdot Ca(NO_3)_2$ is at 50.4 wt. % $Ca(NO_3)_2$. At this composition the degree of dissociation shows a minimum. 2 figures, 4 references.   G.B.

BOOKS

Glass—General Treatise on Glass Technology (Il Vetro—Trattato Generale di Tecnologia Vetraria). FELICE FRANCESCHINI. Published by Ulrico Hoepli, Milan, 1954. 1056 pp., 795 illus., 106 tables. Price Lit 6800.—Part I covers the properties, raw materials, and preparation of glass. F. traces the history of glass and gives the technical definition as a basis for studying the technique of glassmelting. Glasses are classified according to method of fabrication and chemical composition, and the forms, modifications, and structure of silica are treated briefly. The general physicochemical properties of glass are covered, including the vitreous state, devitrification, viscosity, annealing, and chemical resistance, together with special physical properties (mechanical, thermal, optical, and electrical). The chapter on the control of the chemical and physical properties of glass is not completely up to date. Raw materials discussed include acidic and basic oxides, stabilizing oxides, fining agents, colorants, decolorizers, and opacifying agents. Part II covers thermal equipment. A brief history of the technology of heat and combustion is followed by chapters on fuels, firing with gas, melting furnaces (201 pp.) and their operation and control, and refractory materials in the glass industry. Part III deals with the manufacture and annealing of glass. It comprises chapters on the calculation and control of glass batches, selection of the batch, decolorization of glass, reactions in the melt, melting and fining, melting defects, annealing of glass (fundamental theory), the cooling of glass in industrial practice (methods and equipment), and types of glass (bottle, window, optical, opal, radiation, etc.). In part IV, on glassworking, F. gives the fundamental concepts for glass shaping and describes the handworking of glass by blowing, the pressing of glass, laminating of glass, mechanical drawing and blowing of glass, blowing and pressing machines, finishing, decoration, tempered and safety glass, and glass wool and cloth. The book appears to be quite comprehensive in its coverage although not completely up to date with respect to equipment and methods.   GUY E. RINDONE

Structure of Glass—Proceedings of a Conference on the Structure of Glass, Leningrad, 1953. Edited by A. A. LEBEDEV ET AL. Translated from the Russian, 1958. 294 pp., illus. $20. Available from Consultants Bureau, Inc., New York 11. For review see *Ceram. Abstr.*, 1956, Aug., p. 164c.

PATENTS

Apparatus for applying a bead to glass tumblers. PERRY A. BECKER (Owens-Illinois Glass Co.). U. S. 2,836,145, May 27, 1958.—The apparatus is used in applying a surface coating of gold or other colored material to the beaded rims of glass tumblers. A plurality of units is provided, each including a decorating roll of rubber, etc., by which the decorating material is applied. The article to be decorated is mounted for free rotation about its axis and is held in rolling contact with the decorating rolls. The rolls are symmetrically arranged with respect to the workpiece and its support in a manner to apply a balanced pressure, which prevents tilting of the article. The decorating material is continuously applied to the decorating rolls by cylindrical transfer rolls.   H.E.S.

Apparatus for inspecting and classifying glass containers. BURTON A. NOBLE AND JOSEPH F. SCHLESINGER (Owens-Illinois Glass Co.). U. S. 2,849,114, Aug. 26, 1958.   H.E.S.

Apparatus for making tube envelopes. LLOYD S. HARTLEY, JOSEPH B. HENRY, JOHN W. MILLER, AND WILLIAM E. SHAHAN

(General Electric Co.). **U. S. 2,837,870**, June 10, 1958.—The invention relates to the making of glass-to-metal seals and particularly to improved apparatus for fabricating metal type cathode ray tube envelopes. The fabrication is carried out on a rotary machine of the type that is provided with a plurality of work supports or heads which are moved intermittently to occupy positions with respect to stationary work stations so that the parts are subjected to predetermined fabricating operations in each of the successively located stations. The work holders support the parts in the desired position and adjust the glass neck with respect to the metal cone to compensate for variations in the dimensions of the parts. The heads are also provided with means for subjecting the glass to a predetermined amount of pushup during the sealing operation; after the seal is largely made, the vertical force is removed from the neck to allow the same amount of pulldown by the action of gravity on the weight of the glass neck. The face plate seals are accomplished by ring burners which are raised from the envelopes carried by the machine when the machine is moved and are lowered into position automatically after each movement of the machine. After the face plates are sealed, their final position is accurately determined by admitting air under pressure to the interior of the bulb and controlling the admission of air in accordance with the position of the face plate. To insure uniform heating of the metal cones during the preheating and sealing operation, each head is rotated about its own axis.   H.E.S.

Apparatus for the manufacture of glass beads. EMILE PLUMAT (Union des Verreries Mécaniques Belges Soc. Anon.). **U. S. 2,838,881**, June 17, 1958.—Small glass beads are made in an apparatus comprising a vertical tubular column, the lower end of which has opening thereinto an upwardly directed burner which is supplied with fuel, a supporter of combustion, and glass granules and the upper end of which adjoins a centrifugal separator. At least one part of the burner is connected to the source of the supporter of combustion and/or fuel by means of a preheating jacket surrounding at least one refrigeration zone of the column and to the jacket by at least one pipe, into which opens the means for feeding glass granules. The glass granules are preheated rapidly to a temperature slightly or immediately below their softening temperature and then up to the softening temperature by their introduction into, and during their entrainment by, one of the two initially preheated fluids. They are then injected with the fluids into the flame and are heated rapidly to a temperature higher than their softening temperature. The beads thus formed are cooled in three stages: the first is sudden and terminates at the upper point of structural transformation; the second is moderate and terminates at the lower point of structural transformation; and the third is sudden and terminates slightly above 100°. The beads are then separated from the gases and are collected by a centrifuging operation. The flame is formed within an orientatable rising air current, the speed and temperature of which are adjustable.   H.E.S.

Cathode-ray tube filming apparatus. FRANCIS J. KINSCH (Rauland Corp.). **U. S. 2,846,974**, Aug. 12, 1958.   H.E.S.

Cathode-ray tube manufacturing apparatus. JEROME J. O'CALLAGHAN (Rauland Corp.). **U. S. 2,846,973**, Aug. 12, 1958.   H.E.S.

Composite firearm barrel comprising glass fibers. JAMES C. HARTLEY, HARRY I. DAY, AND JOHN L. WILSON (Olin Mathieson Chemical Corp.). **U. S. 2,847,786**, Aug. 19, 1958.   H.E.S.

Electric synchronizer for glass machine feeder. HAROLD E. LARISON (Lynch Corp.). **U. S. 2,846,818**, Aug. 12, 1958.   H.E.S.

Flow spout construction. ALFRED H. BAILEY AND JOHN C. BLAINE (Libbey-Owens-Ford Glass Co.). **U. S. 2,838,880**, June 17, 1958.—The invention relates particularly to an improved outlet or flow spout for continuous melting furnaces. By an improved shoulder and edger block mounting structure, both blocks can be shifted substantially as an integral unit to vary the width of a glass ribbon prior to its formation. Adjustment in the width of formed glass ribbon can be more rapidly carried out by moving the shoulder blocks with the assurance that the cooperating edger blocks will be maintained in their established positions without time-consuming readjustment. Since suitable adjusting means are provided, initial and minor positioning of the edger blocks can be made with respect to both the shoulder blocks and the forming rolls.   H.E.S.

Glass blowing device. KEITH CONRAD AND ROBERT R. DENMAN (Owens-Illinois Glass Co.). **U. S. 2,837,871**, June 10, 1958.—The invention relates particularly to a device for supplying blowing air for the expansion of formed glass parisons of either the pressed or blown type. A blow head mechanism is designed to adapt itself to any mechanical irregularities which may exist in the forming mechanism. The parison blowing device consists of a blow head baffle, a piston movable with the baffle, and a piston rod providing attachment between the piston and baffle. A spring is adapted to contact the lower end of the piston and baffle in a nonblowing position. Means are provided for supplying fluid pressure to the top of the piston, and a metering orifice in the top of the piston is adapted to permit leakage of fluid pressure in metered quantity to permit lifting of the baffle. A neck and a blow mold are also adapted to support a parison in blowing position with respect to the blow head and baffle. Means are provided for supplying air to the inside of the parison and beneath the baffle, and means are also provided to regulate the flow of the top pressure fluid through the metering orifice to control the amount of lift of the baffle.   H.E.S.

Glass compositions. GUY E. RINDONE (Prismo Safety Corp.). **U. S. 2,838,408**, June 10, 1958.—The glass compositions have a high index of refraction (at least 1.90) and are suitable for making small glass beads for use as retroreflective elements. A glass which is chemically stable to weathering contains silicon dioxide, titanium dioxide, and at least two of the oxides of barium, lead, alkali metals (potassium, sodium, or lithium), and arsenic. Example (mole %): SiO$_2$ 33.0, TiO$_2$ 34.0, BaO 25.1, PbO 7.5, and As$_2$O$_3$ 0.4. On slow cooling these glass compositions devitrify completely; rapid quenching in water, however, prevents devitrification and produces transparent particles. Liquid droplets formed by passing crushed and graded particles of the glass through a flame or a radiant-heat stack may be quenched to provide spherical transparent beads.   H.E.S.

Glass grinding machine. JOSEPH SCIURBA. **U. S. 2,847,801**, Aug. 19, 1958.   H.E.S.

Glass sealed centerwire structure. KARL SCHWARTZWALDER AND ROBERT W. SMITH (General Motors Corp.). **U. S. 2,837,679**, June 3, 1958.—A spark plug comprises a tubular metal shell, an alumina insulator secured within the shell and having a bore extending therethrough, a silver electrode spindle positioned in the bore, a resistor element in the bore, a layer of a mixture containing about 30 to 50% glass and the remainder substantially all a metal powder electrically connected to the resistor element and bonded to the walls of the bore between the resistor and the silver electrode spindle to form a gastight seal in the bore, and a compact sintered layer of conductive material in contact with and bonded to the first-mentioned layer and the silver electrode spindle to form a path of low electrical resistance, the conductive material being selected from the group consisting of nickel, silver, iron, cobalt, chromium, silica, and alloys thereof.   H.E.S.

Laminated joint for cathode-ray tube envelope and method of sealing. HARVARD B. VINCENT (Owens-Illinois Glass Co.). **U. S. 2,837,235**, June 3, 1958.—Cathode-ray tubes comprising a prefabricated hollow glass funnel and a face plate having complemental annular sealing edges are sealed together by the use of annular metallic sealing surfaces with a thin gasketing layer of high-melting glass. The jointing is enhanced by the use of an intermediate annular layer of low-melting glass sealing composition interposed between the layers of high-melting glass. The improved joint is durable and vacuum-tight.   H.E.S.

Lamp sealing method. ALEXANDER ROSENBLATT AND JOHN F. BURFIELD (Sylvania Electric Products, Inc.). **U. S. 2,837,880**, June 10, 1958.—The method of sealing and tipping-off an exhaust tube extending from and in communication with the interior of a sealed electrical device filled with gas at a pressure above ambient comprises heating a portion of the exhaust tube, while exposed to ambient pressure, to a temperature sufficient to render it sufficiently plastic to be worked but not sufficiently plastic to be ruptured by the internal gas pressure, pinching the plastic portion of the exhaust tube completely closed, evacuating the exhaust tube below the pinched portion to a pressure below ambient, and heating the exhaust tube below the pinched portion to a temperature sufficient to effect a severance thereof.   H.E.S.

Means for intercepting gobs of molten glass. JOHN E. McLAUGHLIN AND GUY H. ALLGEYER (Owens-Illinois Glass Co.). **U. S. 2,836,934**, June 3, 1958.—The invention is particularly adapted for use with machines in which the mold carriage is rotated at a high speed and mold charges or gobs are severed and dropped into the molds in rapid succession as the molds pass beneath the feeder. The interceptor is operated by an air motor by which it is reciprocated into and out of the path of the falling gobs. The air motor is controlled by a solenoid valve. An electrical control system provides selective means including switches individual to

the molds or mold units on the carriage. These switches may be operated manually to cause selective operation of the interceptor by which the falling gobs are detoured from any selected mold or molds and dropped into a cullet chute.   H.E.S.

Method and apparatus for applying metal to glass. HARRY B. WHITEHURST AND WILLIAM H. OTTO (Owens-Corning Fiberglas Corp.). **U. S. 2,848,390,** Aug. 19, 1958.   H.E.S.

Method of producing glass. ALEXANDER SILVERMAN. **U. S. 2,838,882,** June 17, 1958.—The finely divided glassforming materials are mixed with a binder; shaped at relatively low, even atmospheric, temperatures; and reacted in the presence of oxygen or an oxygen-yielding material. The exothermic heat of reaction, aided, if necessary, by added heat, raises the materials to their fusion point. By adjusting the proportions of the reacting materials and the externally heated environment, the temperature of the molten glass may be raised to give the desired viscosity. The oxidation of the metal used in the glassforming mix in the presence of complementary oxides results in an oxidized product composed of the mixture of the oxide of the metal and the complementary oxides. The process is applicable to molding, die forming, or extrusion.   H.E.S.

Method of providing glass fibers with plural superimposed different oxide coatings and products thereby produced. DOMINICK LABINO (L-O-F Glass Fibers Co.). **U. S. 2,839,424,** June 17, 1958.—Fibers of an alkali silicate are treated with a medium such as an aqueous solution of a chloride of calcium, zinc, or barium. The metal of the chloride replaces a portion of the alkali in the fiber by ion exchange, and the water of the solution is also incorporated in the fiber to a material extent. If the fiber thus formed is heated sufficiently to drive off the water, the porous fiber remaining is highly receptive to solutions of solutes which, upon heating, yield temperature-resistant oxides, e.g., chromic anhydride (CrO_3), cobalt nitrate, zinc nitrate or chloride, and aluminum nitrate or sulfate. The constituents are picked up by and become an integral part of the fiber. When the fibers are fired and the insoluble chromic oxide is attained, the material will resist, without deformation, temperatures of about 3000°F.
                                     H.E.S.

Preliminary pressing of laminated glass. OSCAR D. ENGLEHART, JOHN R. SADESKY, JOHN W. MORRIS, AND ROY S. SHER-

BONDY (Pittsburgh Plate Glass Co.). **U. S. 2,837,453,** June 3, 1958.—A laminated glass assembly, e.g., an automobile windshield, comprising two sheets of glass and a thermoplastic interlayer is supported on a flexible sheet within the area of the sheet that is defined by a continuous rib on its top surface. The assembly is placed so that it is spaced from the rib. A flexible cover sheet having dimensions sufficiently large to completely cover, even during evacuation, the entire area occupied by the rib is placed over the assembly. The two flexible sheets cooperate with the rib to provide a conduit between the rib and the periphery of the laminated assembly. This conduit is evacuated through the rib while at least part of the conduit is maintained in order to evacuate air from between the plastic interlayer and the sheets of glass. The assembly is then heated in at least the marginal area while vacuum is maintained between the two flexible sheets. After sufficient heating of the assembly to seal at least the marginal area, the vacuum is released and the flexible cover sheet is removed. The assembly is sufficiently prepressed by this method that it can be placed in the autoclave in the fluid for final pressing by heat and pressure without the fluid penetrating between the glass sheets and the plastic interlayer.   H.E.S.

Surface treatment of molybdenum and tungsten for glass sealing. JOHN E. STANWORTH, HAROLD RAWSON, AND MARY KNOWLES (British Thomson-Houston Co., Ltd.). **U. S. 2,836,935,** June 3, 1958.—In the manufacture of glass-to-metal seals with molybdenum or tungsten, rapid oxidation of the metal on heating is prevented by passing a volatile halide of silicon over the metal, which is heated to a temperature at which the compound is decomposed at the surface to form an adherent coating. Hydrogen is used as a carrier gas, and the hydrogen halide which is the by-product of the reaction is flushed off in the stream of gas. Silicon tetrachloride may be used as the volatile halide. Pure dry hydrogen is bubbled through the silicon tetrachloride and then passed over the metal, which is heated to 1200° to 1400°C. for 0.5 to 2 hr., depending on the thickness of coating desired. This schedule produces good oxidation-resistant films on the surface of the metal.   H.E.S.

Additional abstract

Sect. III: Hydraulic properties of glasses.

VI—Structural Clay Products

Floor tile. ANON. *Ziegelind.,* 11 [12] 347–60 (1958).—Complete German specifications (DIN 4159 and 4160, parts 1 and 2) are given for all hollow and perforated brick used as cover for reinforced concrete, static-free and non-static-free. 40 figures.
                                     T.W.G.

Mechanical forming of bellmouthed ceramic shapes [sewer pipe]. M. D. ABRAMOVICH. *Steklo i Keram.,* 14 [4] 23–27 (1957).—A vertical vacuum press was used in an attempt to produce curved sewer pipe. A full description is given. 6 figures.
                                     K.S.

New aging method. KURT LEFNAER. *Ziegelind.,* 11 [12] 370–72 (1958).—L. describes the handling of wet clay for aging by means of a crane and suspended grab bucket in the filling and emptying of the aging house. 5 figures.   T.W.G.

Production of ceramic floor tile in Czechoslovakia. L. YA. MISHULOVICH. *Steklo i Keram.,* 14 [4] 30–32 (1957).   K.S.

Significance of size of specimen in determining the strength of building ceramics. I. A. ROKHLIN. *Steklo i Keram.,* 15 [7] 33–36 (1958).—A mathematical treatment for the determination of cold crushing strength is given. 4 figures, 1 reference.   K.S.

Interlocked [building] blocks [design]. LINZA M. MOORE. U. S. 2,847,847, Aug. 19, 1958.   D.J.B.

Tile handling conveyer. PHILIP E. KOPP. **U. S. 2,846,098,** Aug. 5, 1958.—A tile handling conveyer automatically receives hollow clay products in wet condition from extruding and cutting apparatus, moves them along at right angles to the extruder, turns them from the on-side position to the on-end position, and lowers them onto a vehicle which conveys them to the kiln. On engaging a limit switch at the conveyer, the tile are raised on individual slotted pallets by a pneumatic piston, and the pallet with the tile is then pushed onto the conveyer by a second piston. When the tile reaches the other end of the conveyer another limit switch is engaged, and a group of the tile are tilted on end clear of the pallets. This whole section of conveyer is then lowered hydraulically so that the tile are deposited on a slotted deck of a vehicle for transportation to the kiln. The pallets return by an inclined lower conveyer to the original pickup point where they are raised individually to form a stack for picking up new tile, thus completing the cycle.   D.J.B.

VII—Refractories

Acid resistant semidry-pressed brick from local [Bun'kovsk] clays. M. E. BRAVERMAN. *Steklo i Keram.,* 14 [6] 18 (1957).— Details of analyses of materials, grading, and methods of manufacture are given. The Al_2O_3 content is 19.25 to 21.75%, SiO_2 62.29 to 69.51%, and Fe_2O_3 2.09 to 5.69%. The brick are fired at 1060° to 1080° in tunnel kilns.   K.S.

Are metallurgists prepared for 19XX? R. F. THOMSON. *Metal Progr.,* 73 [3] 99–106 (1958).—Future problems and the tools needed to solve them are discussed. Among the high temperature materials covered are thorium oxide and tantalum carbide for furnace resistors, other carbides and cermets as raw materials, and refractories for test furnaces. 4 figures.   D.J.B.

Better ways to fabricate high-temperature materials. ANCN. *Metal Progr.,* 73 [5] 97–101 (1958).—Procedures for use with metals are covered; the method favored for cermets and refractory oxides is slip casting. A very brief general discussion is presented, and the physical properties of high chrome-alumina and high tungsten-chrome-alumina bodies are tabulated. 4 figures.   D.J.B.

Casting of magnesium oxide in aqueous slips. STEPHEN D. STODDARD AND ADRIAN G. ALLISON. *Am. Ceram. Soc. Bull.,* 37 [9] 409–13 (1958).—Fused magnesium oxide, after being subjected to ball milling and aging, may be suspended in water to form a casting slip. Deflocculation is obtained by addition of

the proper amount of acid. Both drain and solid castings in a wide range of shapes and sizes have been produced successfully from these slips. The casting behavior of slips of varying grain size distribution and the properties of the resulting cast pieces are given. Two firing techniques are described, and several physical and mechanical properties of the ware resulting from these firing treatments are summarized. 7 figures, 11 references.

Chemism of the destruction of chrome-magnesite refractories during service in vel'ts furnaces. A. M. DAVIDSON, P. A. POLK-voĬ, AND G. A. RASHIN. *Ogneupory*, 22 [9] 417–25 (1957).— Chemical and petrographic studies led to the following conclusions: (1) the basic cause of wear in furnaces for the production of ZnO appears to be the action of acid iron and calcium silicates on the spinel-forsterite bond of the refractory. (2) Chemical destruction of the bond proceeds mainly by (a) migration of iron oxides from the scum, which form low melting point iron bearing spinelides and silicates, and (b) an increase in the acidity of the cementing bodies in the reaction zone. Under the influence of the acidic melt, in place of the orthosilicate in the bond (forsterite), several pyroxenes are formed (enstatite and the more complex Ca-Mg-Fe pyroxene); the refractory spinelide bond is also replaced by much lower melting silicates. During service of the chrome-magnesite, the chromite grains possess the greatest resistance as shown by comparative analyses of specimens of the original brick and used brick. The chemical changes consist of the formation of magnesite and the replacement of magnesium in the chromite by divalent iron and of aluminum by trivalent iron. These reactions take place only in the reaction zone. The intensity of the destructive processes is aided by nonuniformity of the crystalline structure and especially by the irregular distribution of the mineral phases in the brick. Tests showed that greater uniformity of structure leads to higher resistance in the furnace linings. 5 figures, 5 references.   K.S.

Comparison of physicochemical properties of primary blast-furnace slags with their mineralogical composition. N. L. ZHILO, A. V. RUDNEVA, AND G. A. SOKOLOV. *Izvest. Akad. Nauk S.S.S.R., Otdel. Tekh. Nauk*, 1957, No. 6, pp. 37–42; abstracted in *J. Iron Steel Inst.* (London), 189 [3] 276 (1958).— Data on the phase composition and a comparison of the actual and calculated mineralogical compositions of primary blast-furnace slags (produced during the smelting of basic and foundry iron) with their physical properties are given. The investigation was carried out to establish the cause of variation in the behavior of K_2O in acid and basic slags. The comparison of viscosity, crystallization temperature, and phase composition indicated that the negative influence of alkali on the physical properties of these slags is caused by the formation of high-melting alkali aluminosilicate groupings with a three-dimensional skeletal structure of anionic complexes (of the type of kaliophilite and leucite). See "Investigation. . . ," this section.   V.R.E.

Correcting formulas for sagger mixes. B. N. Ol'SHEVSKIĬ. *Steklo i Keram.*, 14 [6] 19 (1957).   K.S.

Determination of the bulk density of refractories by their absorption of γ radiation. A. N. LYULICHEV AND E. V. LEVINTOVICH. *Ogneupory*, 23 [7] 319–24 (1958).—A suitable setup is shown, and a mathematical treatment of the fundamental principles is presented. The technique can be used for determining the bulk density of refractories having a density of 0.75 to 3.35 $gm./cm.^3$ and a linear dimension of 65 to 180 mm. The authors tested the influence of geometrical factors, chemical composition, and duration of test period on the accuracy of the results. The method was then used for different refractories. Results are tabulated. 3 figures, 7 references.   K.S.

Effect of additions [of alumina and graphite] on the friction properties of sintered copper. W. HOFMANN AND G. PIEPER. *Z. Metallk.*, 49, 80–86 (1958); abstracted in *Brit. Aluminium Co., Ltd., Light Metals Bull.*, 20 [14] 473 (1958).—A 3, 5, or 8% addition of alumina together with graphite increased the coefficient of friction and reduced wear.   V.R.E.

Increased fuel input and basic refractories. J. H. CHESTERS. *Refractories J.*, 34 [6] 280–81, 283 (1958).—New basic oxygen processes are stimulating the development of the open hearth in steelmaking. Recent tests with the all-basic furnace show that with the increased firing rates, roof temperatures may be above the critical point (1650°C.) for as much as 3 hr. in 8 of the charge-to-tap time. The temperature sometimes rises to 1800°C. and even higher when oxygen enrichment is used. Where air is completely replaced by oxygen, all-basic construction is essential. The "Double E" brick, which is essentially an unfired metal-cased basic brick with two additional steel plates inserted in it,

reduces the cross-sectional area of the units to only a third of normal, which should increase the resistance to spalling. Cf. *Ceram. Abstr.*, 1958, Sept., p. 239g.   C.M.C.

Investigation of the viscosity of primary blast-furnace slag. N. L. ZHILO, A. V. RUDNEVA, G. A. SOKOLOV, AND L. M. TSYLEV. *Izvest. Akad. Nauk S.S.S.R., Otdel. Tekh. Nauk*, 1957, No. 2, pp. 27–35; abstracted in *J. Iron Steel Inst.* (London), 189 [3] 276 (1958).— This investigation was made to determine the effect of alkali and FeO in the presence of alkali on the viscosity (I) of primary blast-furnace slags. The chemical compositions of natural and synthetic slags investigated are given. It was found that K_2O decreases I and the temperature of crystallization (II) of acid as well as basic slags not containing Al_2O_3. An increase in the K_2O content in slags with 5 to 10% Al_2O_3 decreases I and II only of acid blast-furnace slags and has an opposite influence on basic slags. FeO decreases I and the temperature of the beginning of crystallization. This influence is more strongly pronounced in acid slags than in basic slags. Alkali additions (3 to 16%) decrease I and II of ferrous slags with a CaO to SiO_2 ratio of 0.61 to 1.16. Increasing CaO/SiO_2 ratio leads to a decrease in I and an increase in II in alkali-containing ferrous slags. The presence of alkalis in slags aids in displacing ferrous iron from slag melts, thus increasing the process of reduction of iron oxides. See "Comparison. . . ," this section.   V.R.E.

Materials for rocket engines. R. C. KOPITUK. *Metal Progr.*, 73 [6] 79–84 (1958).—K. discusses the requirements in rocket engines and the selection and fabrication of materials for both regenerative and nonregenerative types. If improved oxidation and corrosion characteristics are required in the gas generator, which operates at 1900°F., the metals are given a thin refractory ceramic coating, usually alumina, zirconia, or one of the National Bureau of Standards enamels. The same thing is true for the combustion chamber extension cone, but here the temperatures may run a little higher. On the combustion chambers for non-regenerative rocket engines which are not cooled, ceramic bodies and bonding cements are used. Common bonding cements are calcium aluminate cements alone or with flint, plaster of Paris, and alumina-base cermets; the liners are graphite, silicon-carbide coated graphite, carbon-bonded silicon carbide, silicon nitride-bonded silicon carbide, and silicon carbide with a recrystallized silicon carbide bond. 4 figures.   D.J.B.

Molded refractory burners for tunnels—for industrial heating purposes. W. N. SMIRLES. *Gas J.*, 291 [4915] 663–64, 667–68, 673 (1957).—The design, construction, and performance of a special molded refractory burner being tested is described. The principle factors are (1) correct shape, (2) the temperature of the flame and reproducibility of flame characteristics, (3) speed of combustion products as affecting heat transfer rate by forced convection, and (4) silent performance, flame-proofness, etc. 2 figures, 8 references.   V.R.E.

New developments in steelmaking. J. S. CURPHEY. *Refractories J.*, 34 [6] 259–77 (1958).—C. reviews open-hearth furnace design, especially in regard to roof life, fuel, preheat treatment, flame enrichment, and steelmaking processes (modified Bessemer, L-D, Rotor, and Kal-Do). 12 figures, 9 references. Cf. *Ceram. Abstr.*, 1958, Sept., p. 239g.   C.M.C.

Thermal conductivity of magnesia refractories. V. V. PUSTOVALOV. *Ogneupory*, 23 [7] 326–28 (1958).—P. gives details of the relation between thermal conductivity of some Russian magnesite-chromite refractories and temperature. The Cr_2O_3 content varied from 1.8 to 30%. A graph shows that nearly all of the products tested had a negative coefficient of thermal conductivity, or the property remained constant for all temperatures. The apparatus used in the study is described, and the ceramic properties of the materials are given. 1 figure, 4 references.   K.S.

PATENTS

Apparatus for forming refractory bodies. JAMES M. LAMBIE (Pittsburgh Plate Glass Co.). U. S. 2,849,779, Sept. 2, 1958.—1. In a sectional mold structure, a horizontal platform, a pair of spaced base mold sections having opposed inner edge flat surfaces diverging downwardly, spaced transverse members on the platform and spacedly supporting the pair of base mold sections above the platform, the opposed inner edges of the transverse members being spaced apart, a longitudinal mold section having longitudinal sides with flat top portions converging upwardly and removably fitting in wedging relation between the downwardly diverging surfaces of the pair of mold sections, transverse wedge members disposed between the spaced transverse members and

having top surface portions downwardly inclined toward and adjacent their opposed inner edges, the wedge members being supported on the platform and the inclined top surface portions engagedly supporting the longitudinal mold section, and side and end mold sections above the spaced base mold sections and the end portions of the longitudinal mold section defining with the base and longitudinal mold sections an upwardly opening mold matrix for shaping moldable material, the mold sections being formed of plaster of Paris.   D.J.B.

Explosion resistant refractory castable. DONALD F. KING AND ALBERT L. RENKEY (Harbison-Walker Refractories Co.). **U. S. 2,845,360,** July 29, 1958.—An explosion resistant refractory castable consists of refractory aggregate selected from the group consisting of alumina and aluminum silicate aggregate and a high alumina calcium aluminate cement with an Al_2O_3 to CaO ratio of about 2:1 to 6:1 by weight and containing boric acid in an amount of about 0.02 to 1.5% based on the weight of the mixture. The addition of the boric acid to such mixtures permits rapid heating of fabricated units to operating temperatures without explosion. The cement should be the minor portion of the mix, ranging from 10 to 50%. Suitable aggregates are calcined alumina, calcined bauxite, calcined clay, ground fire-clay brick or lightweight aggregates such as perlite. In one example 83% by weight of a graded calcined flint clay (all +65 mesh) was blended with 2% ball clay, 14.85% calcium aluminate cement, and 0.15% boric acid. The cement had an Al_2O_3 to CaO ratio of 4.4 to 1 and contained about 1% sodium citrate as a set regulator. This composition was mixed with water, rammed into a block 18 x 18 x 9 in., air-dried overnight, and installed in the door of a gas-fired test furnace. The temperature was raised to 2550°F. in 2 hr., and there was no explosion or deterioration of the block.   D.J.B.

Hot top. DONALD D. WHITACRE (Whitacre-Greer Fireproofing Co.). **U. S. 2,846,741,** Aug. 12, 1958.—A sectional ceramic hot top for use with ingot molds comprises an inner cylindrical burned clay sleeve portion open at both ends with a central feed opening and a collar having a central opening to receive and encompass the lower portion of the sleeve and having a height about $\frac{1}{3}$ to $\frac{1}{2}$ the height of the sleeve. The collar has an exterior form complementary to the upper end of the ingot mold and is supported on the brim of the mold. The sleeve is characterized by uniform porosity and thickness, low density, low heat capacity, and high insulating value. The density should be about $\frac{2}{3}$ oz./in.^{3}, and the insulating value should be such that under steady conditions an exterior temperature of 200°F. can be maintained when the temperature of the inner surface is 1000°F. The opening of the sleeve is 10 to 50% greater in height than its mean transverse dimension. The collar is of dense, strong, burned clay with density approximately twice that of the sleeve. The hot top has an internal volume of not more than 10% of the volume of the ingot and the crop. The sleeve is made by extrusion from equal parts by volume of fire clay and anthracite silt, to which is added about 20% sawdust or pulverized bituminous coke of the same mesh size as sawdust. A sleeve 2.5 in. thick made with silt and clay had a density of 0.65 oz./in.^{3} when fired at 1400° to 1600°F. The collar is made by extrusion of wet clay alone, and when prepared by normal procedures it has a density of 1.25 oz./cu. in. The sleeve has a wall thickness of 2.75 to 3 in., a mean internal diameter of 15.625 in., and a length of 21.5 in. for molds with an upper opening 2 ft. square. The collar has a height of 9 in.   D.J.B.

Method of chemically disintegrating and pulverizing solid material. RINTARO TAKAHASHI AND TAKEHIKO YUIZE. **U. S. 2,848,313,** Aug. 19, 1958.—9. The process of disintegrating scrap comprising hard metal carbide and a metallic bond comprises treating the scrap with a gas containing carbon monoxide whereby the metallic bond forms a carbonyl powder, the scrap thereby being disintegrated and depositing the hard metal carbide as a powder.   D.J.B.

Method of producing boride coatings on metal. MARGARET A. REID AND ABNER BRENNER (United States of America as represented by the Secretary of Commerce). **U. S. 2,849,336,** Aug. 26, 1958.—1. The method of coating a metal comprises passing a metallic borohydride vapor over the surface of the metal to be coated at a temperature between 400° and 800°C. whereby metallic boride from the vapor is deposited as a coating on the metal.   D.J.B.

Nonmetallic electrical heating elements. EUGENE WAINER AND DONALD E. PLATT (Thompson Products, Inc.). **U. S. 2,848,586,** Aug. 19, 1958.—1. An electrical heating element has a central high-resistance portion and terminal low-resistance portions

integral with the high-resistance portion, the portions being composed of a binder selected from the group consisting of oxides of the second and third group elements of the periodic table and refractory metal silicides selected from the group consisting of the silicides of molybdenum, tungsten, tantalum, zirconium, niobium, titanium, and mixtures thereof, the central portion comprising substantially equal portions by weight of the refractory metal silicide and the binder and the terminal portions comprising a major portion of the refractory metal silicide and a minor portion of the binder.   D.J.B.

Production of refractory metal carbides. WILLIAM H. BLEECKER (Allegheny Ludlum Steel Corp.). **U. S. 2,849,275,** Aug. 26, 1958.—1. In the production of titanium carbide, the steps comprise heating titanium metal in an atmosphere of hydrogen at 325° to 350°C. to form titanium hydride, mechanically comminuting the titanium hydride, screening the comminuted titanium hydride to obtain a predetermined particle size of > 100 mesh, adding a predetermined mass of carbon in the form of fine powder to the titanium hydride, mixing the titanium hydride and carbon to produce a substantially uniformly blended mixture, and vacuum carburizing the mixture at 1800° to 2000°C.
     D.J.B.

Refractory manufacture. EDWARD P. PEARSON AND VAUGHN V. HUGHEY (Basic, Inc.). **U. S. 2,846,326,** Aug. 5, 1958.—1. A method of physically bonding particles of a relatively chemically inactive magnesium compound selected from the group consisting of magnesite and brucite into briquette form comprises the steps of mixing particles of such a compound with a primary bonding agent consisting essentially of the reaction product of chemically active magnesia and an inorganic water soluble iron salt, the magnesia being present in an amount by weight of about 1.5 to 3% of the magnesium compound, and the iron salt being present in an amount by weight of about 1 to 4% of the compound, and causing the reaction product to adhere the particles of the compound to one another to impart mass integrity thereto.
     D.J.B.

Refractory and method. WALTER R. SATTERFIELD (Armco Steel Corp.). **U. S. 2,846,324,** Aug. 5, 1958.—A composition for highly refractory ceramic weld metal retaining products consists essentially by weight of at least 60 Al_2O_3, 6 to 30 MgO, 1 to 30 SiO_2, up to 15 SiC, and 2 to 15% resin selected from the group consisting of phenol-formaldehyde, urea-formaldehyde, melamine-formaldehyde, polyoxyethylene esters, and polyoxypropylene esters. Cup-shaped refractories of such compositions are useful in cladding the base metal stock of internal combustion engine parts, such as exhaust valves, with costly hard-facing alloys. These cups serve as a physical support to hold the articles in the desired welding position and retain the high heat required for the operation. A preferred composition is as follows (by weight): Al_2O_3 (−100 mesh) 71, MgO (−100 mesh) 8, SiO_2 2, SiC (−100 mesh) 11, liquid resin (phenolic type) 6, and water 2%. The cups are pressed at 500 p.s.i., dried at 350°F. for 1 hr., and fired at 2250°F. for 2 hr. The fired piece has a weight ratio of Al_2O_3:-SiO_2:MgO of 87.5:2.5:10.0. This is based on the assumption that SiC is unchanged at this firing temperature. Such cups may be used 15 to 20 times.   D.J.B.

Reinforcing insert for furnace block. DONALD W. MASON AND WILLIAM H. MYERS (Harbison-Walker Refractories Co.). **U. S. 2,846,963,** Aug. 12, 1958.—1. A reinforcing insert adapted to be molded into an upright brick that has a hanger-receiving recess in one side near its upper end comprises an upright metal plate adapted to extend vertically through the brick at one side of its recess and a vertical metal strip extending along a vertical edge of the plate at an angle to the plate and integral therewith, the vertical strip being only long enough to cover a portion of the recessed side of the brick below the recess, and the upper end of the strip having an extension bent in across the plate and then curving upward and outward to form a tonguelike lining for the top and bottom of the hanger recess.   D.J.B.

Rocket motor with recrystallized silicon carbide throat insert. EDWIN C. LOWE (Norton Co.). **U. S. 2,849,860,** Sept. 2, 1958.—1. A rocket motor comprises a hollow chamber made of graphite having a portion of a venturi as an integral part thereof, an exhaust nozzle piece separate from the chamber and also made of graphite and constituting a continuation of the venturi, a throat insert made of recrystallized silicon carbide in the narrowest part of the venturi, a coating of silicon carbide on the inside of the chamber and on the inside of the portion of a venturi, being a continuous coating and being integral with the graphite of the chamber and of the portion of a venturi, a coating of silicon car-

bide on the inside of the exhaust nozzle piece and being integral with the graphite thereof, and a continuous outside coating of silicon carbide on the outside of the chamber and the portion of a venturi and the exhaust nozzle piece and integral with the graphite of the chamber and of the portion of a venturi and of the exhaust nozzle piece.   D.J.B.

Additional abstracts

Sect. I: (*patent*) Electric furnace product. **Sect. VIII:** Beryllium and beryllia.

VIII—Whiteware

Automatic copying of high-tension insulators. WERNER MECHTOLD. *Silikattech.*, **9** [6] 260–64 (1958).—The machine and an installation are described which result in greater and more economical production. 8 figures.   M.HA.

Automatic press for wall tile production. R. S. HARDING AND A. N. GILSON. *Am. Ceram. Soc. Bull.*, **37** [9] 405–408 (1958).—A British automatic tile press widely used in Europe is described. Faults in tile and their remedies are discussed. 7 figures.

Bentonite faience for facing ceramics. M. A. BEZBORODOV AND E. F. POLUEKTOVA. *Steklo i Keram.*, **14** [4] 13–16 (1957).— Bentonite has been used for a decade as a flux and plasticizer for faience in the Turkmen S.S.R. Experiments were made on the use of bentonite containing a large amount of iron compounds to replace certain plastic Chasov-Yar clays in faience bodies pressed into facing ceramics. The rheological and other properties of the bentonites were studied, and analyses, etc., are given. The study proved the advantage of using bentonite for this purpose. A formula for a faience body is 73 Beregorsk kaolin, 15 Gorbsk bentonite, 5 quartz sand, and 7% Baranovsk pegmatite. Its molecular formula is CaO 0.217, MgO 0.512, K_2O 0.166, Na_2O 0.105; Al_2O_3 8.166, Fe_2O_3 0.223; SiO_2 40.884, TiO_2 0.108. The properties of this body are tabulated. The optimum firing temperature is 1150° to 1180°. A great advantage of the bentonite faience body appears to be its high strength when freshly pressed and in the air-dried state. This may favor single-firing techniques; it increases vitrification and reduces water absorption. 2 references.   K.S.

Beryllium and beryllia: I, II. L. DAVID. *Metal. Ind.* (London), **90** [June 21] 519–21; [June 28] 546 (1957); condensed in *Metal Progr.*, **73** [6] 192, 194 (1958).—A compilation of the properties, fabrication, and uses of beryllium and beryllia is given.   D.J.B.

Causes of hair cracks [crazing] in pottery glazes. N. N. STASEVICH. *Steklo i Keram.*, **14** [6] 9–14 (1957).—After discussing the literature on the importance of equating the coefficients of expansion of bodies and glazes, S. gives a detailed account of his experiments on the behavior of glazes with particular respect to structure and quartz form. He concludes that the basic cause of crazing (crackle) in pottery glazes is not the different coefficients of expansion of glaze and body but the microstructure of the glaze, i.e., the presence of a crystal lattice in the main component of the mix (silica). Numerous tests were made to study the effect of varying the SiO_2 content and its form (diatomite, sand, and tripoli). 6 figures, 5 references.   K.S.

Colored ceramic tile for internal walls and fireplaces. *Brit. Standard*, 1958, No. 1281. Price 4s. 6d.—This standard prescribes the dimensions and workmanship of square and rectangular glazed tile for walls and fireplaces and fittings for wall tile only. The quality of the glazed surfaces and the standard sizes and tolerances are stated, and tests for checking squareness and flatness are included.   A.B.S.

Cooling porcelain ware in periodic kilns with forced air supply. M. S. KUZNETSOVA. *Steklo i Keram.*, **15** [7] 27–29 (1958).— Owing to the rarefication of the kiln atmosphere, air from the outer chamber enters the firing chamber through an opening of 210 x 150 mm. and goes out through an opening 150 x 80 mm. in size. Such a cooling technique reduces the temperature from 220° to 100°–120°. Further intensive cooling was needed with kilns firing larger products (electrical insulators), and forced air systems were installed. The setup is shown in a diagram. The cooling period was shortened from 77–88 to 60–62 hr. and later to 52–54 hr. Cooling curves for the various methods of cooling are shown. 2 figures.   K.S.

Determination of the optical characteristics of enamels and glazes. K. P. AZAROV AND V. E. GORBATENKO. *Steklo i Keram.*, **15** [7] 36–40 (1958).—Existing apparatus for determining the whiteness and brilliance of enamels and glazes does not take into account their colors and is unsuitable, e.g., for controlling deep ware of small diameter. Suitable nondestructive tests were de-

veloped by the authors, and the apparatus is described. It consists of a whiteness meter, an ammeter, and a voltage regulator. A full description of the electrical and optical components and setup is given. The mathematical principles are considered, and the results are tabulated. 5 figures, 8 references.   K.S.

Development of a production line for fine-ceramic tableware. HORST SCHILLING. *Silikattech.*, **9** [6] 256–59 (1958).—An installation for the continuous manufacture of cups and saucers is described. 7 figures.   M.HA.

Glazed facing tile in Czechoslovakia. L. F. SHULIKO. *Steklo i Keram.*, **14** [6] 26–28 (1957).—The production methods of two factories, Rako and Gornaya Briza, are described. Raw materials include local clays with kaolins, feldspar, whiting, and dolomite. The clays contain kaolinite as the main mineral constituent. No quartz sand is used in the body; the SiO_2 content is 10% (Rako) and 15% (Gornaya Briza). Grog is added as calcined kaolin (1350° to 1420°) in amounts of 55%, i.e., 15% more than in Russian plants. This composition gives little cracking during manufacture. The clays, etc., are blended by the slip method in ball mills (2.5 to 3% on a sieve of 10,000 apertures/cm.^{2}). Filter presses use cotton cloths immersed in phenolic solution. Nylon has been tried successfully. Gradings of the press powders are 10 to 12% >1 mm., 25 to 28% 1 to 0.5 mm., 22 to 25% 0.5 to 0.2 mm., and 35 to 40% <0.2 mm. Tile 108 x 108 mm. are pressed on British automatic presses. Pressures are 160 to 170 kg./cm.^{2} (6 mm. thickness) and 230 to 250 kg./cm.^{2} (4 mm. thickness). Drying and biscuit firing (saggerless) are done in 90 hr. at an end temperature of 1280° in Dressler muffle kilns (fired with gas regenerated from brown coal). The tile are glazed by a conveyer method. Glaze formulas are given, and the setting of colored and white glazed tile is described in detail. S. pinpoints the main differences between Czechoslovakian and Russian methods and emphasizes the high quality and low loss of the former. 2 figures.   K.S.

Influence of the physical properties of the glaze on its quality. Z. A. NOSOVA. *Steklo i Keram.*, **14** [5] 12–18 (1957).—Seventeen glazes (analyses given) were studied in the laboratory, and the following data are shown: viscosity-temperature curves (1125° to 1350° and 800° to 1200°), spreadability compared with viscosity, wetting angle on semiporcelain, pottery, and ceramic facing bodies. Conclusions: To prevent boiling of the glaze, firing, especially in open flame, should be done at that temperature at which the viscosity of the glaze is < 6000 to 9000 or > 400 poises. In the first case gases from the body and glaze will not rise to the surface; in the second case they pass through the glaze layer and escape while the holes formed are closed by melting. The viscosity at which the glazes investigated melted on the body and possessed adequate brilliance was located in the range 60,000 to 14,000 poises. The boiling temperature can be controlled in practice by determining the temperature of pouring of the glaze and the length of spread when poured into the ceramic molds. Additions of 6 to 7% bentonite ensure good strength and adherence to the body before and during firing (in the initial stage). 3 figures, 3 references.   K.S.

New body compositions for glazed facing ceramics. L. F. SHULIKO. *Steklo i Keram.*, **14** [4] 16–19 (1957).—To develop bodies more resistant to cracking and deformation during drying and firing, the following raw materials were used: Novo-Shveitsarsk clay, Prosyanov kaolin, quartz sand, tile grog, kaolin fired at 1350°, dolomite, and lime. The best mixtures were, respectively, as follows: (*a*) 28, 22, 7.5, 12, 30, 0.5, 0; (*b*) 28, 22, 17.5, 12, 20, 0.5, 0; and (*c*) 28, 20, 37, 7, 0, 0, 8. The glaze used with these bodies was 42.2 SiO_2, 9.2 Al_2O_3, 8.1 CaO, 10.3 R_2O, 3.5 ZnO, 7.2 B_2O_3, and 19.5% PbO. The ware was fired in saggers in tunnel kilns at 1250° to 1280° and at 1160° to 1180° (biscuit 60 hr., glost 35 hr.). The effects of the components in relation to the above faults are discussed.   K.S.

New method of packing glazed shapes in saggers. G. I. SHUVALOV. *Steklo i Keram.*, **14** [4] 27–28 (1957).—The method is used for placing tile. Diagrams show the different ways of

setting the tile. Increases of 33, 166, and 211% of the utilized available space resulted with different types of ware. 2 figures.
K.S.

Reclaiming body scrap at fine china dinnerware plant. ANON. *Ceram. News*, 7 [7] 13 (1958).—The principle of multiphase mixing with a Cowles dissolver is described. This equipment permits the reclaiming of green scrap and eliminates the necessity of drying and ball milling. 7 figures. D.J.B.

Saggerless firing of sanitary technical faience ware in periodic kilns. P. A. CHERNYAK AND YU. I. VOROB'EVA. *Steklo i Keram.*, 15 [7] 43–44 (1958).—Fire-clay tile and pillars were used to make a series of boxes into which the ware was placed. This new method of placing reduced the firing cycle from 21 to 17 hr. The cycle was as follows: 210° to 850°, 100°/hr.; 850° to 1100°, 70°/hr.; and 1100° to 1250°, 30°/hr. The capacity of the kiln was increased by 30%. 4 figures. K.S.

Strains in glazed ceramic bodies. J. R. FINLAYSON. *Dissertation Abstr.*, 17, 2231 (1957); abstracted in *J. Appl. Chem.* (London), 8 [7] ii–54 (1958).—Correlations were attempted between calculated and observed strains in open rings glazed only on the outer cylindrical surface. V.R.E.

Three ceramic products with high strength. ANON. *Materials in Design Eng.*, 48 [1] 126–28 (1958).—Low expansion ceramics having high thermal shock resistance are made from lithium-aluminum-silicate compositions. Pyroceram (Corning Glass Works) cement and tubing are also discussed. Physical properties are tabulated. 4 figures. Cf. *Am. Ceram. Soc. Bull.*, 36 [7] 279–80 (1957). D.J.B.

PATENTS

Method for making ceramic articles. JOSEPH R. FISHER (Bell Telephone Laboratories, Inc.). U. S. 2,847,314, Aug. 12, 1958.—1. The method of making a shaped body of ceramic materials comprises mixing the finely divided ingredients of the ceramic material, water, and 3 to 6% by weight of polymethacrylic acid, calculated on the basis of the dry ingredients, removing excess water to give a plastic mass, forming the mass into a shaped body, drying, and firing the body. D.J.B.

Method of making ceramic-metal seal. MORTIMER EBER (United States of America as represented by the Secretary of the Navy). U. S. 2,848,801, Aug. 26, 1958.—1. A method of forming a vacuum-tight seal between a zircon porcelain disk and a Kovar ring disposed circumferentially about the disk includes disposing a layer of soldering material closely about the periphery of the disk, fitting the ring closely about the solder, fitting a resilient metal clamp about the exterior surface of the ring for yieldably pressing the ring into intimate contact with the solder, and heating the assemblies sufficiently to melt the solder for forming the vacuum-tight seal, the clamp being formed of a material having a coefficient of thermal expansion substantially the same as that of the disk but less than that of the ring, the clamp further having a compressive strength during the heating sufficiently greater than the rigid strength of the Kovar ring whereby the clamp effectively restrains heat expansion of the metal ring away from the disk during the heating. D.J.B.

Method of soft soldering to nonmetallic refractory bodies. DANIEL W. LUKS (Frenchtown Porcelain Co.). U. S. 2,848,802,

Aug. 26, 1958.—1. A method of joining a metallic body to a nonmetallic refractory body comprises coating the nonmetallic refractory body with a composition consisting essentially of a metallic glass base, the base consisting essentially of 60 to 94.5% by weight of a powdered heavy metal selected from the group consisting of nickel, cobalt, and iron, between 0.5 and 30%, calculated as MnO_2, of a powdered manganese constituent, and between about 5 and 30% powdered glass in combination with a vehicle, firing the coated refractory body at a temperature between about 1300° and 2100°F. in a reducing atmosphere, and soldering the metallic body directly to the coated body with soft solder. D.J.B.

Multiple [ceramic] tile unit. ELDRED A. TALBOTT. U. S. 2,844,955, July 29, 1958.—1 A multiple tile unit comprises plural rows of tiles in edge-to-edge abutment, each tile being provided with protruding edge lugs and the lugs of adjacent tiles being engaged and defining through spaces between the adjacent tiles and along the line where they join, and a separate flexible tape disposed along each line joining adjacent rows of tiles and adhesively connected to the tiles to connect the tiles of each row and the rows of tiles together, the tape being substantially narrower than a row of tiles to leave an expanse of such row of tiles exposed between the tapes. D.J.B.

Pottery transfer brushing machine. ANNA C. RESCHKE. U. S. 2,849,820, Sept. 2, 1958.—1. A pottery transfer brushing machine comprises a worktable having a vertical tubular guide mounted therein, a sleeve bearing slidably mounted in the guide, a spindle journaled in the sleeve and having a work holder affixed on its upper end adapted to support a plate for rotation, a thrust bearing acting between the holder and the upper end of the sleeve, means for continuously driving the spindle, means mounted below the table including a lever operatively connected to the sleeve for elevating the sleeve in the guide, and a standard on the table having an oscillating brush depending toward the work holder, the brush oscillating in a plane parallel with the table and through a path which lies laterally spaced from the axis of the spindle and which is substantially symmetrical to a radius extending from the axis to the midpoint of the path. D.J.B.

Tile holding tool for use in [ceramic] tile cutting. JOHN PEPI (Edward C. Houlette). U. S. 2,842,115, July 8, 1958.—1. A tile retaining press construction for supporting a tile element in a state of predetermined compression required for a selective hole breaking operation includes a four-sided frame, the frame having two of its sides meeting to form a fixed corner, tile supporting base portions extending inwardly along the opposite sides of the frame, a bottom portion having a hole therethrough, a pair of pressure bars adjustably disposed in the frame at right angles to one another and oppositely to the fixed corner, the pressure bars being adapted to engage and hold the tile element against the fixed corner with an unsupported bottom of the tile element occurring over the hole, and screw means for tightening the respective pressure bars to exert compressive forces on the tile element. D.J.B.

Additional abstracts

Sect. IV: Description and measurement of white surfaces.
Sect. V: (*patent*) Glass sealed centerwire structure.

IX—Electronics

Air-gap test cell for measuring properties of sheet dielectrics. S. I. REYNOLDS AND D. A. KOLLATH. *Rev. Sci. Instr.*, 29 [4] 295–96 (1958).—An air-gap capacitor was designed to measure the dissipation factor and dielectric constant of sheet insulating materials, including Pyrex glass, without making contact with the dielectric. Tests indicate that the loss tangent and dielectric constant values obtained are comparable to those obtained with intimate-contact electrodes. This method provides a means of measuring, over a wide range of thickness, sheet materials which cannot have electrodes intimately fastened to their surfaces. 3 figures, 7 references. V.R.E.

Dielectric properties and phase transitions of $NaNbO_3$ and $(Na,K)NbO_3$. G. SHIRANE, B. NEWNHAM, AND R. PEPINSKY. *Phys. Rev.*, 96 [3] 581–88 (1954).—Optical, dielectric, and structural studies were made on $NaNbO_3$ and the solid solution $(Na,K)NbO_3$, both single crystals and ceramics being used. No evidence for ferroelectricity in $NaNbO_3$ was found, and the crystal seems to be antiferroelectric in accordance with the nonpolar structure reported by Vousden. It is shown that a small addition of

$KNbO_3$ to pure $NaNbO_3$ produces a new ferroelectric phase, the existence of which suggests a possible explanation of the conflicting dielectric and structural properties previously reported. The phase diagram of $NaNbO_3$-$KNbO_3$ is given. This, together with the optical and X-ray studies of pure $NaNbO_3$, shows that the three phase transitions in $NaNbO_3$ are quite different in nature from the $BaTiO_3$-type transitions in $KNbO_3$. 7 figures, 2 tables, 24 references. J.J.D.

Domain formation and domain wall motions in ferroelectric $BaTiO_3$ single crystals. WALTER J. MERZ. *Phys. Rev.*, 95 [3] 690–98 (1954).—The nucleation and growth of ferroelectric domains in barium titanate was studied as a function of applied electric field and temperature. Optical and electrical measurements were made on thin single crystal plates normal to *c*, the polar direction. When the electric field applied along this direction was reversed, new domains with opposite polarization were formed. The growth of these domains was almost never by sidewise motion of the 180° side walls, as in ferromagnetics, but by the formation of many new antiparallel domains which were extremely thin

$(10^{-4}$ cm.). The wall thickness was of the order of one to a few lattice constants and wall energy about 10 ergs/cm.^{2}. Electrical pulsing experiments showed that both the nucleation rate of new domains and the rate of growth of the new domains increased with increasing temperature. Data were also obtained on switching current and switching time as a function of applied electric field, temperature, and size of sample. 17 figures, 17 references.

J.J.D.

Effects of anisotropy on thermodynamic properties of antiferromagnets. J. A. EISELE AND F. KEFFER. *Phys. Rev.*, 96 [4] 929–33 (1954).—In antiferromagnets, because of interplay with exchange energy, a small anisotropy can have a huge effect on thermodynamic properties. Detailed calculations are given, by use of the spin-wave theory, of this effect on sublattice magnetization, specific heat, and parallel susceptibility of a cubic or uniaxial antiferromagnet. The theory is extended to orthorhombic symmetry, and reasonable agreement is found with existing experimental data on $CuCl_2 \cdot 2H_2O$. 2 figures, 1 table, 22 references.

J.J.D.

Infrared spectrum of barium titanate. R. T. MARA, G. B. B. M. SUTHERLAND, AND H. V. TYRELL. *Phys. Rev.*, 96 [3] 801–802 (1954).—The infrared absorption of barium titanaté between 2 and 33μ was found to be identical with that of pure strontium titanate. The spectrum contains two broad bands, one centered near 550 cm.$^{-1}$ and the other beyond 300 cm.$^{-1}$. There is no difference between the spectra of hexagonal and tetragonal BaTiO$_3$ over the range 2 to 15μ. No change in the spectrum of ceramic BaTiO$_3$ was observed on heating to 150°C. 2 figures, 4 references.

J.J.D.

Low-temperature acoustic relaxation in Ni-Fe ferrites. M. E. FINE AND N. T. KENNEY. *Phys. Rev.*, 96 [6] 1487–88 (1954).—An acoustic relaxation effect occurs near 40°K. in Ni$_{0.73}$Fe$_{2.25}$O$_4$, and it is attributed to a stress-induced change in the distribution of Fe^{2+} and Fe^{3+} similar to that occurring in magnetite. The process involves electron diffusion. The activation energy is between 0.026 and 0.055 e.v./electron jump. 2 figures, 6 references.

J.J.D.

Magnetic anisotropy constants of ferromagnetic spinels. R. S. WEISZ. *Phys. Rev.*, 96 [3] 800–801 (1954).—The first order magnetic anisotropy constants of NiFe$_2$O$_4$ and CoFe$_2$O$_4$ were calculated to be $K_1 = -4.0 \times 10^4$ ergs/cm.^{3} and -3.4×10^6 ergs/cm.^{3}, respectively. These values were calculated from initial permeability and saturation magnetization values obtained on pure polycrystalline materials, by the use of a formula based on the assumption that the initial permeability of sintered polycrystalline ferromagnetic spinels is predominantly due to spin rotation. Values of K_1 determined directly on flame-fusion single crystals of the nickel and cobalt ferrites are higher and lower, respectively, than those calculated, in accordance with the idea that the single crystals are not pure but contain some magnetite in solid solution. 1 figure, 12 references.

J.J.D.

Magnetic and crystalline behavior of certain oxide systems with spinel and perovskite structures. LOUIS R. MAXWELL AND STANLEY J. PICKART. *Phys. Rev.*, 96 [6] 1501–1505 (1954).—A series of substitutions were performed on nickel ferrite by which the Fe^{3+} was replaced, in varying amounts, by In^{3+}, Sc^{3+}, Y^{3+}, Gd^{3+}, and La^{3+}. In^{3+} went into solid solution with nickel ferrite to form a spinel structure whose lattice constant a_0 increased linearly with increasing amounts of In^{3+} to a maximum value of 8.708 a.u. for 1.5 In^{3+} ions per molecule. The saturation magnetization (μ_0) obtained by extrapolation to absolute zero increased with increasing amounts of In^{3+} in a manner indicating that the In^{3+} preferred A sites. In the case of Sc^{3+}, cell size increased up to $a_0 = 8.41$ a.u. for 0.75 Sc^{3+} ions per molecule. μ_0 decreased with increasing Sc^{3+} content and approached a compensation point similar to that found previously with Al^{3+} substitution. It is concluded that trivalent metal ions having a rare gas electronic structure, by showing a preference for the B sites, give rise to compensation points and Néel P-type curves. Curie temperatures for the substitution of In^{3+} and Sc^{3+} show a nearly linear decrease with concentration but with slopes greater and less, respectively, than the slope of the single curve found previously to represent both the Al^{3+} and Ga^{3+} substitutions. The Y^{3+}, Gd^{3+}, and La^{3+} substitutions resulted in a mixed solution of nickel ferrite and corresponding perovskite structures formed with Fe^{3+}. 6 figures, 1 table, 6 references.

J.J.D.

Measurement of the complex tensor permeability of ferrites. J. H. ROWEN AND W. VON AULOCK. *Phys. Rev.*, 96 [4] 1151–53 (1954).—The components of the permeability tensor of a ferrite, as well as its real and imaginary dielectric constants, can be de-

termined from the frequency shift and change in Q produced by inserting a thin ceramic ferrite disk in a degenerate-mode cavity. 1 figure, 3 references.

J.J.D.

Nonmagnetic ions in an antiferromagnetic. K. F. NIESSEN. *Philips Research Repts.*, 13 [4] 327–34 (1958).—A method is given for determining the distribution of a relatively small number of foreign nonmagnetic ions between the two sublattices of an antiferromagnetic, in which they replace the same number of original magnetic ions. The influence of the foreign ions on several measurable quantities was investigated. This influence can be used to determine some specific constants of the antiferromagnetic. In the anisotropy energy, besides the usual terms, an interaction term between the two sublattices is taken into account. Use is made of the spontaneous magnetization, the parallel and perpendicular susceptibilities, the critical field strength, and the antiferromagnetic resonance. 3 references.

J.J.D.

Observation of paramagnetic resonances in single crystals of barium titanate. A. W. HORNIG, E. T. JAYNES, AND H. E. WEAVER. *Phys. Rev.*, 96 [6] 1703 (1954).—Electron resonances are not observed with pure barium titanate, but they are observed in single crystals containing small amounts of iron. Above the Curie temperature, the spectroscopic splitting factor, g, is 2.0. Between the Curie temperature and about 0°C. there are four components, whose g values are 3.52, 2.72, 2.41, and 1.79. Below 0°C. there are two principal lines approximately symmetrically located about a g value of 2. 2 figures.

J.J.D.

Reversible susceptibility of ferromagnetics. D. M. GRIMES AND D. W. MARTIN. *Phys. Rev.*, 96 [4] 889–96 (1954).—An expression is given relating the magnetization dependence of the reversible susceptibility normal to the field direction to that of the parallel reversible susceptibility. Modification of these susceptibility dependences due to the trapping of domain walls in metastable positions by potential holes is considered. The reversible susceptibilities of three ferrite specimens were measured and found to agree favorably with the theory. 4 figures, 1 table, 11 references.

J.J.D.

Processes taking place during the sintering of plastic steatite bodies. V. G. AVETIKOV AND E. I. ZIN'KO. *Steklo i Keram.*, 15 [7] 29–33 (1958).—The body studied, TK-21, contained 70% talc, and the clay components were Chasov-Yar clay and Oglanlinskiǐ bentonite. Belgorod whiting served as a flux. The mass was prefired at 1300° to 1350°, and the processes were studied by thermographic methods with simultaneous recording of shrinkage and weight loss. Graphs show the relation between loss on ignition and temperature, the influence of firing temperature on the content of dissolved CaO and SiO$_2$, and the relation between water absorption and shrinkage and temperature. The study showed that the first stage of the sintering process (up to 1000°) is characterized by reactions in the solid state. As a result of these, finely dispersed magnesium metasilicates are formed, owing to the recombination and rearrangement of the talc and chemically low resistant Ca silicates (chiefly due to the CaO which is freed during decarbonization of the CaCO$_3$) and the SiO$_2$ from the clays and bentonite. Since dehydration of the talc proceeds after decomposition of the clay materials, CaO freed during the breakdown of the whiting has already combined with the silica from the clay. The SiO$_2$ from the talc, therefore, takes part in forming calcium silicates in a less marked degree than does the silica from the clay. The second stage of the sintering (in the range 1100° to 1280°) is characterized by the presence of melts. Here the metasilicates increase owing to the continued recombination of the products of decomposition of the talc. Eutectic melts are formed in which the Mg metasilicates and decomposition products of talc and clays dissolve. Part of the clinoenstatite present in the sintered steatite is formed as a result of recrystallization from the melt during cooling. This stage of sintering is accompanied by intensive densification and strengthening of the steatite body. 7 figures, 11 references.

K.S.

Temperature dependence of elastic constants and the velocity of propagation of ultrasonic waves in high permittivity ceramics. KIYOSHI OKAZAKI AND RYUSUKE KONO. *Yogyo Kyokai Shi*, 66 [750] 139–44 (1958).—The speed of propagation of ultrasonic waves was determined by the rotation method in which the angle of total reflection of the incident beam is measured while the specimen is rotated. From the velocities of longitudinal and transverse waves of 5 mc. in barium titanate at 10° to 140°C., temperature dependence of Young's modulus, Poisson's ratio, Lamé's constant, bulk modulus, and compressibility were calculated. The measurements were extended to TiO$_2$, CaTiO$_3$, NiSnO$_3$, CuZrO$_3$, and BaTiO$_3$-BaSnO$_3$. The velocities found in

TiO₂ and various titanates were 7000 to 9000 m./sec. The elastic constants of barium titanate showed slight fluctuations according to the method of preparation of the samples. 13 figures, 12 references.   K.Y.

Electrical resistor and method and apparatus for producing resistors. NATHAN PRITIKIN. U. S. 2,849,583, Aug. 26, 1958.—1. A resistor comprises an insulating base, an oxidizable metallic resistance film adhering to the base, a pair of terminals electrically connected to spaced points on the resistance film, and a layer of silicon monoxide covering substantially all the exposed surface of the resistance film.   D.J.B.

Electrically conductive cement and brush shunt connection containing it. KENNETH R. MATZ (Union Carbide Corp.). U. S. 2,849,631, Aug. 26, 1958.—16. An embedded shunt connection for electrical brushes and contacts has a cavity therein and in the cavity a flexible conductor of electricity secured therein by a conductive cement consisting of 60% by weight of silver flakes, the largest dimension of which does not exceed 65μ, 25.2 to 36% of an epoxy resin, 4 to 12% of finely divided quartz filler material, and 2.8 to 4% by weight of triethanolamine.   D.J.B.

Electroluminescent lamp. ERIC L. MAGER (Sylvania Electric Products, Inc.). U. S. 2,848,637, Aug. 19, 1958.—2. An electroluminescent lamp comprises two spaced conductors in close proximity to each other and a coating therebetween of phosphor embedded in an insulating material, the dielectric constant and resistivity of the embedding material being high compared to those of the phosphor.   D.J.B.

Electroluminescent materials. ROBERT M. MAZO AND SIMON LARACH (Radio Corp. of America). U. S. 2,847,386, Aug. 12, 1958.—1. A method for producing an electroluminescent material comprises heating together in a bromine-containing atmosphere at temperatures of about 1000° to 1200°C. a mixture comprising about 50 to 70 mole % of zinc sulfide, about 50 to 30 mole % of zinc selenide, and about 0.08 to 0.2% by weight of copper activator.   D.J.B.

Method of making single crystal ferrites. JOSEPH P. REMEIKA (Bell Telephone Laboratories, Inc.). U. S. 2,848,310, Aug. 19, 1958.—1. A method of making single crystals of ferrite comprises heating lead oxide and the constituent components of a polymetallic ferrite having a spinel crystal structure to a temperature above 880°C., at which the ferrite is dissolved in the lead monoxide, and crystallizing the ferrite material out of solution by reducing the temperature of the melt at a rate less than 30°C./hr.   D.J.B.

Method of making thorium oxide cathodes. JAMES E. CLINE AND JOHN P. JASIONIS (United States of America as represented by the Secretary of the Army). U. S. 2,847,328, Aug. 12, 1958.—1. A method of making thorium oxide cathodes of large areas for high power magnetrons comprises mixing in powdered form about 50 parts by weight of thorium oxide, about 50 parts of molybdenum, and about 1 part of ruthenium into an organic solvent to make a paste, pasting the mixture into a wire mesh consisting of molybdenum, and firing the coated mesh at about 1800°C.   D.J.B.

Monocrystalline nickel titanate boule. ARTHUR LINZ, JR., AND LEON MERKER (National Lead Co.). U. S. 2,850,355, Sept. 2, 1958.—Monocrystalline nickel titanate boule is formed synthet-

ically by introducing powdered nickel titanate into a stream of oxygen, surrounding the stream of oxygen with a stream of hydrogen and forming a flame having a central oxygen cone, melting the powdered nickel titanate in the flame, forming the monocrystalline nickel titanate at a temperature of 1620° to 1680°C., crystallizing the molten nickel titanate in the form of a boule adjacent the end of the oxygen cone, maintaining the flame about the boule, and subsequently annealing the boule by heating at 650° to 1500°C. for 6 to 24 hr. to remove the strains therefrom.   D.J.B.

Morphotropic piezoelectric ceramics. BERNARD JAFFE, ROBERT S. ROTH, AND SAMUEL MARZULLO (United States of America as represented by the Secretary of the Army). U. S. 2,849,404, Aug. 26, 1958.—3. A piezoelectric ceramic composition comprises a solid solution consisting of the compounds of lead titanate, lead stannate, and lead zirconate, the compounds having proportions such that if the proportion of one of the compounds were considered fixed, the proportions of the remaining two compounds would be within about 10 mole % of the morphotropic phase boundary of the solid solution, the boundary being approximately determined by the smooth curve drawn through the points of four boundary compositions on a composition diagram of the ternary system lead stannate–lead titanate–lead zirconate, the four boundary compositions being substantially as follows (mole %): 58 lead stannate, 42 lead titanate; 40 lead stannate, 45 lead titanate, 15 lead zirconate; 20 lead stannate, 48 lead titanate, 32 lead zirconate; and 46 lead titanate, 54 lead zirconate.   D.J.B.

Semimetallic resistive filaments. MAURITZ L. ANDERSON AND FREDERICK T. HILL (Raytheon Mfg. Co.). U. S. 2,845,515, July 29, 1958.—A resistive filament for a cathode of a thermionic discharge device consists of a mixture of about 40 to 55% finely divided molybdenum and the remainder of dielectric refractory particles formed into a self-supporting body and covered by an insulating coating with conductors inserted into the body of the filament at each end. The conductive material should be selected from the group W, Ti, Ta, and Mo; these metals are capable of operating at 1100° to 1200°C. without melting or reacting with such refractory materials as Al₂O₃, MgO, ZrO₂, or other oxide, silicon carbide or nitride, or a mixture of any of these materials. The optimum content of tungsten is 53% when it is used with a nonconductive refractory. If the refractory contains some conductive material, such as SiC, the metal content must be reduced accordingly to attain the desired resistance. The raw materials are blended with water and an extrusion aid, formed into the desired shape, dried, and fired at 1650°C. in a hydrogen or other reducing atmosphere. The resistor is then coated with alumina to form an insulating coating and refired.   D.J.B.

Thermionic cathode. OTTO G. KOPPIUS (North American Philips Co., Inc.). U. S. 2,848,644, Aug. 19, 1958.—1. A thermionic dispenser cathode comprises a body of refractory metal having a porous portion and a supply within the body of a mixture of an alkaline earth metal tungstate and a refractory metal different from that of the body and selected from the group consisting of thorium, tantalum, and zirconium.   D.J.B.

Additional abstracts

Sect. VIII: (*patents*) Method for making ceramic articles. Method of making ceramic-metal seal. Method of soft soldering to nonmetallic refractory bodies.

X—Production Equipment and Unit Operations

Automation of a four-column hydraulic press. E. M. MEN AND N. P. SHEVERDYAEV. *Steklo i Keram.*, 14 [5] 18–21 (1957).—The operation of the press is described with full details of construction. 3 figures.   K.S.

Ball-mill grinding: II, Application of laboratory tests in industry. J. NIJMAN. *Brit. Chem. Eng.*, 3 [8] 414–17 (1958).—N. recommends recording the results of laboratory tests on (1) the relation of grinding speed to mill load, (2) grinding speed as a function of mill load, (3) realized separation of the breakage velocity into components of cascading and cataracting, (4) relation of the breakage velocity constant to differences in the initial sizes of the particles, and (5) the results of experiments at 50% of the critical mill speed, showing the dependence of the breakage velocity constant on mill load. Different methods of scaling-up drawings for commercial plants from laboratory results are briefly described on the basis of two considerations: (a) a particle-size spectrum

obtained by milling has the same form as that obtained by the fracture law, whereby the probability of breakage is assumed to be equal to unity; and (b) the resulting size spectrum is independent of the original size of the particles. Various theories of other investigators are criticized, and the conclusion is reached that, to be acceptable, any theory must include particle-size distribution after a single breakage, the probability of breakage through cascading, and the probability of breakage through the cataracting of the balls. N. concludes that the fineness of the product is due not only to the distribution function but also to the breakage velocity constant of each of the different sizes of particles at various stages in the grinding. 4 figures. For part I see *Ceram. Abstr.*, 1958, June, p. 151h; cf. *ibid.*, 1958, Aug., p. 208d.   A.B.S.

Combined grinding and drying of clays in a shaft mill. E. L. ROKHVARGER. *Steklo i Keram.*, 14 [2] 1–8 (1957).—The follow-

ing factors were studied, and the results are discussed in detail: capacity and suitability of the assembly, influence on moisture and fineness of sandy and plastic clays, relation between fineness of grinding and speed of gas travel in the system, relation between water content of powder and temperature of drying agent on entry into the mill, heat consumption for extracting 1 kg. of moisture at optimum production, relation between consumption of electricity and mill production, and best cycle for producing materials suitable for dry-pressed brick. Exhaust gases from the cooling zone can be used for drying wet materials. As the method could lead to automation, it should be widely introduced in Russian practice. 10 figures.   K.S.

Economics through synchronizing handling with operations. P. W. PEEL. *Glass*, 35 [7] 311–12 (1958).—The use of mechanical methods for moving the materials of production and the finished product has invariably resulted in a lower production cost and increased output for the same amount of equipment. V.R.E.

Effect of methods of preparing clay powders on the physicomechanical properties of ceramics. E. L. ROKHVARGER. *Steklo i Keram.*, 14 [5] 8–12 (1957).—Combined drying and grinding of clays permits automation of these processes, and powders with consistent grading and water content for semidry pressing can be obtained. Tests at a Russian plant using a shaft mill gave promising results. About 100,000 bricks were pressed with the clay obtained. The shaft mill method was compared with the drum drier and disintegrator method. Gradings from the shaft mill showed 41.85% <1 mm.; the disintegrator product was 32%. Other properties were also compared. The data include (1) specific surface areas of the two products, (2) compressive strength curves for samples made from both products, (3) relation between bending strength and water content (shaft mill material had higher values), and (4) compressive strengths vs. moisture. R. concludes that the method can be used for the manufacture of brick, refractories, acid resistant ceramics (by semidry method), and plastic-shaped pipe, block, etc. 5 figures. K.S.

Electrostatic precipitators. R. J. PLASS AND H. H. HAALAND. *Rock Prods.*, 61 [7] 104–10, 136–40 (1958).—The design and functions of the precipitator in the cement industry are discussed. The problem of dust return to the kiln as related to alkali build-up and air pollution is considered, and a flow sheet is included. Recommendations are given for wet process, dry process, and the ACL system, as well as new applications in raw material driers and in the grinding room. 4 figures. D.J.B.

High temperature gaseous jets as applied to some manufacturing processes. J. B. HENWOOD. *Gas J.*, 291 [4915] 656–63 (1957).—Combustion must take place in a minimum time and a minimum space, and it must use the maximum energy level with the high-temperature gases transferring heat to the object in a controlled manner. Both the speed and temperature of the jet must be developed to solve process problems involving simultaneous heating, mechanical forming, and conveying. H. proposes ideal conditions under which new processes and products can be developed. 14 figures, 7 references. V.R.E.

Influence of gaseous surroundings on the firing of ware made from clays containing carbonates. V. I. KOTOV. *Steklo i Keram.*, 14 [2] 8–11 (1957).—To clarify the nature of changes in ware made from carbonate clays during firing in different atmospheres, thermographic analytical methods were used. Specimens were fired together with a sample of refractory prefired at 1300° as a comparison. The clay group tested had the following composition: 53.3 SiO₂, 13.8 CaO, 12.1 Al₂O₃, 0.9 MgO, 4.8 Fe₂O₃, and 14.9% loss on ignition. The mineral composition mainly comprised clay substance, CaCO₃, Fe₂O₃, quartz, and particles of mica. The thermal effects obtained with the analysis are discussed. Conclusions: Firing of ware made with carbonate clays proceeds favorably under oxidizing conditions. Reducing conditions at 1125° to 1155° form black iron spots fused on and below the surface. The clay was badly sintered and had a low vitrification range. Under oxidizing conditions the range was 75°, with initial sintering at 1100° and maximum shrinkage 6% at 1165°; under reducing conditions the range was 25°, with initial sintering at 1125° and maximum shrinkage 1.2% at 1150°. Reducing firing at 1130° to 1165° led to clinkering of the material. 3 figures, 4 references. K.S.

Influence of shape and arrangement of clay particles on shrinkage of the ware. G. L. EFREMOV. *Steklo i Keram.*, 14 [6] 14–17 (1957).—The particle size, shrinkage, and wettability of several Russian kaolins and ball clays were studied. E. reviews the present knowledge of the subject and suggests that plaster molds should be rotated during slip casting to remove any strains in the

body by destroying orientation of the particles. 6 figures, 1 reference. K.S.

Infrared drying. R. A. ELLIOTT. *Can. Mining Met. Bull.*, 51 [550] 111–13 (1958); abstracted in *Mine & Quarry Eng.*, 24 [8] 376–77 (1958).—A stainless-steel belt running under a radiant infrared panel was found to be the best of several types of equipment considered. Data and costs are presented. V.R.E.

Pump and pipeline calculations. D. A. WEBB. *Cement, Lime & Gravel*, 33 [1] 7–13 (1958).—W. describes the calculations necessary for determining the pressure or head against which a pump will have to operate and some of the features of pipes used in pumping liquids, slurries, etc. 8 figures. V.R.E.

Theoretical delivery volume in an auger machine. GOTTRAM TEUBNER. *Ziegelind.*, 11 [13] 403–405 (1958).—There can be no increase in speed of the bar passing the die, the theoretical volume of issue being the product of the rate of advance of the screw and the free die cross section. The screw shaft diameter can be calculated leading to the explanation of the laminated structures due to backing up. As long as the speed of issue corresponds to the theoretical speed of advance of the screw and as long as the bar is filled out, there can be no backing up. 2 figures, 17 references. T.W.G.

PATENTS

Air filter. JOHN TURNER (Koppers Co., Inc.). U. S. 2,850,-113, Sept. 2, 1958.—1. A gaseous fluid filtering apparatus comprises a casing having a dirty gas inlet and a clean gas outlet, an endless sheet material filtering element adapted to travel endwise in the casing, the filtering element having a dirty gas face and an opposite clean gas face, rollers positioned to support the element on the clean gas face, bearings for the end portions of the rollers, journal boxes for the bearings adjacent to side edges of the filtering element, and means for subjecting the bearings within the boxes to clean gaseous fluid pressure conditions slightly higher than the pressure of the dirty gaseous fluid to be filtered thus maintaining the bearings clean and simultaneously discharging fluid under pressure away from the clean gas face and around the filtering element to float the filtering element for free travel and to prevent escape of fluid to be filtered around the margins of the filtering element. D.J.B.

Apparatus for coating particulate material by thermal evaporation. CHARLES A. BAER AND ROBERT W. STEEVES (National Research Corp.). U. S. 2,846,971, Aug. 12, 1958.—1. In apparatus of the type in which a coating is applied to discrete particles of a material, the improvement comprises means for holding the particles in a circumferential course by centrifugal force above a source material, means for reducing the pressure within the system, means for heating the source material to a temperature high enough to cause vaporization of the material at the existing pressure, and means for causing the discrete particles to tumble, thereby exposing all surfaces to the coating vapors. D.J.B.

Apparatus for filtering gas. MARCEL DRU (Préparation Industrielle des Combustibles). U. S. 2,850,112, Sept. 2, 1958.—1. Apparatus for filtering fluids such as dust-laden gas comprises a plurality of filter compartments arranged in a circle about a common vertical axis, a plurality of elongated flexible permeable filter sleeves mounted in each of the filter compartments, means including conduits for directing a flow of the gas to be treated through the filter sleeves, means mounted in each of the filter compartments for shaking the filter sleeves therein including a manifold pipe carrying a plurality of bellows, each connected to one of the sleeves, a distributor assembly associated with the filter compartments including a conduit connected to a source of pulsated air and positioned to be successively brought into communicative engagement with the manifold pipes, and means for intermittently rapidly rotating the distributor assembly to bring the conduit into successive engagement with the manifold pipes so that the bellows carried thereby will be operated to shake the filter sleeves connected thereto. D.J.B.

Control valves for hydraulic presses. JOHN M. TOWLER (Electraulic Presses, Ltd.). U. S. 2,848,874, Aug. 26, 1958. D.J.B.

Device for slowing down the movement of the press piston in hydraulic presses. MILAN VLTAVSKY (CKD Ceska Lipa narodni podnik). U. S. 2,846,980, Aug. 12, 1958. D.J.B.

Dust separating aggregate of small cyclones. CLAES ALLANDER AND BENGT LANNE (Aktiebolaget Svenska Fläktfabriken). U. S. 2,848,061, Aug. 19, 1958.—1. A multiple-cyclone dust-separating aggregate in a partition between a common inlet cham-

Ceramic Abstracts

ber for raw gas and a common outlet chamber for clean gas of the aggregate consists of a number of cyclone units arranged in vertical and horizontal rows, the units in each vertical row being spaced a given vertical distance, each of the cyclone units comprising at least one casing having a cylindrical upper part having a tangential raw-gas inlet open to one side of the partition and a conically tapered lower part terminating in a dust outlet, a central tube coaxially arranged in the cylindrical upper part as a clean-gas outlet open to the other side of the partition, and a vertical open-ended pipe integral with the unit having a length corresponding to the vertical spacing of the units, the dust outlet of each unit terminating in a wall opening of the pipe, the pipes of the units in each vertical row being in endwise abutting vertical alignment to constitute a common vertical outlet conduit for dust, each cyclone unit also being provided with an outwardly projecting vertical member constituting a rectangular disk angularly disposed with respect to the longitudinal axis of the casing, the vertical and horizontal dimensions of the disk corresponding to the vertical and horizontal spacing between adjacent rows of units, the disks having joining means for fastening the units together to form an aggregate of any desired size, the disks constituting the partition between the inlet and outlet chambers of the separating aggregate. D.J.B.

Electrically heated vibrating screen. JOSEPH J. SCANLON AND JOHN J. SCHROTH (Link-Belt Co.). **U. S. 2,850,163,** Sept. 2, 1958.—11. In a vibrating screen, a screen frame having transversely spaced side walls, a screen deck comprised of a plurality of longitudinally spaced screen cloths supported between the side walls, means for electrically insulating the screen cloths from each other and from the side walls, means for distributing electricity along each side edge of each screen cloth, means to bridge the gap and to provide an electrical connection between adjacent screen cloth side edges, one only of the means being provided for each gap and the means being staggered so that successive gaps are bridged on opposite sides of the screen deck leaving a first side edge and a second side edge at the feed and discharge ends of the screen deck, respectively, each without an electrical connection to any other side edge, and means for supplying electricity to the screen deck including one set of supply conductors connected to the first side edge at the feed end of the screen deck and another set of supply conductors connected to the second side edge at the discharge end of the screen deck. D.J.B.

Electrostatic precipitators. WILLIAM J. ROOS (Westinghouse Electric Corp.). **U. S. 2,847,082,** Aug. 12, 1958.—1. An electrostatic precipitator comprises an air guiding enclosure having an open air inlet and an open air outlet, a mat of conductive filaments extending crosswise of the enclosure between the inlet and outlet, a first plurality of spaced-apart conductors having insulation therearound in contact with the side of the mat facing the inlet, a second plurality of spaced-apart conductors having insulation therearound in contact with the side of the mat facing the outlet, and means for establishing electrostatic fields between the first conductors and the mat and between the second conductors and the mat. D.J.B.

Feeder for fibrous materials. WARREN S. BLUNDIN (Babcock & Wilcox Co.). **U. S. 2,850,183,** Sept. 2, 1958.—1. A feeder for the controlled delivery of wet fibrous materials comprises a housing having an inlet opening in the top, an inclined bottom plate of the housing having an outlet opening in the lower portion thereof, an overhead bin for the wet fibrous materials, an upright spout connecting the bin with the inlet opening of the housing, an endless chain positioned in the housing beneath the spout, a plurality of spaced fingers projecting outwardly of the chain, means for operatively supporting the endless chain in an inclined position with the lower end of the chain adjacent the outlet opening, a siftings hopper positioned below the inclined bottom plate of the housing, and drive means for moving the upper run of the endless chain downwardly to discharge the wet fibrous material through the discharge opening. D.J.B.

Friction press. NORMAN B. OWEN AND FRANK W. OWEN. **U. S. 2,846,747,** Aug. 12, 1958.—In a friction press such as used in molding ceramic tile, an improved nut for the lead screw cannot become frozen in place, can be readily removed for replacement by a hammer blow, and provides support for the screw to minimize any bending forces thereon. The nut also provides for readily replaceable means to take up wear and hold the lead screw in alignment. D.J.B.

Grinding charge for ball mills. WILLIAM W. HARTMAN. **U. S. 2,847,169,** Aug. 12, 1958.—2. For use in a ball mill, a new and improved grinding element the shape of which conforms ap-

proximately to the interstice within a group of four balls symmetrically stacked so that the centers of each three of the four balls lie approximately at the vertices of four substantially identical equilateral triangles formed by straight lines joining the centers of each three of the four stacked balls, and the surface of the grinding element having four concave grinding depressions registering approximately with the adjacent portion of the convex surfaces of the four symmetrically stacked balls. D.J.B.

Pellet making. EMIL BLAHA (Selas Corp. of America). **U. S. 2,847,702,** Aug. 19, 1958.—4. Apparatus for forming pellets includes, in combination, a first endless belt provided with a plurality of perforations, a pair of parallel reels over which the belt is placed, means to mount the reels on parallel axes so spaced that the belt is taut, a second endless belt longer than the first belt, the second belt being placed over the reels within the first belt, guide means between the reels around which the second belt passes to take up the slack therein, means engaging the first belt at a point where it is supported by the second belt and one of the reels operative to fill accurately the perforations with a material, and means located between the belts adjacent to the guide means to remove material from the perforation of the first belt. D.J.B.

Rotary tablet press. RAYMOND G. FRANK (F. J. Stokes Corp.). **U. S. 2,846,723,** Aug. 12, 1958. D.J.B.

Self-clearing feeder. WARD J. HEACOCK (Link-Belt Co.). **U. S. 2,850,145,** Sept. 2, 1958.—1. A feeder for bulk material comprises a material supply hopper having a bottom opening and a forward end wall having a bottom edge adjacent the bottom opening, an endless conveying member, means mounting the conveyer for endless conveying movement below the bottom opening and with an upper run normally extending forwardly beyond the bottom edge for carrying material from the bottom opening under the edge, means for mounting the conveying member for bodily endwise movement parallel to the path of the upper run, stop means for limiting such movement, biasing means for holding the conveying member with the upper run in the normal position, and driving means for imparting the endless conveying movement to the conveying member, the driving means being effective when pieces of material become jammed between the upper run and the bottom edge to drive the conveying member in the bodily endwise movement away from the edge to allow the jamming material to drop free. D.J.B.

Sieves and strainers. JUSTIN HURST (Russell Constructions, Ltd.). **U. S. 2,848,110,** Aug. 19, 1958.—1. A sieve comprises, in combination, a sieve-supporting flyweight casing, a flyweight therein, outwardly extending members on the casing, suspension rods flexibly secured to the outwardly extending members in substantially the same plane as the flyweight, means for supporting the suspension rods flexibly, a sieve base secured to and spaced from the flyweight casing, a sieve element secured to the sieve base, and means for driving the flyweight to produce circular vibration in the casing and parts mounted thereon. D.J.B.

Spring mounted compound motion ball mill. ELMER H. EVERETT AND ERNST CZERLINSKY (United States of America as represented by the Secretary of the Air Force). **U. S. 2,849,190,** Aug. 26, 1958.—1. In a ball mill, a container, means including a driving plate for rotating the container, one set of stiff springs, and one set of lighter springs for supporting the container and connected to the driving plate for flexibly driving the container for eccentric motion about the axis of rotation of the driving means to produce a tumbling action. D.J.B.

Suppressor electrode for a perforated type of electrostatic separator machine. WILLIAM A. BRASTAD (General Mills, Inc.). U. S. 2,847,124, Aug. 12, 1958.—10. An electrostatic separator comprises spaced upper and lower electrodes, the upper electrode having a plurality of openings therein through which material attracted from the lower electrode may pass onto the upper surface of the upper electrode, means for feeding a stream of material along the lower electrode, means for maintaining a difference of potential between the electrodes, suppressor means including an elongated member spaced with respect to one of the electrodes and located adjacent the discharge edge thereof, and means for maintaining the elongated member at a preferred potential which will reduce the field intensity in the region of the elongated member and thus prevent undesired displacement of particles in the region in a direction having a component normal to the electrodes. D.J.B.

Vibrating screen device. JOSEPH R. GUESS. **U. S. 2,849,119,** Aug. 26, 1958.—4. A material-screening device comprises at least two pairs of posts, a pair of tubes extending between each pair of posts, a pair of rotatable shafts within the tubes, the shafts

being mounted by bearings in the posts, an eccentric on each end of each of the shafts, a pair of rods running between the posts parallel to the shafts, the rods and the shafts being interconnected by a strap encircling the eccentrics, a set of hubs suspended from the rods, the hubs encircling the tubes adjacent the ends thereof, a compressible member disposed between the hubs and tubes, and a

screen suspended from the hub and tube combination, the screen being adapted to reciprocate upon rotation of the shafts.

D.J.B.

Additional abstracts

Sect. VI: (*patent*) Tile handling conveyer.   **Sect. VIII:** Automatic press for wall tile production.

XI—Instruments and Test Methods

Calibration of thermocouples. AIMONE CAMARDELLA. *Bol. INT* (*Inst. nacl. tecnol.*) (Rio de Janeiro), **5** [13] 37–46 (1954).— After discussing several theoretical considerations, C. explains the calibration methods used by the National Bureau of Standards. 1 figure, 6 references.   V.R.P.

Method for the rapid and precise determination of the densities of liquids. G. L. GAINES AND C. P. RUTKOWSKI. *Rev. Sci. Instr.*, **29** [6] 509–10 (1958).—A device based on Archimedes' principle and involving the use of a sensitive quartz spiral as a measuring element was constructed to permit the rapid measurement of the density of liquid samples.   1 figure, 7 references.

V.R.E.

Simple, automatic, high-temperature thermal analysis apparatus. S. J. LLOYD AND J. R. MURRAY. *J. Sci. Instr.*, **35** [7] 252–54 (1958).—A high-temperature high-vacuum thermal analysis apparatus is described.   The sample, in a chamber which may be evacuated to better than 10^{-5} mm. of mercury at 1000°C., is heated by a molybdenum element, and the thermal arrests are indicated by the differential method.   By placing the sample in direct contact with the thermocouple hot junction, solid state phase changes may be detected in samples as small as 0.3 gm. Alternatively, samples of 20 to 80 gm. may be contained in crucibles; using the arrangement, thermal arrests have been detected at temperatures up to 1550°C.   2 figures, 3 references.

V.R.E.

Simple density apparatus. J. W. SMITH. *Chem. & Ind.* (London), **1958**, No. 28, pp. 885–86.—S. describes an instrument based on the displacement method for measuring the true density of active carbons, coals, and cokes.   2 references.   V.R.E.

Some high-pressure high-temperature apparatus design considerations: equipment for use at 100,000 atm. and 3000°C. H. TRACY HALL. *Rev. Sci. Instr.*, **29** [4] 267–75 (1958).—Three items of equipment are described in detail: (1) a simple piston and cylinder device capable of generating pressures to 50,000 atm. simultaneously with temperatures of 8000°C., (2) a tetrahedral-anvil device that has been successfully tested at 100,000 atm. and 3000°C., and (3) a stepped piston device capable of developing pressures to 200,000 atm. at room temperature.   In addition, consideration is given to such problems as (*a*) geometrical elements of design, (*b*) higher strength materials, (*c*) use of mechanical anisotropy in design, (*d*) electrical leads, (*e*) thermal and electrical insulation, (*f*) solid pressure transmitting media, (*g*) binding rings, (*h*) internal generation of pressure, (*i*) multistaging, and (*j*) calibration.   12 figures, 14 references.   V.R.E.

BOOK

Instrumental Methods of Analysis. 3d ed. HOBART H. WILLARD, LYNNE L. MERRITT, JR., AND JOHN A. DEAN.   D. Van Nostrand Co., Inc., Princeton, N. J., 1958.   626 pp. $7.50.— This is a textbook intended for the student rather than a reference book for the working chemist.   It also serves as a laboratory manual.   Detailed instructions for experiments are appended to each chapter.   An unusual feature is that complete, step-by-step instructions are given for the operation of the analytical instruments most commonly found in school and research laboratories. Since this is in addition to a photograph of each instrument and, usually, a line drawing or diagram illustrating its construction and operation, the student is given a very real familiarity with the instruments, even though they may not be available at his school. The text is straightforward and lucidly written and includes a good deal of theoretical discussion of the methods and instruments covered.   Problems, questions, and general references conclude each chapter.   Practically all of the basic instrumental methods are covered, including visual and photoelectric colorimetry; ultraviolet, visible, and infrared spectrophotometry; potentiometric, coulometric, and amperometric titrations; polarography, turbidimetry, and fluorescence analysis; flame photometry; X-ray fluorescence analysis; gas chromatography; radioactive techniques; mass spectrometry; nuclear magnetic resonance and emission and Raman spectrography.   The book is recommended.

J.J.D.

PATENTS

Apparatus for applying marks to a test specimen. ORVAL W. WADE.   U. S. 2,849,803, Sept. 2, 1958.—1.   An apparatus for applying marks to a test specimen comprises a base adapted to rest upon a supporting surface, at least two spaced standards rising from the base, a platform extending over the top ends of the standards and connected to the standards for movement toward and away from the top ends, a horizontally disposed shaft spaced above the base and rotatably supported in the standards intermediate the ends thereof, spring means operatively connected to the platform and the standards for biasing the platform away from the upper ends of the standards, there being an opening in the platform, the upper face of the platform being adapted to support a test specimen in registering relation with respect to the platform opening, at least two spaced marking wheels on the shaft and in registry with the platform opening, and hand actuatable means on the shaft for effecting the rotation of the latter, the platform being manually movable against the action of the spring means toward the top ends of the standard when a test specimen is supported on the upper surface of the platform in registering relation with respect to the platform opening to project peripheral portions of the marking wheels through the opening and into contacting engagement with the underface of the specimen.

D.J.B.

Apparatus for supersonic examination of bodies. EDWARD E. SHELDON.   U. S. 2,848,890, Aug. 26, 1958.—1.   A device for reproducing supersonic images comprises, in combination, an examined body, a source of supersonic radiation for irradiating the body and producing a supersonic image of the body, a vacuum tube having piezoelectric means sensitive to supersonic radiation, the piezoelectric means receiving the supersonic image and converting the image into an electrical pattern, the piezoelectric means being supported by the wall of the tube, means for producing a broad nonscanning beam of electrons, the beam being modulated by the electrical pattern on the piezoelectric means, and means spaced apart from the piezoelectric means for receiving the modulated broad electron beam.   D.J.B.

Apparatus for ultrasonic testing. JOSEPH E. HUNTER, JR., AND NORMAN W. SCHUBRING (General Motors Corp.).   U. S. 2,848,-891, Aug. 26, 1958.—1.   In a device for the determination of the size of grains in a given article, the combination of means for recurrently generating variable high frequency electrical oscillations at a predetermined sweep frequency, a first electromechanical transducer electrically coupled to the first means and mechanically coupled to a surface of the article, a second electromechanical transducer mechanically coupled to an opposite surface of the article and actuated by mechanical vibrations transmitted therethrough, a sweep generator having a sweep frequency identical to that of the means for generating oscillations, an oscilloscope having pairs of beam deflecting plates, one of the pairs of deflecting plates being electrically coupled to the second transducer and the other pair of deflecting plates being connected to the sweep generator, a calibrated screen on the oscilloscope correlating the oscilloscope trace with the size of grain in the article, and means connected in circuit with the second transducer and the sweep generator and responsive to the lowest frequency oscillations produced by the means for generating oscillations to initiate the operation of the sweep generator.   D.J.B.

Automatic controller for high temperature electric furnaces. EUGÈNE JOUMIER (Ateliers d'Appareils de Mesure et de Laboratoire (Soc. Anon.)).   U. S. 2,850,597, Sept. 2, 1958.   D.J.B.

Humidity determination. DONALD R. BLUMER (Minneapolis-Honeywell Regulator Co.).   U. S. 2,848,306, Aug. 19, 1958.—1. The method of determining the water vapor content of a gaseous mixture includes passing a standard reference gas through a first chamber wherein its relative thermal conductivity may be measured, passing a sample of a gas of unknown composition through a metal hydride bed wherein the water vapor is converted to molecular hydrogen, and thence passing the converted gas through a second thermal conductivity chamber wherein its thermal conduc-

tivity may be measured and compared with that of the reference gas.   D.J.B.

Method and apparatus for determining the surface tension and viscosity of molten substances. ANTONÍN NOVOTNÝ. **U. S. 2,846,870,** Aug. 12, 1958.—1. A method for simultaneously determining the surface tension and viscosity of molten substances which are solid at normal temperatures comprises the steps of heating the bottom end of a solid rod of the substance to be tested to form a molten drop thereof which, after overcoming the surface tension, drops from the remainder of the solid rod, and measuring the changes in length of the rod during the formation of the molten drop and its removal from the remainder of the rod, which changes in length are characteristic of the surface tension and viscosity of the substance in molten condition.   D.J.B.

Spectrochemical analysis device. HERBERT FRIEDMAN AND JOHN J. MAGUIRE (J. J. Maguire Co.). **U. S. 2,848,624,** Aug. 19, 1958.—1. A device for spectrochemical analysis comprises a source of primary radiations, a test specimen on which primary radiations are directed, a spectrograph detecting system comprising a detector and counter detecting and counting respectively fluorescent radiations from the test specimen, a monitor detecting system comprising a monitor detector and monitor counting means detecting and counting respectively the monitor radiations derived from the source, a relay device connected to the monitor counting means, the contacts of the relay being operated to interrupt the counting of the spectrograph detecting system upon a predetermined count being made by the monitor counting means, and means interposed between the source of primary radiations and the monitor counting means causing the last-named means to count only radiations having substantially the same quality and being proportional to the quantity of the radiations of the spectrograph detecting system.   D.J.B.

Temperature indicator. CHARLES M. MACDONALD. **U. S. 2,849,518,** Aug. 26, 1958.—3. A thermocouple temperature indicator comprises a tubular metal casing, a thermocouple comprising metal leads supported by and extending axially of the casing, an elongated metal tube enclosing the metal leads of the thermocouple, insulating material disposed between the metal leads and the metal tube, a cylindrical shaped metal cup having a coefficient of expansion substantially that of glass snugly fitting in the outer end of the casing and extending coaxially thereof, the metal cup having a cylinder-shaped inner end portion defining a chamber, a ceramic plug fitted into the inner end portion and sealing the chamber, the plug and the metal cup having substantially the same coefficient of expansion and the plug being of substantially uniform thickness throughout its length, and lead-in conductors extending through the plug, sealed thereto, and connected to the thermocouple leads within the chamber.   D.J.B.

Viscosity meter. KARL T. KÄLLE. **U. S. 2,846,873,** Aug. 12, 1958.—1. A viscosity meter for continuously indicating the viscosity or concentration of flowing liquids and suspensions comprises a vertical stationary tube having an open upper end, means for supplying liquid to be measured into a lower section of the tube to provide an upstream therein, the open tube end serving as an overflow outlet defining an overflow edge for the tube, a rotary member rotatable around a vertical axis and having the form of an elongated truncated cone with its inwardly tapering end directed vertically downwardly, mounting means supporting the rotary member and holding the rotary member only partly below the overflow edge of the tube, whereby the rotary member is only partly immersed in the fluid contained in and overflowing the tube, means for rotating the member, and means indicating the resistance against its rotation caused by varying viscosity of the liquid.   D.J.B.

XII—Kilns, Furnaces, Fuels, and Combustion

Automatic equipment for regulating the temperature in the central channel of a drier. A. E. EFIMOV. *Steklo i Keram.*, **14** [5] 28 (1957).—E. gives the electrical circuit and describes the equipment. 1 figure.   K.S.

Energy exchange between cold gas molecules and a hot graphite surface. LOTHAR MEYER AND ROBERT GOWER. *J. Chem. Phys.*, **28** [4] 617–22 (1958).—Methane and ethane do not decompose on clean graphite surfaces up to 2300°C. as long as the mean free path of the gas molecules exceeds the dimensions of the reaction cell. An investigation of the energy exchange between a hot graphite surface and cold molecules impinging on it revealed an accommodation mechanism of temporary adsorption followed by evaporation at critical temperatures essentially independent of the filament temperature as long as the latter is higher than the former. The evaporation temperature for methane is far below its decomposition temperature. 11 figures, 17 references.   V.R.E.

Engineering research with a solar furnace. PETER E. GLASER. *Solar Energy*, **2** [2] 7–10 (1958).—Instruments and techniques are suggested for the measurement of temperature, heat flux, thermal conductivity, thermal expansion, heat content, and spectral emissivity in the infrared region. 7 figures, 10 references.   J.J.D.

Factors of dust suppression in small- to medium-size rotary kiln systems: I. WOLF G. BAUER. *Pit and Quarry*, **50** [11] 134–35, 138–40, 148 (1958).—B. covers the sources and nature of dust within the system which, besides constituting a neighborhood nuisance, shows loss of raw material and probably thermal and mechanical inefficiencies in the processing. Suggestions are made for removal from kiln feed and for minimizing dust generation in the kiln and in transfer from kiln to cooler. 4 figures. **II.** *Ibid.*, **51** [1] 185–86, 190 (1958).—The secondary phase of dust suppression, for dust that escapes the kiln and collection system, is covered. Various code dust emission limits are tabulated and evaluated, showing that there are wide discrepancies.   D.J.B.

Kiln ring removal. ANON. *Pit and Quarry*, **50** [11] 154, 166 (1958).—A summary of methods and problems involved in ring removal in cement, lime, and refractory plants is presented. Tabulations are given on the number of shells fired and the rate.   D.J.B.

Lepol kilns with a heat consumption of 750 kcal./kg. of clinker by utilization of waste heat. G. RUPPERT. *Zement-Kalk-Gips*, **11** [5] 212–16 (1958).—Two installations are described, one of which was charged with the usual type of batch and the other with a charge consisting of Ca(OH)$_2$, limestone (CaCO$_3$), and clay. The former required 808 kcal./kg. of clinker, and the other, 762 kcal. By utilizing exhaust air from the cooler, the requirements could be reduced to 744 and 748, respectively. Heat balances are given, and means for reducing the heat requirement still further by reducing radiation losses are discussed. 3 figures, 6 references. Cf. *Ceram. Abstr.*, **1956,** June, p. 122j.   M.HA.

Measurement of flame speeds by a nozzle burner method. CARL HALPERN. *J. Research Natl. Bur. Standards*, **60** [6] 535–46 (1958).—The literature records numerous measurements, using stationary flames on burners, of the speed with which flame moves through combustible mixtures of gases. Although the method seems reasonably simple, the results obtained by various investigators are often not in good agreement. A program of research on combustion includes a study of the reasons for the differences among recorded values of flame speed measured by the burner method. The primary objective of this task has been to develop the precautions that should be observed in applying the method, rather than to evolve numerical values of flame speed. H. describes progress that has been made since the apparatus was originally described in 1951 and presents values of flame speeds of methane-air mixtures obtained since then, together with comparisons of these values with those obtained by two flame theories. 15 figures, 14 references.   M.J.K.

Sampling exhaust gases in glassmelting furnaces. V. A. KRECHMAR. *Steklo i Keram.*, **15** [7] 24–25 (1958).—A brief description is given of an apparatus for sampling gas. It consists of a sampling pipe made from three concentric tubes, the two inner being of brass and the outer of steel. A special aspirator for continuous sampling is shown, and the performance of the complete setup is discussed. 2 figures.   K.S.

Technical limits of heat consumption of the coke-fired shaft limekiln. H. EIGEN. *Zement-Kalk-Gips*, **11** [6] 258–62 (1958).— The heat consumption (per kg. of lime) is determined by the gas-material temperature difference at the boundary between the preheating and firing zones; as the useful heat, the heat of reaction at 20°C. is used. Small-lump limestone and a high preheating zone result in a particularly low temperature interval at the boundary and thus in a very low heat consumption. By reducing this temperature interval to 30°C., the thermal efficiency of the coke-fired kiln can be increased to 90% and the heat consumption reduced to 774 kcal./kg. of lime with 93% free CaO. 6 figures, 8 references.   M.HA.

PATENTS

Apparatus for measuring and/or controlling surface temperatures under non-black-body conditions. WILLIAM T. GRAY (Leeds & Northrup Co.). **U. S. 2,846,882,** Aug. 12, 1958.

D.J.B.

Chamber lining. GEORGE P. REINTJES. **U. S. 2,846,867,** Aug. 12, 1958.—A chamber lining comprises a supporting structure, a tile lining for the structure comprising a plurality of rows of identical abutting tile, each pair of adjacent tile having their abutting side edges formed with recessed flanges conjointly forming a T-shaped slot opening through the rear face of the tile, rows of spaced studs projecting in fixed relation from the supporting structure and having threaded ends received within the T-slots, rectangular anchor castings having their opposite longitudinal edges received within the recessed flanges of each pair of adjacent tile, the rectangular castings have a diagonal slot receiving the studs and permitting longitudinal and lateral displacement of the castings on the studs to compensate for misalignment of the T-slots in relation to the stud location, and clamp nuts threaded on the studs on opposite sides of the castings to secure the castings in fixed position on the studs.

D.J.B.

Drying method. JAMES E. LAWVER (International Minerals & Chemical Corp.). **U. S. 2,847,123,** Aug. 12, 1958.—1. The method of preparing relatively soft and attritionable nonmetallic ore for electrostatic separation comprises subjecting the washed comminuted ore to drying gases under agitation conditions in a first stage of drying where the solids are moved by hot drying gases having a velocity in excess of that for maintaining a teetering condition for the largest particles being dried, removing the partially dried solids from suspension at a temperature in the range of 175° to about 210°F., and subjecting the partially dried particles in a final stage of moisture removal to drying gases under conditions giving a time of agitation in the range of about 0.1 sec. to 15 min., the shorter periods of agitation being utilized when the agitation is greatest, and a heat transfer permitting attainment of a solids temperature in excess of about 250°F. during the period of agitation, electrically charging the dried ore particles, and subjecting the charged dry ore to an electrostatic separation to beneficiate it.

D.J.B.

Gas and liquid fuel burner assembly. ROBERT D. REED, JOHN S. ZINK, JR., AND ROBERT P. DUNCAN (John Zink Co.). **U. S. 2,847,063,** Aug. 12, 1958.—In a fuel burner assembly for firing into a ceramic-lined opening in a furnace wall, a cup-shaped frame adapted to be secured to the wall, an end portion on the frame adapted to be spaced from the wall, an annular refractory member carried by the end portion having a smaller diameter than the cup-shaped frame, the end portion having an opening therethrough registering with the interior of the upstream end of the annular refractory member, a plurality of mixing tubes arranged in circumferentially spaced relation around the exterior of the refractory member, each extending substantially parallel to the axis of the refractory member, a pipe rigidly connected to the downstream end of each mixing tube and disposed at an angle with respect to the axis of the associated mixing tube, a burner head carried by the downstream end of each pipe having a discharge orifice aligned with the axis of the associated pipe, each of the mixing tubes extending through an opening in the end portion, a member surrounding each mixing tube carried by the end portion for supporting the mixing tubes with each tube rotatable about its axis, a manifold including means associated therewith for supplying gaseous fuel into each mixing tube, means for supporting the manifold on all of the tubes, the cup-shaped frame member having circumferentially spaced windows therein, an annular shutter surrounding the cup-shaped frame and the windows and supported for rotation thereon, the shutter having circumferen-

tially spaced openings therethrough, and means for controlling the volume of air admitted through the opening in the end portion for movement into the interior of the refractory member.

D.J.B.

Furnace structure. JAMES KNIVETON (Selas Corp. of America). **U. S. 2,848,206,** Aug. 19, 1958.—1. In a furnace, the combination of mechanism including a horizontal frame with means to move the frame in a vertical direction and in a horizontal direction, an elongated furnace floor subject to changes in length due to changes in furnace temperature, the floor being mounted on the frame, means between the floor and frame operative to permit relative longitudinal movement between the two, a connection between the frame and one point on the floor whereby the remainder of the floor, upon expansion and contraction thereof, may move relative to the frame, and structure forming furnace side walls and roof above the floor and separate therefrom.

D.J.B.

High-intensity carbon-arc surface heater. RICHARD FRIEDMAN. **U. S. 2,850,554,** Sept. 2, 1958.—1. An electrical heating unit comprises a hollow metallic housing having a plurality of spaced lateral apertures, conductive refractory means mounted in the housing and disposed between the apertures, a layer of conductive refractory disposed in parallel relation to the housing and insulated therefrom, a plurality of elongated conductive refractory members projecting laterally from the layer of refractory and extending into the apertures for electrical cooperation with conductive refractory means in the housing to produce an arc and high temperature.

D.J.B.

Induction heating apparatus for fusing vitreous enamel. EUGENE J. LIMPEL (A. O. Smith Corp.). **U. S. 2,848,566,** Aug. 19, 1958.—1. An apparatus for firing a vitreous enamel to a steel article comprises an induction heating element, means to energize the element and induce a current in the article to heat it to a temperature sufficient to fuse the vitreous enamel coating to the steel article, means for reflecting the heat radiated from the article back toward the article, the metal being selected from the group consisting of aluminum, silver, gold, and copper, and means to cool the reflective surface to prevent oxidation and tarnishment thereof.

D.J.B.

Modular suspended wall. GEORGES P. REINTJES. **U. S. 2,847,849,** Aug. 19, 1958.—A furnace wall construction comprises a series of vertically spaced horizontally extending stringers, tile-supporting clips horizontally and vertically adjustable on the stringers, each of the clips having a downwardly opening hook and an underlying shelf, a plurality of horizontally spaced tiles defining horizontal courses along the stringers, each tile being supported by one of the clips and having an upper groove engaging a hook thereof and a bottom recess in seating engagement with the shelf of the same clip, each tile having complementary tongues and grooves on its top and bottom surfaces and on its two opposite side surfaces, a plurality of horizontal courses of stretcher brick being supported by each of the courses of the tile, each of the stretcher brick having top and bottom tongues and grooves, each brick of one of the courses of stretcher brick being disposed end to end with each end supported on one of the tile in a course directly beneath and with the portion of each brick between its ends spanning the space between a pair of adjacent tile, each stretcher brick in the one course having a tongue and groove interlock with the tile providing the support therefor, header brick having tongues and grooves on the top, bottom, and side surfaces and being positioned in the spaces between the tile, another course of the stretcher brick directly underlying a course of the tile supporting the one course of stretcher brick, and the header brick having tongue and groove interlock with the spaced tile, the stretcher brick in the course underlying the tile, and the stretcher brick supported by the tile.

D.J.B.

XIII—Materials

Abrasive materials. HENRY P. CHANDLER AND GERTRUDE E. TUCKER. *U. S. Bur. Mines Minerals Yearbook* (preprint), 1956, Vol. I, 19 pp. 4 figures. 15¢. **Asbestos.** D. O. KENNEDY AND ANNIE L. MATTILA. *Ibid.,* 13 pp. 1 figure. 10¢. **Bauxite.** RICHARD C. WILMOT, ARDEN C. SULLIVAN, AND MARY E. TROUGHT. *Ibid.,* 21 pp., 2 figures. 15¢. **Clays.** BROOKE L. GUNSALLUS AND ELEANOR B. WATERS. *Ibid.,* 24 pp. 3 figures. 15¢. **Diatomite.** L. M. OTIS AND ANNIE L. MATTILA. *Ibid.,* 8 pp., 1 figure. 10¢. **Feldspar, nepheline syenite, and aplite.** TABER DE POLO AND GERTRUDE E. TUCKER. *Ibid.,* 9 pp. 10¢. **Gem stones.** JOHN W. HARTWELL AND ELEANOR B. WATERS. *Ibid.,*

13 pp. 10¢. **Graphite.** DONALD R. IRVING AND ELEANOR B. WATERS. *Ibid.,* 12 pp. 10¢. **Gypsum.** LEONARD P. LARSON AND NAN C. JENSEN. *Ibid.,* 15 pp. 3 figures. 10¢. **Jewel bearings.** HENRY P. CHANDLER AND ELEANOR B. WATERS. *Ibid.,* 4 pp. 5¢. **Kyanite and related minerals.** BROOKE L. GUNSALLUS AND GERTRUDE E. TUCKER. *Ibid.,* 3 pp. 5¢. **Minor nonmetals.** D. O. KENNEDY, ALBERT E. SCHRECK, AND ANNIE L. MATTILA. *Ibid.,* 3 pp. 5¢. **Perlite.** L. M. OTIS AND ANNIE L. MATTILA. *Ibid.,* 6 pp., 1 figure. 5¢. **Quartz crystal (electronic grade).** WALDEMAR F. DIETRICH AND GERTRUDE E. TUCKER. *Ibid.,* 5 pp. 5¢. **Review of the mineral industries (metals and nonmetals**

except fuels). WILLIAM A. VOGELY. *Ibid.*, 44 pp. 15¢. **Statistical summary of mineral production.** KATHLEEN J. D'AMICO. *Ibid.*, 52 pp. 20¢. **Talc, soapstone, and pyrophyllite.** DONALD R. IRVING AND ELEANOR B. WATERS. *Ibid.*, 12 pp., 1 figure. 10¢. **Vermiculite.** L. M. OTIS AND NAN C. JENSEN. *Ibid.*, 6 pp. 1 figure. 5¢.   M.J.K.

Adjustment of land derived clays to the marine environment. MAURICE C. POWERS. *J. Sediment. Petrol.*, 27 [4] 355–72 (1957). —The predominant clay minerals found in river waters in the Chesapeake Bay area consist of a well-formed to weathered illite with minor amounts of kaolin and a trace of weathered chlorite. Mixed-layer clays observed in the estuaries are related to and difficult to distinguish from differentially hydrated monomineralic clays when these clays are in a weathered condition. A regularly stacked mixed-layer illite-chlorite was observed at one locality in the James Estuary. A chlorite-like and a vermiculite clay are forming in estuaries along the Atlantic coast. Thermal stability of the diagenic chlorite increases with increasing salinity of the environment and to less extent with depth in the sediment. The chloritic material arises principally from the diagenesis of weathered illite in the Atlantic coastal environment and probably passes through a vermiculite stage. Montmorillonoid and, to less extent, illite are altered to chloritic material in the Gulf of Mexico and along the Pacific coast. The first phase planned for the study of the geochemical relation of chloride, sodium, calcium, potassium, and magnesium in the clays of an estuary has been completed. The chemical data are used to support a hypothesis that a chloritic-vermiculitic clay mineral is being constructed by the alteration of weathered illite and montmorillonoid and the reconstitution of a trace amount of chlorite.   S.A.F.

Alteration of volcanic ash near Denver, Colorado. JULIUS SCHLOCKER AND RICHARD VAN HORN. *J. Sediment. Petrol.*, 28 [1] 31–35 (1958).—A vitric, crystal, lithic volcanic ash near Denver consists predominantly of fresh highly vesicular rhyolitic glass shards and smaller amounts of partly altered platy glass shards. The alteration products of the platy shards are predominantly illite randomly interlayered with a small amount of montmorillonite and also containing a small amount of free montmorillonite. Among the lithic and crystal particles in the ash is biotite, probably of volcanic origin, which is partly altered to vermiculite, part of which is randomly interlayered with biotite. Some of the altered biotite crystals are long and vermicular and appear to be authigenic.   S.A.F.

Bucket drill pinpoints aggregates in deposit. J. M. WELLS. *Rock Prods.*, 61 [7] 86–88, 142 (1958).—Bucket-type drilling equipment for sampling permits careful screening and analysis of the actual physical content of the material. Procedures used and results obtained at the Glen Canyon Dam are given; they show that the data was obtained at one-fifth the cost of hand labor. 4 figures.   D.J.B.

Bucket drill yields superior data. JOHN J. HECK. *Rock Prods.*, 61 [6] 103–104, 107, 120, 122 (1958).—This equipment can be used for subsurface exploration for sand, gravel, etc. The drilling tool is a large cylindrical bucket 14 to 48 in. in diameter with a hinged bottom. The bottom is concave up and contains two cutter blades positioned like the cutting edges on a wood auger. Some test results are given indicating a drilling rate of 4.6 ft./hr. in a sandy deposit. Holes were drilled to a depth of 156 ft. Very accurate samples may be obtained from any portion of the boring. 5 figures.   D.J.B.

Critical considerations in clay preparation. R. PELS-LEUSDEN. *Ziegelind.*, 11 [14] 430–37 (1958).—A new French process (Grimal) using superheated steam is discussed. 13 figures.   T.W.G.

Hydrocyclone for improving refractory clays. S. V. GLEBOV. *Ogneupory*, 23 [7] 334–35 (1958).—G. attempts to prove that clays can be successfully enriched by this equipment. The work was done in a Polish faience factory, and results are promising.   K.S.

Hydrothermal alteration of Phosphoria mudstones. LAWRENCE F. ROONEY. *J. Sediment. Petrol.*, 27 [4] 453–59 (1957).— Samples of phosphatic mudstone collected from several measured sections in the Retort phosphatic shale member of the Phosphoria formation near Divide, Montana, contain an abundance of montmorillonite, locally associated with kaolinite and talc. Of several possible modes of origin, hydrothermal alteration of preexisting illite to montmorillonite best accords with related geologic phenomena. These include the presence of intrusives within and/or adjacent to the formation, the associated hydrothermal alteration of the underlying dolomite to talc, the associated low-

grade metamorphism of the phosphatic mudstone itself, the network of calcite and quartz veins within the mudstone, and the association of talc and montmorillonite. The kaolinite, which occurs in very carbonaceous mudstones, may be (1) further hydrothermal alteration of montmorillonite, (2) an authigenic mineral formed in a restricted part of the Retort Basin with acidic bottom conditions, or (3) a detrital mineral.   S.A.F.

Liquefaction behavior and chemical-physical properties of some refractory clays. HANS ROSENBERGER. *Silikattech.*, 9 [7] 303–309 (1958).—A number of refractory clays of East Germany used for the production of fire-clay brick were tested with regard to their liquefaction behavior in electrolytes, electrolyte mixtures, and protective colloids. Bivalent cations exert a negative influence on the liquefaction, complete liquefaction taking place only when the cations are univalent. All clays with higher contents of organic substance can be liquefied almost completely, even if bivalent cations are present. The negative action of the anions, especially $SO_4{}^{2-}$ and Cl^-, on the slip is small. The water requirement of the slip depends also on the surface and the grain structure of the clays. Diagrams and tables give data for the behavior. 12 figures, 12 references.   M.HA.

Material which absorbs X rays. HANS FEIERABEND. *Silikattech.*, 9 [5] 213–15 (1958).—The new material is made of barite of different grain sizes and with different binders (mainly blastfurnace cement 225); it is used in brick sizes of 490 x 238 x 75 mm. for building up walls. The necessary thickness of a protective layer of lead for X rays up to 200 kv. and the curve for selecting the equivalent thickness of the new material are given. For > 200 kv., barite only with a specific gravity of 2.4 gm./cc. is used. 4 figures, 8 references.   M.HA.

Mountfield sub-Wealden gypsum mine. W. S. GIBSON. *Mine & Quarry Eng.*, 24 [8] 333–39 (1958).—G. describes the history, geology, mining, preparation, and handling of gypsum at the Mountfield mine. 14 figures.   V.R.E.

New technique for measuring roundness of sand grains. D. A. ROBSON. *J. Sediment. Petrol.*, 28 [1] 108–10 (1958).—Because the Wadell (1935) process is laborious and time consuming, a special graticule has been devised which, together with a new procedure, makes it possible to measure up to 50 grains per hour.   S.A.F.

Occurrence of palygorskite and barytes in certain parna soils of the Murrumbidgee region, New South Wales (Australia). J. A. BEATTIE AND A. D. HALDANE. *Australian J. Sci.*, 20 [9] 274–75 (1958).—Clay aggregates had white paperlike skins 0.1 to 0.2 mm. thick, translucent when moist. The skins were almost pure palygorskite and surrounded aggregates of quartz, kaolinite, illite, and montmorillonite. Some skins contained in addition quartz, kaolinite, and manganese oxides. The quartz and kaolinite formed an inner layer between the palygorskite and the manganese oxides. Barytes occurred as white chalky nodules 0.5 to 5.0 mm. in diameter accompanying the clay aggregates. The various minerals were associated with parna sheets, i.e., sheets of an aeolian calcareous clay. 10 references.   W.O.W.

Pennsylvanian underclays—potential bonding clays for use in foundries. HAYDN H. MURRAY. *Indiana Dept. Conserv. Geol. Survey Rept. Progr.*, 1958, No. 11, 27 pp. 50¢.—Laboratory tests show that five underclays from western and southwestern Indiana are potential sources of bonding clay for foundries. Green and dry strength tests were determined for each sample, and the results of these tests were compared with the results of tests obtained from a commercially used bonding clay. The particle-size distribution and the mineral composition of the underclays are most important in interpreting the results of physical tests. The samples which had a high clay content and a rather high percentage of montmorillonite produced the best green and dry strength test results. Five areas in Indiana are most favorable for commercial production of bonding clays. 6 figures.

Proposed classification and terminology of rocks in the series bauxite-clay-iron oxide ore. JIŘÍ KONTA. *J. Sediment. Petrol.*, 28 [1] 83–86 (1958).—Chemical composition is used in only a small number of rock types as the main criterion in their petrographic classification and terminology. A new classification and terminology of rocks in the series bauxite-clay-iron oxide based on their quantitative mineral composition is proposed. The terms laterite and bauxite are defined from their substantive and genetic standpoints. Laterite is a relatively untransported weathered product containing free aluminum hydroxide, derived *in situ* from the parent rock, whereas bauxite is a transported weathered product (detrital mode of occurrence). Both of these rocks, however, have the same mineral composition.   S.A.F.

Rubidium depletion in feldspars. S. R. TAYLOR AND K. S. HEIER. *Nature*, **182** [4629] 202–203 (1958). 2 figures, 9 references.   V.R.E.

Search for industrial minerals in Canada. G. M. HUTT. *Western Miner and Oil Rev.* (Vancouver), **31** [6–7] 33–43 (1958). —The search for any industrial mineral in Canada should be confined to areas of favorable geology with suitable transportation facilities and favorable markets. Minerals that merit investigation and the sections where they may be found are listed.   G.M.H.

Spectrochemical analysis for trace elements. *Am. Soc. Testing Materials Spec. Tech. Publ.*, 1958, No. 221, 84 pp. $2.75.

Study of new boron carbide materials for use in nuclear energy. C. FICAI AND L. CINI. *Ceramica* (Milan), **13** [6] 51–53 (1958).— Further data are given in diagrams on the neutron absorption of boron carbide and on its resistance to attack by air and CO_2 at 550°C. Cf. *Ceram. Abstr.*, 1958, Sept., p. 239*j*.   M.HA.

Surficial sediment in Lake Mead. B. N. ROLFE. *J. Sediment. Petrol.*, **27** [4] 378–86 (1957).—The surficial sediment along a 70-mile reach in Lake Mead was examined as to texture and mineralogical composition in order to determine possible relations to diagenesis and deposition. Mineralogically, montmorin-type clays dominated the dispersed clay fraction upstream, whereas illite was predominant downstream.   S.A.F.

X-ray and electron microscope study of several Brazilian kaolins. YVONNE STOURDZE VISCONTI AND BLANCHE NICOT. *Bol. INT* (*Inst. nacl. tecnol.*) (Rio de Janeiro), **5** [11] 22–34 (1954).— Two samples of Georgia kaolin were used as comparison in the study of several Brazilian kaolins from Minas Gerais, Bahia, Paraná, and São Paulo states. According to X-ray diffraction and electron microscope observations the crystal structures of the Brazilian kaolins differ; in general, the crystals are in the form of tubes, many broken fractions can be seen, and impurities such as quartz are present in high concentration. Perfect kaolinite crystals were seldom observed. 22 figures. Cf. *Ceram. Abstr.*, 1957, Feb., p. 50*j*.   V.R.P.

BOOK

Gypsum and Anhydrite. A. W. GROVES. Overseas Geological Surveys, Mineral Resources Division. H. M. Stationery Office, London, 1958. iv + 108 pp. Price 8*s*. 2*d*.—This is a monograph on the properties, mode of occurrence, mining and quarrying, beneficiation, uses, preparation, standard specifications, world production, prices, and valuation of gypsum. The second half of the volume gives descriptions of gypsum and anhydrite mines, deposits, occurrences, and industries in British and other countries. 400 references.   V.R.E.

PATENTS

Alumina compositions. EVERET F. SMITH (Standard Oil Co.). U. S. 2,847,387, Aug. 12, 1958.—1. A method for preparing alumina from aluminum comprises reacting aluminum metal with water, in the presence of about 0.1 to 2% by weight of gallium as catalyst, at a temperature above about 140°F. for a time sufficient to form hydrous alumina.   D.J.B.

Apparatus for producing powders by atomization of liquid carriers. JOHAN E. NYROP (Niro Corp.). U. S. 2,850,085, Sept. 2, 1958.—1. In a device for the production of powders by atomization of a liquid having a drying chamber, a disk-shaped vane wheel suspended in the chamber, a shaft secured to the wheel, means for rotating the shaft, the wheel having a central opening from which the vanes of the wheel extend to the periphery of the wheel, each of the vanes being shaped as a wall and defining a channel of substantially uniform breadth with one of the other vanes, the channels extending from the central opening to the periphery of the wheel, means for supply of liquid to the channels through the central opening in the wheel, the channels being curved from the radial direction in the direction of motion of the wheel as defined by the means for rotating the shaft, the magnitude of the curvature being such that the centrifugal force derived from the rotation of the wheel has a component at right angles to the channel and the angle between the tangent to the curvature of the channels and the radius through the point of tangency being only a little < 90° for all points of a channel.   D.J.B.

Colloid mill. LANCELOT H. REES AND HAROLD C. BECK (Manton-Gaulin Mfg. Co., Inc.). U. S. 2,850,246, Sept. 2, 1958.—1. In a colloid mill provided with a housing which forms a working chamber having an inlet and an outlet port and a rotor shaft extending through the housing into the chamber, the hous-

ing being split to form sections partible axially of the shaft for access to the working chamber, and means for releasably holding the sections together, a rotor removably secured to the shaft within the working chamber, an annular stator surrounding the rotor, the rotor and stator having opposing closely spaced faces constituting the working surfaces of the mill, the stator being removably received in the housing between the sections thereof and forming a seal between them, a removable liner surrounding the shaft in spaced relation thereto and confined between the stator and the housing, a sleeve on the shaft within the liner and adjacent the rotor, the sleeve and liner being spaced peripherally and having oppositely directed circumferential flanges and sealing means confined between the flanges, the sleeve being formed to provide an annular space between it and the shaft adjacent the rotor, an annular bearing received in the space and forming a seal between the sleeve and shaft, the bearing being slidable axially of the shaft within the sleeve, and spring means biasing the bearing against the rotor to form a rotary seal therewith.   D.J.B.

Grinding apparatus. KLAUS GUSTKE AND ERICH KUHLS (Anni Guenther). U. S. 2,850,245, Sept. 2, 1958.—1. A multiple stage colloid mill comprises, in combination, a stationary mill housing having a frustoconical interior wall with grinding teeth separated by grooves, a hollow rotor with a frustoconical exterior wall and an interior wall defining a material inlet chamber, the rotor being mounted within the housing for rotation about a substantially vertical axis and the interior wall of the mill housing being spaced from the exterior wall of the rotor to define a milling gap therebetween, the wall of the rotor surrounding the material inlet chamber defining openings for passage of material from the chamber to the milling gap by centrifugal force upon rotation of the rotor and the exterior rotor wall surrounding the chamber having grinding teeth forming an acute angle to the vertical and separated by corresponding grooves, the above-mentioned grinding teeth of the housing and the rotor forming a pregrinding zone of the mill; a coarse grinding zone arranged below the pregrinding zone, the latter zone being formed by substantially parallelogram-shaped grinding teeth defined by two sets of parallel grooves in the exterior wall of the rotor, each set of grooves being inclined in the same direction but at a different angle in relation to the vertical, and corresponding grinding teeth in the interior wall of the mill housing; a third zone below the coarse grinding zone receiving the coarsely ground material therefrom, the third zone being formed by generally downwardly extending channels in the exterior wall of the rotor and the interior wall of the housing, the channel cross sections being so correlated with the preceding grinding teeth that they correspond to the grain size of the coarsely ground material; and a fourth or fine milling zone formed by roughened surfaces of irregular formation and finer grain than the grinding teeth on the exterior wall of the rotor and the interior wall of the housing.   D.J.B.

Indicating powder composition. TABER DE FOREST (Magnaflux Corp.). U. S. 2,848,421, Aug. 19, 1958.—1. A dry indicating powder composition comprises 80 to 20 parts by weight of particles of a silica aerogel carrier and 20 to 80 parts of pigment particles having a particle size of less than about 10μ and loosely adhering to and carried by the carrier.   D.J.B.

Vanadium-bearing ceramic pigment. THOMAS D. CARNAHAN AND EDWIN H. RAY (B. F. Drakenfeld & Co., Inc.). U. S. 2,847,-317, Aug. 12, 1958.—A method of preparing a vanadium-bearing pigment to remove uncombined vanadium oxide still present in the calcine comprises incorporating in the calcined pigment an alkaline-reacting metal compound in an amount sufficient to react completely, in the presence of water, with the uncombined vanadium oxide. Such uncombined oxides cannot be removed by simple leaching of the calcined pigment, and they are the cause of welting or dimpling of the finished glaze in which the pigment is used. For most commercial formulations about 3 to 10% of the alkaline compound based on the dry weight of the pigment will be satisfactory. It forms insoluble vanadates and eliminates the undesirable characteristics of the uncombined vanadium. Typical reacting metal compounds are salts and hydroxides of sodium, potassium, lithium, magnesium, calcium, barium, zinc, strontium, and mixtures of these; the carbonates and hydroxides are preferred for economic reasons. In one example a tin vanadium yellow pigment was made from a mixture of 10 parts by weight of SnO_2 for each part of NH_4VO_3 by calcining at 2300° to 2400°F., resulting in a theoretical composition of 94.5% SnO_2 and 5.5% V_2O_5. The calcine was ground in water in a ball mill to a suitable fineness. An addition of 6% $MgCO_3$ based on the dry weight of the calcine, was mixed with the slurry and the slurry was heated

to 150°F. to accelerate the reaction. The end of the reaction was noted by the cessation of bubbling, and the pigment was filtered and dried. When used as an underglaze or glaze stain no dim-

pling was noted. A similar calcine without the treatment, although washed several times with hot water, produced many dimples when used in test glazes.   D.J.B.

XIV—Chemistry and Physics

Carbides of niobium. G. BRAUER, H. RENNER, AND J. WERNET. *Z. anorg. u. allgem. Chem.*, **277** [5] 249–57 (1954).—Niobium carbides in the composition range from $NbC_{1.0}$ to NbC_0 were prepared by reaction of niobium with highly carburized carbides. These latter compounds were obtained by sintering NbO_2 with carbon at 1600°C. in vacuum. Nb_2O_5 could not be used because of its violent reaction with C. Therefore NbO_2 was prepared first by reduction of Nb_2O_5 in hydrogen at 1150° to 1250°C. The direct carburization of niobium with CH_4 at 1200°C. can also be used for the preparation of the carbides. X-ray investigations showed the presence of 3 phases in the system Nb–C: (1) A monocarbide phase in the homogeneity range from $NbC_{1.00}$ to $NbC_{0.72}$ has the rock-salt structure; the lattice constant decreases from 4.4572 to 4.4243 kX. (2) The subcarbide phase, which is homogeneous from $NbC_{0.00}$ to $NbC_{0.52}$, has the Nb atoms in the hexagonal close-packing arrangement; *a* decreases from 3.1131 to 3.1109 kX and *c* from 4.949 to 4.944 kX. The metallic phase has a homogeneity range from Nb to $NbC_{0.02}$ corresponding to solutions of C in niobium. All the results apply to samples prepared at 1600° to 1700°C. 4 figures, 7 references.   G.B.

Color of ruby and the $(Al,Cr)_2O_3$ solid solutions. E. THILO, J. JANDER, AND H. SEEMANN. *Z. anorg. u. allgem. Chem.*, **279** [1–2] 2–17 (1955).—The following properties of Al_2O_3-Cr_2O_3 solid solutions were investigated: lattice constants, densities, color and its temperature dependence, reducibility, and magnetic susceptibility. Only solid solutions having less than 8 mole % Cr_2O_3 show a pure red color. Above that concentration the green color of Cr_2O_3 begins to appear. The lattice constant and the density and reducibility curves also show inflections at 8 mole % Cr_2O_3. From these results and from measurements of the magnetic susceptibility it is concluded that the red color at low concentrations is due to isolated Cr^{3+} ions, whereas at higher concentrations (above 8 mole % Cr_2O_3) the Cr^{3+} ions are in contact with each other, giving green colored solid solutions. 7 figures, 24 references.   G.B.

Conductometric determination of immiscibility in silicate melts. C. KRÖGER AND K. LIECK. *Z. anorg. u. allgem. Chem.*, **279** [5–6] 300–12 (1955).—The method is described, and as examples the systems PbO–B_2O_3 and PbO–B_2O_3–SiO_2 were studied. The temperature of beginning immiscibility was determined from resistance measurements with two pairs of Pt electrodes arranged one above the other. The degree of immiscibility was estimated from the temperature and concentration dependence of the conductivity of the boundary phases. 7 figures, 6 references.   G.B.

Crystal morphology of dehydration products of aluminum oxide trihydrate. W. HÜTTIG AND H. GINSBERG. *Z. anorg. u. allgem. Chem.*, **278** [1–2] 93–107 (1955).—Microscopic and X-ray investigations on the morphological changes attending the dehydration of γ-$Al_2O_3 \cdot 3H_2O$ to α-Al_2O_3 are described. Dehydration and transformation of the lattice are not synchronous. Persistent pseudomorphism is reported. The importance of this fact for bulk density and other properties is discussed. 17 photomicrographs, 21 references.   G.B.

Differential thermal analysis above 1200°C. TERRY F. NEWKIRK. *J. Am. Ceram. Soc.*, **41** [10] 409–14 (1958).—Differential thermal analysis techniques and equipment for use at temperatures up to 1550°C. are described. Proper electrical shielding eliminates the spurious effects ordinarily encountered above about 1200°C. For nonvolatile materials a pellet method requiring no container and only 0.1 to 0.2 gm. of sample has been developed. For systems containing volatile components, covered crucibles are used. Examples are given of typical DTA curves obtained from pellets of CaO-Al_2O_3-Fe_2O_3 mixtures. The interpretation of DTA heating curves to give precise solidus and liquidus data is discussed briefly. 5 figures, 8 references.

Effect of oxide additions on sintering of magnesia. JAMES W. NELSON AND IVAN B. CUTLER. *J. Am. Ceram. Soc.*, **41** [10] 406–409 (1958).—The effect of transition metal, alkali, alkaline-earth, and heavy metal oxide additions on the sintering of magnesia was determined by measuring bulk density and shrinkage. Polished specimens were made of selected compositions, and the

grain structure was photographed. The unusual effect of titanium, zirconium, silicon, lithium, iron, and zinc oxides in promoting high sintered densities is explained on the basis of the defective crystal structure produced by these additions. ' 6 figures, 9 references.

Effects of ultrasonics on heat transfer by convection. GILBERT C. ROBINSON, C. M. McCLURE III, AND RUDOLPH HENDRICKS, JR. *Am. Ceram. Soc. Bull.*, **37** [9] 399–404 (1958).—An investigation was made of the effect of 400-kc. sound waves on the temperature drop between heated air and a solid and between heated oil and a solid. It was found that ultrasonic energy can alter this temperature drop only when the fluid is capable of transmitting the sound energy. Several pieces of equipment especially constructed for this investigation are described, including an air to solid heat exchanger, a liquid to solid heat exchanger, a device for coupling ultrasonic energy to high-temperature specimens, and a vibration pickup. 8 figures, 11 references.

Electron microscope and electron diffraction studies of sintering of magnesite. A. PANDE AND RABINDAR SINGH. *J. Am. Ceram. Soc.*, **41** [10] 394–97 (1958).—Electron micrographs and electron diffraction patterns of chemically pure and natural magnesite samples heated from 400° to 1050°C. showed, in general, that at lower temperatures (400° to 600° C.) small MgO particles were formed by the decomposition of $MgCO_3$ ($MgO + CO_2$). As temperatures were increased (600° to 800°C.), these particles grew into large secondary aggregates showing higher porosity. The porosity of the main particles (unchanged $MgCO_3$) also increased. Sintering began at 850°C.; the particles seemed to adhere more strongly to each other, and aggregation and porosity decreased. Sintering was completed at 1050°C., and numerous sharply defined cubic crystals varying from 0.1 to 0.35μ were observed. In natural magnesites that contained traces of iron and aluminum oxides the decomposition began at higher temperatures than in the chemically pure samples, but the recrystallization process was delayed, which was contrary to expectations. 6 figures, 2 references.

Sintering of high-purity nickel oxide. YOSHIO IIDA. *J. Am. Ceram. Soc.*, **41** [10] 397–406 (1958).—The results of an investigation of densification and grain growth during the sintering of high-purity NiO in various atmospheres are presented. The sintering of NiO powders is divided into three stages. Grain growth during the third stage follows the empirical equation $D^3 = Kt$, where D is the average grain diameter, K is a rate constant, and t is the sintering time. The activation energy of grain growth was found to be 55 kcal./mole. The shrinkage and weight loss during the sintering process in vacuum were larger than in argon, air, and oxygen. Grain growth during sintering also differed with the sintering atmosphere. It is concluded that the sintering process is not explained reasonably by the theory of a semiconductor. 16 figures, 17 references.

Studies on polytypism of silicon carbide: I, Correlation between color and polytype of silicon carbide. HIROSHIGE SUZUKI. *Yogyo Kyokai Shi*, **66** [745] 4–10 (1958).—Various samples of silicon carbide were examined by the X-ray diffractometer. Type 4H was not found in the pale green, green, and yellow varieties. Type 15R is found in yellow crystals in fairly large amount, and nearly all crystals of any color contain a small amount of it. Type 6H is found in both green and black crystals. Black silicon carbide found in American and German brick consists mainly of type 6H, while type 4H is the most common variety of black silicon carbide found in products of Japan. 5 figures, 9 references.   K. Y.

Ternary systems BaO–TiO_2–SnO_2 and BaO–TiO_2–ZrO_2. G. H. JONKER AND W. KWESTROO. *J. Am. Ceram. Soc.*, **41** [10] 390–94 (1958).—An investigation of the ternary systems BaO–TiO_2–SnO_2 and BaO–TiO_2–ZrO_2 led to the discovery of two new compounds belonging to the system BaO–TiO_2. These compounds, $Ba_2Ti_5O_{12}$ and $Ba_2Ti_9O_{20}$, are stabilized by minute additions of SnO_2 or ZrO_2. The known compound $BaTi_2O_5$ can be obtained only from the molten phase, and it decomposes below 1300°C. into $Ba_2Ti_9O_{12}$ and $BaTiO_3$. In these systems no ternary compounds are found. The ternary phase diagrams can be divided into re-

gions with high and low dielectric losses, which are in accordance with the phase relations. Crystallographic data of the new compounds are included. 2 figures, 8 references.

Thermal decomposition of dolomite. YOSHIAKI SANADA AND KIYOSHI MIYAZAWA. *Sekko to Sekkai*, **1955**, No. 17, pp. 20–22.— To elucidate the thermal decomposition mechanism of dolomite, materials such as precipitated calcium carbonate, magnesite, talc, or serpentine were added, and differential thermal analysis was made of the mixtures. When precipitated calcium carbonate was added, its decomposition temperature was identical with the second decomposition temperature of dolomite. When magnesite was added, however, its decomposition temperature was entirely different from that of dolomite. Four samples of pulverized dolomite were heated at 650°, 700°, 750°, 800°, and 850°C. Determination of their contents of free magnesia and free lime showed that in some samples the total amount of $MgCO_3$ does not completely decompose at the initial decomposition temperature, but the undecomposed residue tends to decompose at the second decomposition temperature. This is due perhaps to the fact that the dolomite consists of not one kind but several kinds having different properties. 1 figure.   Y.S.

Thermal formation of tridymite and of cristobalite from precipitated amorphous silica. JEAN PAPAILHAU. *Compt. rend.*, **245** [17] 1443–45 (1957).—Silica gel crystallizes easily in the presence of fluorides and carbonates of potassium and sodium with temperature rise into the state of tridymite or cristobalite by passing through an intermediary crystalline state between the amorphous state and cristobalite when the mineralizer is sodium fluoride or potassium fluoride.   M.HA.

Transport numbers of iron ions in molten iron silicates. O. A. ESIN AND A. K. KIR'YANOV. *Izvest. Akad. Nauk S.S.S.R., Otdel. Tekh. Nauk*, **1956**, No. 8, pp. 20–27; abstracted in *J. Iron Steel Inst.* (London), **188** [3] 286 (1958).—An electrolyzer for the determination of transport numbers of iron cations in melts of the $FeO-SiO_2$ system was developed. As an indicator, Fe^{59} was used. It was established that transport numbers of iron cations in melts saturated with silica as well as those of calcium in the $CaO-SiO_2-Al_2O_3$ system are near to unity. In this way the cation character of the electrical conductivity in the above melts and a low mobility of complex anions in such melts were confirmed. In liquid slags of the system $FeO-Fe_2O_3-SiO_2$ the transport number of iron cations decreases continuously with increasing FeO content. This decrease is explained by two factors, viz., increasing electron conductivity and participation in the transport of oxygen ions. An attempt was made to explain the predominantly electronic conductivity of $FeO-Fe_2O_3$ melts.   V.R.E.

Viscosity of kaolin suspensions. L. ZAGAR AND C. SCHUMANN. *Ziegelind.*, **10** [18] 585–90 (1957).—The specific hydrodynamic volume according to the Bingham equation yields fairly constant values in all investigated concentrations, being equal in the mean to 1.0. From this it cannot be concluded that the kaolin particles in watery suspension did not enlarge, since the calculated value of φ_0 from the old Bingham formula for the calculation of the φ values was placed into the equation. The specific hydrodynamic volumes calculated from the Einstein formula show no constancy; instead, they increase perceptively, a further proof of the fact that the assumptions for the equation are not fulfilled. With the extended Einstein law, however, the specific hydrodynamic volumes show satisfactory agreement up to a weight concentration of about 15%, and they are >1. It follows that by the application of the extended Einstein formula, experimental results are correctly obtained up to a certain concentration. From this point on, the flow properties of kaolin suspensions are basically changed, which makes an extension of the law necessary. Within the area of correctness of the law, the suspended kaolin particles display a volume 2.8 times as great as that in the dry state. 6 figures, 9 references.   T.W.G.

Viscosity of molten slags of the system manganese oxide–silica–alumina. SH. M. MIKIASHVILI, A. M. SAMARIN, AND L. M. TSYLEV. *Izvest. Akad. Nauk S.S.S.R., Otdel. Tekh. Nauk*, **1957**, No. 1, pp. 115–22; abstracted in *J. Iron Steel Inst.* (London), **188** [3] 285–86 (1958).—The viscosity of molten slags of the system $MnO-SiO_2-Al_2O_3$ corresponding in composition to the products of deoxidation of steel in the region of the lowest melting temperature was investigated. With increasing content of silica, the viscosity of homogeneous liquid slags increases; it is determined mainly by the size of silicate anions. The viscosity of heterogeneous liquid slags at 1400° to 1590°C. increases with decreasing silica content and is determined by the proportion of solid phase present. The lowest viscosity (0.5 to 10 poises) was observed for

melts with $MnO:Al_2O_3 = 6$ and a silica content of 20 to 30%. With decreasing $MnO:Al_2O_3$ ratio, the viscosity of the melts increases. An addition of alumina causes a slight increase in the viscosity of homogeneous liquid melts. The most fluid melts are those with $MnO:SiO_2 = 2.6$ and up to 22% alumina. With decreasing $MnO:SiO_2$ ratio, the viscosity of the melts increases. An increase in the content of manganese oxide decreases the viscosity of homogeneous liquid slags. Melts of the lowest viscosity correspond in composition to tephroite.   V.R.E.

Work of Soviet scientists in the field of physical chemistry and in ceramic technology. P. P. BUDNIKOV. *Silikattech.*, **8** [11] 470–73 (1957).—A review. 7 references.   M.HA.

BOOKS

Dislocations and Mechanical Properties of Crystals. Edited by J. C. FISHER, W. G. JOHNSTON, R. THOMSON, AND T. VREELAND, JR. John Wiley & Sons, Inc., New York, 1957. xiv + 634 pp., 407 illus. $15.—This book contains the entire proceedings of a small international conference on dislocations and mechanical properties of crystals held at Lake Placid, New York, in September 1956. It consists of 42 papers and the subsequent discussions arranged under eight headings: (I) Direct observations of dislocations, (II) Deformation of pure single crystals, (III) Work hardening and recovery, (IV) Alloy crystals, impurities, and yield point phenomena, (V) Dislocation damping and fatigue, (VI) Theory of dislocations, (VII) Whiskers and thin crystals, and (VIII) Radiation damage. The printed discussions were prepared by the editors from tape recordings, except for a few comments which were submitted in writing after the conference and which are designated as such. The editors are to be congratulated; the discussions are not only valuable for their content but also increase the readability of the book and give the reader a feeling of the stimulating atmosphere which must have existed at the conference. Most of the papers are profusely illustrated, and this is an important asset because many of the ideas are geometrical and the figures greatly facilitate their understanding. The papers vary so much in subject matter and in length (from 2 to 87 pages) that a general discussion is difficult. The experiments involving direct observations of dislocations by etch pit or impurity techniques are particularly impressive when it is recalled that ten years ago dislocation theory was vulnerable to the accusation that direct and unequivocal evidence for the existence of dislocations was lacking. The direct observation experiments, however, have revived the old and difficult question of the origin of dislocations. This problem was once thought to be solved by the theory that some dislocations must be formed during growth and others developed from them by the operation of Frank-Reed sources. However, Gilman's observations of dislocations in lithium fluoride suggest that dislocations can develop out of regions which apparently do not contain Frank-Reed sources. Perhaps the most interesting general conclusion from all the papers is that important contributions can still be made at all levels to both the experimental and theoretical sides of this field. There is no question about recommending this book to metallurgists and solid-state physicists who are interested in mechanical properties; for such people it should be close to indispensable. For ceramists, the recommendation must be qualified because the reviewer found no mention of specifically "ceramic" materials and because the material in this book probably cannot be put to immediate use in practical ceramic problems. The book is strongly recommended, however, to ceramists interested in the fundamental mechanisms of deformation in ceramics. The impact of dislocation theory on this field is just beginning to be felt, but it seems safe to say that further progress depends on understanding the properties of lattice defects and that the present book will be a standard reference for many years.   J. B. WACHTMAN, JR.

Main Congress Lectures, Sixteenth International Congress of Pure and Applied Chemistry, Paris, 1957. Birkhäuser Verlag, Basel, 1957. 355 pp. $7.50.—A series of eighteen invited lectures was a feature of the Sixteenth Congress. The six lectures on organic chemistry need not be mentioned here. Of interest were the following papers which represent fine modern reviews by outstanding scientists: "Recent research in the actinide elements," by G. T. Seaborg. "Study of combustion by kinetic spectroscopy," by R. G. W. Norrish.—N. discusses flash photolysis and kinetic spectroscopy, a technique for the determination of the vapor species in an explosion as a function of time. 23 references. "Some properties of water in crystals," by R. M. Barrer.—B. reports on his interesting study of the various associations of water in crystals. He reviews the nine methods for

studying the associations and the results of the application of these methods to various chemicals and minerals. 47 references. "Thermodynamic theory of diffusion," (in French), by S. R. de Groot.—G. discusses the derivation of a general expression for entropy for the diffusion phenomena in a mixture of charged and uncharged chemical components from the thermodynamics of irreversible processes. 11 references. "Study of fast reactions by means of mass spectrometry," (in French), by C. Ouellet.—O. discusses the identification of vapor species in flames, etc., by mass spectrometry. 33 references. "Chalcogenides of the transition elements," (in German), by H. Haraldsen.—H. reviews the recent crystal chemistry of the sulfides, etc., and oxides of the transition elements. "New developments in boron chemistry," (in German), by E. Wiberg.—W. discusses the crystal chemistry, chemical bonds, and reactions of the compounds of boron. "Protoactinium and neighboring elements," by A. G. Maddock. "High temperature chemistry—a pioneering field," by L. Brewer. —B. emphasizes the unexplored nature of the high temperature field and the lack of guide lines to predict reactions, etc., at high temperature. He illustrates his points with examples of the vaporization process and the rather unpredictable nature of the vapor species above a subliming solid. The case of phases stable at high temperature but unstable at low temperature is also discussed. The case of SiO is mentioned. 22 references. "Synthesis and properties of inorganic compounds of germanium," (in French), by H. Nowotny and A. Withmann.   S. ZERFOSS

PATENTS

Catalyst and method of preparation therefor. CYRIL ROMANOVSKY AND THOMAS E. JORDAN (Publicker Industries, Inc.). U. S. 2,850,463, Sept. 2, 1958.—5. A method for manufacturing a catalyst useful for the direct catalytic conversion of ethyl alcohol to butadiene comprises forming a solution of calcium ions, nickel ions, and phosphate ions, the solution containing 7.5 to 9.2 atoms of calcium per atom of nickel, rendering the solution nonacidic and precipitating a normal metal phosphate material composed of phosphate radicals chemically combined with calcium and nickel in the relative proportion of 7.5 to 9.2 atoms of calcium per atom of nickel, and commingling a minor weight percentage of the normal metal phosphate material with a major weight percentage of magnesia and silica to form a substantially homogeneous mixture having improved catalytic conversion characteristics for catalyzing the direct conversion of ethyl alcohol to butadiene.   D.J.B.

Method of and apparatus for spectrochemical analysis. ALAN WALSH (Commonwealth Scientific and Industrial Research Organization). U. S. 2,847,899, Aug. 19, 1958.—1. A method of determining spectrochemically the concentration in a substance of a member of the group consisting of an element and isotopes of that element comprises the steps of converting the substance into an atomic vapor which emits radiation, passing through the atomic vapor a beam of radiation the spectrum of which contains an atomic spectral line characteristic of a member of the group, and measuring the ratio between the incident and emergent intensities of the beam, which ratio is determinative of the concentration of the member.   D.J.B.

Preparation of active contact masses from kaolin clays. JOSEPH J. DONOVAN AND THOMAS H. MILLIKEN, JR. (Houdry Process Corp.). U. S. 2,848,422, Aug. 19, 1958.—2. A method for forming a hydrocarbon conversion catalyst comprises contacting a kaolin clay at about 650° to 900°F. with a gas containing about 6 to 45 mole % sulfur trioxide for a period at least sufficient to effect incorporation of about 22% SO_3 by weight in the clay and then desulfating the clay by contacting it with a reducing gas at elevated temperatures.   D.J.B.

Preparation of kaolin catalysts. GEORGE A. MILLS AND GERHARDT TALVENHEIMO (Houdry Process Corp.). U. S. 2,848,423, Aug. 19, 1958.—1. A process of preparing granular aggregates of a catalytic contact material from kaolin clay includes the steps of subjecting a plastic kaolin clay containing particles of $>2\mu$ size and finer sized particles to a procedure effective in separating the particles to form a fraction composed of $<80\%$ particles of 2μ size and smaller, shaping the fraction consisting predominantly of such 2μ size and smaller particles of such plastic kaolin into granular aggregates, subjecting such aggregates to an elevated temperature treatment to form attrition resistant aggregates, subjecting such heat-treated aggregates to a gas stream containing hydrogen sulfide at $<1200°F.$ to form partially reacted aggregates, subjecting such partially reacted aggregates at an elevated temperature to a reactant gas containing ammonium chloride for the selective removal of a portion of the iron content of the kaolin to purify the kaolin, and subjecting the purified aggregates to further heat-treatment to prepare granular aggregates of a cracking catalyst possessing a significantly higher activity for the cracking of high boiling hydrocarbons to hydrocarbons of the gasoline boiling range than granular aggregates prepared from particles having a particle size $>2\mu$.   D.J.B.

Silica-alumina-chromium fluoride catalytic compositions, their preparation, and their use in hydrocarbon conversions. ALFRED E. HIRSCHLER (Sun Oil Co.). U. S. 2,849,382, Aug. 26, 1958.—1. A catalyst for the conversion of hydrocarbons consists essentially of a synthetic silica-alumina composition impregnated with 4 to 19% by weight, based on the final composition, of chromium fluoride, the radius of the pores of the catalyst being 135 to 300 a.u., and the surface area of the catalyst being 20 to 90 m.²/gm.   D.J.B.

Additional abstract

Sect. III: Thermodynamic investigation of the solid reactions in silicate systems.

XV—General

Ceramics and nuclear energy. CELESTINO FICAI. *Faenza*, 44 [2] 40–46 (1958).—The principles of nuclear energy, the theories involved, and methods of practical utilization are explained. Apparatus and installation are described, and ceramic materials utilizable in the construction of equipment, in control, and in protection from radiation are discussed. 1 figure.   M.HA.

Ceramographic exhibit. ANON. *Am. Ceram. Soc. Bull.*, 37 [9] 419 (1958).—Three winning photomicrographs are shown. Cf. *ibid.*, 36 [7] 283 (1957).

Economic trends in the ceramic industry. C. W. PLANJE. *Am. Ceram. Soc. Bull.*, 37 [9] 414–15 (1958).

Glamour course for other engineering students. LANE MITCHELL. *Am. Ceram. Soc. Bull.*, 37 [9] 417 (1958).—The Georgia Institute of Technology offers an elective course in ceramic materials and processes for students enrolled in other curricula. Since it was initiated, more than 5000 men have taken the course.

Guide to materials standards and specifications: 5, Nonmetallics (except plastics and rubber). S. P. KAIDANOVSKY. *Materials in Design Eng.*, 48 [1] 93–95 (1958).—Standards and specifications prepared by Government agencies and national organizations are compiled. Of ceramic interest are those tabulated under glass, mica, asbestos, and mineral wool and some under the miscellaneous group, such as thermal insulation, cemented carbides, and ceramics for electrical uses.   D.J.B.

Materials for a space traveler. RODNEY A. JONES. *Metal Progr.*, 74 [1] 78–82 (1958).—J. summarizes the effect of high vacuum, solar radiation, meteorite dust, cosmic rays, zero gravity, and ionized atoms on materials used in space vehicles. No specific materials are mentioned. 2 figures.   D.J.B.

New developments in ceramics. JOHN H. KOENIG. *Materials in Design Eng.*, 47 [5] 121–36 (1958).—K. discusses ceramics for nuclear, high temperature, electrical, and mechanical uses. Recent developments in the most important materials in each field are covered. Properties are discussed and tabulated with some suggested uses. This review is very complete and forms Manual No. 148 of *Materials in Design Eng.* It is available as a separate reprint. 11 photos, 15 references. Cf. *Ceram. Abstr.*, 1958, Feb., p. 60a.   D.J.B.

A Request to Authors:

To assure the best handling by review committees, editors and printers the following suggestions are offered to those preparing manuscripts

Manuscripts should be submitted in duplicate. They should be typewritten with double spacing. A third copy will speed the reviewing process, for earlier publication.

Title should be descriptive and as short as clarity will permit.

Abstract should be brief, yet include scope of the paper, the results, and its application in the industry.

Tables should be mentioned chronologically in the text. All tables must have descriptive headings.

Drawings should be made with India ink on tracing cloth or good quality white paper. They are usually reduced to column width ($3^1/_3$ in.) and after reduction should have lettering $^1/_{16}$ in. high.

Photographs must be glossy prints, black and white only. Identify each on back with Fig. number and author's name, taking care the writing does not punch through to spoil the print.

Captions should be typed on a separate sheet.

References should be listed on a separate sheet in the order in which they are cited. Use triple-spaced typing. Style should be that adopted by *Chemical Abstracts*.

Formulas should be numbered and the names for all symbols penciled in margins. Special care should be taken to identify symbols in the text.

Units of Measurement should always be included in tables and figures.

R. S. V. P.

Dear Author:

Division program chairmen are already
scouting around for outstanding papers for the
61st Annual Meeting of The American Ceramic
Society.

If you are working on a ceramic research
project or other material that can be developed
for presentation at the May meeting, now is the
time to get in touch with the program chairman
of the appropriate Division. He will appreciate
hearing from you soon.

Early papers will get first consideration
in the Divisions that find it necessary to limit
the number of papers they can find time to hear
and discuss.

The 61st Annual Meeting will be held May
17–21, 1959, in the Palmer House, Chicago, Ill.

Division Program Chairmen

Basic Science
Samuel Zerfoss
Mineral Products Div.
National Bureau of Standards
Washington 25, D. C.

Design
F. J. Von Tury
Vontury, Inc.
Perth Amboy, N. J.

Electronics
William W. Coffeen
1024 Boulevard
Westfield, N. J.

Enamel
Robert F. Patrick
Pemco Corp.
5601 Eastern Ave.
Baltimore 24, Md

Glass
Ralph K. Day
307 W. Harrison Ave.
Maumee, Ohio

Materials & Equipment
Chester Gulick
Kentucky-Tennessee Clay Co.
Mayfield, Ky.

Refractories
Edwin Ruh
789 Fruithurst Dr.
Pittsburgh 34, Pa.

Structural Clay Products
Wayne E. Brownell
State University of New York
College of Ceramics
Alfred, N. Y.

White Wares
Willard D. Packman
Edwin M. Knowles China Co.
Newell, W. Va.